

# POLITECNICO DI TORINO

Department of Mechanical and Aerospace Engineering

Master's Degree Course  
in Mechanical Engineering



## BIOMECHANICAL ANALYSIS OF AUGMENTS IN TOTAL KNEE ARTHROPLASTY

**Supervisors:**

Prof.Cristina Bignardi

Prof.Bernardo Innocenti

**Candidate:**

Alessandra de Pinto

232567

A.Y. 2018-2019



*Alla mia famiglia,  
che mi ha sempre supportata*



## List of Contents

Abstract .....	1
Chapter 1: Literature review .....	3
1.1 Knee joint anatomy .....	3
1.2 Knee kinematics .....	6
1.3 Revision Total Knee Arthroplasty (rTKA) .....	7
1.3.1 Management of bone defects.....	8
Chapter 2: Porous Metals .....	11
2.1 State of the art .....	11
2.2 Metal Properties necessary for orthopaedic applications.....	13
2.3 Manufacturing technologies.....	18
2.4 Advanced Manufacturing Technologies of porous metals and coatings.....	21
2.4.1 Non AM procedures .....	21
2.4.2 AM procedures .....	24
2.4.3 Surface modification techniques .....	26
2.5 Advanced Porous biomaterials.....	28
2.5.1 Limitations of Traditional Porous Metals .....	28
2.5.2 Trabecular Metal (Zimmer Biomet).....	31
2.5.3 Tritanium (Stryker) .....	37
2.5.4 Regenerex (Zimmer Biomet) .....	40
2.5.5 Gription (Depuy).....	43
Chapter 3: Finite Element Modelling.....	45
3.1 Introduction .....	45
3.2 Knee joint model .....	47
3.2.1 Femur and Tibia Material Properties and Geometry.....	48
3.2.2 TKA prosthesis model and material properties.....	49
3.2.3 Ligaments model and material properties .....	54
3.2.4 Block Augments model and material properties .....	55
3.2.5 Boundary and Load conditions .....	59
3.2.6 Interactions and contact Properties .....	61
3.2. Mesh.....	62
Chapter 4: Results .....	66
4.1 Tibial model .....	67
4.1.1 Von Mises Stress: flexion angle 0° .....	67
4.1.2 Von Mises Stress: flexion angle 45° .....	70
4.1.3 Von Mises Stress: flexion angle 90° .....	73

4.1.4	Shear stress: flexion angle 0° .....	76
4.1.5	Shear stress: flexion angle 45° .....	79
4.1.6	Shear stress: flexion angle 90° .....	82
4.2	Femoral model.....	86
4.2.1	Von Mises Stress: flexion angle 0° .....	86
4.2.2	Von Mises Stress: flexion angle 45° .....	91
4.2.3	Von Mises Stress: flexion angle 90° .....	96
4.2.4	Shear stress: flexion angle 0° .....	101
4.2.5	Shear stress: flexion angle 45° .....	106
4.2.6	Shear stress: flexion angle 90° .....	111
Chapter 5: Discussion.....		117
Bibliography.....		
Acknowledgements .....		



# Abstract

Revision total knee arthroplasty (TKA) is advised when aseptic loosening, infection, osteolysis occur or when the range of knee motion is affected [58]. The extent of bone injuries determines which prosthesis should be implanted. Currently, a variety of solutions are commercially available:

- Small bony deficiencies can be addressed with cement or allografts.
- Broader defects can be dealt with augments, metal wedges, bone grafts or personalized prosthesis.
- Stems and screws can be used to provide more stability [58,59]

The great challenge for revision total knee arthroplasty (TKA) is to provide adequate pain relief for the patient and ensure greater knee stability, proper alignment and a longer lifespan of the implanted prosthesis [58].

Modular augments and wedge are recommended when there is a lack of bone support which is more than 40% [58]. Nowadays, different shapes (rectangular or wedge-shaped) and sizes (several thicknesses), whose selection is related to the extent of bone defect, are commercially available, while there are not guidelines for the selection of the porous material best fitting specific clinical requirements [59]. Furthermore, it is important to investigate how bone response changes varies if the material has been changed.

Among several modelling approaches, finite element analysis (FEA) allows to deal with a variety of biomechanical problems which could compromise knee functions and the longevity of the implanted prosthesis. Therefore, FEA gives the possibility to analyse bone and implant stress distribution and interactions under different conditions, by comparing these results to those of a physiological knee. Finite element modelling represents a powerful tool through which is possible to develop clinical strategies and enhance the success of TKA, by ensuring a long-term stability and fixation of the implant [63].

For the reasons stated above, this study will focus on the development of a 3D model of the knee joint where tibial and femoral bone defects are addressed with porous metal augments because these biomaterials ensure a faster bone regeneration and they also need a little bony

resection. Therefore, the aim of this work is to carry out a finite element analysis in order to investigate the change in tibial and femoral bone stress response to the placement of an augment, both locally and globally. Different thicknesses (5, 10 and 15 mm), positions (distal, proximal and posterior) and materials (porous and solid) are considered in order to compare the different bone responses.

The results obtained by this analysis demonstrate that the insertion of an augment made of any material induces a change in terms of bone stress, in particular in the region which surround the wedge. Furthermore, it will be possible to notice that an augment made of a porous metal induces a stress distribution that is similar to that of the reference model where no augment is inserted, while conventional metals cause more significant variations. So, it is possible to conclude that porous metals are a good alternative to the dense because of their stiffness that is closer to that of the bone. Consequently, porous biomaterials ensure the best implant performance.

# Chapter 1

## Literature Review

### 1.1 Knee joint anatomy

One of the most important joint in our body is the knee: it is characterised by a complex structure which consists of bones, ligaments, tendons, muscles in order to form two different joints: *tibiofemoral* and *patellofemoral*. It is also very vulnerable, especially for athletes [1].

As shown in (Figure 1), it includes several bones:

- the thigh bone (*femur*) shows two bumps known as femoral condyles (medial and lateral) at the end of the bone;
- the shine bone (*tibia*) possesses two bulges named *tibial tubercles* and two tibial condyles called also *tibial plateau* where are located the *menisci* (medial and lateral) which ensure a good stability of the knee;
- the kneecap (*patella*) is placed between the femoral condyles, whose function is to reduce the friction forces when we move the knee;
- the *fibula* is placed close to the tibia and linked to the tibiofibular joint: its function is to offer a surface where muscles and ligaments are fixed [2].

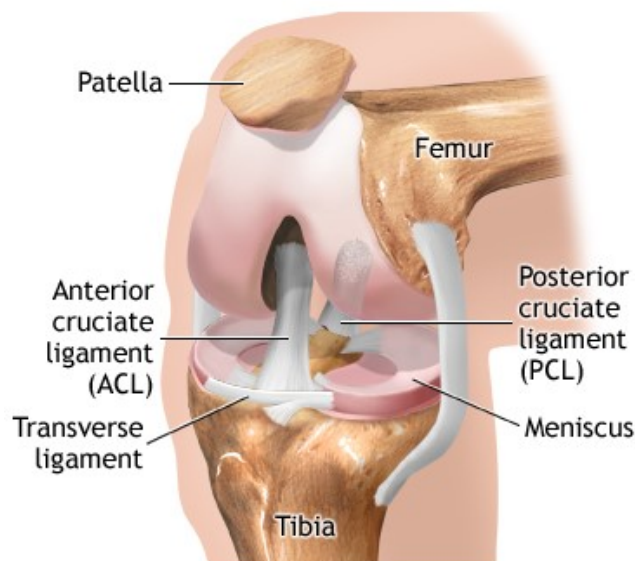
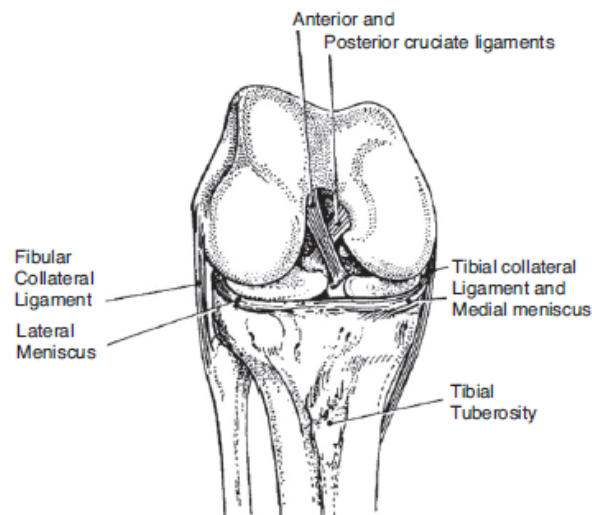


Figure 1 - Structure of the knee joint [4].

If we considered the knee joint without menisci, it would be unstable because the surfaces of the tibia and femur which are in contact do not adhere exactly, due to the presence of the protuberances. In fact their most important task is to improve the surface of contact between the femoral and the tibial condyles in order to facilitate the articulation between the femur and the tibia, but also to direct the range of motion of the knee. In this way, menisci allow the stability of the knee [6].

*Coronary ligaments* attach menisci to the tibia: these connections restrict the relative motion existing between the tibial surface and the menisci (*Figure 2*). Furthermore, while a stronger link exists between the edge of the medial meniscus and the *medial collateral ligament* (MCL), the lateral meniscus is not attached to the *lateral collateral ligament* (LCL): this justifies the higher mobility of the latter [2].



**Figure 2** - Anterior view of menisci and ligaments [7].

The knee is a synovial joint which can be classified as uniaxial joint because it allows only the movements in one plane and a little rotational movement. Between the ends of the bones which are involved in the knee joint, there is a cavity containing the *synovial membrane* (*Figure 3*) which produces the *synovial fluid*: it plays the key role to protect and also feed the cartilaginous structures [3].

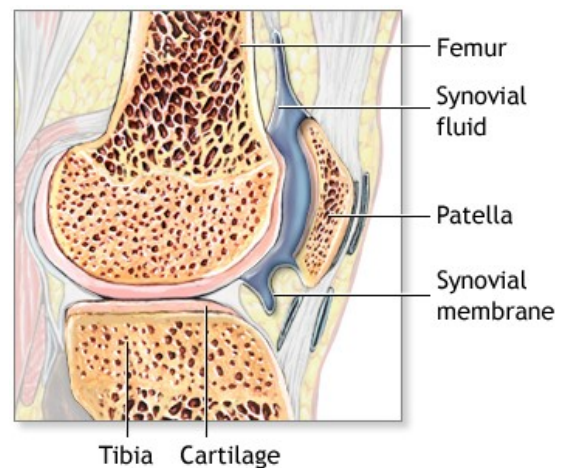


**Figure 3** - Cut section view of the knee joint [5]

The four leading ligaments made of collagen fibres play the primary role of ensuring the stability of knee joint: they avoid that any quick movements could affect the relative position of the structures to which they are attached, preserving the alignment of the bones [8].

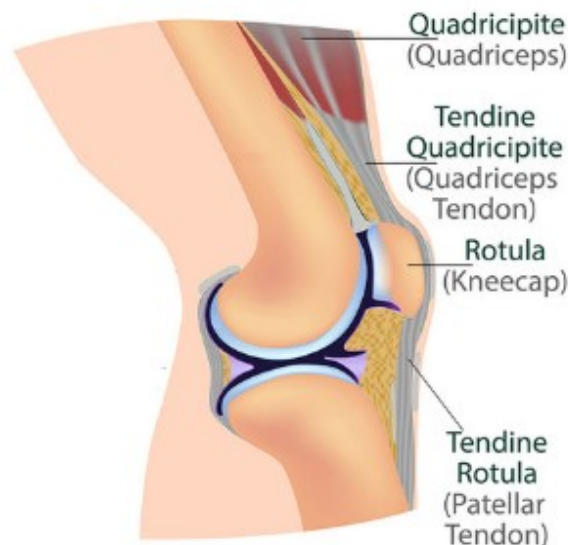
The ligaments which connect two bones each other are classified as follows:

- the *medial* and *lateral collateral ligaments* secure the medial and the lateral stability of the knee respectively;
- the *anterior* and *posterior cruciate ligaments*, placed in the centre of the knee, keep the knee stable during the anterior and posterior movements.

In addition, MCL and LCL together with ACL and PCL avoid excessive rotation during the extension [6].

The performance of the knee movements is allowed by the presence of the muscles together with the tendons, an assembly of fibres, which ensure the attachment of the muscles to the bones (*Figure 4*). Although the tendon and the ligament are fibrous structures, the main difference is that the former connect the muscle to the bone, the later attaches two bones [9].

- The knee extensor is the *quadriceps* which consists of four muscles: the vastus medialis, the vastus intermedius and the vastus lateralis and the rectus femoris which are located in the anterior part of the thigh. These muscles share a tendon which is connected to the patella and the tibia. The quadriceps are responsible for the extension of the leg.
- The hamstrings is characterised by three muscles which are placed in the posterior part of the thigh: their function is to guide the flexion movement [2,6,9].

**Figure 4** - Lateral view of the knee: muscles and tendons [9].

## 1.2 Knee kinematics

The knee joint is very complicated to model because it consists of three rigid bodies: patella, femur and tibia and due to the presence of ligaments, tendons, menisci and muscles which work all together in order to allow the motion of the knee during the activities of daily life.

Observing the tibiofemoral movement, the knee joint kinematics can be analysed by *six degrees of freedom movement* which is characterised by three rotational movements: *flexion-extension*, *external-internal rotation* and *varus-valgus rotation*) and three translations: *anterior-posterior*, *medial-lateral shift* and *superior-inferior translation*, [11] as shown in the *Figure 5*.

According to the literature [12], *Good* and *Suntay* described the motion of the knee joint defining an anatomical coordinate system. It is not a fixed coordinate system, but it consists of two fixed body axis (tibial mechanical axis around which occurs the internal – external rotation of the tibia and flexion – extension axis which corresponds with transepicondylar axis of the femur approximately) and a third floating axis, obtained from the previous axes through the right hand rule.

The complex interactions between the different components of the knee joint can be simplified, considering the resultant transmitted forces and torques by the several structures which take action during the motion of the knee [10].

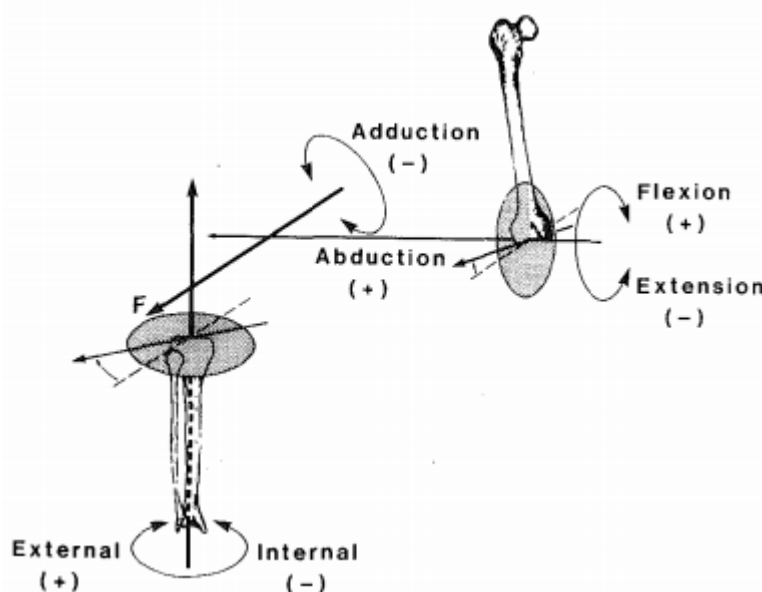


**Figure 5** – Knee joint coordinate system and degrees of freedom [12].

### 1.3 Revision Total Knee Arthroplasty (rTKA)

The leading aim of Total Knee Arthroplasty (TKA) is to reduce pain, guarantee a stable knee and also restore the normal range of motion. TKA is a surgical treatment which is required when serious diseases, such as osteoarthritis, affect the physiological performance of the knee. The outcomes achieved through this surgical practice should last for a long time, but it could occur that the implanted prosthesis fails [13], due to different causes. When it happens, the knee becomes unable to performance the normal daily life activities and so a *revision surgery* is necessary.

The prostheses implanted during a primary TKA is chosen according to the disease that affects the knee, the extension of the bone deficiency and the age of the patient.

The three main kinds of knee prostheses used, are classified as follows:

- *Unconstrained prostheses*: implanted when a very small part of cartilage or tissue is damaged (uncompartmental knee arthroplasty), keeping the original frame of the articulation;
- *Semiconstrained prostheses*: adopted for superficial joint replacement and they are divided in two groups in accordance with the necessity or not of removing the posterior cruciate ligament;
- *Constrained prostheses*: used when there is a big extent of bone deficiency and the knee stability is affected seriously [14].

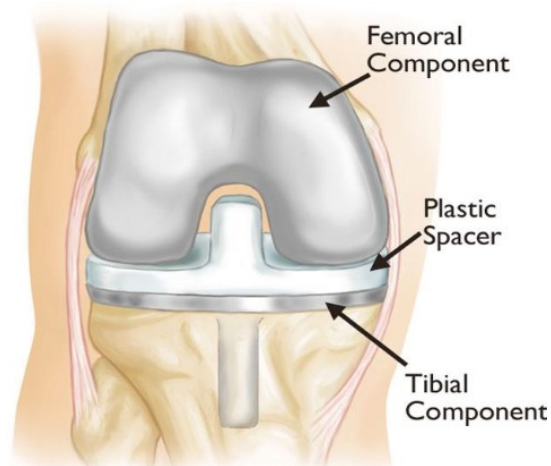
During the primary surgery, the surgeon removes the damaged surfaces of the tibia and the femur and resects them in order to fit to the surfaces of the implanted components, using special tools (*Figure 6*).



**Figure 6** – Steps of primary Total Knee Arthroplasty [15].

Although *Revision Total Knee Arthroplasty* is a surgical procedure which is performed to achieve the same aims of the primary TKA - for instance to ensure adequate range of knee motion during the normal activities and to reduce pain – revision TKA is much more complicated than primary TKA because surgeons have to plan the surgery carefully and they have to adopt special surgical tools [16].

According to the mechanism of failure of the primary knee joint replacement, the extent of bony defects, a full or partial replacement of the components of the prosthesis (femoral, tibial and patellar) could be necessary (*Figure 7*).

**Figure 7** – Components of prosthesis during a primary TKA [16].

### 1.3.1 Management of bone defects

When rTKA has to be performed, new implant stability and fixation could be compromised by a severe bony loss. This goal represents a hard challenge to deal with surgeons since it compromises components' right alignment and does not provide a good stability at the interface. The method of bone reconstruction and the kind of material for rTKA had to be also chosen according to patients' life expectancy and everyday activities.

In most cases remaining bone is of low quality, so the aim of rTKA is to preserve residual bone and to reconstruct the lacking bone in order to achieve long-term outcomes. In less severe cases (bone defects less than 5 mm) the surgeon can intervene using more cement (with or without screws). However, it cannot provide good long-term results and it is often used for elderly

people. In more severe cases (bone defects greater than 5 mm) augments are implanted or bone grafts are used.

The evaluation of surgical treatments is challenging because of the lack of a well-defined bone defect classification. The AORI (Anderson Orthopaedic Research Institute) classifies bone loss according to the severity of bony insufficiency observed in the revision surgery. The three categories are described in the table below.

**Table 1** – Bone loss classification according to AORI [87].

Defect type	Identifying features	Treatment
F1/T1	no component subsidence or osteolysis; no cancellous defects in the peripheral rim; cancellous bone that will support an implant; defects can be filled by small amounts of particulate bone graft or cement; a normal joint line is present  <i>femur</i> —full condylar profile <i>tibia</i> —component above the fibular head and a full metaphyseal segment	no augments (>4 mm), structural grafts, or cement fill (>1 cm);  no stemmed components necessary
F2/T2	cancellous bone inadequate to support the implant; cancellous defects may require bone grafts; the component used requires augmentation to restore the joint line; osteolysis may be more extensive than radiographs indicate  <i>femur</i> —reduced condylar profile <i>tibia</i> —component is at or below the tip of the fibular head and the tibial flare is reduced	joint line restored with an augmented component (>4 mm), particulate autograft or allograft, or cement fill (>1 cm);  stemmed components should be used
F3/T3	marked component migration; knee instability; deficient metaphyseal segment  <i>femur</i> —loss of collateral ligament attachments from one or both condyles; severe condylar bone loss from osteolysis or a comminuted supracondylar fracture	structural graft, augment or cement, or a hinged component used to reconstruct the condyle or plateau;  stemmed components required

Several studies [87, 88] demonstrated the absence of differences between the use of bone grafts and cement in the first two type of defects, but the former methodology is biologically better. It allows a load transfer more physiological, even if they can lead to transmission of viral and bacterial infections. The use of augments provides a quick application, but problems linked to wear and corrosion could occur. Angled wedge augments lead to shear stresses and leave distal bone unloaded, while step wedge augments could need of a major bone resection, but they make compression forces to act at the interface. Hockman *et al.* studies [89] demonstrated that the combined use of modular augments and structural allograft increased rate of implant survival. Rand *et al.* [90] found that 100% of patients with augments including wedges augments reported positive results. On the other hand, Brand *et al.* [91] noticed that wedges augments were better for elderly patients with severe peripheral tibial defects.

Cuckler *et al.* [93] suggested that the use of augments is more appropriate if 40% or more of the implant-bone projection is not supported by remaining bone, or when 25% or more of the

cortical rime shows peripheral defects. Other studies [94,95,96] claimed the use of rotating-hinge or custom-made prostheses in patients with severe defects because they assure a better mechanics and survival. Nonetheless, custom-made implants are expensive and require more time for realisation. Furthermore, they could not fit well, so a more bone resection is necessary in order to have a good stability.

More innovative methodology concerns the use of metaphyseal filling metal cones. They can provide a better components stability in the presence of large defects due to sclerotic bones. However, they require the use of cement in order to be fixed to the implant. It is possible to combine cones and porous materials (like porous tantalum) with the aim to improve metaphyseal fixation because it promotes and accelerates bony ingrowth [97]. These technique shows good short-term results for type-2B and type-3 defects [98], on the other hand the medium- and long-term results are not yet well-known [92].

## Chapter 2

# Porous Metals

### *2.1 State of the art*

All over the world, people continue suffering pathologies which require the implantation of a prosthesis in order to relieve pain and re-establish the normal function of the joint. Therefore, a great challenge is to develop biomaterials which ensure a high performance of the implant and a long lifespan [44].

During the last decades, it has been observed a great development of porous biomaterials in orthopaedic field due to particular properties offered by porous metals, such as *porosity*, *coefficient of friction* and *modulus of elasticity* [18].

Overall, porous biomaterials offer a variety of advantages which have revolutionized the field of total joint reconstruction, such as hip and knee replacements. These surgical practices allow the restoration of the joint function, bringing relief from pain, but to achieve a satisfactory result of these medical procedures is necessary to pay attention to biological fixation: coarse porous biomaterial surfaces have shown an enhancement in osteointegration [19].

A crucial aspect for the bony restoration is represented by the structure and the functions of bone: it is able to regenerate tissue in presence of some bone deficiencies but if serious pathologies, an extended bone defect or a cancer resection occur, bone grafting will be necessary [37].

The natural bone consists of composite material, as shown in the following *Figure 8* organic material is composed by fibres of collagen while inorganic material contains hydroxyapatite which is composed by calcium, phosphorus and a lesser quantity of magnesium. These materials ensure a certain level of stiffness. As concerns the framework of the bone, it consists of:

- cortical bone, composed essentially by calcium and phosphate, represents the outer rigid and dense part of the bone; it is characterised by a low porosity that accounts for 5-10% approximately.

- spongy bone is the internal part, characterized by a high level of porosity (around 50-90%); in fact, its structure is organized in lamellar trabeculae composed by blood vessels and tissue. This porous framework allows to obtain a specific surface which is much greater than that of cortical bone.

Nowadays, the great challenge is to be able to replicate a biomaterial with a structure which resembles to that of the original bone as much as possible [46].

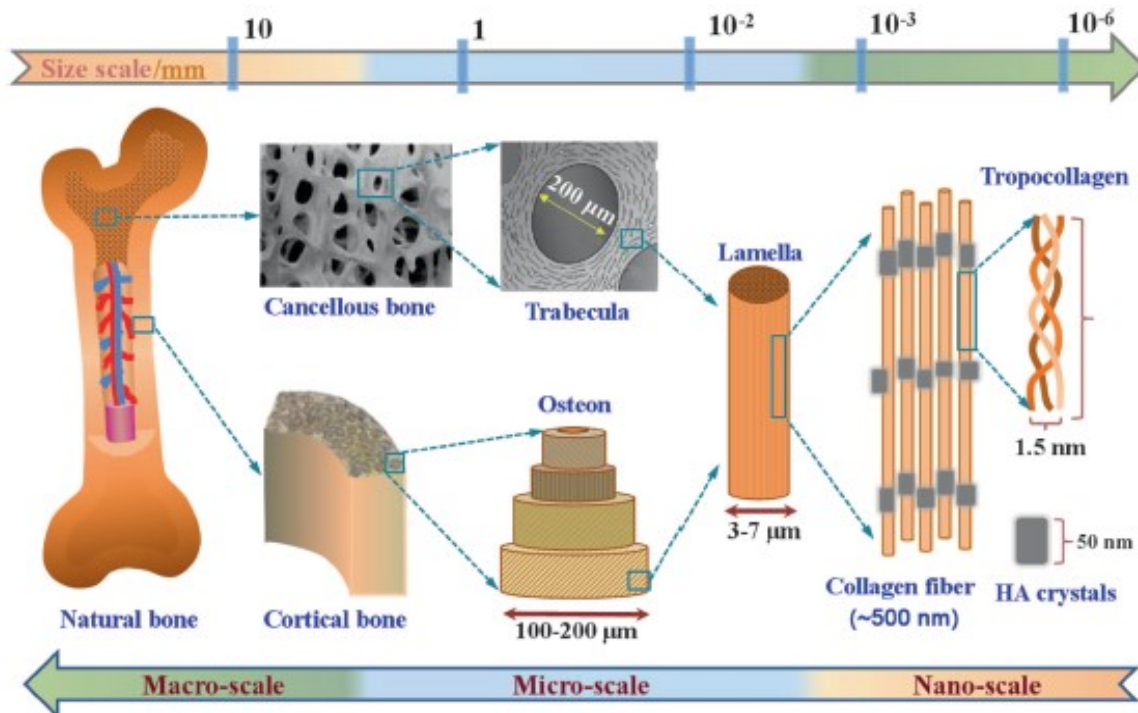


Figure 8 – Composition and structure of the natural bone [46].

In order to achieve this goal, biomaterials have to fulfil different requirements:

- Biodegradable, bioactive and biocompatible.
- Non-toxic.
- They have not only to close the bone defects but also to degrade constantly as the new tissue regrow, in order to preserve the bone capabilities.
- Proper mechanical properties and stability with the purpose of offering support for the bone regeneration.
- High porosity of the structure for ensuring the presence of void spaces, necessary for the proliferation of the cellular tissues and the formation of the cellular matrix, the vascularization, the supply of nutrients and the oxygenation, fundamental for the growth of the tissue.

- Implanted biomaterial and the cells have to react to each other in an effort to promote some processes, such as: proliferation and differentiation.
- Osteoinductivity plays a key role in the tissue regeneration because it ensures an appropriate correspondence between the biomaterial and the original bone, allowing a close fixation [46].

In orthopaedic field, revision surgery is conducted when primary surgery fails [20]:

- Loosening: the implant loses the attachment to the underneath bone (56.4%)
- Dislocation (14.5%)
- Infections (11.1%)
- Fracture (8.8%).

Due to the complexity and the additional expense of this surgical procedure, people who require a total joint replacement desire that the implanted prosthesis has a longer lifespan in order to avoid the revision surgery.

For the purpose of tackling these challenges, porous biomaterials play a key role especially in orthopaedic applications because the mechanical properties shown demonstrate their ability to overcome the drawbacks of solid metals, for instance: stress shielding, loosening of the implant, low volumetric porosity, high modulus of elasticity, limited bone ingrowth and osseointegration. In fact, these materials offer a porous surface that facilitates the locking between the host bone and the implant [21, 22]. Furthermore, biomaterials offer another important property: *permeability*, necessary to feed and oxygenate the cells provided by the porous biomaterial, in order to replicate the behaviour of the bone [17].

## *2.2 Metal properties necessary for orthopaedic applications*

During the last decades, porous metals have experienced a great success due to the improvements which they have allowed in total joint arthroplasty: they have enhanced several functions, for example: the attachment of the implant to the bone, the osseointegration and a longer lifespan of the implanted prosthesis [32].

To ensure the success of a total joint replacement is necessary that the material, used for the manufacturing of the prosthesis, fulfils those requirements (previously mentioned), which are explained thoroughly in the following paragraph.

- The permanent attachment of the implant to the bone is fundamental in order to avoid that the transfer of the load could cause relative movements between the prosthesis and the underlying bone [23]. The direct contact between the implant and bone, known as “*osteointegration*”, depends on:
  - Prosthesis shape and size;
  - Manufacturing procedure of prosthesis;
  - Materials used for the manufacturing of prosthesis;
  - Characteristics of the interface bone – implant.
  
- During a surgical procedure an ideal prosthetic component, implanted in order to restore a bone defect, should perform in the same way of the original bone in terms of transferring and spreading load to the underneath bone. Actually, the implanted prosthesis distributes loads in a different manner: it is linked to the fact that prosthetic stiffness is higher than that of original bone which has been replaced by the prosthesis. In this way, implant carries much of the applied load due to its greater stiffness and so it is overloaded, while the surrounding bone is subjected to lower loads [24]. Hence, this leads to the phenomenon called “*stress shielding effect*”: the decrease of the stress over the bone which surrounds the prosthesis, causes a gradual bone loss with the passing of the time [25].

For instance, during the surgical treatment of revision TKA it could be possible to implant a long stem into the tibia, in addition to the tibial, femoral and patellar components in order to ensure an enhanced attachment between the prosthesis and the host bone [26]. A finite element analysis is carried out in order to compare the different response of the host bone in terms of stress distribution, considering different characteristics of the stems. By comparing the intact tibia with the configurations with prosthetic implants, it has been proven that the effect of stress shielding has resulted in a reduced density bone (*Figure 9*) and a decrease of load nearby the tibial component, that compromises bone integrity [27].

Furthermore, the phenomenon of stress shielding leads to the lack of mechanical stability, in addition to the bone demineralization.

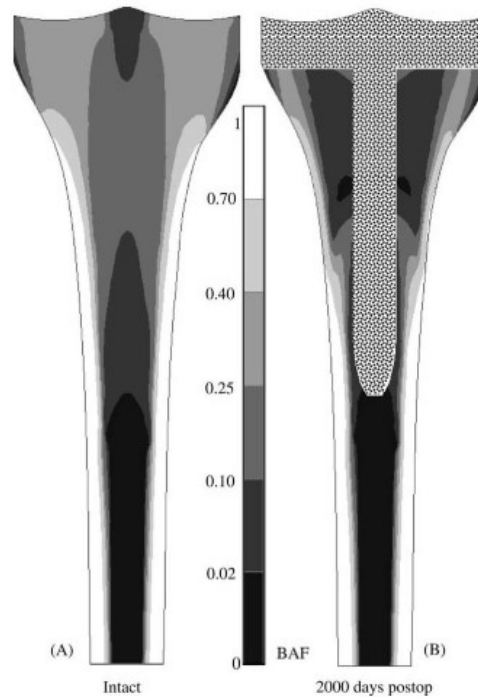


**Figure 9** – Comparison between the intact tibia and the tibia 2000 days after the insertion of the implant, looking at bone loss (BAF – bone area fraction) [28].

- The ideal porous metal has to be *biocompatible*: it must react with host bone without causing inflammatory reaction when the prosthesis is implanted, but it must be *bioactive*, i.e. promoting cellular regrowth, the vascularization and it has also to be osteoconductive and osteoinductive. It has to be capable to ensure the osseointegration with the underlying bone, but it must not have dangerous and toxic impact to the surrounding bone [31].
- The implant material should have *mechanical properties* (in terms of *strength* and *stiffness*) which are as similar as possible to those of host bone [32]. In fact, bone presents a structure that is characterised by a cortical bone (strength: 52 – 219 MPa and stiffness: 7.1 – 27.6 GPa) and a cancellous bone with lower properties (strength 1.6 - 3.9 MPa and stiffness: 0.1 – 10.4 GPa) [33]. It is fundamental that stress distribution over the implant and the surrounding bone resembles as much as possible to that of the original bone in order to avoid bone resorption (stress shielding effect) and to stimulate bony regeneration [32].

- The implanted *material modulus of elasticity* plays a key role to prevent the risks related to the stress shielding. This issue has been tackled by designing prostheses defined “isoelastic”, i.e. they show a Young modulus which is similar to that of bone [23]. For example, while stainless steel, cobalt-chromium and titanium alloys show an elastic modulus which is higher than that of bone, bone cement (PMMA) Young modulus is an order of magnitude fewer than that of bone [29]. If there was a mismatch between the implant elastic modulus and that of original bone, this could cause implant loosening [33]. In order to avoid this issue, it is fundamental that Young modulus is similar to that of bone, between 10 and 30 GPa) [34]. According to some studies, conducted by Brett Levine [47], he discovered that materials with trabecular structures have elastic modulus which is similar to that of cortical bone or cancellous bone [34].
- Another important role is played by the *porosity*: it represents the ratio between the pore space volume and the total volume of the considered material and it is characterised by three different kinds of pores: closed, through and blind pores. The crossing of fluids is partially and totally allowed by the blind and through pores, respectively. In orthopaedic field, “open porosity” is widely used because it helps the regeneration of bone tissue (osteointegration), by promoting the vascularization and the growth of cells. To safeguard the restoration of bone tissue is necessary to keep under control size, interconnectivity and distribution of the pores. Furthermore, *mass transport properties* (such as *permeability* and *diffusion*) are fundamental for ensuring the growth and the feeding of the cells [31]. Recent studies have demonstrated that bone ingrowth is facilitate by those surfaces which are characterised by a higher curvature [33]. Porosity, Young’s modulus and mechanical strength are related. In fact, it is important that the ratio between porosity and strength is appropriate in order to give the opportunity of using these materials for orthopaedic applications. For instance, porous structures realized by sintering procedures present a lower level of porosity, as compared with that obtained through other technologies, due to the morphology of the adopted powder (shape and dimension). Electron or laser beam melting manufacturing processes ensure a high level of porosity because they are influenced only by the three – dimensional models [34].

- To achieve a good mechanical stability at the contact surface between the implant and the bone, interface bonds play a crucial role. Some technologies, such as EBM and lost wax casting, and those which realize a partial remelting of the underlying layers allow a proper interlocking. Other processes need appropriate treatments [34].
- Moreover, another important material property is the *roughness of the prosthesis surface* because if it were smooth, the implant would not attach to the host bone and relative sliding movements could occur, leading to the stress shielding [23]. If the contact surface between the prosthesis and the underlying bone were porous, the biological fixation could be more effective, keeping more stable the mechanical contact [31]. A technological solution widely adopted is the use of hydroxyapatite coatings (*Figure 10*): hydroxyapatite, a calcium phosphate which has the same chemical composition of the mineral bone, so it is able to establish strong chemical bonds between the implant and the host bone tissue. This kind of coating facilitates osseointegration [30] but on the other hand, superficial roughness plays a key role in fatigue cycle: it could cause the initiation of a fatigue crack [34].

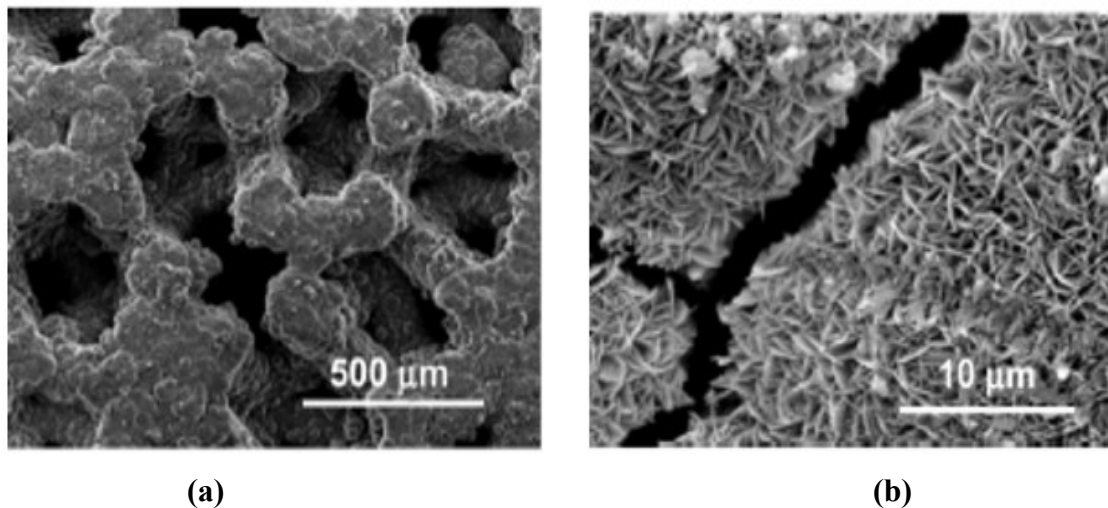


**Figure 10** – (a) hydroxyapatite coating on the surface. (b) microstructural features of the hydroxyapatite coating on a Ti6Al4V [30].

- *Corrosion and biocompatibility*: nowadays, CoCr and titanium alloys are adopted for orthopaedic applications because they are biocompatible but also they allow a high level of corrosion strength. A crucial aspect is about the metallic ions scattered during the

chemical reactions which occur. They could be harmful for the healthcare of the human body: these elements would cause the appearance of little defects over the implant surface. This effect, called “pitting”, could compromise the mechanical stability and it occurs in porous morphology because of the ratio between the area and the volume is high particularly, if it is compared to that of metallic bulk materials [34].

- *Production expense* should not be particularly expensive and furthermore the surgical procedure that has to be adopted, should be easy and simple to replicate [32].

In summary, the greatest challenge is to achieve a proper trade – off between the several features which are required [34]:

- Tensile, torsional and fatigue strength in order to support the different loads to which prosthesis is subjected;
- Low modulus of elasticity to avoid stress shielding effect and consequent bone demineralization;
- High interconnected porosity to enhance a stable fixation of the implant to the bone;
- Corrosion strength;
- Biocompatibility.

### 2.3 Manufacturing technologies

Porous metals which are used orthopaedic field are generated adopting different production processes whose complexity is related to the size, distribution and interconnectivity of the pores which plays a key role in the osteointegration [31].

- *Porous beads*: the raw material adopted to realize porous beaded surfaces is a CoCrMo alloy. The first production step consists in the addition of a ligand which has the property of being soluble in water, in order to attach the beads to the implant’s surface, applying a mechanical force. This ligand allows the adhesion between the particles of powders: it is a sort of glue. After that, this film is exposed to a sintering process in order to facilitate the evacuation of the ligand and the phenomenon of diffusion between these

beads and the underlying implant surface. This process is realized in a vacuum chamber and it takes place due to the fact that the component has been heated up until high temperature. This procedure is reiterated in order to obtain the necessary coating thickness. It is also characterized by a framework with a porosity that is approximately 35% and a pore size of about 425  $\mu\text{m}$ : this allows the attachment between the prosthesis and the surrounding bone [19].

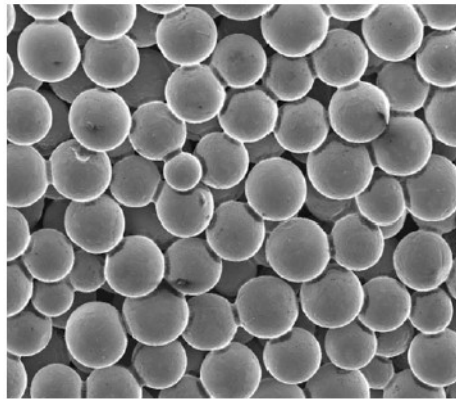


**Figure 11** – Sintered Co-Cr beads [19].

- *Wire arc deposition*: during this manufacturing process a row metal material is sprinkled in order to achieve the desired roughness of the implant surface. This coating (*Figure 12*) is obtained through the melting of a collection of titanium particles, using a special gun: it is continuously supplied by two CPTi wires because they work as two electrodes in order to form an electrical arc. Afterwards, there is a pulverisation of the titanium particles through the passage of a high pressure inert gas (argon): these steps continue until the achievement of the appropriate thickness. This process is realized in a protected chamber, keeping under control different parameters [19].

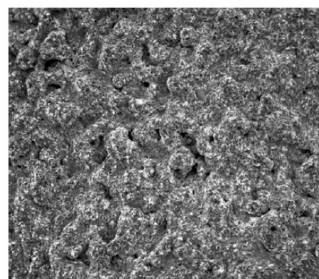


**Figure 12** – Arc deposited Ti [19].

- *Plasma spray*: this process involves the use of a specialized gun: it consists of two electrodes which form a plasma flame in which the Titanium powder, necessary to form

the coating, is injected. A constant stream of plasma heats the particles of powder, and after that the molten material, accelerated properly, is pressed onto the surface which needs to be coated where this powder solidifies (*Figure 13-a*). This process is carried out into an inert chamber in order to avoid every kind of contamination [19]. Keeping under control the processing parameters, a porous coating is realized (*Figure 13-b*).

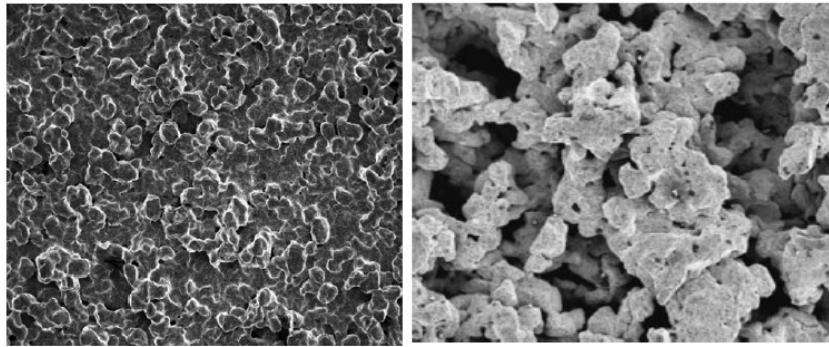


**Figure 13** – (a) Plasma sprayed Titanium [19] – (b) Regenerex structure (Biomet) [34].

- *Fiber metal mesh*: It is another method to manufacture porous coatings: it is a process based on solid state diffusion in order to join the porous cluster – which consists of metal fibres of Commercial Pure Titanium – and underneath surface [18,19]. The goal is to achieve better mechanical properties, improving osteointegration. The coatings could be realized using fibres of Titanium and the obtained porosity is around 50% (*Figure 14a*). On the other hand, it is possible to use a powder of Titanium: the porosity is monitored by controlling the pressure that is adopted to mold the product. The porosity that is possible to reach is about 55% (*Figure 14b*) [19]. The process is conducted in a vacuum chamber [18].

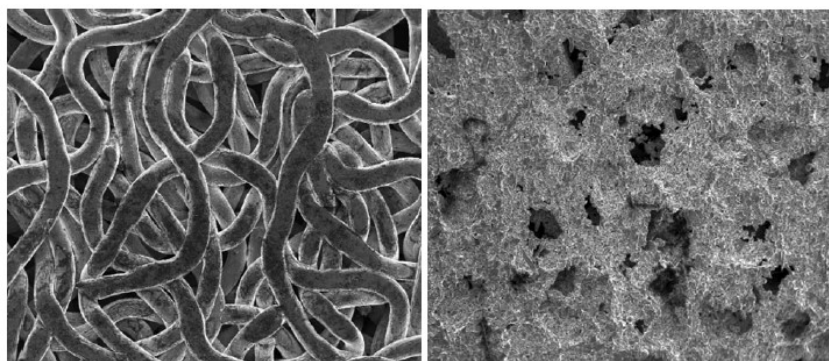


**Figure 14** - (a) Diffusion – bonded CPTi fibres - (b) Diffusion – bonded CPTi powder [19].

## 2.4 Advanced manufacturing techniques of porous metals and coatings

The innovative field of biomaterials is constantly evolving because of the need to treat particular pathologies: the contact surface implant – bone is the most critical and the positive outcome of the total joint arthroplasty (for instance knee, hip, shoulder) depends on the efficacy of this fixation. The contact surface has been revolutionized: at first, it was smooth and so the bond prosthesis – host bone was weak. Then, it has become rough, allowing a better adhesion, and recently, the research has led to a porous surface. The idea is to combine metals and non-metals in order to put together the advantages of both materials: metals which are characterized by a high strength and polymers, with the purpose of achieving a higher capacity of osteointegration [37]. In order to achieve these goals is necessary that the material is characterised by interconnected pores with the purpose to allow biocompatibility, vascularization, fluid flow and osteoconduction and tissue formation [38].

Particular attention is payed to biomaterials characterized by high porosity which could be subjected to a chemical treatment with the target of improving the tissue ingrowth, mechanical stability and reducing the risk of infection [37]. This purpose has led to the development and the combination of different approaches in order to guarantee a longer lifespan of the implant [37]. Among the several available manufacturing techniques, those which involve the production of open porous morphology will be argued in the following paragraph. The technologies which are used in orthopaedic field can be classified in:

- *Non additive or traditional methods;*
- *Additive manufacturing procedures.*

### 2.4.1 Non AM procedures

The main difference between these two groups is the fact that AM techniques allow to control more accurately the sizes, shape, distribution and connection between the pores. The level of porosity that it is possible to achieve through these procedures is lower than that of AM techniques [33]. In the following, some of these processes are described.

- *“Space holder technique”*: this process requires a blending of metal powder and a space holder material which could be metallic or not [35]. This technique gives us the opportunity of fabricate metal component characterized by a distribution of pores which

is not homogeneous: the obtained metal product presents a high open porosity [31]. Some pre admixtures are added in order to reduce friction and to promote bonding [35]. The next step consists in applying a high pressure in order to compact the mix, obtaining the “green part”. The following step is “primary sintering”: a heat treatment is conducted with the purpose of dissolving the holder material, while the metallic particles remain attached. Then a high temperature sintering is carried out to achieve the desired density level [31,35]. In this way, it is possible to realize a high porosity (60-80%) [31]. High porosity metal foams are produced by this method: this structure, characterized by interconnected pores which lead to a high surface density and the open cell framework, favours heat diffusion (mechanism shown in *Figure 15*) [36].

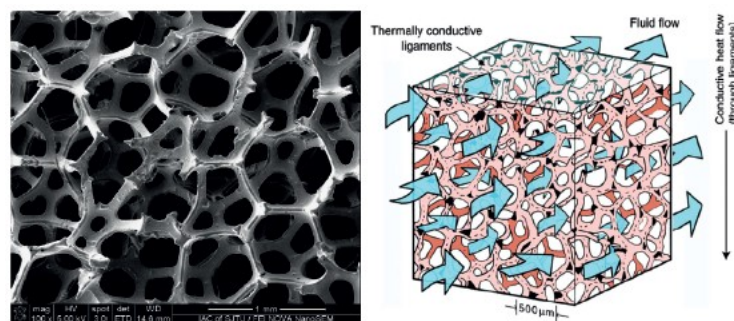


**Figure 15** – Metal foam: structure (left); mechanism of flow mixture (right) [36].

- *Replication*: this method is similar to the previous one – it consists of three stages: at first we have the preparation of the model, then there is the infiltration and finally it is necessary to remove the model, reaching the desired level of porosity. This approach is used to produce porous titanium and titanium alloy components [31]. For instance, polyurethane foam (*Figure 16*) is used as a binder: it is coated by a layer of Titanium powders and it is evacuated through a thermal treatment in order to obtain the desired metallic structure [19].

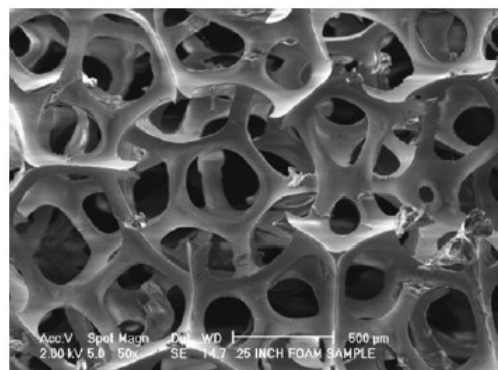


**Figure 16** –Polyurethane foam is used as a sacrificial material [19].

- *Combustion synthesis*: a technique which is adopted to realize a high level of porosity using especially powder mixture of Ni-Ti alloys. It is based on an exothermic reaction which involves this mixture, obtained by mixing and pressing the powder and the binder: thermal explosive reactions involve the entire mixture as a combustion wave [31].

The type of structure that it is possible to achieve is showed in the following *Figure 17*.

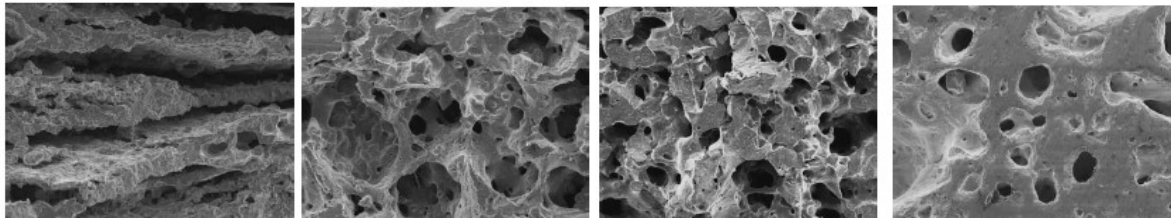


**Figure 17** – High level of porosity reached by the combustion synthesis [38].

- *Chemical vapour deposition*: it is a process which leads to the deposition of a solid material onto the surface that must be coated, through a chemical reaction between the heated substrate and a reactant gases carried by a carrier gas. Keeping under control the parameters of the gaseous reaction is it possible to vary the porosity of the coating layer [31, 39].
- *Freeze – drying technique*: This is a method which is applied to produce porous scaffolds. It involves the use of polymers which are dipped into a solvent. The porous framework is obtained from this mixture dissolving the solvents through a freeze drying process: at first, the material is iced and then, adequate heat is provided in order to allow the sublimation of the material, achieving the desired porous structure (*Figure 18*). In the emulsion – freezing (a similar process), it is necessary less time for preparation of this admixture and better interconnection of the pores [40]. The level of porosity achieved in these scaffolds is higher than 90% [31].

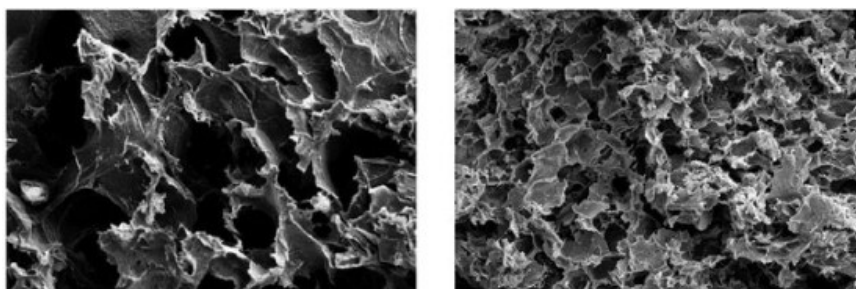


**Figure 18** - Scaffolds produced through emulsion freezing/ freeze – drying method [41]

- *Electrospinning*: it is a technique which produces electrospun nano size fibres, characterized by a high porous structure. This process starts with polymers mixture where salt particles (NaCl or CaCO<sub>3</sub>) are added. A key role is played by these salt particles in achieving a particular pore size and distribution (*Figure 19*) [42].

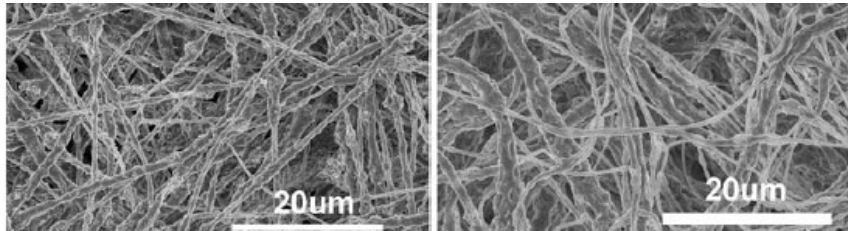


**Figure 19** – Porous structure of electrospun fibres [42].

- *Lost-wax casting*: the most relevant feature of this technique is the possibility to produce complicated structures due to a mould which is realized through a model. The wax is poured into the mould in order to produce the wax model. After that, it is coated with refractory ceramic. Subsequently, metal is melted and poured within the model and finally the wax is dissolved. In order to obtain a trabecular structure (*Figure 20*), it is possible to use a wax model realized with trabecular features [34].

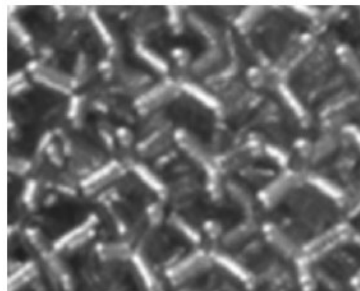


**Figure 20** – Trabecular structure obtained through low – wax casting [34]

### 2.4.2 AM procedures

In order to allow a better performance of the implanted prosthesis - better restoration of bone deficiencies, a relief of the risk of infection a long term survival of the implant - has been developed a production process called 3D printing [43]. This manufacturing technique gives the opportunity to create complex morphology with a correspondence between the characteristics of the bone which is necessary to restore and the implant, by overcoming the limitations encountered with the bio – inert materials (Ti and CoCr alloys).

As stated above, 3D printing is a layer-by-layer technique which ensures not only a monitored size and distribution of the pores, allowing a framework which replicates the matrix of the lost bone and hence a better osteointegration, but also mitigates the risk of the shear stress effect.

By starting from computer tomography (CT) scans of the patient, data are collected in order to produce a 3D model which replicates the real anatomical morphology. Then, the CAD model is converted in data which can be read by rapid prototyping machines. Through this procedure, it is possible to provide a detailed check with regard to interconnected porosity necessary for bone regeneration and feeding fundamental for the regrowth of the new tissue [45].

One of the most critical aspect of this technology is the capability to reproduce a new vascular grid, means of channelling nutrients to the tissue: it is crucial for the success of the tissue regeneration. Nowadays, the realization of this network is a challenge for 3D printing because it must not undermine the vascular system that already exists. Compared to the traditional manufacturing processes, 3D printing is able to create routes within the structure. This process is more expensive than conventional methods because it requires the use of special tools and the gathering of data necessary for the replication of the model, but on the other hand it has been noticed an enhancement of the surgery result, avoiding the risk of a secondary surgical practise [44].

Other AM technologies are represented by Selective Laser Melting (SLM) and Electron Beam Melting (EBM), based on the use of a powder bed. They are able to produce a very porous structure, built in the following way:

- A powder layer is deposited on a solid platform;
- A fiber laser or an electron beam is used to melt the powder where is necessary, following what is showed in the CAD file;
- In order to allow the compaction between the layers, it is carried out a partial recast of the previous layer;
- The platform goes down and another layer of powder is deposited.

The process continues until the whole product is replicated. The EBM process is conducted in a controlled atmosphere in order to avoid the dispersion of the electron beam [33].



- The anode is necessary to close the electric circuit;
- An aqueous solution which works as an electrolyte.

Through the passage of the electric current, the oxidation reaction occurs at the anode, while the reduction reaction happens at cathode: this is responsible for the electrodeposition process [48].

- *Biomimetic*: this process consists of two stages with the aim of making the biomaterial bioactive, necessary property for the realization of a strong interface bonding. The first one involves a superficial preparation of the orthopaedic implant surface in order to activate the external surface of the biomaterial with the purpose of forming apatite, subsequently [49]. The second phase requires the use of a solution which is similar to the human blood plasma, called simulated body fluid (SBF), in which the biomaterial is plunged: in this way, the apatite coating occurs. This technique gives the opportunity of producing a bone like hydroxyapatite layer [20].
- *Sol gel method*: the deposition of the hydroxyapatite coating is obtained at low temperature in two different ways. It is possible to use organic or inorganic precursors in a colloidal solution, as reactants. Several studies were conducted analysing the effects of these precursors in order to choose the most effective coating. The hydroxyapatite layer, obtained by using inorganic precursors, showed a density which was lower than that realized adopting an organic solution, while both layers presented uniform composition [20].
- *Titanium dioxide*: titanium has the capability of reacting spontaneously with the surrounding atmosphere, forming a layer of titanium dioxide which protects the metallic substrate from corrosion. It also possesses some properties which allow it to interact with the tissue, forming a very strong bonding. Different treatments are applied in order to improve this property for the orthopaedic applications [50]. The deposition of this coating occurs on porous biomaterial through electrophoretic sol-gel coating method or anodization. This last method involves the use of an electrolyte: it is important to keep under control several parameters, for instance concentration, temperature, etc. Several studies were conducted in order to prove the effectiveness of this coating: TiO<sub>2</sub> ensures a better fixation. According to literature, Lee et al. [20] manufactured porous titanium

by following a new manufacturing process which involved the use of a sacrificial polymeric sponge which was extended and then treated providing heat. After that, the porous titanium structure underwent the anodization process with the purpose of coating the metallic substrate with a layer of TiO<sub>2</sub>.

Furthermore, TiO<sub>2</sub> coatings provide a better performance of biomaterials in orthopaedic applications due to their capability of promoting cellular regeneration. In addition to their bio – activity, they are also able to avoid the diffusion of bacteria. These methodologies, applied to improve the behaviour of biomaterials, need to be designed thoroughly. Some researches carried out on biomaterials underline that the understanding of connections existing between different bioactive materials is crucial for the production of orthopaedic implants [50].

## *2.5 Advanced porous biomaterials*

### *2.5.1 Limitations of Traditional Porous Metals*

Some solid metallic biomaterials (stainless steel, titanium and CoCr alloys) are applied in a lot of load-bearing surgical applications due to their capability of resisting to high tensile loads, to fatigue load cycles and to corrosion and being biocompatible. Despite these undeniable advantages, they are bio-inert and they are unable to establish strong bonds at the interface implant-bone. Consequently, this unsuitable fixation could cause aseptic loosening, osteolysis and other pathologies, which would result in the failure of the prosthesis [30]. Furthermore, the success of the implant could be compromise by the presence of Ti and CoCr alloys due to the inflammatory reaction and the risk of infections [44]

In order to overcome these limitations, these metallic biomaterials can be subjected to the chemical superficial treatments (previously discussed): in this way, it is possible to allow bioactivity through the deposition of a porous coating. This modification leads to a strong implant-bone anchorage, a higher lifespan and a better osteointegration [20,51]

Although the positive outcomes achieved through the superficial modifications, traditional porous biomaterials - for instance CoCr sintered beads, fiber metal and plasma spray Ti - continue to show different limits:

- They can be used only as porous coatings onto solid metals and not as bone graft substitute or bone augmentation because they do not have the adequate mechanical properties.
- Limitations in terms of size and geometry.
- Inability of responding to the modification of the surrounding environment.
- Weak attachment of the implant to the host bone.
- It is necessary to improve the level of porosity with the purpose of making the bone-implant contact still more effective and more rapid.
- Low coefficient of friction.
- High elastic modulus which causes the stress shielding phenomenon [18,51].

In the following *Table 2*, mechanical properties of cortical and spongy bone, and some biomaterials adopted for orthopaedic implant are summarised in order to underline the mismatch existing between the elastic modulus of the bone and a lot of traditional biomaterials [20].

Material	Elastic modulus GPa	Tensile strength ( $10^{-3}$ ) GPa
Cortical bone	20	150
Cancellous bone	3	5
Stainless steel	200	700
Co-Cr-Mo alloys	230	500
Titanium	110	500
Ti-6Al-4V	110	950
Hydroxyapatite ceramics	20	100*
Glass ceramics	30	200*
PMMA	3	80

**Table 2** - Mechanical properties of cortical and cancellous bone and some orthopaedic biomaterials [20]

Some porous biomaterials available for orthopaedic applications are described in the following *Table 3* [50,51]

Name	Description	Processing	Applications	Limitations
Actipore™	Fully porous NiTi alloy. Porosity ~ 65% Pore Size ~ 215 µm	Not reported	Spine and shoulder surgeries.	Low mechanical properties and limited part geometries.
Regenerex™	Fully porous Ti. Porosity ~ 67% Pore Size ~ 300 µm Modulus ~ 1.6 GPa	Porous plasma processing	Hip and shoulder surgeries.	Low strength, limited sizes and only acetabular components and augments are available
Titanium™	Porous Ti coating. Porosity ~ 60% Pore Size ~ 616 µm Modulus ~ 106–115 GPa	Low temperature arc vapor deposition of polyurethane foam shell	Hip surgeries	It is not manufactured as a stand-alone structure, and it is only available in acetabular components. The manufacture process is also limited at this time to large sized components
CSTi™	Porous Ti coating. Porosity ~ 50–60% Pore size ~ 400–600 µm, Modulus: 106–115 GPa.	Powder sintering with pressure.	Hip and knee surgeries.	Simple and limited part geometries, low fatigue resistance.
Stktite™	Porous Ti coating. Porosity ~ 60% Pore Size ~ 500 µm Modulus ~ 100–110 GPa	Porous plasma processing	Hip and knee surgeries.	Simple and limited part geometries, low fatigue resistance.
Trabecular Metal™	Open cell fully porous Ta. Porosity ~ 75–85% Pore Size ~ 550 µm Modulus ~ 2.5–3.9 GPa	Chemical vapor deposition/infiltration of carbon skeleton.	Hip and knee surgeries.	Relatively high cost of manufacture, inability to produce a modular all tantalum implant
CoCr Beads	Porous CoCrMo coating. Porosity ~ 30–50% Pore Size ~ 100–400 µm Modulus ~ 210 GPa	Powder sintering	Hip surgeries.	Simple and limited part geometries, low fatigue resistance.
Fiber Metal	Porous Ti coating. Porosity ~ 40–50% Pore Size ~ 100–400 µm Modulus ~ 106–115 GPa	Sintering	Hip surgeries.	Simple and limited part geometries, low fatigue resistance.

**Table 3** - Porous materials for orthopaedic applications [51].

Therefore, in order to allow long lifespan of the implanted prostheses, the idea is to exploit the advantages (high mechanical strength) and overcome drawbacks of traditional metallic biomaterials, by improving their morphology. It is necessary a high interconnected open cell porous structure to stimulate cellular regrowth allowing the supply of nutrients [20]. In order to manufacture this trabecular framework, at first a sacrificial model in polyurethane foam is realized and then its surface is coated by titanium or tantalum. The remarkable advantage is that in this way there aren't limits on geometries and dimensions: this is fundamental in the orthopaedic field. These structures, characterized by a high level of porosity (60-80%), ensure a high coefficient of friction, a stronger interlocking between the new prosthesis and the surrounding bone, a higher resistance to the bacteria, a better osteointegration and a lower

Young's modulus which should be similar to that of cancellous bone as much as possible [18,20].

As described previously, a key role is played by additive manufacturing technologies because they allow to fabricate complex structures characterized by an open porosity, fundamental for ensuring: a low Young's modulus in order to reduce the risk of stress shielding effect, the necessary mechanical resistance, a higher coefficient of friction, important for a stronger attachment and a longer lifespan.

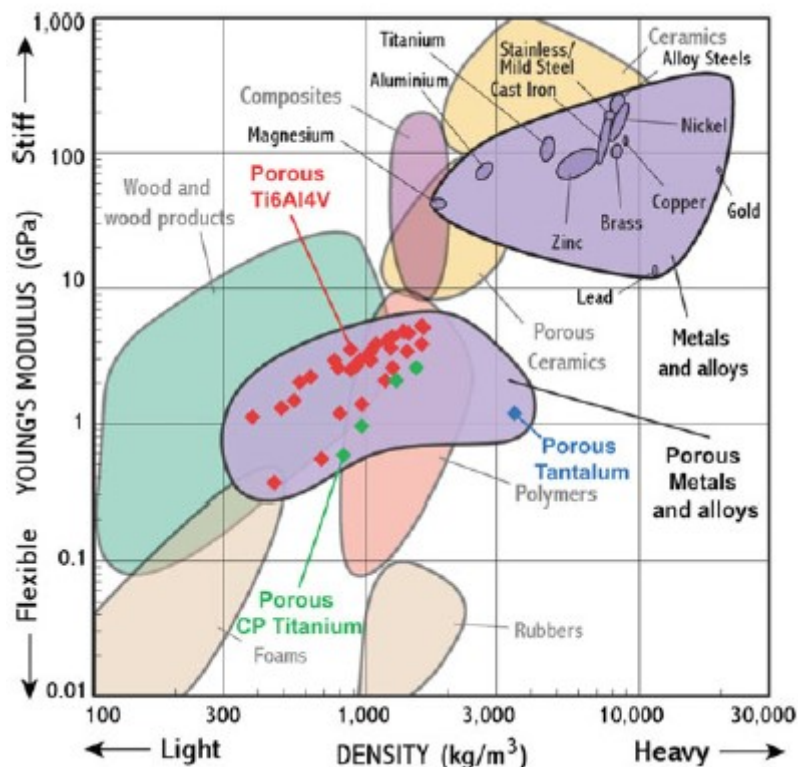


Figure 22 – Young's modulus of new porous biomaterials [33]

Looking at the *Figure 22*, we can see that the stiffness ensuring by these new porous metals is lower than that of solid metals of around an order of magnitude.

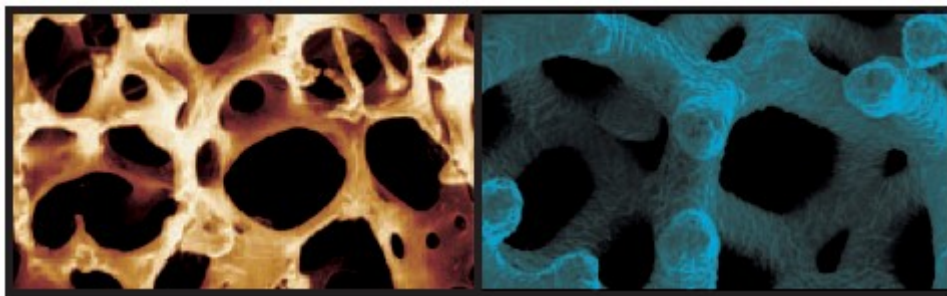
For the reasons stated above, different new porous metals have been developed for the realization of orthopaedic implants. Some of them are mentioned in the *Table 3* and they are described in detail in the following paragraphs.

### 2.5.2 Trabecular Metal (Zimmer Biomet)

Tantalum represents a biomaterial of great interest for surgical applications due to its capability of resisting to corrosion because it is able to manufacture a protective layer  $Ta_2O_5$  itself [44]. Furthermore, it allows a strong contact at the interface bone-implant, ensuring a better bone

ingrowth and fixation which could improve the survival of the implant [52]. In addition, it could be used not only as a porous coating but also as standalone material, especially for joint replacement. A harmful aspect for the orthopaedic applications is its high Young's modulus (186 GPa) which will cause the stress shielding effect because its mismatch with that of cortical (12-18 GPa) and spongy (0.1-0.5 GPa) bone [44].

**Zimmer Biomet** has manufactured a porous biomaterial, known as **Trabecular Metal**™ which is tantalum characterized by a high open porosity. The process adopted to produce this porous material consists in the manufacturing of a reticular polymer foam - which shows a structure with internal interconnected pores – and then, CP tantalum is poured onto the surface of this polymer scaffold via the process of chemical vapour deposition [18, 19]. The advantage is that this material could be used to produce several kinds of knee prosthesis in terms of shape and size. Furthermore, its structure is close to that of cancellous bone as it is possible to notice in the *Figure 23* [53].



(a)

(b)

**Figure 23** – (a) Cancellous bone – (b) Trabecular Metal™ [53]

Trabecular Metal properties could be summarized as follows:

- ✓ The modulus of elasticity (3.1 GPa) is similar to that of cancellous bone but lower than that of cortical bone, as shown in *Graph 1*. The elasticity is lower than that of titanium, and CoCr alloys. This causes a decrease of the risk of the stress shielding effect. It could also be seen a comparison between different alloys [53]
- ✓ Interconnected porosity between 75% and 85%: it allows a better ongrowth (strong bonds at implant-bone interface) and ingrowth (*Figure 24*) [52,53].
- ✓ Fibrous tissue ingrowth: Hacking et al [54] discovered that porous tantalum ensures a high tissue ingrowth not only at the interface but also within the prosthesis, with a consequent stronger fixation.

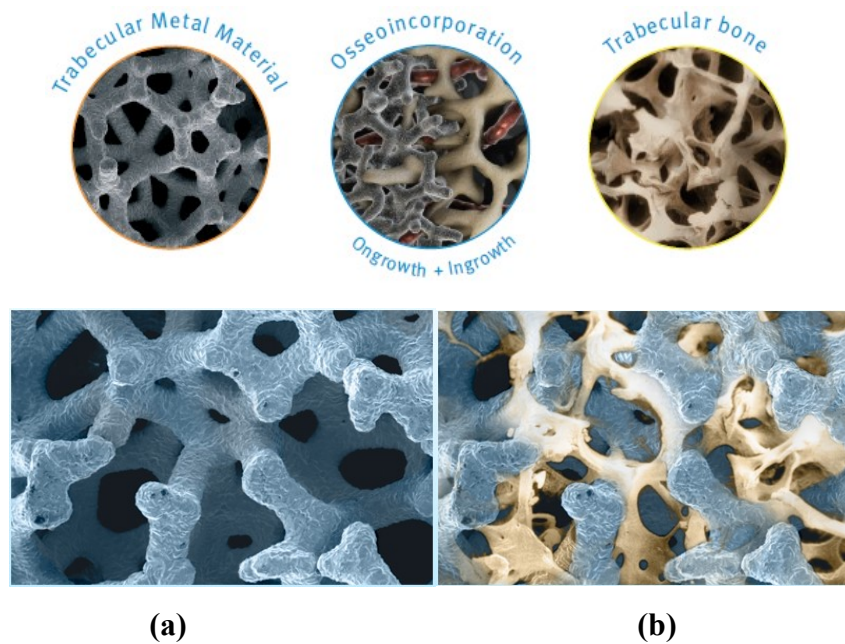


**Figure 24** – Structural features of Trabecular Metal compared to that of cancellous bone: (a) morphology of Trabecular Metal – (b) osteintegration [53].

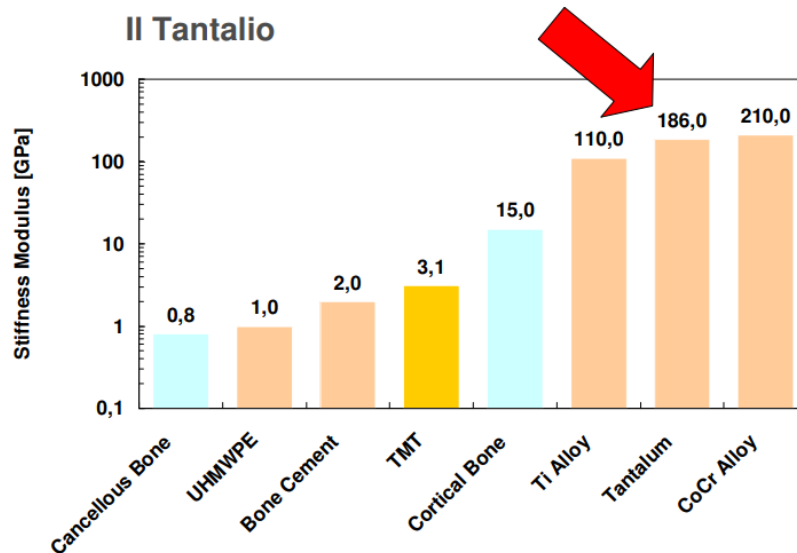
- ✓ High coefficient of friction around 0.88 which ensures a stability that is higher than that of sintered coatings (0.60) and a better longevity of the implant, and also a higher endurance to physiologic loads [18,52].
- ✓ High mechanical strength: if we look at compressive strength, we can see that it is around 50 – 80 MPa midway between that of cortical (130-150 MPa) and trabecular bone (10-50 MPa) [53]. A comparison between the mechanical properties of different biomaterials available in orthopaedic field is shown in *Table 4* [52].

Mechanical Property	Tantalum	Titanium	Cobalt Chromium
Modulus of elasticity (GPa)	2.5-3.9	106-115	210
Ultimate strength (MPa)	50-110	780-1050	430-1028
Yield strength (MPa)	35-51	860	827
Compressive strength (MPa)	50-70	N/A	N/A
Tensile strength (MPa)	63	N/A	N/A
Bending strength (MPa)	110	N/A	N/A

Abbreviation: N/A = not applicable

**Table 4** – Mechanical properties of different biomaterials available in orthopaedic field [52]

- ✓ A good corrosion resistance: tantalum differs from other biomaterials due to its passivation – it is able to protect itself from corrosion, realizing an inert protective layer  $Ta_2O_5$  [52].
- ✓ A high level of biocompatibility and bioactivity: ability to establish strong bonds between implant and bone, allowing a strong attachment via the formation of a layer of apatite which mimics the composition of the mineral bone.



**Graph 1** – Young’s modulus of different biomaterials available in orthopaedic field [53]

### Applications of Trabecular Metal™

Several causes trigger the failure of primary total knee arthroplasty, such as osteolysis, loosening caused by the lack of bone ingrowth of the tibial component. Furthermore, for the attachment of the implant, some screws were necessary, so the holes realized for the implantation induced polyethylene wear and the risk of corrosion.

In order to overcome the encountered limits during the implantation of the prosthesis in primary TKA, Zimmer Biomet develops a *Trabecular Metal monoblock tibial component* (Figure 26) which ensures:

- ✓ a great level of stability.
- ✓ a strong attachment.
- ✓ a proper alignment.
- ✓ low elastic modulus and high compressive strength reduce the risk of the stress shielding effect due to a better transfer of the loads to the proximal tibia.
- ✓ Micromotion which occur at the interface bone – implant are reduced: this allows a decrease of the backside wear of the polyethylene.
- ✓ Tibial pegs, made of Trabecular Metal, improve not only the initial stability, a stronger fixation but also the osteointegration (figure 25) [53].



**Figure 25** – Zimmer Biomet Tibial pegs structures [53]

These positive outcomes are due to a thorough designing in order to allow a better stress transmission: polyethylene powder resin is pressed into TM tibial tray until a depth of 2 mm [52,53]



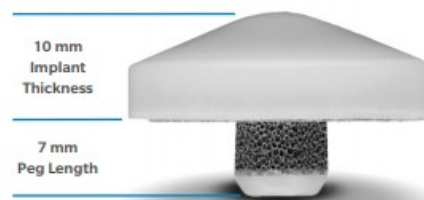
**Figure 26** - Zimmer Biomet Trabecular Metal Tibial Component [53]

A drawback is represented by the impossibility of using additional screws, if it is necessary for an inappropriate initial stability or for a revision surgery [52,53]

Moreover, Zimmer Biomet develops *Trabecular Metal Monoblock Patella* (Figure 27): a controlled process allows a close fixation of the polyethylene into the reticular structure of the Trabecular metal with a penetration of approximately 1.5 mm, avoiding the risk of any possible micromotions and separation between the implant and the metal [53].



**(a)**



**(b)**

**Figure 27** – (a) Compression molding process – (b) Trabecular Metal Patellar component [53]

Other applications involve the secondary surgery which is necessary to restore bone defects, or improper alignment of the joint line. Zimmer Biomet provides *Trabecular Metal tibial, femoral and patella augments* in order to repair large bone deficiencies, instead of bone grafts or those produced in titanium which need to be fixed with cement. Furthermore, tantalum augments can be fixed cement or not, or with screws. There are also manufactured Trabecular Metal tibial cones of different shape and size which are used to treat large cavitory injuries and which reveal a long term endurance. At first, the lesion is adapted in terms of shape and size to those of the TM cone and then the cone is pressed into the defect in order to fill the bone deficiency and allow a better stability of the prosthesis. They reproduce the bone structure and its elasticity, by guaranteeing a rapid bone integration [53].

In addition, Zimmer Biomet offers alternative solutions for treating total hip arthroplasty:

- TM acetabular cups improve the bone reconstruction and they offer a higher support.
- TM acetabular augments are another option to bone allografts, ensuring a closer direct contact bone – prosthesis.

Zimmer Biomet also produces shoulder, dental and spinal solutions, which ensure a better stability, attachment and a more effective restoration of bone injuries, which are represented in the following *Figure 28 – 29* [53]



**Figure 28** – Zimmer Biomet Trabecular Metal Tibial and Femoral Cones [53]

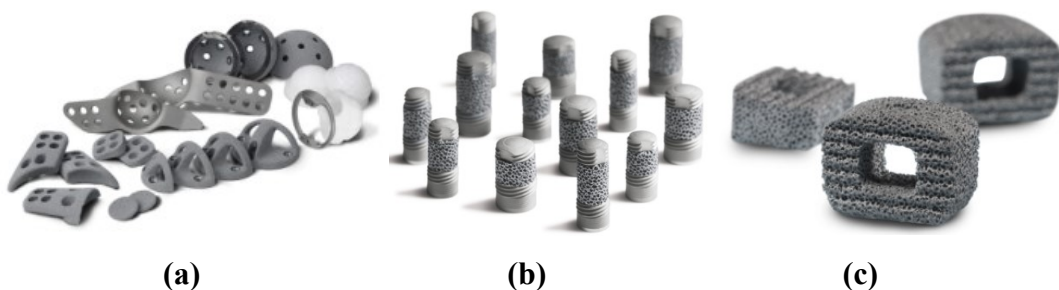


**Figure 29** – Zimmer Biomet Trabecular Metal (a) Revision solutions – (b) dental implants – (c) spine devices [53]

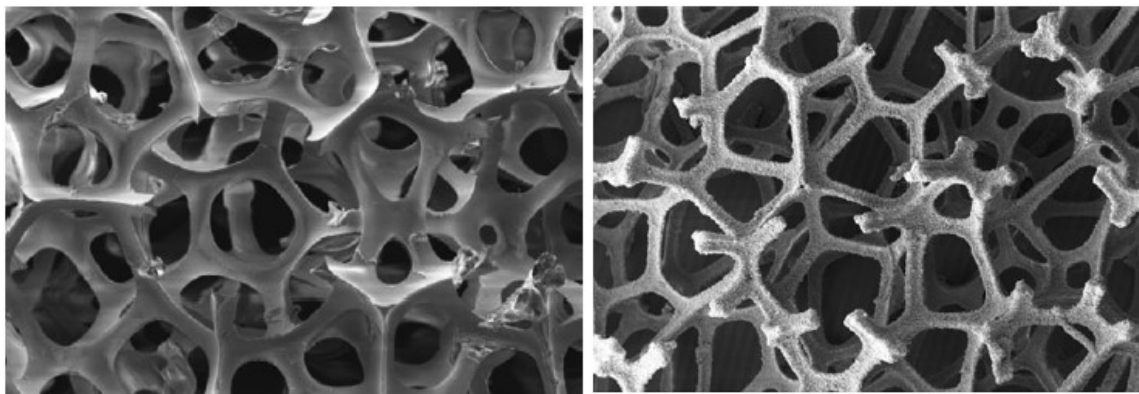
### 2.5.3 Tritanium (Stryker)

Several studies, conducted using animal models in order to analyse thoroughly the properties and the evolution of the interfacial contact bone – titanium implant, showed not only an intimate contact between the prosthesis and the surrounding bone but also a good bone ingrowth. A bony regeneration occurs at the interface bone – implant because of natural response of the body to the presence of titanium. In fact, titanium alloys promote the growth of osteoblast cells which are responsible of the tissue formation, and this phenomenon is closely related to the surface roughness: the more it is high, the more the bone formation is encouraged.

Therefore, the bone ingrowth capability of titanium alloys, which are able to resist to physiological loads, is improved by developing a porous metal which similar to bone in terms of structure and mechanical properties: Tritanium. This is the aim of the studies carried out by Striker: a new technology is developed in order to control the pore size of the structure and create a surrounding environment which improves bone regeneration [55].

The process adopted to manufacture Tritanium consists of several steps:

- A sacrificial scaffold is produced by modelling polyurethane foam to a structure characterized by a reticular and open porosity as shown in the *Figure 30*.



(a)

(b)

**Figure 30** – (a) Polyurethane foam – (b) Sintered CP Titanium [19]

- The commercially pure titanium powder is poured on the fabricated foam in order to create a fine coating through a low temperature arc vapour deposition.
- All the structure is located onto the dense titanium alloy and subjected to a sintering process in order to remove only the polyurethane.
- In this way, it is possible to obtain a porous material characterized by a substrate of Ti alloy, covered by a sintered commercially pure Ti as shown in the *Figure 30*.

Subsequently, after the addition of a polymeric ligand, all the assembly is subjected to a further sintering in order to ensure a stronger fixation of the powder. This phase is repeated until the achievement of the desired thickness, which is related to the attainment of the wished level of strength [19]. In this way, it is possible to control the size of the pores as it is possible to see in the following *Figure 31*.

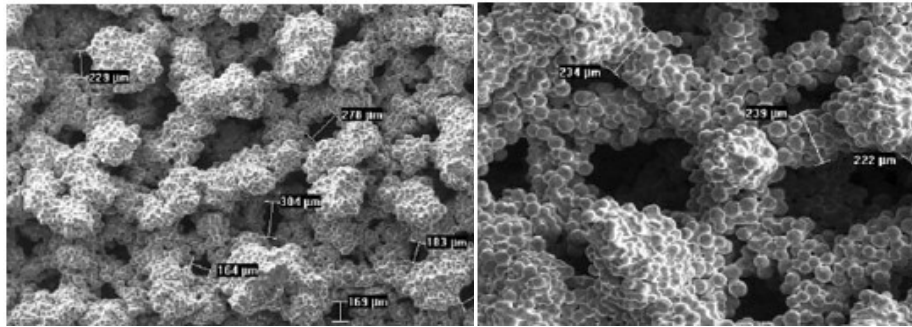


**Figure 31** – Different sizes of the pores of the titanium structure [19]

Stryker develops an alternative process: a sacrificial foam, a polymeric ligand and CP Ti powder are mixed all together, poured in a cast and pressed under low temperature, by obtaining the “green part”. Then, it is subjected to a sinter process in order to ensure compaction of the powder [19].

One of the most important property is the binding existing at the interface bone – implant, crucial for the proper transfer of the loads between the prosthesis and the host bone. It is fundamental that the porous implant remains firmly attached to the underlying bone [19].

Looking at the material properties, they can be summarized as follows:

- Initial stability is allowed by a very high coefficient of friction, if compared to that of sintered CoCr and titanium alloys, and Trabecular Metal (*Figure 32*)

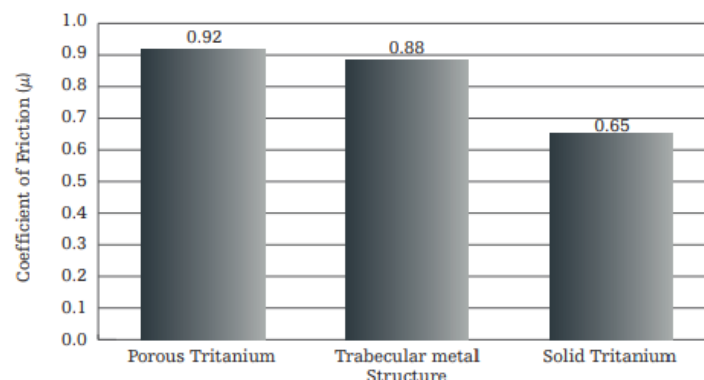


**Figure 32** – Comparison between different biomaterials looking at the coefficient of friction [55]

- In terms of elasticity, it ensures a Young’s modulus (6.2 GPa) which falls between that of cancellous and cortical bone (*Figure 33*)

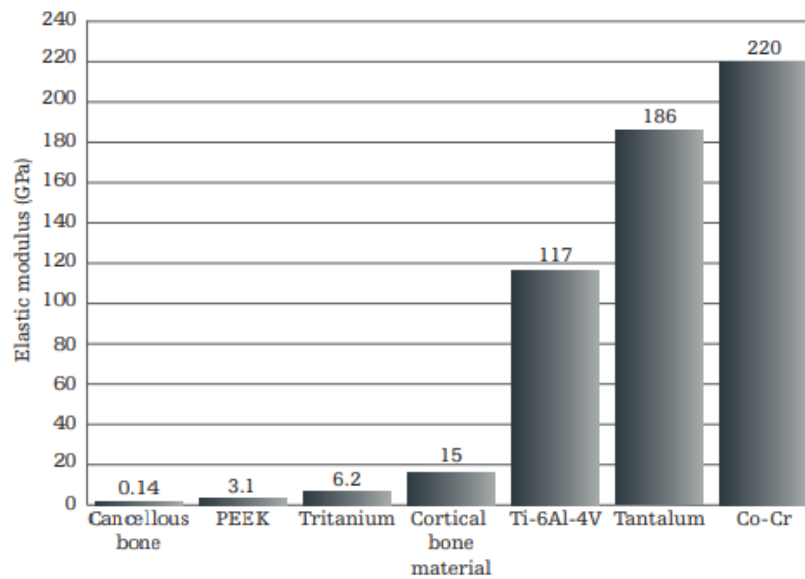


**Figure 33** - Comparison between different biomaterials looking at the elasticity [55]

Stryker's Tritanium In-Growth Technology has enhanced the biological attachment and tissue regeneration, producing a particular porous framework which is able to stimulate osteoblast cell proliferation (cells responsible of the tissue formation). So, Stryker tries to replicate the structure of the spongy bone as much as possible, by adopting additive manufacturing techniques. This technology manufactures controlled porous morphologies which resemble to that of cancellous bone with the purpose of maximising bone restoration.

- Mean pore size range: 400 – 500  $\mu\text{m}$  (compared to that of spongy bone 1 mm) which allows vascularization, fundamental for the transport of the nutrients to the tissue and the oxygen.
- Interconnected porosity range: 55 – 65% which improves tissue regeneration [55].

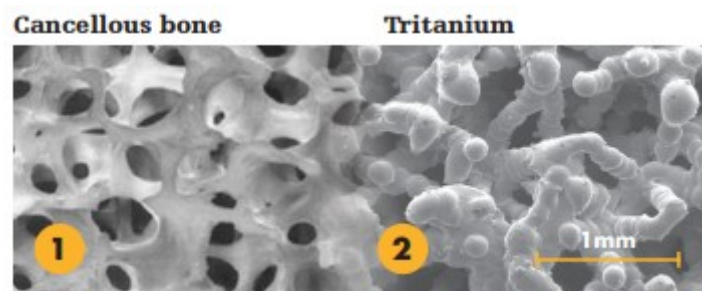


**Figure 34** – (1) Cancellous bone compared to (2) Tritanium structure [55].

- Tritanium material is also able to favour the capillarity necessary for the transport of the nutrients, which play a central role in the infiltration, attachment and proliferation of the osteoblasts through the pores of the Tritanium structure [55].

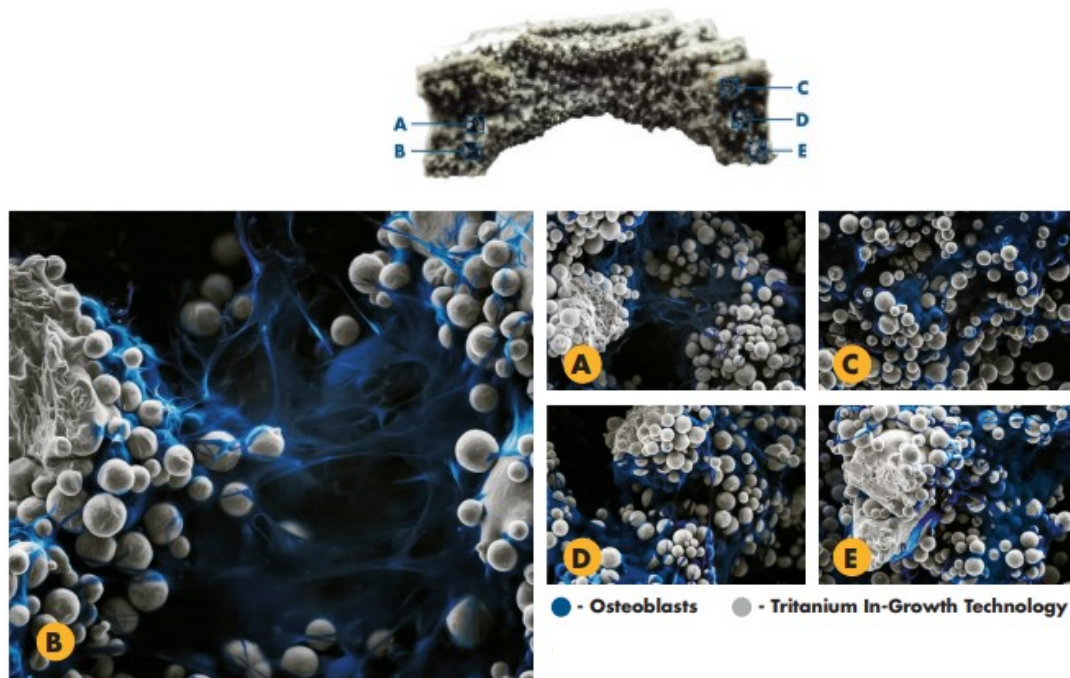


**Figure 35** – Tritanium In-Growth Technology: beneficial environment [55]

#### 2.5.4 Regenerex (Zimmer Biomet)

Zimmer Biomet' strategy aims to develop innovative solutions in order to create a correspondence between the patients' needs and the technical assistance for the surgeons. Each solution has to comply with some requirements:

- ✓ Surgical practice must be invasive as little as possible.
- ✓ Use of advanced biomaterials.
- ✓ Patients' satisfaction [53]

Regenerex is characterized by an advanced porous structure of the titanium alloys which can be used not only as a coating but also as an independent bone substitute. It is produced by using the same powder titanium alloy adopted in the porous plasma spray technology, developed by Biomet: it consists of the powder's deposition on a sacrificial scaffold at a low temperature. In this way, it is possible to ensure the 90% of the mechanical resistance. Particles of different size impact the surface of the substrate, by ensuring a rough surface and a larger contact surface. These irregularities allow a strong stability and fixation between the host bone and the implant. Furthermore, the use of different sizes for the particles produces a structure characterized by smaller pores which are fundamental for the primary stability because they allow a faster

refilling of the bone defects, while the bigger pores ensure a long term attachment. Bone fixation plays a key role the transmission of the loads [53].

Regenerex material ensures the following properties:

- Interconnected porosity of about 67%.
- Average pore size: 300  $\mu\text{m}$  which allows the formation of blood vessels.

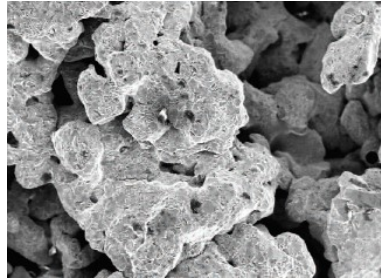


Figure 36 – Regenerex porous structure [53]

- Rapid bone ingrowth: canine studies demonstrate that Regenerex prostheses already show bone integration and vascularization after two weeks from the implantation.

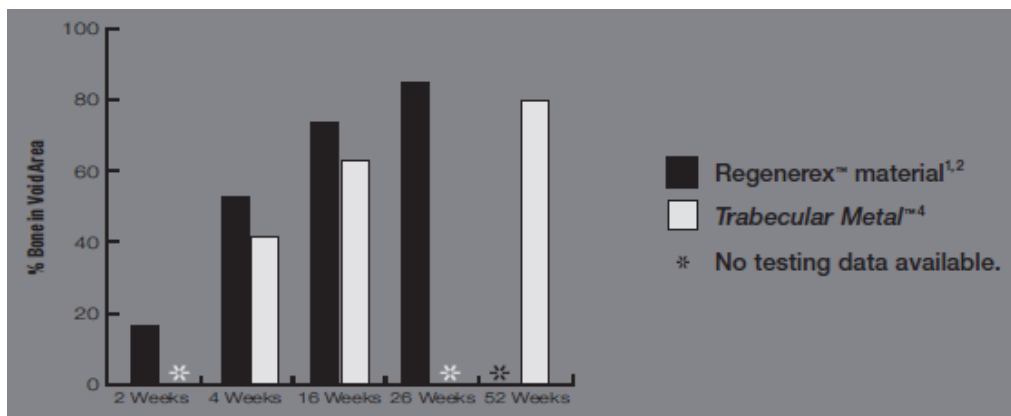


Figure 37 – Regenerex bone ingrowth [53]

- Roughness is 16% higher than that of Trabecular Metal.

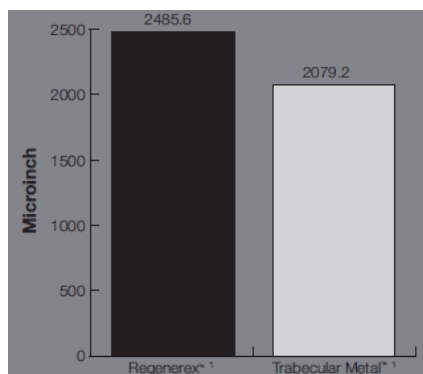


Figure 38 – Regenerex roughness [53]

- In presence of compressive loads, Regenerex structure shows a resistant capability that is 300% higher than that of Trabecular Metal: the elastic modulus is similar to that of cancellous bone: 1.9 GPa.

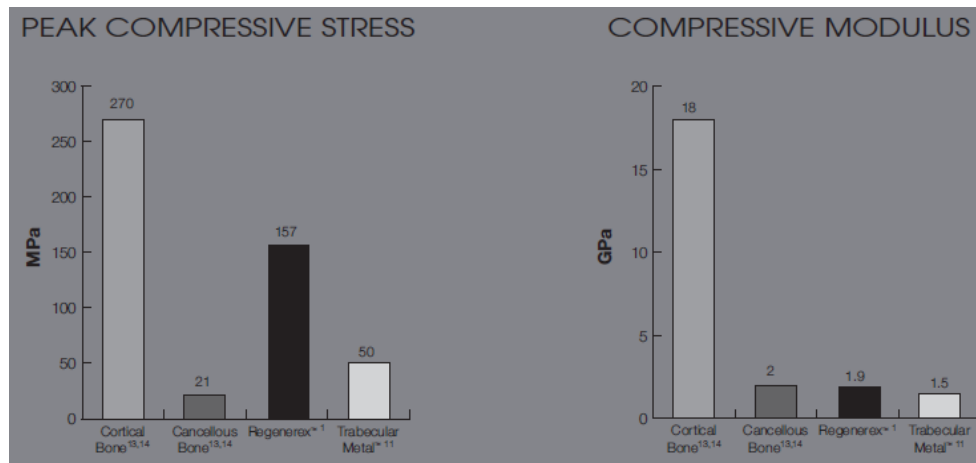


Figure 39 – Regenerex mechanical properties [53]

This advanced biomaterial can be used as bone substitute as acetabular augments in particular surgical applications, or as a modular tibial tray when dense titanium substrate is coated with Regenerex powder. This biomaterial could be used in knee, shoulder and hip arthroplasty.



Figure 40 – Regenerex (a) Tibial Tray – (b) Acetabular cup [53]

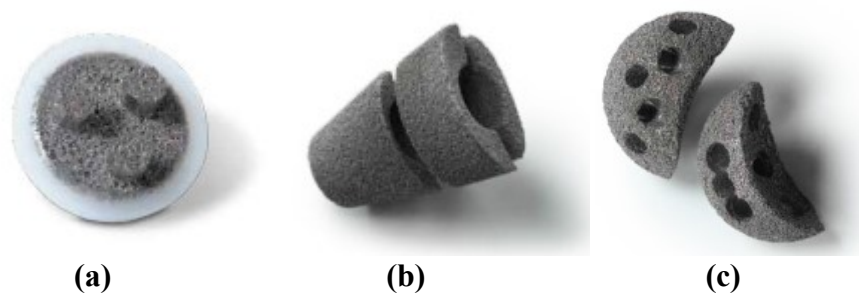


Figure 41 – Regenerex (a) Patella – (b) Cone Augments – (c) Acetabular Augments [53]

### 2.5.5 Gription (Depuy)

Other advanced biomaterial is Gription which is fabricated by Depuy, used as a high porous coating for treating different bone deficiencies, in several surgical applications: total hip and knee arthroplasty. Depuy's strategy combines three goals:

- ✓ Advanced biomaterial.
- ✓ Advanced instrumentation.
- ✓ Advanced fixation [56].

The aim is to improve bone fixation, necessary especially for resisting under high compressive loads: an increase of the contact surface roughness enhances the coefficient of friction and so implant attachment to the bone because it promotes osteoblasts proliferation and attachment [18].

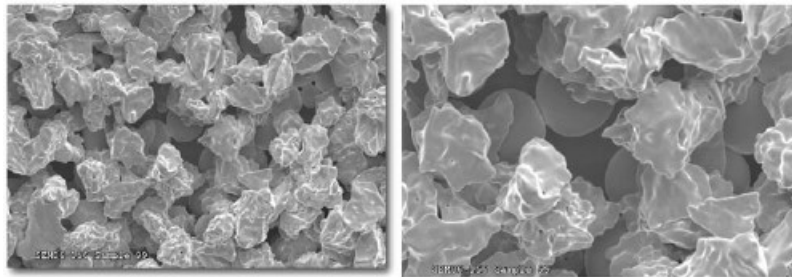


Figure 42 – Gription porous structure [18]

Gription's mechanical properties are summarized in the following *Figure 43*.

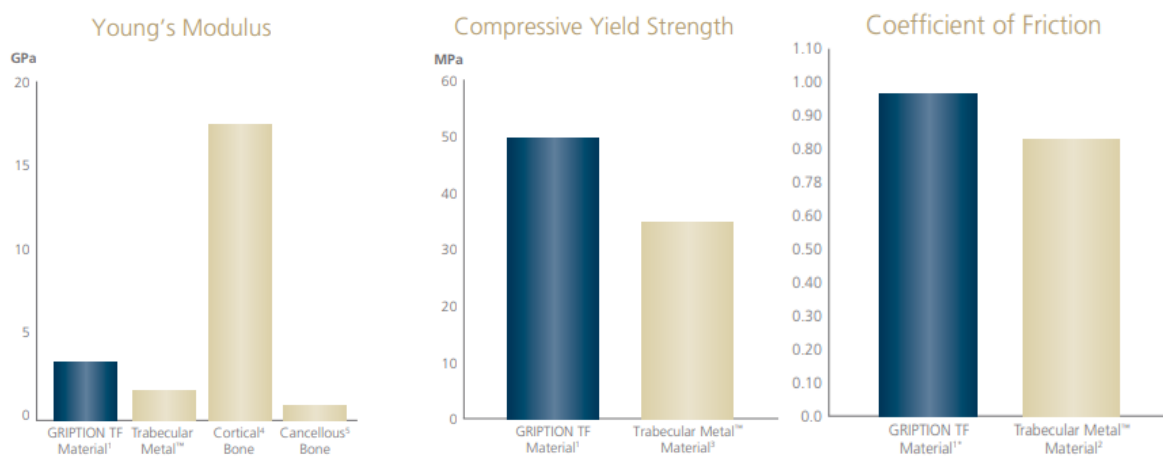


Figure 43 – Gription's mechanical properties [56]

Gription biomaterial is adopted to fabricate: acetabular augments which are necessary to restore large bone defects, buttresses, adopted to provide support for shells and screws for a stronger attachment to the host bone in order to avoid a premature implant loosening [56].



**Figure 44** – Gription' Acetabular augments, buttresses [56].

# Chapter 3

## Finite Element Modelling

### *3.1 Introduction*

Revision total knee arthroplasty (TKA) is advised when aseptic loosening, infection, osteolysis occurs or when the range of knee motion is affected [58]. The extent of bone injuries determines which prosthesis should be implanted. Currently, a variety of solutions are commercially available:

- Small bony deficiencies can be addressed with cement or allografts.
- Broader defects can be dealt with augments, metal wedges, bone grafts or personalized prosthesis.
- Stems and screws can be used to provide more stability [58,59].

With the purpose of achieving strong implant stability, modular augments and wedge are recommended when there is a lack of bone support which is more than 40% [58]. In fact, according to the Anderson Orthopaedic Research Institute (AORI) [60], femoral and tibial Type II and Type III bone deficiencies - which involve a major bone portion - would be more appropriately dealt with highly porous metal augments. Femoral defects occur on posterior and distal surfaces and they could be addressed with the attachment of metal augments. On the other hand, tibial bone deficiencies take place on the proximal side of the tibia and they are treated with metal wedge or rectangular block [58].

Nowadays, different shapes (rectangular or wedge-shaped) and sizes (several thicknesses), whose selection is related to the extent of bone defect are commercially available, while there are not guidelines for the selection of the porous material best fitting specific clinical requirements [59].

As detailed in literature, a variety of clinical research are carried out in order to show experimental evidence of the benefits obtained by treating larger bone defects with metal augments. For instance, Lee *et al.* [61] addressed proximal tibial defects  $\geq 4\text{mm}$  with rectangular metal augments in 43 patients and he monitored them for the following five years: clinical results revealed that this surgical practise is fitting for peripheral tibial defects due to

the lack of failures. Sachi-yuki Tsukada, Motohiro Wakui and Munenori Matsueda *et al.* [62] compared the clinical results of 33 knees subjected to a primary TKA by implanting rectangular augments for treating tibial bone defects to a control group characterized by 132 varus knees without bone deficiencies. These patients were monitored for a postoperative period of 3/6 years: metal block augmented knees revealed clinical outcomes which were comparable to those of the control group. Furthermore, other research demonstrated that rectangular augments are able to ensure a torsional load transmission, tibial tray-bone, which is more suitable than that of the wedge-shaped augments. These kind of inserts allows a reduction of shear stress [62].

The great challenge for revision total knee arthroplasty (TKA) is to provide adequate pain relief for the patient and ensure greater knee stability, proper alignment and a longer lifespan of the implanted prosthesis [58].

Nowadays, the use of numerical analysis, which is increasing due to the opportunity of having a simpler access to the computational data and the refinement of the calculation algorithms, encourages orthopaedic research in order to develop new strategies for treating knee pathologies much more efficiently. Over the years, these numerical techniques have undergone significant change: in the past, it was possible to carry out simplified bi-dimensional models which allowed to analyse only a single structure, while looking at the present, the implementation of detailed three-dimensional numerical models enable to reproduce and investigate the behaviour of tissues, biological multi-structures (bones, cartilages, ligaments) and multi-joint systems (knee, shoulder, hip) [63]. In particular, if we look at knee joint, this numerical analysis plays a crucial role in the design and validation of a prosthesis but it is very difficult to replicate the real behaviour of the joint due to its complexity. It involves a wide range of motions: primary movements (flexion and extension, rotation, anterior and posterior translation, varus and valgus movements) and passive motions (the ligaments and the articular surfaces interact with each other) [57].

Among several modelling approaches, finite element analysis (FEA) allows to deal with a variety of biomechanical problems which could compromise knee functions and the longevity of the implanted prosthesis. Therefore, FEA gives the possibility to analyse bone and implant stress distribution and interactions under different conditions, by comparing these results to those of a physiological knee. Finite element modelling represents a powerful tool through which is possible to develop clinical strategies and enhance the success of TKA, by ensuring a long-term stability and fixation of the implant [63]. Furthermore, in order to achieve all these goals, it is necessary a close cooperation between the clinicians and the engineers: each of them

has to be able to understand the specific language of the other. This communication could be summarized in the following *Figure 45* [65].

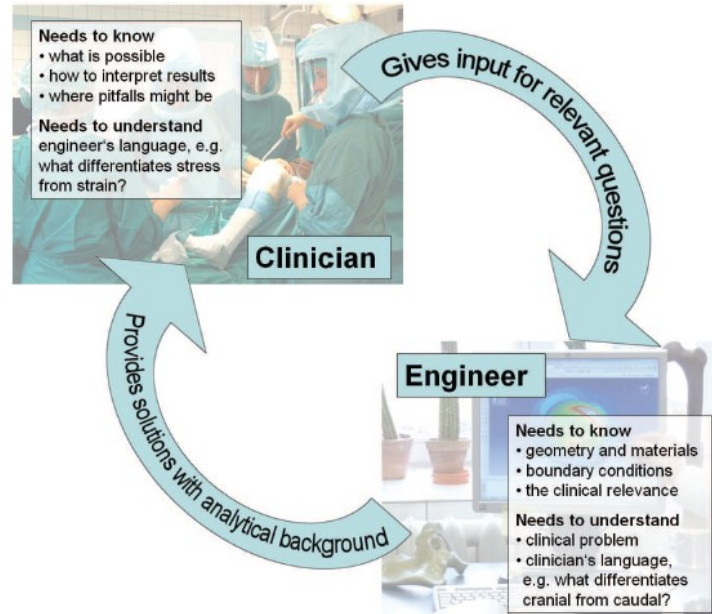


**Figure 45** – Interconnections between clinicians and engineers [65].

For the reasons stated above, this study will focus on the development of a 3D model of the knee joint where Type II and Type III tibial and femoral bone defects are addressed with porous metal augments because these biomaterials (described in the previous chapter) ensure a faster bone regeneration and they also need a little bony resection. Therefore, the aim of this work is to carry out a finite element analysis in order to investigate the change in tibial and femoral bone stress response to the placement of an augment. Bone stress distribution is investigated by considering several characteristics of the inserted augment in terms of different solid and porous biomaterials, thicknesses and positions.

### 3.2 Knee joint model

Knee numerical modelling allows to predict the possible cause of failure of the implanted prosthesis. Several approaches exist, such as:

- *Musculoskeletal modelling*: it considers bones as rigid body and it mimics muscular actions; so it is able to analyse the joint's dynamics.
- *Deformable modelling*: it gives the opportunity to deal with several pathologies which occur in orthopaedic field, by analysing stress and strain distribution which cannot be examined through clinical studies [66].

In this study, deformable models will be considered because the purpose of this analysis is to investigate the changes in bone stress distribution caused by the placement of different augments in terms of shape, size and material: stress distribution is fundamental for understanding and evaluating the effects of the implanted prosthesis in the patient.

The leading challenge for stress analysis in biomechanical field is to mimic the real conditions because of the complexity of the knee multi-joint systems, in terms of geometries, material properties, interactions between the different components, constraints and boundary and loading conditions. Moreover, the accuracy of the numerical results is related to the assumptions used to solve the 3D model. So, it is fundamental a thorough reconstruction of the joint to investigate every kind of injury mechanism. Different hypotheses, which will be adopted, will be described subsequently. First of all, this model will focus on only tibio-femoral joint, neglecting the existence of patella-femoral joint. These features are outlined in the following paragraphs.

### *3.2.1 Femur and Tibia Material Properties and Geometry*

The three-dimensional model of the tibio-femoral joint adopted in this work derives from a published model which was validated through a comparison between its numerical outcomes and the results obtained by carrying out an experimental trial on the same knee: a good correspondence between the FEA and experimental results was demonstrated [64].

The reconstruction process of the model consists of different steps:

- Physiological femoral and tibial bone structures were reconstructed rearranging those data acquired from Computed Tomography (CT) and Magnetic Resonance Imaging (MRI) scans of a healthy native left cadaveric knee, which shows no evidence of injuries.
- CT and MRI images were processed using a suitable software (Materialise Mimic) in order to reconstruct knee 3D model from the scan data.
- Knee 3D model is imported in an adequate software in order to carry out the finite element analysis (ABAQUS).

In FEA, one of the most crucial aspect is represented by the definition of material properties due to the complexity of the behaviour of the hard and soft tissues **Errore. L'origine riferimento non è stata trovata.**] A close relationship exists between the complex bone structural hierarchies - macrostructure (cortical and spongy bone), micro and nano-structures – and its mechanical behaviour. The components of each hierarchical level are allocated and oriented in different directions. Consequently, the resulting structure is heterogeneous, viscoelastic and anisotropic [67,71]

Currently, there are not enough available data about the mechanical behaviour at the micro and nano structural level [67]. Therefore, according to literature [59, 67,69], it is assumed that all the materials adopted in this model are considered linear elastic and this hypothesis provides the possibility to compare the behaviour of all the materials adopted qualitatively. Furthermore, it isn't taken into account the porosity of the bone structure because this work isn't interested in the investigation of the implant-bone behaviour at microscopic level [59].

Therefore, taking into consideration these hypotheses, the bony structures behaviour is assumed transversely isotropic for the cortical bone, while linear isotropic for cancellous bone [70] as shown in the following *Table 5*.

**Table 5** – Mechanical properties for cancellous and cortical bone according to literature [70]

		Young's Modulus [GPa]			Poisson's Ratio		
		E <sub>1</sub>	E <sub>2</sub>	E <sub>3</sub>	ν <sub>12</sub>	ν <sub>13</sub>	ν <sub>23</sub>
Cortical Bone	Transversely	11.5	11.5	17	0.51	0.31	0.31
	Isotropic						
Cancellous Bone	Linear	2.13				0.3	
	Isotropic						

The third axis is parallel to the anatomical axis of each bone [59]

### 3.2.2 TKA Prosthesis Model and Material Properties

After the 3D modelling of femur and tibia geometries obtained by processing data extrapolated from imaging scans, these models are adapted to the TKA prosthesis which is implanted: a GEMINI® SL® FIXED BEARING PS (WALDEMAR LINK GmbH & Co. KG, Hamburg, Germany) which is implanted following the surgical techniques specified by the producer is considered for this finite element analysis.

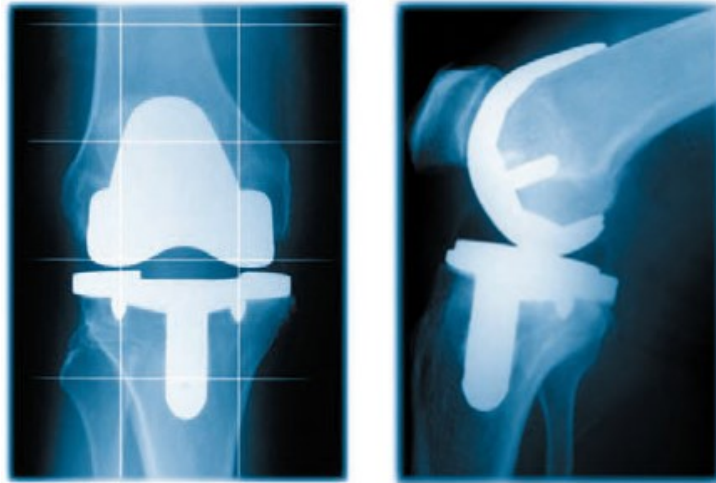


**Figure 46** – Implanted GEMINI® SL® FIXED BEARING PS prosthesis [72]

LINK® GEMINI® knee implant provides a wide range of solutions for treatment of knee injuries with the purpose of achieving some targets, such as: prosthesis longevity and an implant which replicates the real knee anatomy. Different sizes and MOBILE or FIXED BEARING solutions are available: for this study it is chosen a medium size and fixed bearing posterior stabilized tibial components. Furthermore, this prosthesis provides a superficial texture and a double TiCaP® coating (Titanium and Calcium Phosphate) which ensures additional attachment for the cementless implantation.

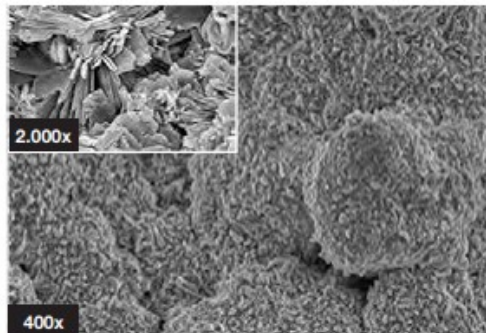


**Figure 47** – TiCaP® coating [72]

This coating, which is characterized by a porous layer of titanium which is covered by a layer of CaP, enhances bone ingrowth on the contact surface implant-bone [72].

FIXED BEARING PS prosthesis consists of the following components:

- Cobalt-chrome alloy (CoCr) femoral component allows long-term stability due to the friction existing between the coupling surfaces: those of the resected femur with the internal surfaces of the femoral component. The external part component is shaped in

order to mimic the real knee joint. Furthermore, the posterior stabilized (PS) solution ensures a better coupling between the implant and bone, a reduction of the bony resection and this stabilizing cam on the femoral component avoids femur subluxation [73].

- Titanium alloy (Ti6Al4V) tibial tray is designed thoroughly in order to replicate the knee anatomy. It also provides blades, fixation pegs and stem for protecting the surrounding bone from rotational and shear forces [73].
- An ultra-highmolecular-weight-polyethylene (UHMWPE) is used for the tibial insert, whose concave surfaces allow enough space for the flexion in order to allow for natural motions [73].

Additionally, in order to avoid the failure for aseptic loosening, it is essential that not only a thorough implant designing is carried out but also it is necessary to choose an adequate cementing technique for the tibial and femoral components because a strong fixation and the longevity of the implant depend on the characteristics of the contact surface bone-implant. Several studies [77, 78, 79] were conducted by analysing the mechanical effects of different thicknesses of the cement skin and the comparison of different cementing techniques. It was found out that an adequate thickness is 3-4 mm of cement penetration because higher thickness could cause thermal injuries at bone-cement interface [79]. Furthermore, according to literature [77, 78], the cementing techniques which enable the implant to perform more efficiently and effectively are:

- Apply a cement layer on the distal and anterior surfaces of the femur, and on the posterior flanges of the femoral component [77]
- Apply a cement layer not only on the bottom surface of the tibial tray, but also on tibial cut surface [78]

In this work, it is applied a cement (polymethylmethacrylate PMMA) layer with a penetration depth of 3 mm to the femoral and tibial severed surfaces in order to ensure a longer lifespan of the prosthesis [59].

The behaviour of all materials used for the implant components is considered isotropic, linear and elastic [59, 69], as stated above for the bone material model. According to literature [59, 75, 76], material's properties are indicated in the following *Table 6*.

**Table 6** – Material properties adopted in this model [75, 76]

Material Model	Young's Modulus		Poisson's Ratio	Reference
	[GPa]	E	$\nu$	
CoCr	Linear	220	0.3	[75]
	Isotropic			
UHMWPE	Linear	0.685	0.4	[75]
	Isotropic			
Ti6Al4V	Linear	110	0.3	[76]
	Isotropic			
PMMA	Linear	2.62	0.3	[75]
	Isotropic			

Starting from the real prosthesis (*Figure 48*), its surfaces are acquired through specialized software in order to replicate the equivalent 3D model.

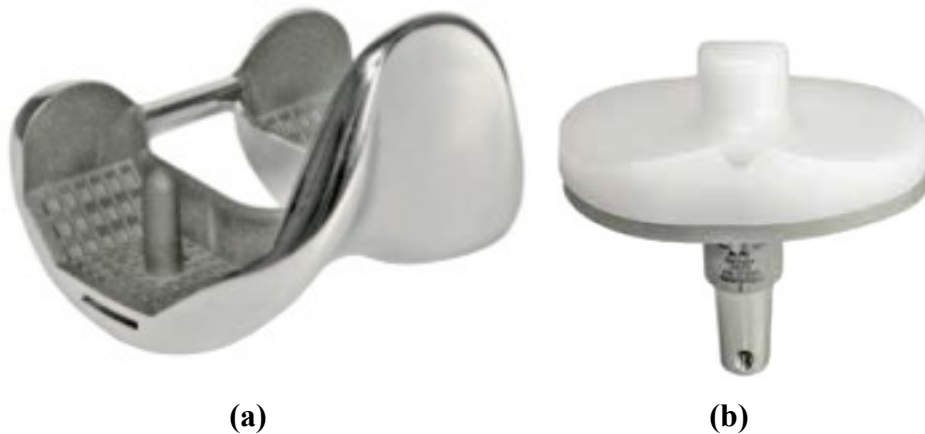


**Figure 48** – GEMINI® SL® FIXED BEARING PS: (a) PS femoral component – (b) Tibial components Fixed Bearing PS [73]

The correspondent 3D model is shown in the following *Figure 49*.

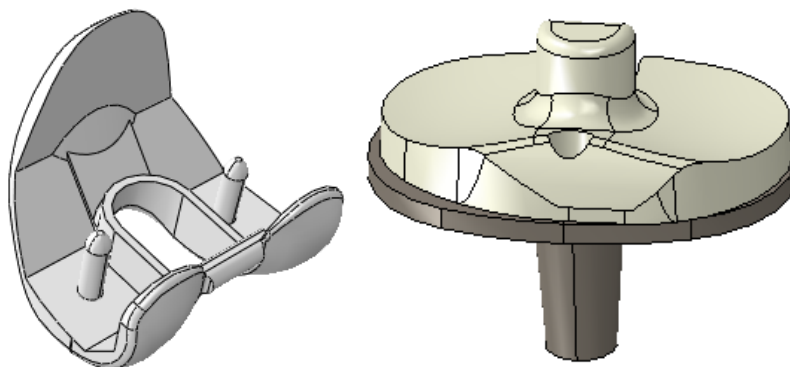


**Figure 49** – Prosthesis 3D model.

The distal part of the femur and the proximal part of the tibia undergo to bone resections as follows (Figure 50).

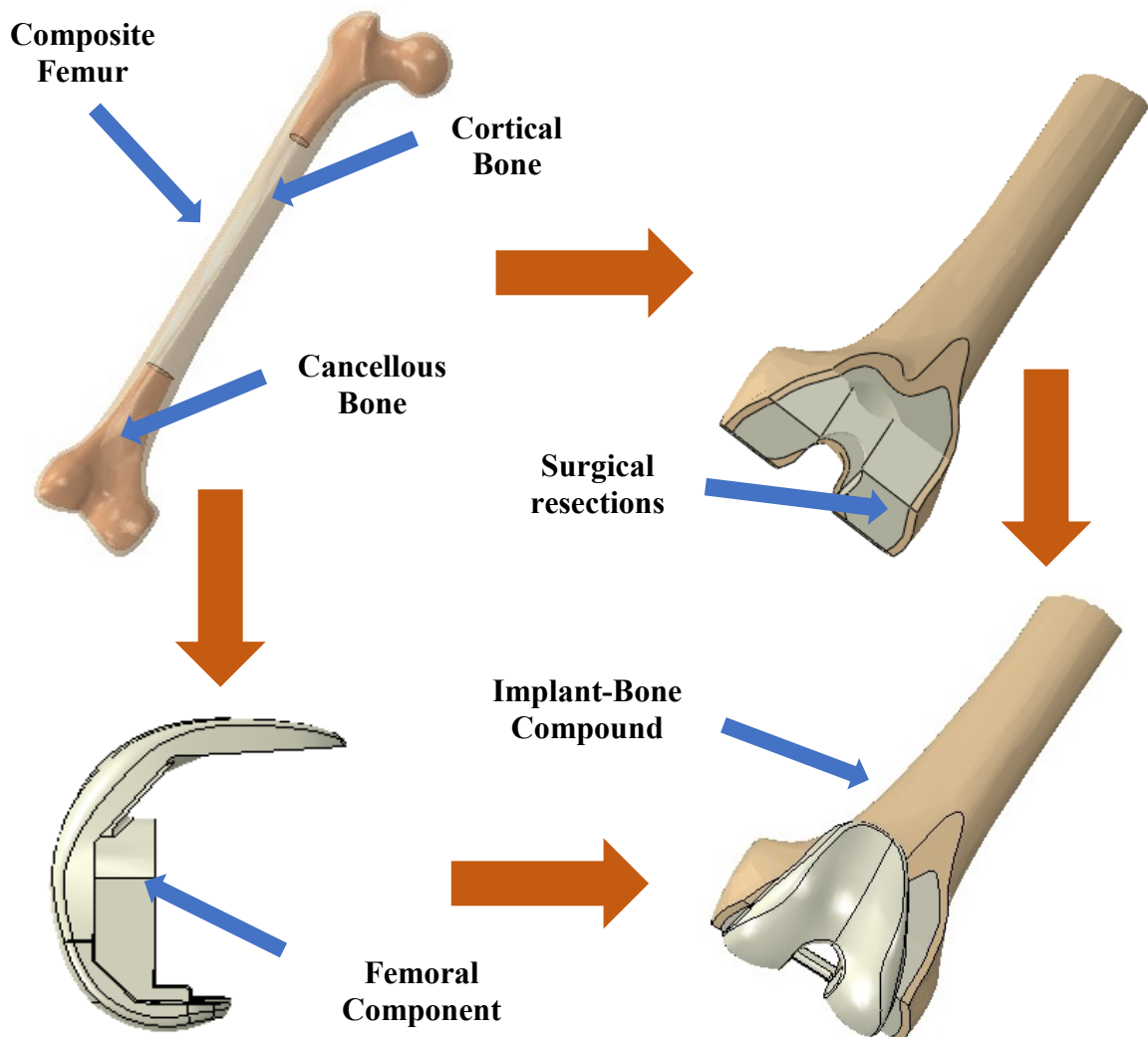


Figure 50 – Steps necessary for implanting the femoral component.

To sum up, femur and tibia geometries obtained by processing data extrapolated from imaging scans should be adapted to the implanted prosthesis through a series of bone resections which are described in the surgical procedures provided by the manufacturer *Figure 51*.

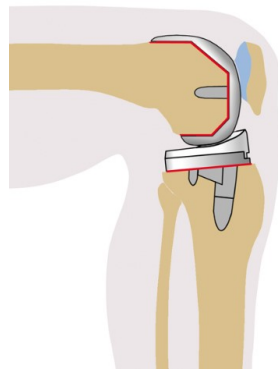
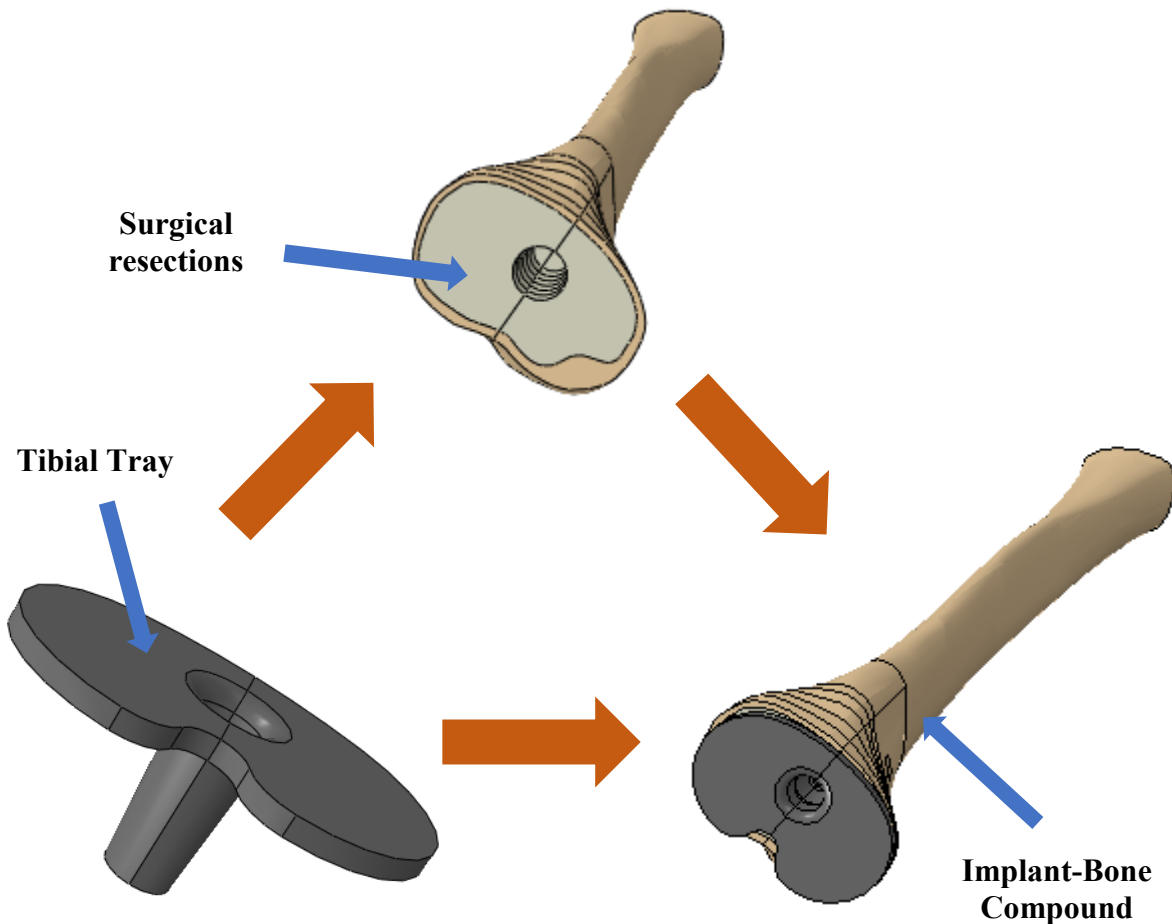


Figure 51 – Surgical guidelines provided by the manufacturer: WALDEMAR LINK GmbH & Co. KG [80]

The same procedure is followed for the tibia:



**Figure 52** - Steps necessary for implanting the tibial tray.

### 3.2.3 Ligaments Model and Material Properties

According to literature [81], a crucial function is played by the ligaments for a good analysis of the kinematics and stress distribution of the knee, but they are made of soft tissue and they present a complex hierarchical structure which is difficult to implement. The ligaments help to ensure a high range of mobility but also a good stability, avoiding the dislocation of the joint. Several studies were conducted in order to mimic the ligaments behaviour and different approaches were followed:

- ✓ Uni-dimensional model: the ligaments are modelled as springs, beams or trusses but only tensile loads could be withstood, and not compression or shear forces.
- ✓ Three-dimensional model: the ligaments are modelled as solid element. MRI scans helps the replication of the real geometry, in terms of the anatomy of the ligaments. These imaging scans help also the acquisition of the insertion point of the ligaments.

- ✓ Bi-dimensional model: the ligaments are modelled as membrane or shell. This approach ensures a simple implementation and a better replication of their anatomy.

In this work, also the medial and lateral collateral ligaments are implemented in order to ensure a better investigation of the stress distribution and a true replication of the working conditions. According to previous validated models [59, 64], a linear elastic isotropic material model is assumed. These ligaments are modelled as beams where a preload is applied. Their properties, in terms of material, preload and cross-sectional area, are listed in the following *Table 7*.

**Table 7** – Mechanical properties of the ligaments [64]

<b>Ligaments</b>	<b>Young's Modulus [MPa]</b>	<b>Poisson's ratio</b>	<b>Initial strain <math>\epsilon_r</math></b>	<b>Cross-sectional area [mm<sup>2</sup>]</b>
LCL	111	0.45	0.05	18
aMCL	196	0.45	0.04	14
pMCL	196	0.45	0.03	14

### 3.2.4 Block Augments Model and Material Properties

The most commonly used classification of bone loss (AORI) states that those defects which damage a large portion of metaphyseal bone (femur and tibia) or the cortical rim can be treated through a modular augmentation: wedge or block augments which could be combined with morsellised bone grafts. It is important that bony reconstruction ensures a strong stability for the new implant in order to allow a better load transmission to the bone and long-term satisfactory results [82].

According to some studies [61], bone deficiencies usually affect distal femur or proximal tibia which could be healed through the implantation of modular augments: this kind of treatment of bone defects is supported by the results of experimental tests, which will be discussed in the following paragraphs. Furthermore, current innovations offer biological solutions: they provide for the use of new porous biomaterials which can be paired with adequate coatings in order to achieve a series of advantages, particularly used for younger patients [82].

Therefore, the aim of this work is to combine the use of rectangular augments of different thicknesses and porous biomaterials with several collocations of the implant, by analysing three flexion angles: 0°, 45° and 90°.

With the purpose of investigating bone stress distribution caused by the implantation of an augment for treating bone injuries, the first step is to consider bone defects by replicating surgical resections in order to remove the damaged bone tissues. In this way, it is possible to prepare the bone surface which will come into contact with the prosthesis.

Hence, this study will analyse the bone response, in terms of stress distribution, to the insertion of different augments. Several positions and extensions of the bone defects, all collocated in the medial condyle:

- For the tibia, proximal position with three different thicknesses (Figure 53) 5, 10 or 15 mm;
- For the femur, distal and posterior position with two different thicknesses: 5 or 10 mm (Figure 54-55).

Consequently, bone resections will be conducted to different depths in order to allow the insertion of these augments. Moreover, the contours of the augments will be tailored to the geometry of the femoral and tibial components because their original features are dictated by the products which are commercially available.

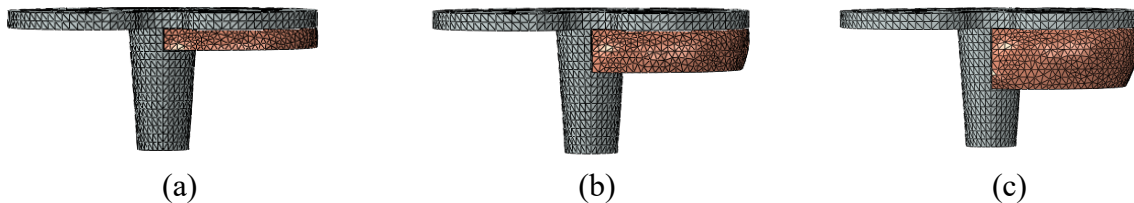


**Figure 53** – Augment placed proximally on the tibial medial side, with different thickness: (a) 5 mm, (b) 10 mm and (c) 15 mm.

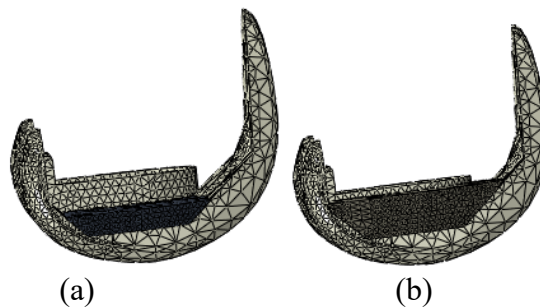


**Figure 54** – Augment placed distally on the femoral medial side with a thickness of: (a) 5 mm and (b) 10 mm.

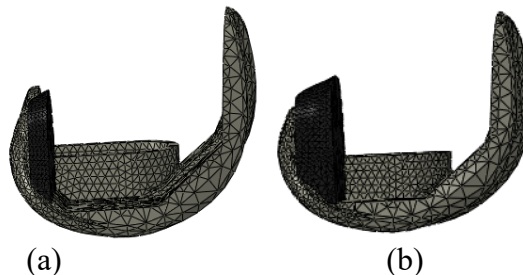


**Figure 55** – Posterior augment placed on the femoral medial side with a thickness of: (a) 5 mm and (b) 10 mm.

Furthermore, the innovation market provides a broad range of porous biomaterials, based on tantalum or titanium alloys which could be coupled with additional coatings, by guaranteeing a number of benefits. These materials try to mimic the real cancellous bone in terms of mechanical properties. Their matrix could allow:

- **High strength** – which is between that of cortical and cancellous bone – is preserved during the regeneration process of the bone and under dynamic loads [83].
- **High interconnected porosity** – which goes up to 80% and above – ensures an osteoconductive matrix and so a favourable environment for the bone regeneration and rapid fixation [83].
- **High roughness** of the surface in contact to the bone which favours a better attachment.
- **High biocompatibility** and **bioactivity** reduce the risk of adverse immunological response [83].
- **High rate of bone ingrowth** if compared to that of sintered beads (CoCr and Ti alloys): these materials don't show inflammatory reaction, but they demonstrate a high incorporation into the host bone [83].
- **High coefficient of friction** affords not only the initial stability at the interface bone-implant but also reduces the risk of micromotions which will compromise bone-prosthesis fixation. A strong biological fixation is fundamental for ensuring a deep bone ingrowth because this give the possibility to hold the implant stable and to minimize the use of bone cement [83].
- **Low elastic modulus** – which is close to that of cancellous bone – enables the natural transmission of the physiological loads between the implant and surrounding bone and this could reduce radiolucent lines and stress shielding [83].

Moreover, the companies, specialized in the orthopaedic field, allow a versatile design in term of shape and dimensions: these structures could have additional holes for a better fixation through screws [83].

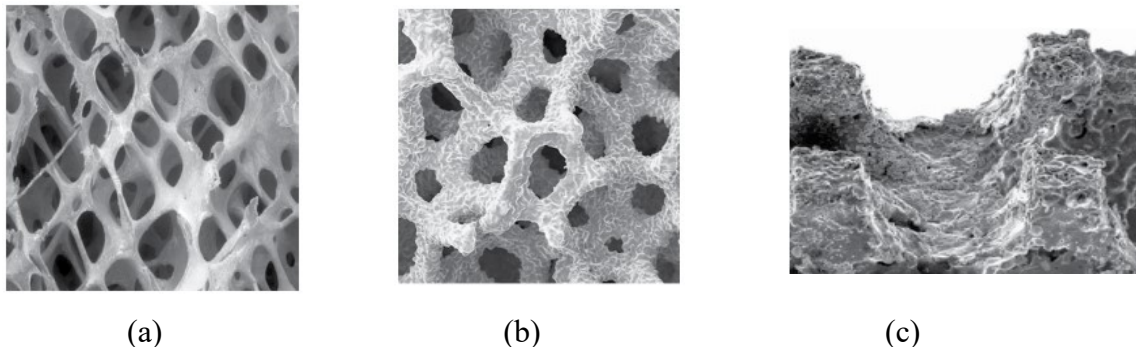


**Figure 56** - (a) Cancellous bone – (b) porous biomaterial – (c) Level of roughness that could be achieved [83]

Looking at the configurations, showed in (Figure 57), each model will be realized by considering different porous and solid materials in order to discuss their bone stress response, by comparing them to a control configuration which is defined considering only the prosthesis but without augment, and so in the absence of bony defects. Furthermore, all these defined model will be considered for three different flexion angles:  $0^\circ$  -  $45^\circ$  -  $90^\circ$ .

As stated previously, the behaviour of porous biomaterials is modelled as linear elastic, homogenous and isotropic [59]. A detailed summary of their properties are described in the following Table 8.

Table 8 – Porous material properties.

Porous Metals	Modulus of elasticity [MPa]	Average pore size [ $\mu\text{m}$ ]	Porosity [%]
Trabecular Metal	2500 - 3900	550	75 - 85
Regenerex	1600	300	67
Tritanium	2700	546	72
Gription	3500	300	63

*These properties were analysed in the previous chapter.*

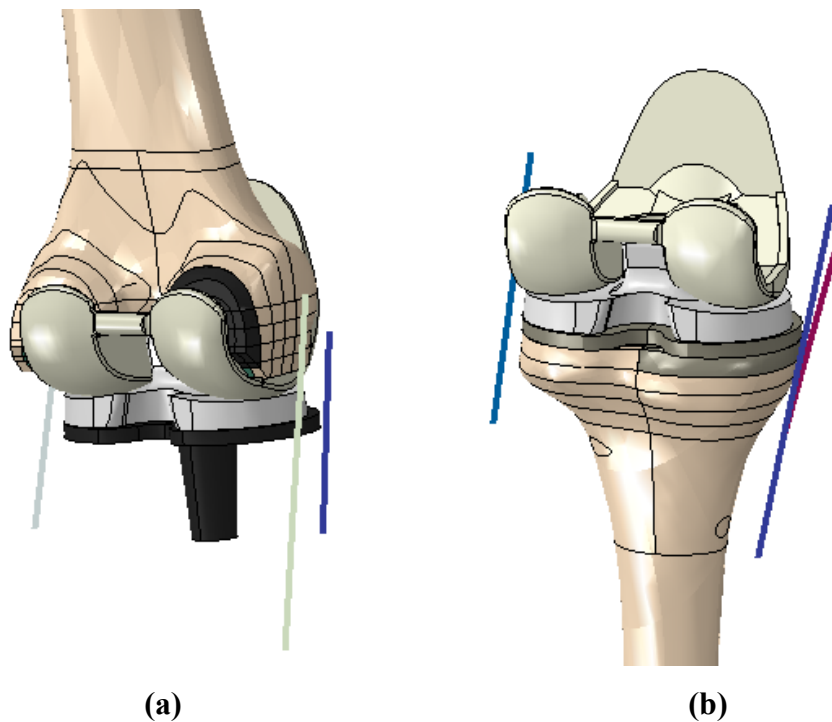


Figure 57 –An example of configurations: (a) femoral model where an augment of 5 mm is placed on the medial and posterior side – (b) tibial model where an augment of 5 mm is placed proximal on the medial side.

### 3.2.5 Boundary and Load Conditions

The long-term success of a surgical treatment of revision TKA is related to the capability of restoring an adequate transmission of the physiological loads, by creating a stable environment. The contact forces which act within the joint and the loads borne by bone depend on the muscular forces which are performed during daily activity. It is very difficult to measure the *in vivo* loading conditions which act in a human knee because it is a complex multi-joint system and the loading environment depends on body weight, gender and activity performed (walking, squat, stair climbing) [84].

According to literature, Taylor *et al.* [84] analysed the *in vivo* loads which occur in tibio-femoral joint, by considering a model already validated for hip in two scenarios: walking and stair climbing. It was found out that the average axial force during a gait cycle is 3.1 times body weight.

The assigning of load conditions to the 3D model is really difficult. Adequate hypotheses are assumed: leading joints (hip, knee and ankle) are considered cylindrical. A scheme of the loads acting on the knee joint are represented in the following *Figure 58*.

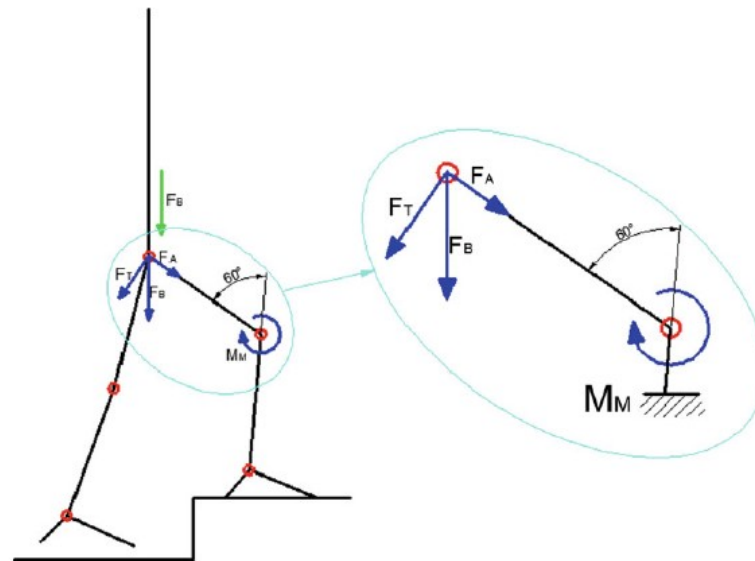


**Figure 58** – Scheme of the loads applied on the knee joint [86]

When both feet touch the ground, the body weight  $F_B$  is shared among the two legs: the most critical condition is that  $F_B$  is borne by a single leg and it is transferred to the femur by means hip joint.  $F_B$  can be divided in two components: axial force  $F_A$  which acts along the anatomical femoral axis and transversal force which is perpendicular to it. By assuming that the distal part of the tibia is fixed and the knee joint is cylindrical, the knee is able to bear only the axial load

$F_A$ , while  $F_T$  and the moment  $M_M$  imposed by the equilibrium of the system are balanced by the muscular actions [86]

In this study, only the axial loads ( $F_A$  and the axial muscular reactions) are considered while the tangential force and the moment acted by the muscles are neglected because they are not relevant for the contact stress femoral component – tibial insert.

According to previous implemented studies [59, 84, 85, 86], an axial load of 2500 N, which is approximately 3.1 times a body weight of 80 kg, is applied in the centre of the femoral head along the femoral mechanical axis, obtained by joining the centres of the femoral head and the ankle. In all the configuration the worst case will be considered: all the axial load is applied on a single leg and it is not split between the two legs.

All configurations (no augment and plus augments) are subjected to the same loading conditions: an equivalent body diagram system is obtained by transporting the axial load in the joint centre (defined as loading application point), maintaining the same loading direction and applying an equilibrium moment. Furthermore, a continuum distributing coupling interaction is applied between the loading application point and the area of application in order to ensure a uniform loading distribution as shown in the *Figure 59*.

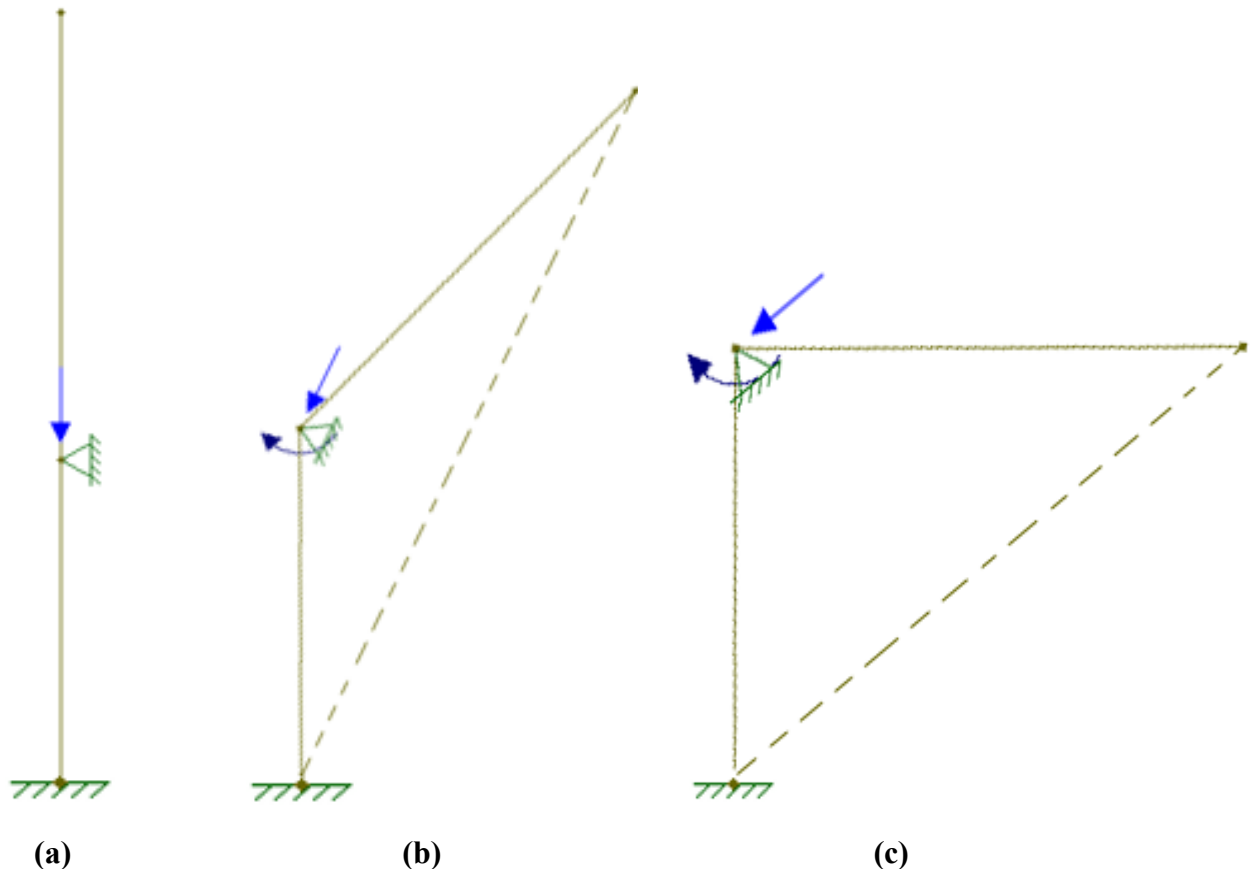


**Figure 59** – Free diagram body for each flexion angle: (a) 0° - (b) 45° - (c) 90°.

By analysing the boundary conditions, if we consider the global model (tibia + femur + prosthesis +augment) the distal part of the tibia is fixed in all the considered configurations, while focusing on the femoral bone, it is allowed only the translation along the loading axis and the rotations around it as shown in *Figure 59*.

In this study, the following models will be analysed:

- when the augment is located onto the distal or posterior side of the femur, the free body diagram involves: prosthesis, augment and femur. In this case, the head of the femur will be totally fixed through the insertion of an encastre, while the load – applied in the centre of the joint – will be distributed onto the underneath surface of the tibial tray.
- Another scenario is represented by the insertion of the augment onto the proximal part of the tibia: in this case the model consists of the prosthesis, the augment and the tibia. So, tibia is distally fixed, whereas the load is applied the underneath surface of the tibial tray.

For both cases, the loading application point is constrained as follows: it is allowed only the translation and the rotations around the loading axis (mechanical femoral axis).

### 3.2.6 Interactions and Contact Properties

As previously mentioned, different fixation techniques exist for the femoral and tibial components: the use of bone cement ensures good primary stability, while cementless implant is directly implanted in contact with the bone for the purpose of promoting biological fixation **Errore. L'origine riferimento non è stata trovata.**] In this study, a cement layer with a penetration depth of 3 mm is applied onto the femoral and tibial severed surfaces which are in contact to the femoral and tibial tray respectively, in order to ensure a longer lifespan of the prosthesis.

In all analysed models, all of the contact surfaces are perfectly bonded through a tie contact in order to avoid the risk of micromotions, except for the interface femoral component – tibial insert where a node to surface contact is applied using a tangential behaviour penalty friction formulation. Innocenti *et al.*[75] provided a value of friction coefficient of 0.2. All the contact properties are shown in the following *Table 9-10*.

**Table 9** – Contact properties for the tibial model.

<b>Model</b>	<b>Interface</b>	<b>Material in contact</b>	<b>Type contact</b>
Tibia + Implant	Femoral component- Insert	Co-Cr - Polyethylene	Node to surface
	Insert-Tibial tray	Polyethylene - Ti	Perfectly bonded
	Tibial tray-Augment	Ti – Porous metal	Perfectly bonded
	Tibial tray - Tibia	Ti - Bone	Perfectly bonded
	Augment- Tibia	Porous metal - Bone	Perfectly bonded

**Table 10** - Contact properties for the femoral model.

<b>Model</b>	<b>Interface</b>	<b>Material in contact</b>	<b>Type contact</b>
Femur + Implant	Femoral component- Insert	Co-Cr - Polyethylene	Node to surface
	Insert-Tibial tray	Polyethylene - Ti	Perfectly bonded
	Femoral component- Augment	Co-Cr – Porous metal	Perfectly bonded
	Augment - Tibia	Porous metal - Bone	Perfectly bonded

### 3.2.7 Mesh

All the components of these models are meshed considering linear tetrahedral elements: a good compromise between accurate results and an acceptable computational time is to divide the femur and tibia into different section in order to apply different element size for the mesh. The regions of interest are set in order to evaluate if the insertion of an augment could affect the stress distribution on the surrounding bone and to highlight if the wedge have also an effect (always in terms of stress) at the global level. For these reasons, the local region of interest close to the augment is deep 10 mm while the global region of interest presents a depth of 50 mm: they are defined for each model as follows:

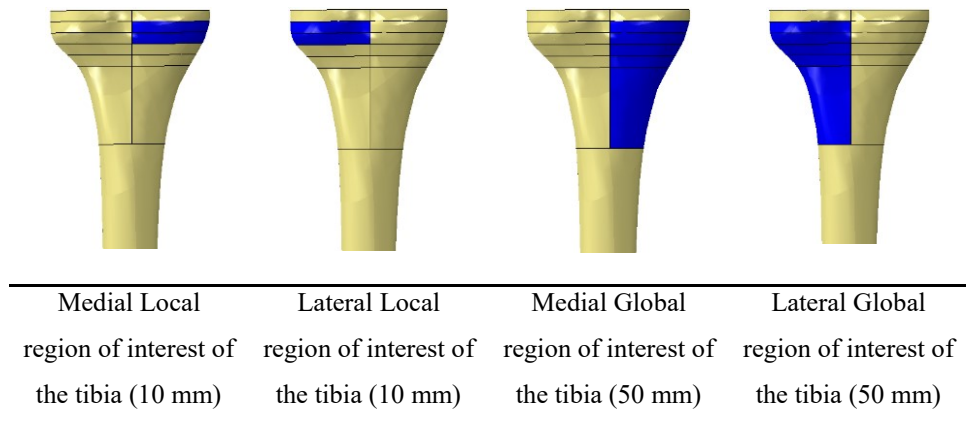


**Figure 60** – Local and global regions of interest for a tibial augment with a thickness of 5 mm, placed proximally.

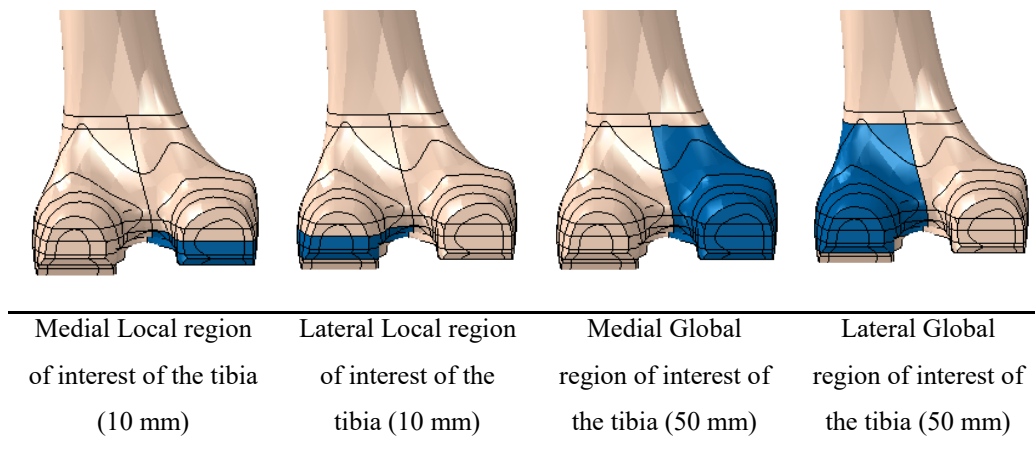


**Figure 61** - Local and global regions of interest for a femoral augment with a thickness of 5 mm, placed distally

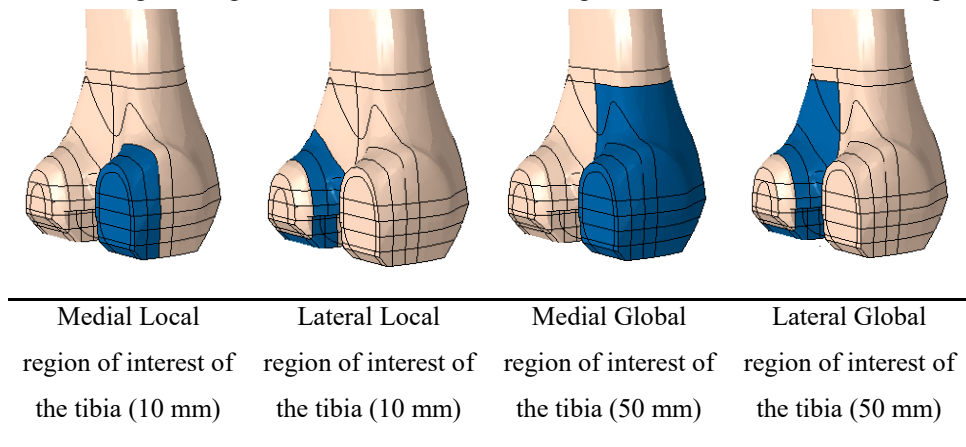


**Figure 62** - Local and global regions of interest for a femoral augment with a thickness of 5 mm, placed posteriorly.

Moreover, a partition of the external surface of the femoral component is realized in order to allow a better contact between the femoral component and the polyethylene insert. Once the most crucial regions for the finite element analysis have been identified, it is possible to use a

finer mesh in order to ensure a better tetrahedral approximation, minimizing the risk of a discontinuity in the distribution of the variables of interest (*Table 11*).

**Table 11** – Summary of the mesh size

	<b>Region</b>	<b>Element Type</b>	<b>Mesh Size</b>
Bone	Local region of interest	Linear tetrahedral elements	2 mm
	Global region of interest	Linear tetrahedral elements	2 mm
Implant	Femoral component	Linear tetrahedral elements	5 mm
	Insert	Linear tetrahedral elements	5 mm
	Contact region Insert-Femoral component	Linear tetrahedral elements	1 mm
	Tibial tray	Linear tetrahedral elements	5 mm
	Augment	Linear tetrahedral elements	2 mm

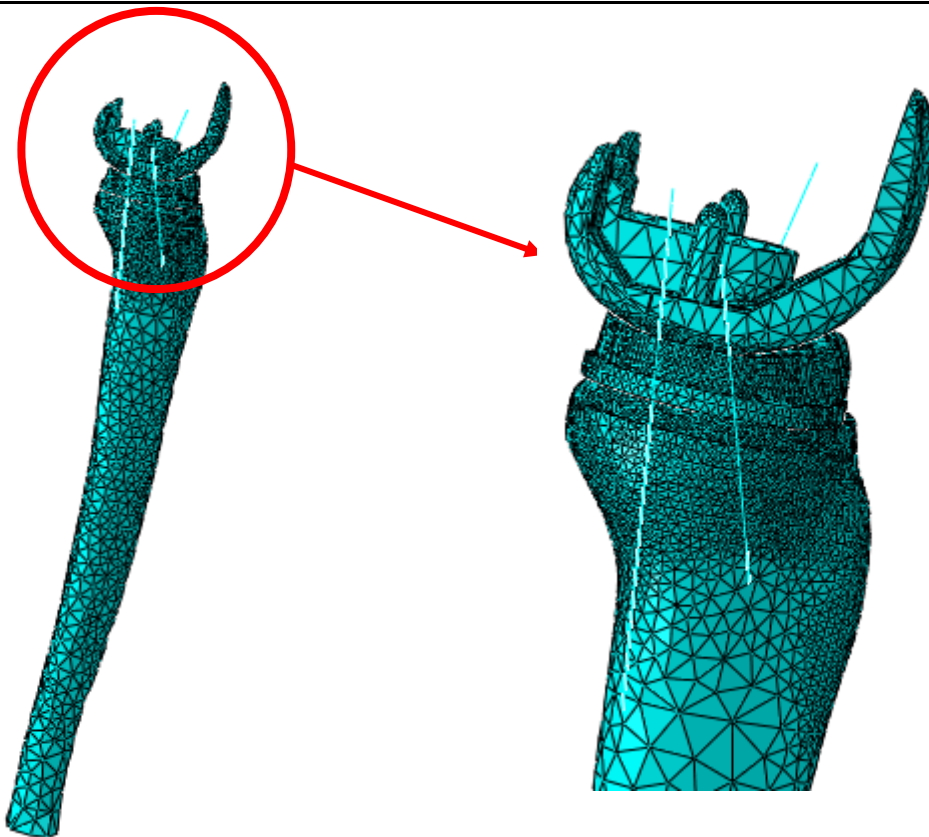


**Figure 63** – Mesh assembly: Tibial model.

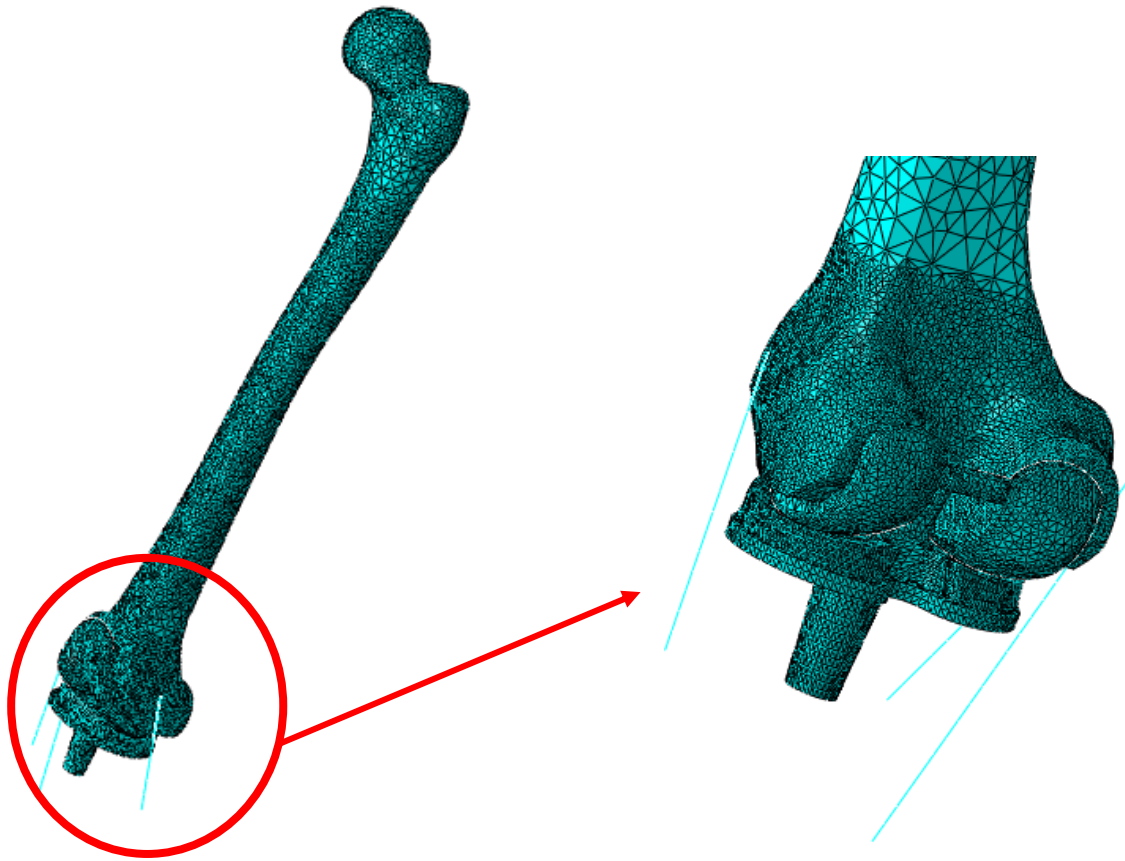


**Figure 64** - Mesh assembly: femoral model.

## Chapter 4

### Results

All simulations were performed on Abaqus/Standard version 6.14-1 (Dassault Systèmes, Vélizy-Villacoublay, France). Results were obtained considering three flexion angles ( $0^\circ$  -  $45^\circ$  -  $90^\circ$ ) for each model, as stated in the previous chapter.

The variables considered in the present study are:

- the average Von Mises stress
- the average Shear stress

All these output variables are analysed in the regions of interest defined in section 3.2.7:

- ✓ the local region, close to the augment is deep 10 mm
- ✓ the global region presents a depth of 50 mm

These regions are set in order to evaluate if the insertion of the augment could affect the stress distribution on the surrounding bone and to highlight if the wedge have also an effect at the global level. These variables will be analysed for each configuration defined in the previous chapter, and they are compared not only to the respective control model (no augment) but also to the other configurations.

This analysis has been carried out in order to demonstrate if the use of an augment made of a porous biomaterial could be a good alternative for dense metals: this goals can be achieved if the change in bone stress due to the presence of a porous augment is smaller than that of a solid augment. For ensuring a satisfactory long-term performance of the implant, it is fundamental to decrease the alterations, in terms of stress, on the surrounding bone.

## 4.1 Tibial model

In this section the results obtained from the FEA are shown in terms of the average Von Mises and shear stress at the interface bone-augment, taking into account the three flexion angles ( $0^\circ$  -  $45^\circ$  -  $90^\circ$ ), the three different thicknesses for the proximal tibial augment (5-10-15 mm) and the several biomaterials (porous: Trabecular Metal, Regenerex, Tritanium and Gription; solid: Cobalt – Chrome and Titanium). Each analysed configuration will be compared to the others and to the control model.

### 4.1.1 Von Mises stress: flexion angle of $0^\circ$

In this paragraph, the change in bone Von Mises stress caused by a proximal tibial augment of 5 – 10 – 15 mm, placed on the medial side of the tibia is investigated, comparing all the porous and solid biomaterials. For each configuration, a flexion angle of  $0^\circ$  is set and the “Control Model” is defined as that model where no augment is implanted. With the purpose of comparing the effects of the insertion of an augment, a graphical representation of the Von Mises stress distribution at the bone-augment interface is shown in the following figures.

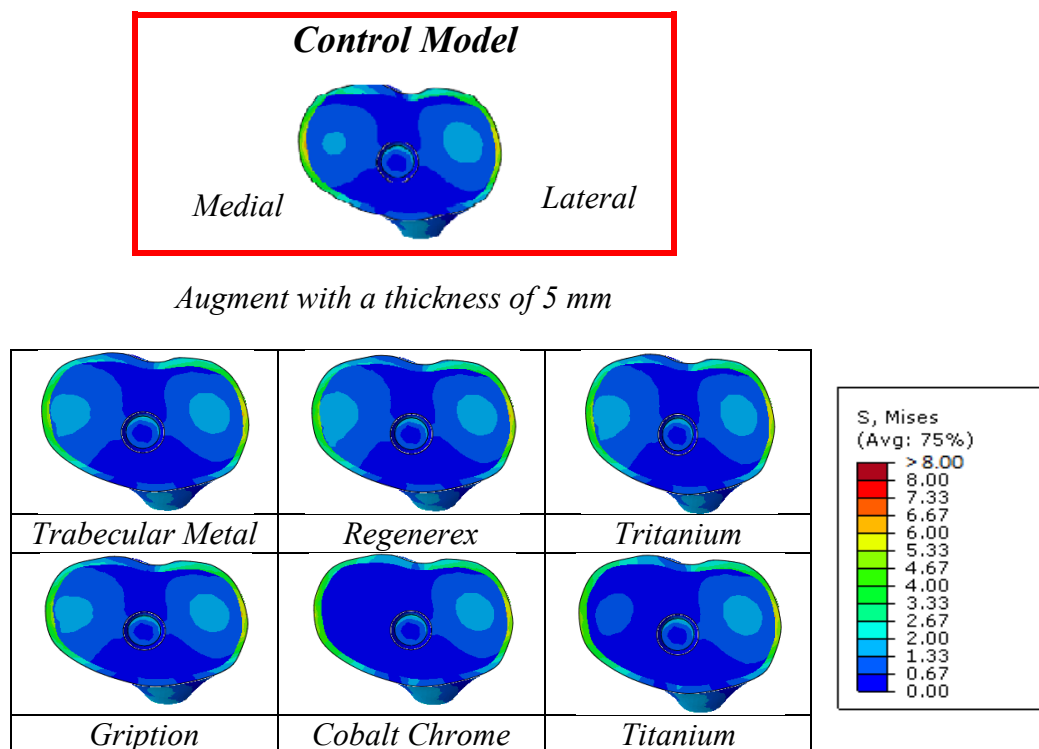


**Figure 65** – Von Mises stress distribution at tibia – augment interface for a flexion angle of  $0^\circ$  and an augment of 5 mm.

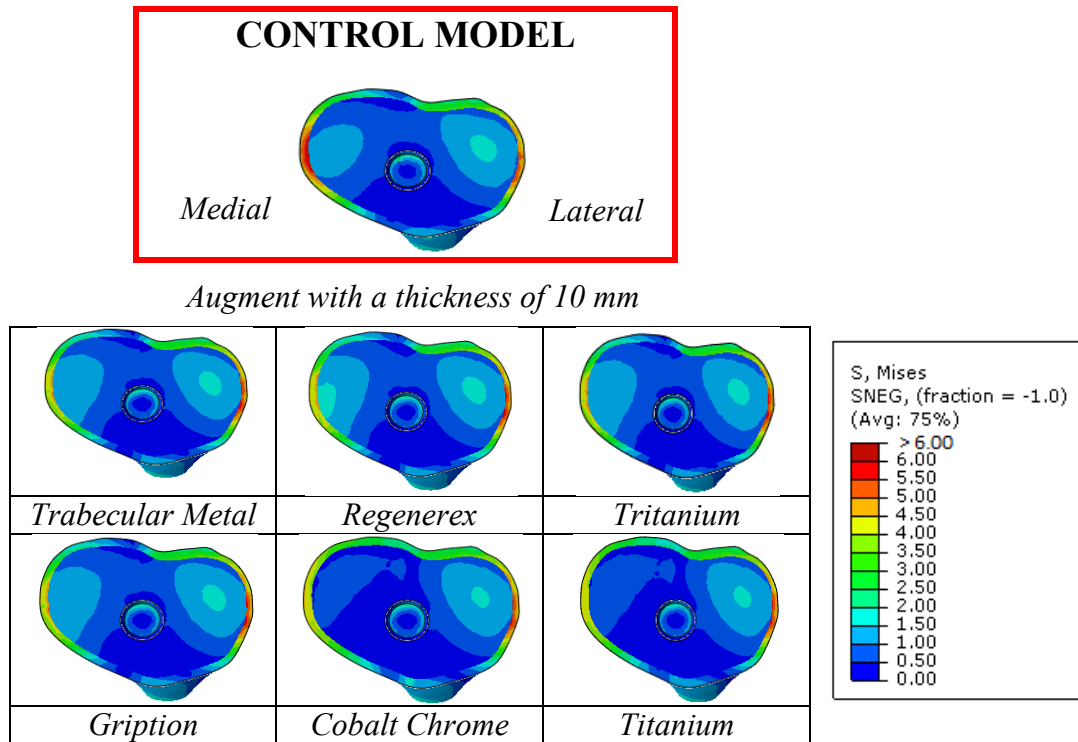


**Figure 66** - Von Mises stress distribution at tibia – augment interface for a flexion angle of 0° and an augment of 10 mm.

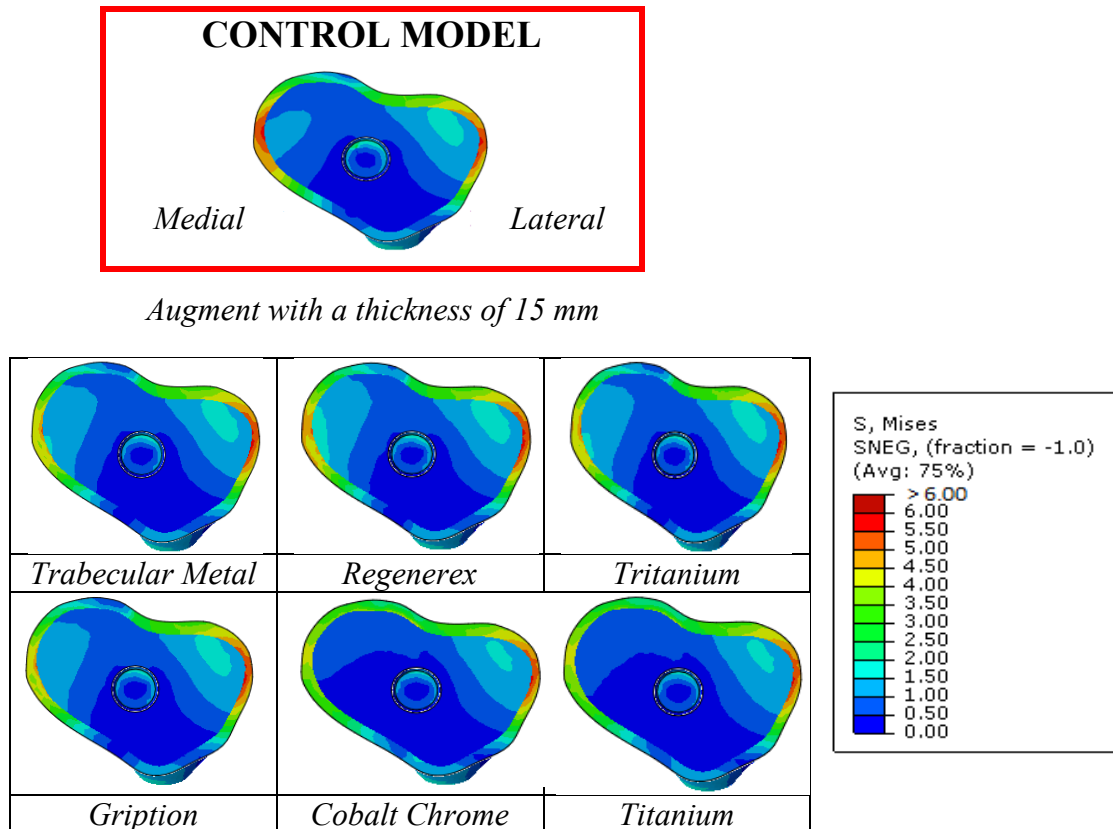


**Figure 67** - Von Mises stress distribution at tibia – augment interface for a flexion angle of 0° and an augment of 15 mm.

A first graphical analysis of the previous figures highlights the same trend for all the analysed thicknesses: Von Mises stress distribution at tibia – augment interface (tibial medial side) is very similar to that of the control model for the porous metals, while a greater discrepancy appears for the solid materials. Looking at the lateral side, by comparing all the biomaterials considered, both porous and solid, it is possible to notice the same trend which is close to that of control model. A proof of this trend is given by the following bar graphs (Figure 68): Von Mises stress is investigated in the local region of interest and in the global one.

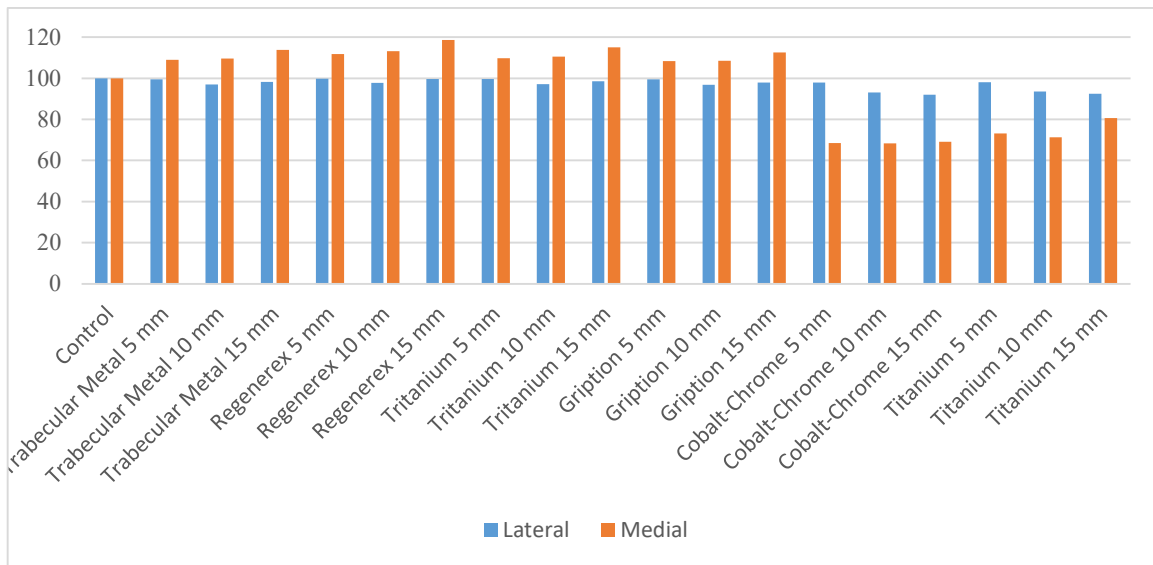


**Figure 68** – Flexion 0°: Average Von Mises bone stress analysing the local region of interest (depth of 10 mm) and comparing all the trend of all the thicknesses and all the biomaterials to the control model and among them.

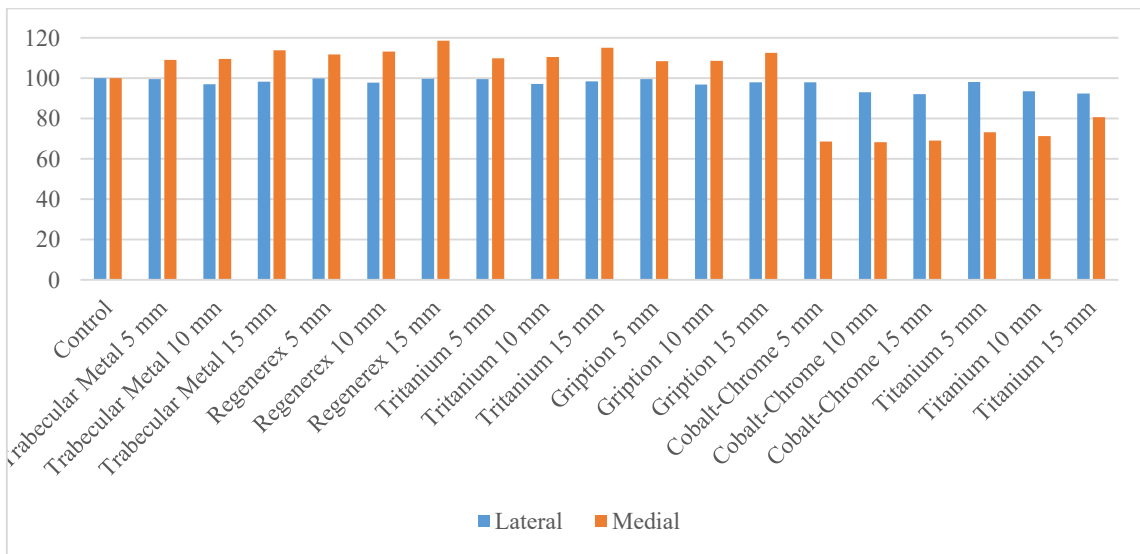


**Figure 69** – Flexion 0°: Average Von Mises bone stress analysing the global region of interest (depth of 50 mm) and comparing all the trend of all the thicknesses and all the biomaterials to the control model and among them.

All these values are obtained by normalizing with the respect of the average Von Mises bone stresses of the control model.

By analysing the change in Von Mises bone stress close to the augment (*Figure 69*), it is possible to notice that the region which is more influenced by the presence of an augment is the tibial medial side, for each material and for each thickness. In particular, the porous biomaterials cause an increase of the Von Mises stress in the medial side of approximately 10 – 20% for all thicknesses, while Cobalt-Chrome and Titanium induce a decrease of about 30 % for all thicknesses. On the other hand, there is no change in the lateral side if it is used a porous augment, while a solid metal induces a slight decrease (about 6.5%) both locally and globally.

#### 4.1.2 Von Mises stress: flexion angle of 45°

As the previous section, the change in bone Von Mises stress caused by a proximal tibial augment of 5 – 10 – 15 mm, placed on the medial side of the tibia is investigated, comparing all the porous and solid biomaterials. For each configuration, a flexion angle of 45° is set and the “Control Model” is defined as that model where no augment is implanted. With the purpose of comparing the effects of the insertion of an augment, a graphical overview of the Von Mises stress distribution at the bone-augment interface is shown in the following figures.

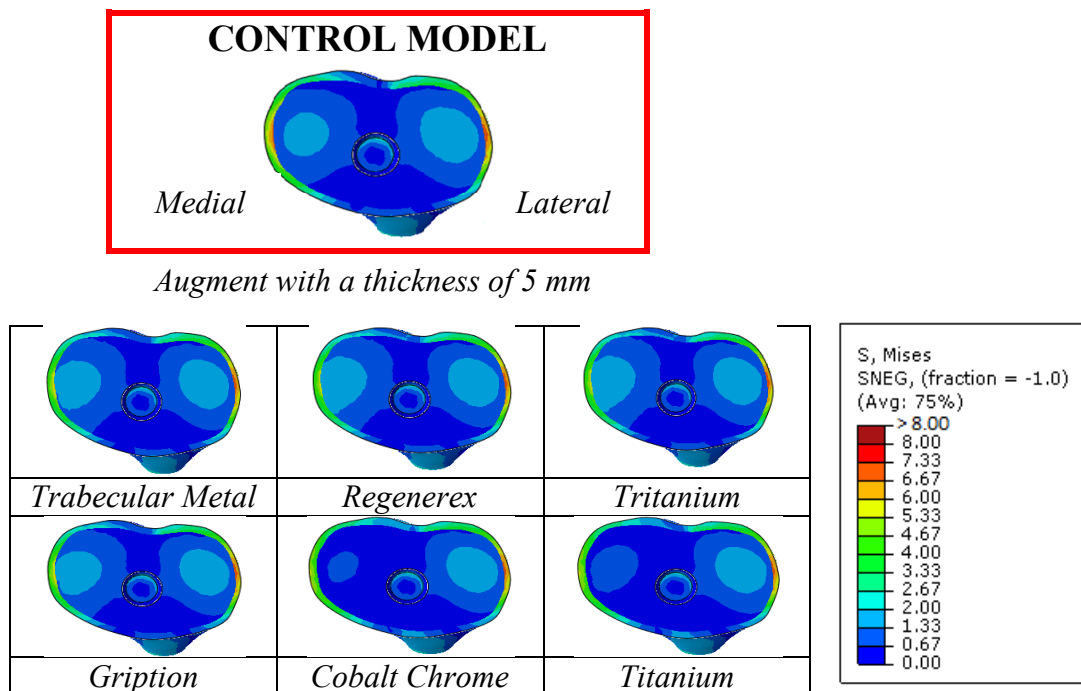


**Figure 70** - Von Mises stress distribution at tibia – augment interface for a flexion angle of 45° and an augment of 5 mm.

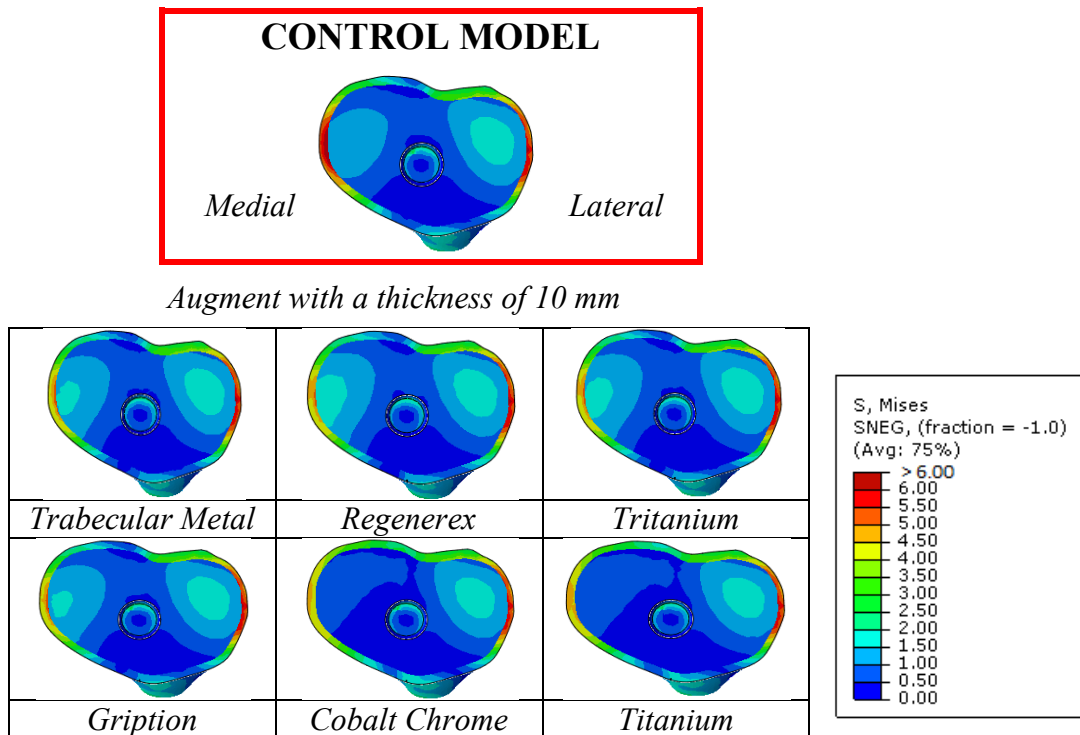


**Figure 71** - Von Mises stress distribution at tibia – augment interface for a flexion angle of 45° and an augment of 10 mm.

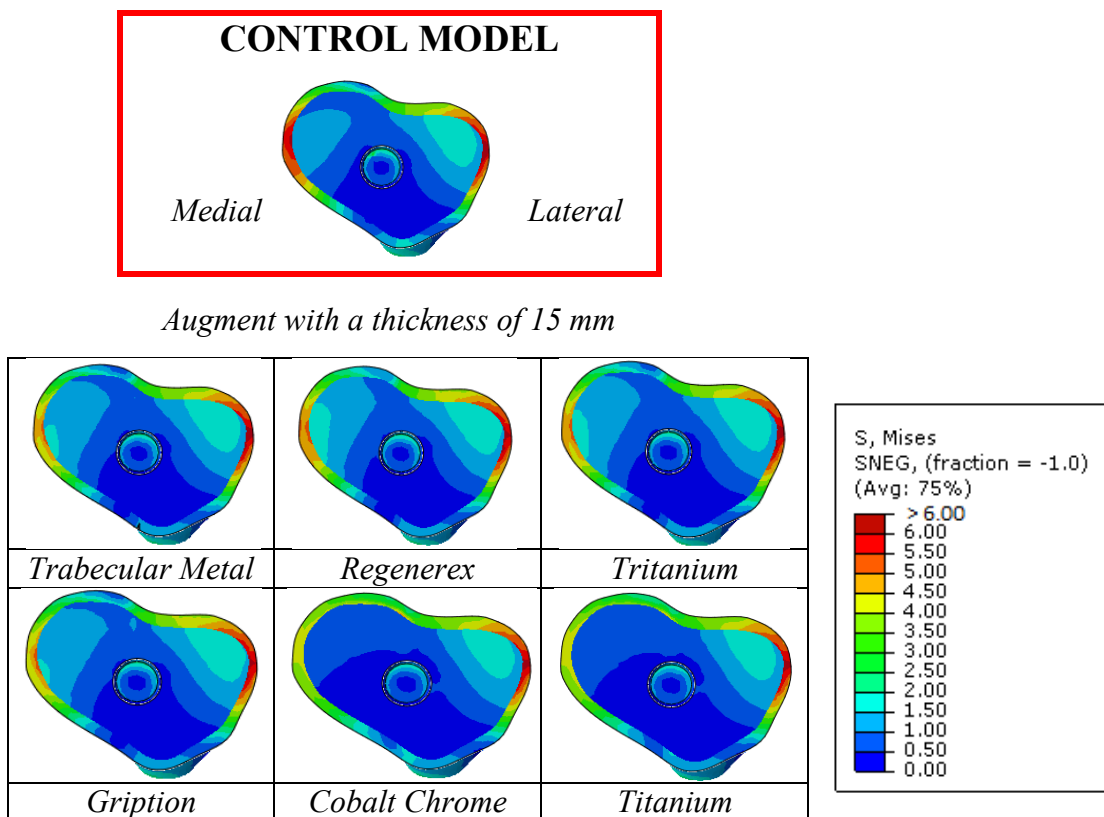


**Figure 72** - Von Mises stress distribution at tibia – augment interface for a flexion angle of 45° and an augment of 10 mm

Also for a flexion angle of 45°, the previous figure shows the same pattern that it is possible to see for a flexion angle of 0°. The leading effect of an augment placed on the medial side of the tibia is induced in the region close to the augment (medial side), while the stress distribution at the tibial bone interface is close to that of the reference model.

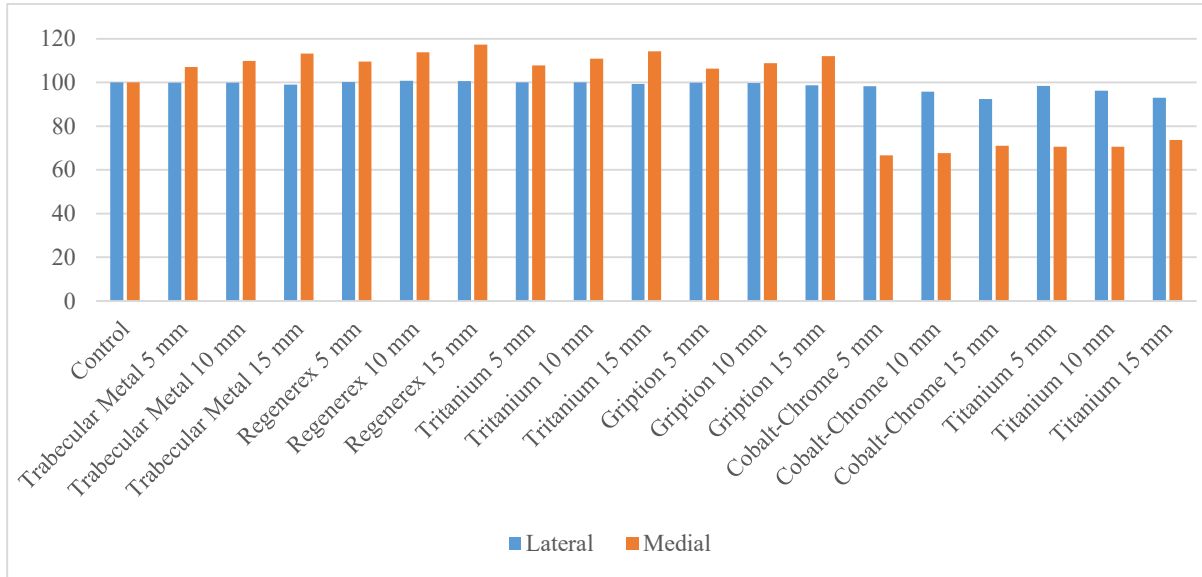


**Figure 73** – Flexion 45°: Average Von Mises bone stress analysing the local region of interest (depth of 10 mm) and comparing all the trend of all the thicknesses and all the biomaterials to the control model and among them.

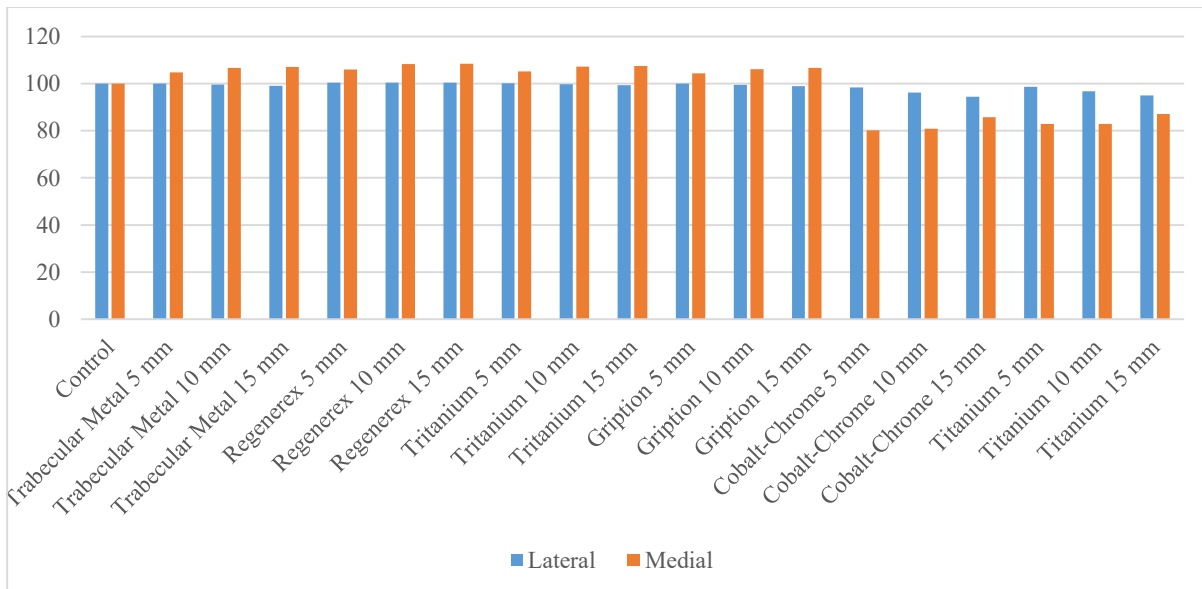


**Figure 74** - Flexion 45°: Average Von Mises bone stress analysing the global region of interest (depth of 50 mm) and comparing all the trend of all the thicknesses and all the biomaterials to the control model and among them.

Locally, porous biomaterials lead to a rise of the bone stress: the average Von Mises stress, normalized with the respect to that of the reference model, grows with the increase of the

thickness (up to approximately 20% for an augment of 15 mm, made of Regenerex; for the other porous metals is slightly lower). On the contrary, there is no effect on the lateral side. This trend is common to all porous metal.

By contrast, the solid metals, such as Co-Cr and Ti, cause a drastic fall of the average stress of about 35% for the augment of 5 mm, made of Co-Cr. By increasing the thickness, this reduction decreases slightly: in fact, the augment of 15 mm, made of Co-Cr, induces a decrease of 30%. Look at the lateral side, also here there is a slight decrease that reach the minimum if the augment's thickness is 15 mm (reduction of about 10%).

Globally, the gap existing between the medial and the lateral side, for both porous and solid metals is reduced.

### 4.1.3 Von Mises stress: flexion angle of 90°

For each configuration, a flexion angle of 90° is set and an augment of 5 – 10 – 15 mm is placed on the medial side of the tibia. In the following figures, a graphical overview is reported:

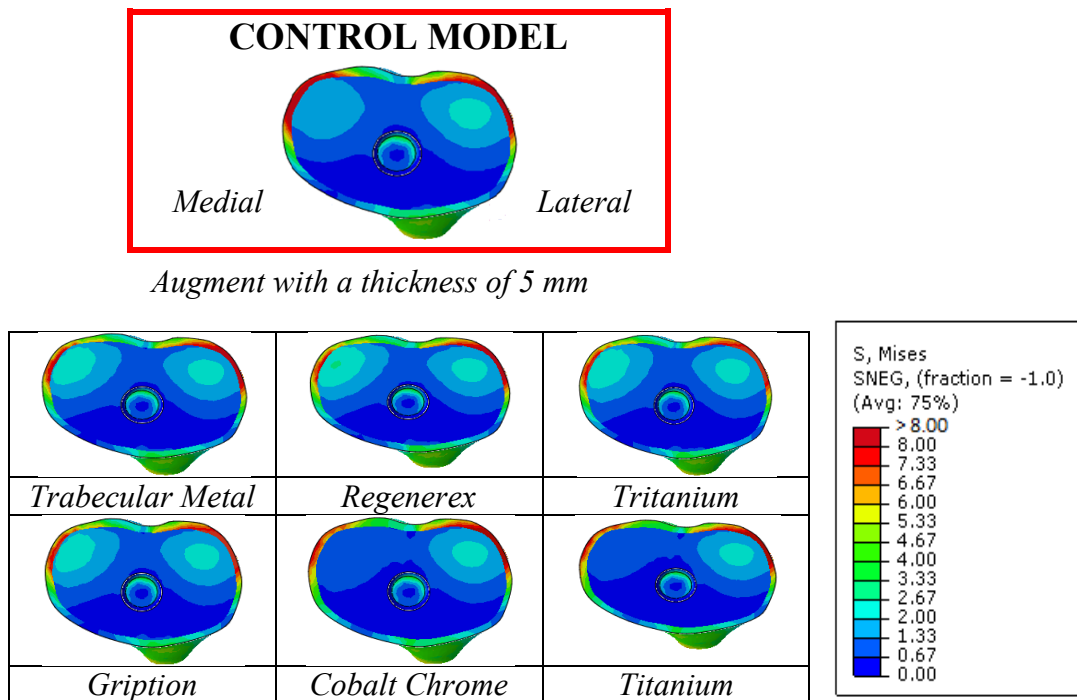


**Figure 75** - Von Mises stress distribution at tibia – augment interface for a flexion angle of 90° and an augment of 5 mm

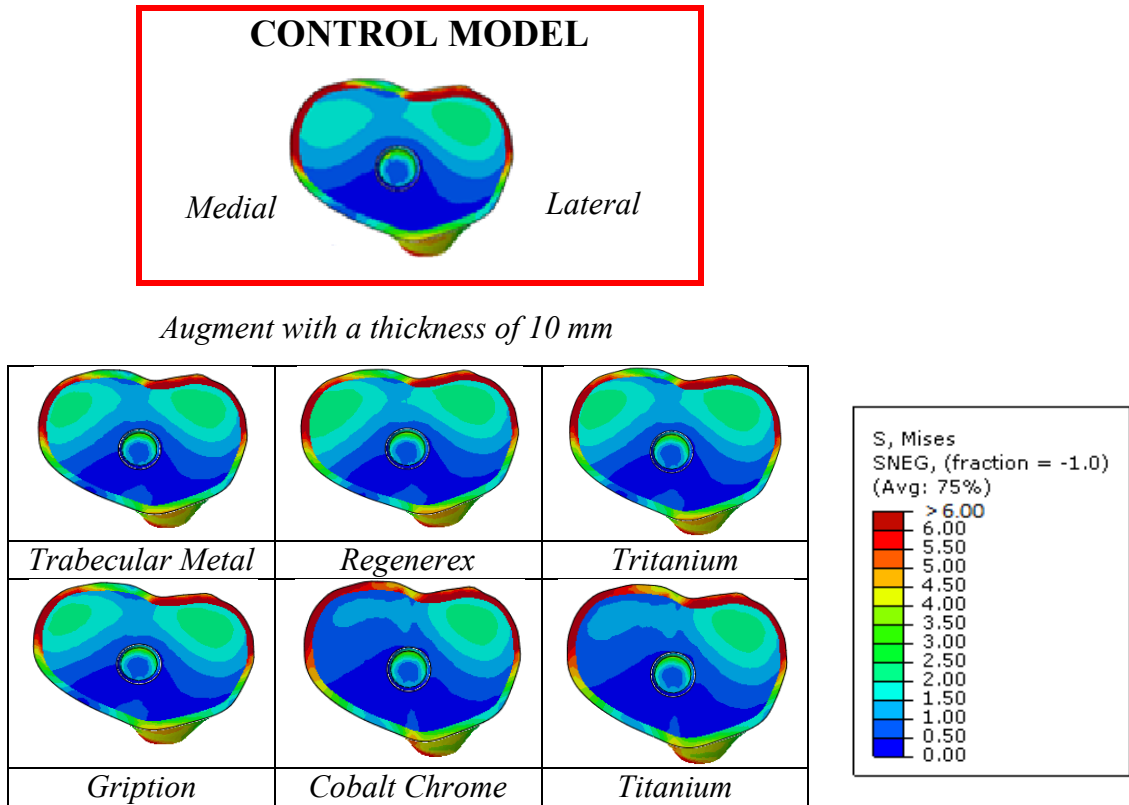


**Figure 76** - Von Mises stress distribution at tibia – augment interface for a flexion angle of 90° and an augment of 10 mm

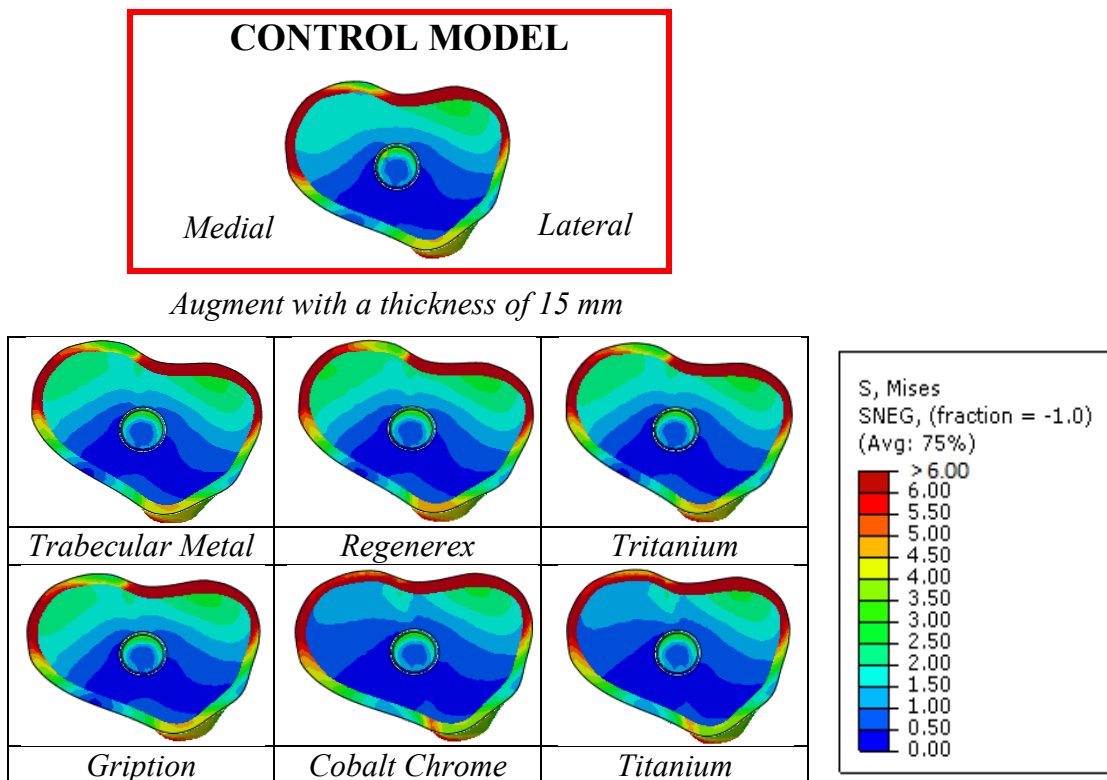


**Figure 77** - Von Mises stress distribution at tibia – augment interface for a flexion angle of 90° and an augment of 15 mm

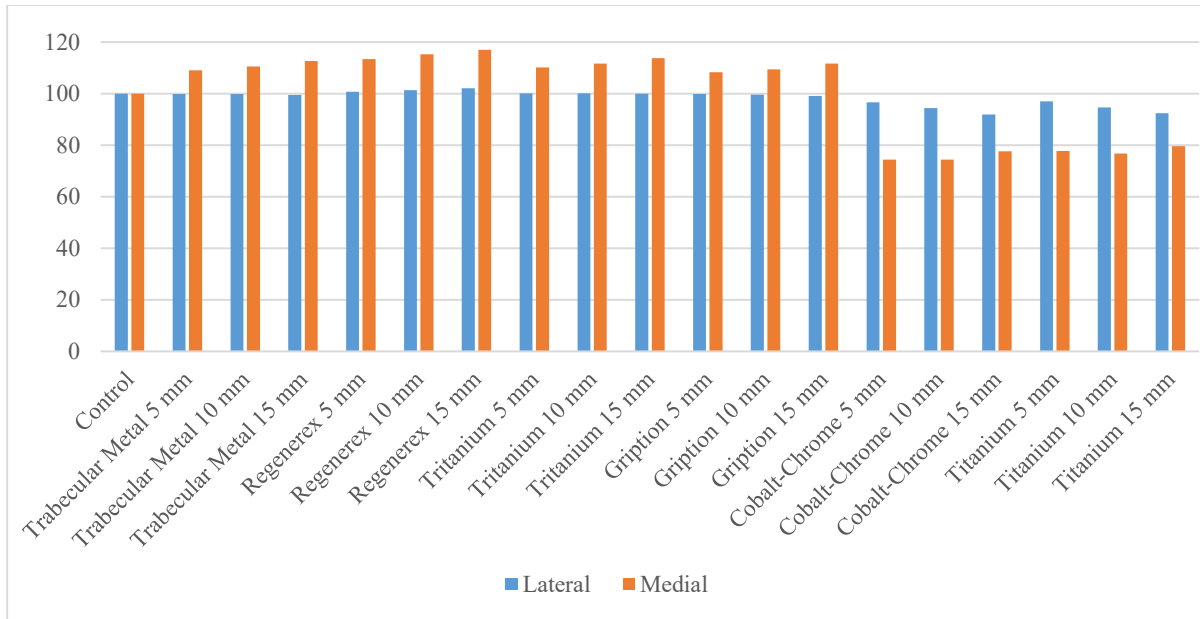


**Figure 78** - Flexion 90°: Average Von Mises bone stress analysing the local region of interest (depth of 10 mm) and comparing all the trend of all the thicknesses and all the biomaterials to the control model and among them.

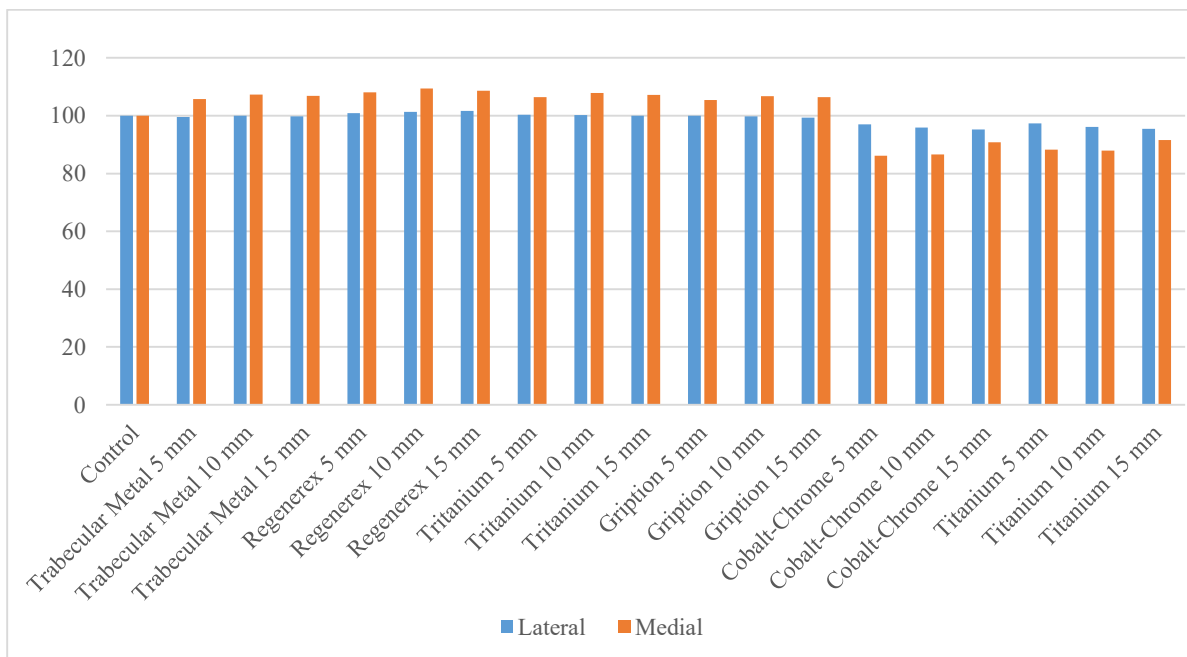


**Figure 79** - Flexion 90°: Average Von Mises bone stress analysing the global region of interest (depth of 50 mm) and comparing all the trend of all the thicknesses and all the biomaterials to the control model and among them.

Analysing both the graphical representation of the Von Mises stress distribution at the tibia – augment interface and the results in terms of percentages (locally and globally), the trend is the same of the other flexion angle.

So, it is possible to conclude that analysing different thicknesses of the augment placed proximally on the tibial medial side, different flexion angles and different porous metals which have Young's modulus similar to that of cancellous bone, no significant change results. On the contrary, if the behaviour of the porous metals is compared to that of convention metals, a relevant change in terms of bone stress is reported: locally, solid metals leads to a reduction of the average Von Mises stress of about 30%, regardless of the flexion angles.

Therefore, it is possible to demonstrate that Von Mises stress distribution is more sensible to the stiffness of the material rather than the flexion angle or the thickness of the augment.

#### 4.1.4 Shear stress: flexion angle of $0^\circ$

In this section, the change in bone Shear stress caused by a proximal tibial augment of 5 – 10 – 15 mm, placed on the medial side of the tibia is investigated, comparing all the porous and solid biomaterials. For each configuration, a flexion angle of  $0^\circ$  is set and the “Control Model” is defined as that model where no augment is implanted. With the purpose of comparing the effects of the insertion of an augment, a graphical representation of the Shear stress distribution at the bone-augment interface and the results are shown in the following figures.

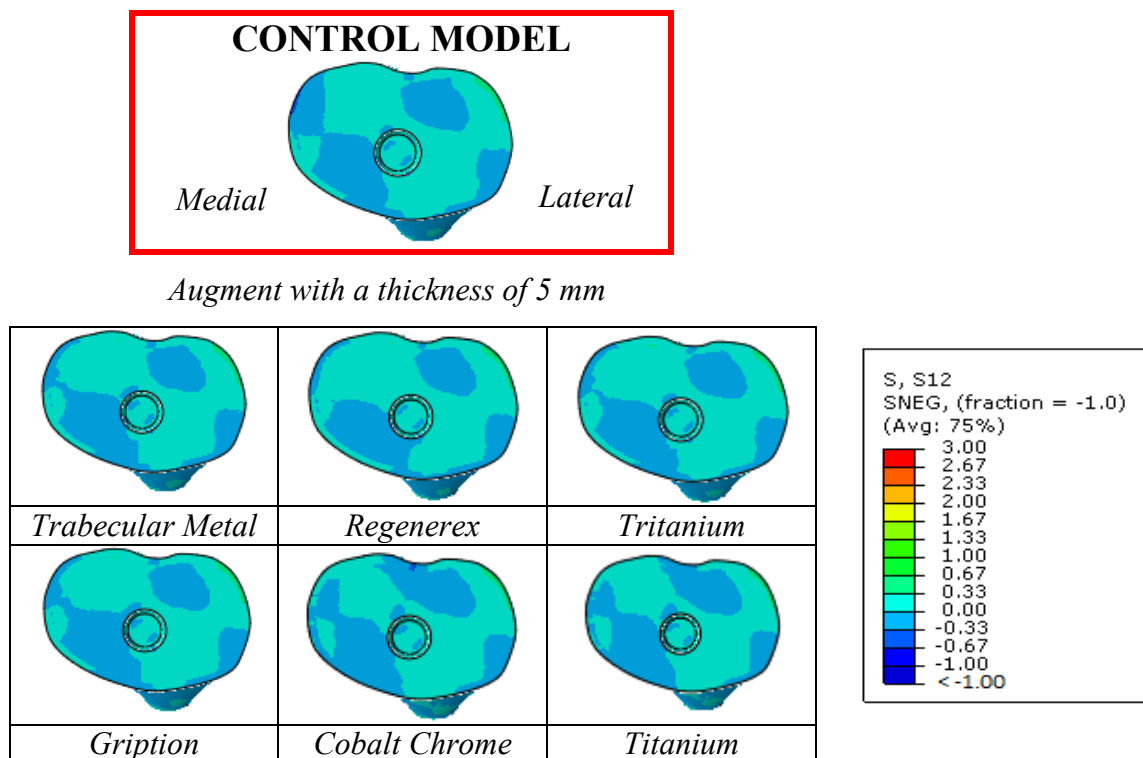


**Figure 80** - Shear stress distribution at tibia – augment interface for a flexion angle of  $0^\circ$  and an augment of 5 mm

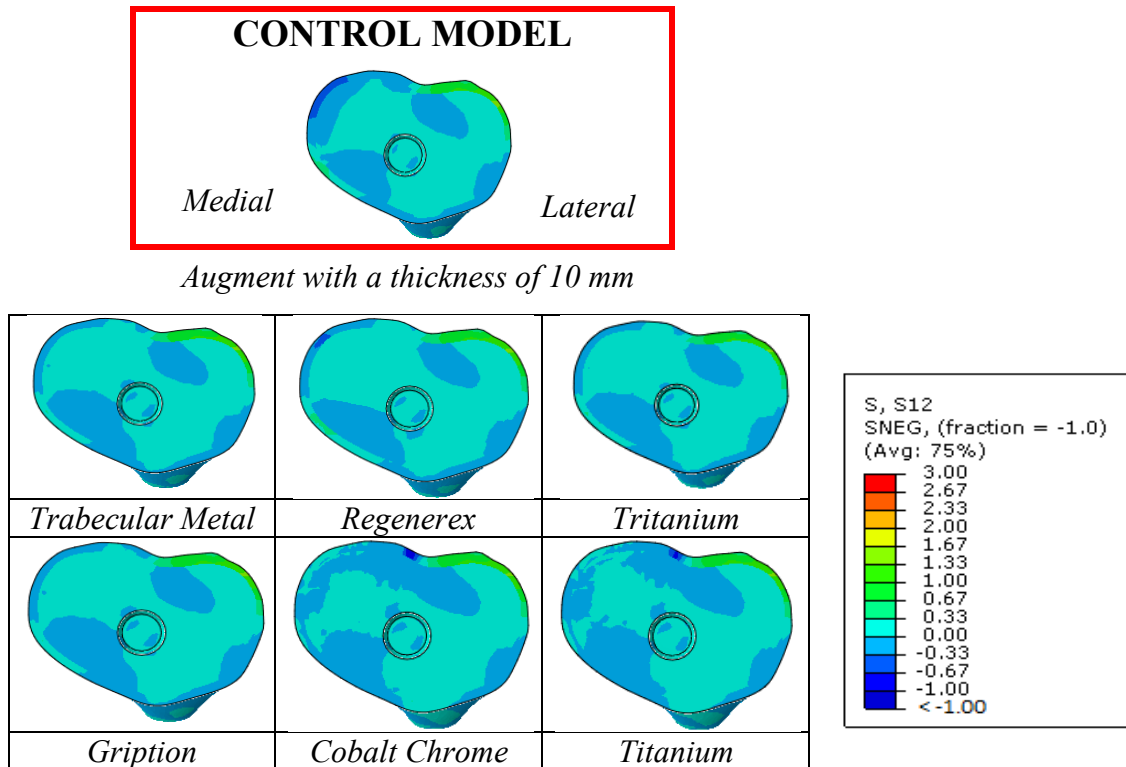


**Figure 81** - Shear stress distribution at tibia-augment interface for a flexion angle of 0° and an augment of 10 mm.

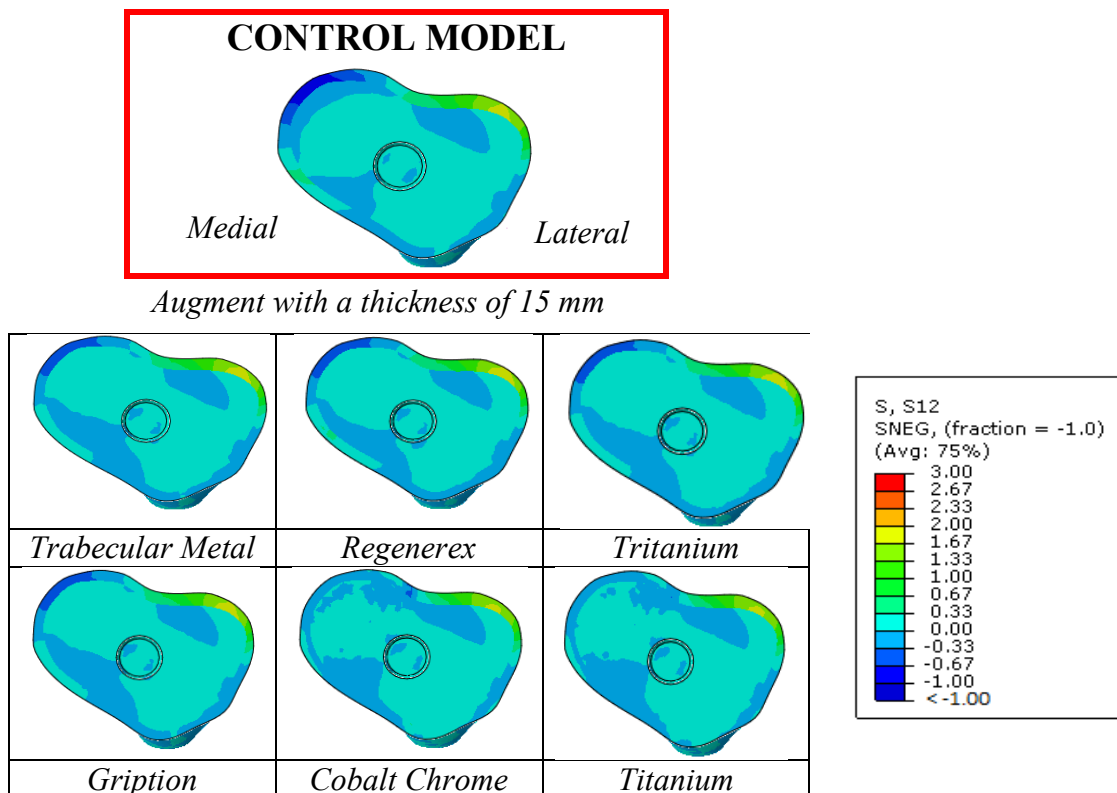


**Figure 82** - Shear stress distribution at tibia-augment interface for a flexion angle of 0° and an augment of 15 mm.

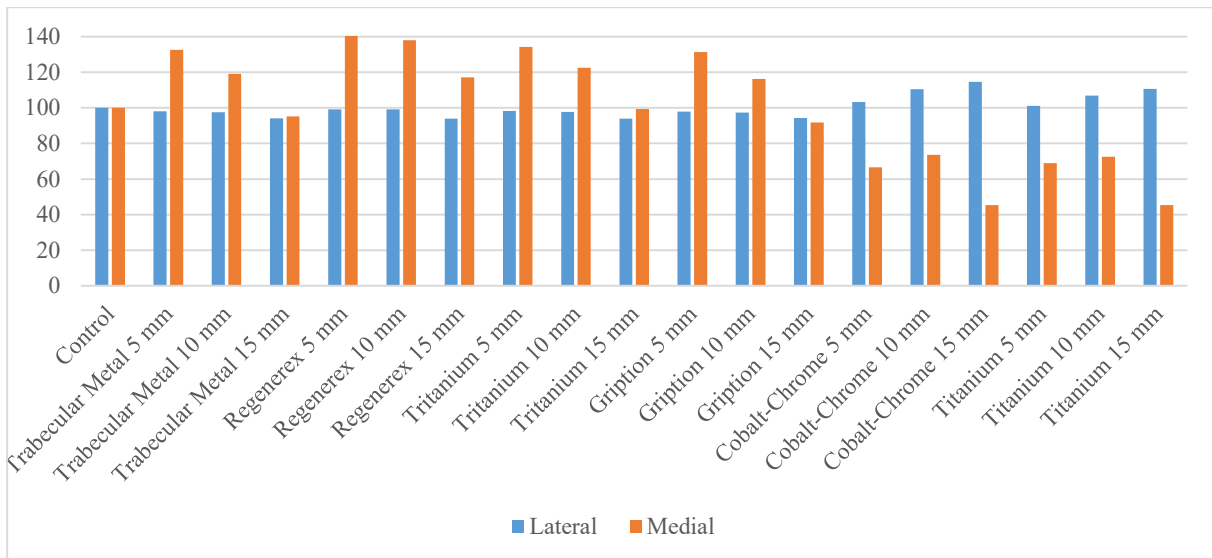


**Figure 83** - Flexion 0°: Average Shear bone stress analysing the local region of interest (depth of 10 mm) and comparing all the trend of all the thicknesses and all the biomaterials to the control model and among them.

Analysing the behaviour of the porous metals, it is possible to notice that no change is visible on the lateral side, regardless of the thickness, while the main variation is reported on the medial side: an increase in terms of bone stress up 40% for a distal augment made of Regenerex, with a thickness of 5 mm. By contrast, conventional metals induce not only a change on the medial side (reduction up to around 60% for the Co-Cr with a thickness of 15 mm) but also an increase of the Von Mises stress on the lateral side (less than 20%).

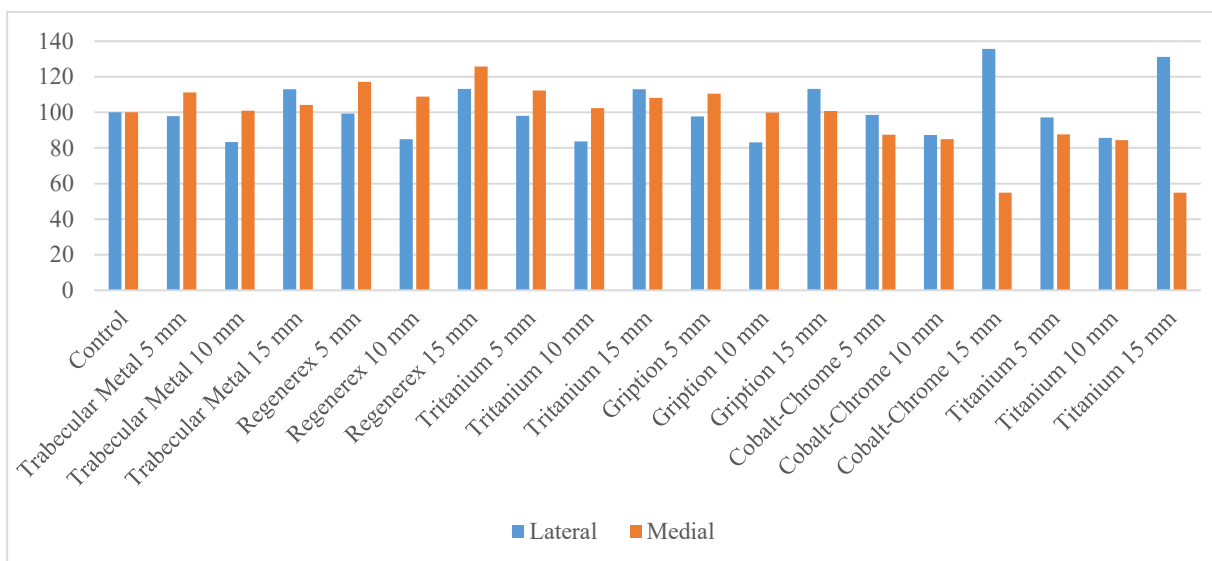


**Figure 84** - Flexion 0°: Average Shear bone stress analysing the global region of interest (depth of 50 mm) and comparing all the trend of all the thicknesses and all the biomaterials to the control model and among them.

Globally, looking at porous metal, it is possible to see that there is also a variation on the lateral side, but the gap is reduced. Conventional metals cause an increment (up to approximately 40% for a thickness of 15 mm) in terms of shear stress on the lateral side, while the distribution has improved on the medial side.

#### 4.1.5 Shear stress: flexion angle of $45^\circ$

As stated above, the change in bone Shear stress caused by a proximal tibial augment of 5 – 10 – 15 mm, placed on the medial side of the tibia is investigated, comparing all the porous and solid biomaterials. For each configuration, a flexion angle of  $45^\circ$  is set and the “Control Model” is defined as that model where no augment is implanted. With the purpose of comparing the effects of the insertion of an augment, a graphical overview of the Shear stress distribution at the bone-augment interface is shown in the following figures.

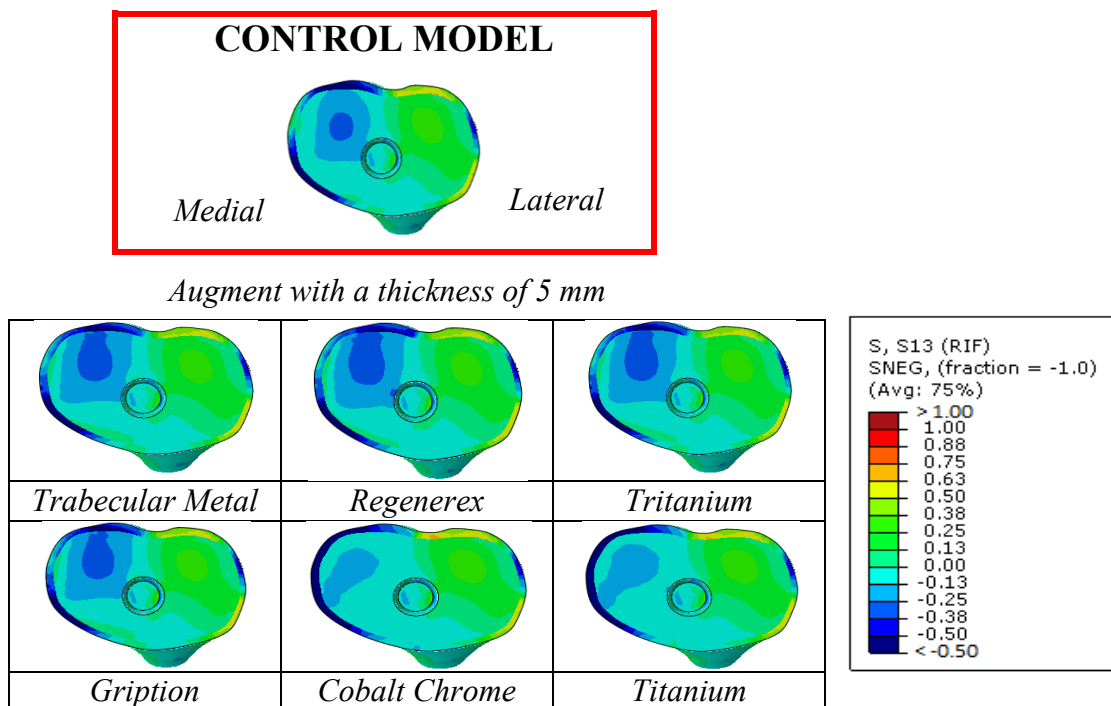


**Figure 85** - Shear stress distribution at tibia-augment interface for a flexion angle of  $45^\circ$  and an augment of 5 mm.

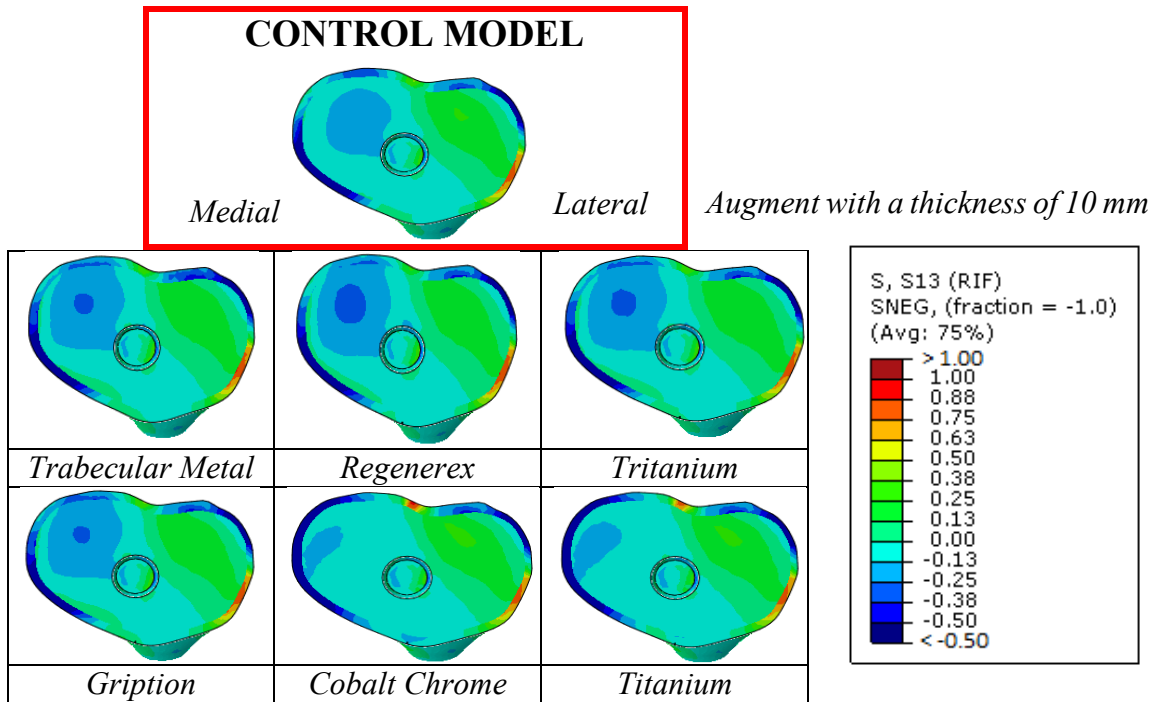


**Figure 86** - Shear stress distribution at tibia-augment interface for a flexion angle of 45° and an augment of 10 mm.

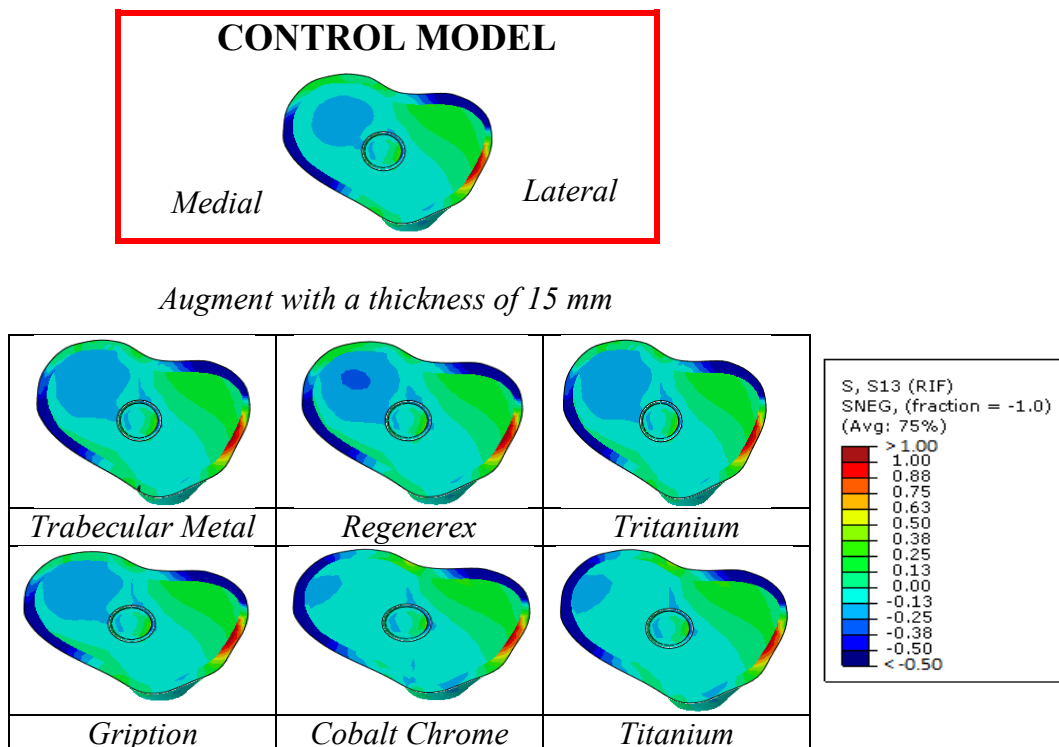


**Figure 87** - Shear stress distribution at tibia-augment interface for a flexion angle of 45° and an augment of 10 mm.

By analysing the distribution of the shear stress at the interface bone – augment, it is possible to see that the bone shear stress changes mainly in the region close to the augment (medial side) both for the porous and for the conventional metals. On the lateral side, there is no significant variation.

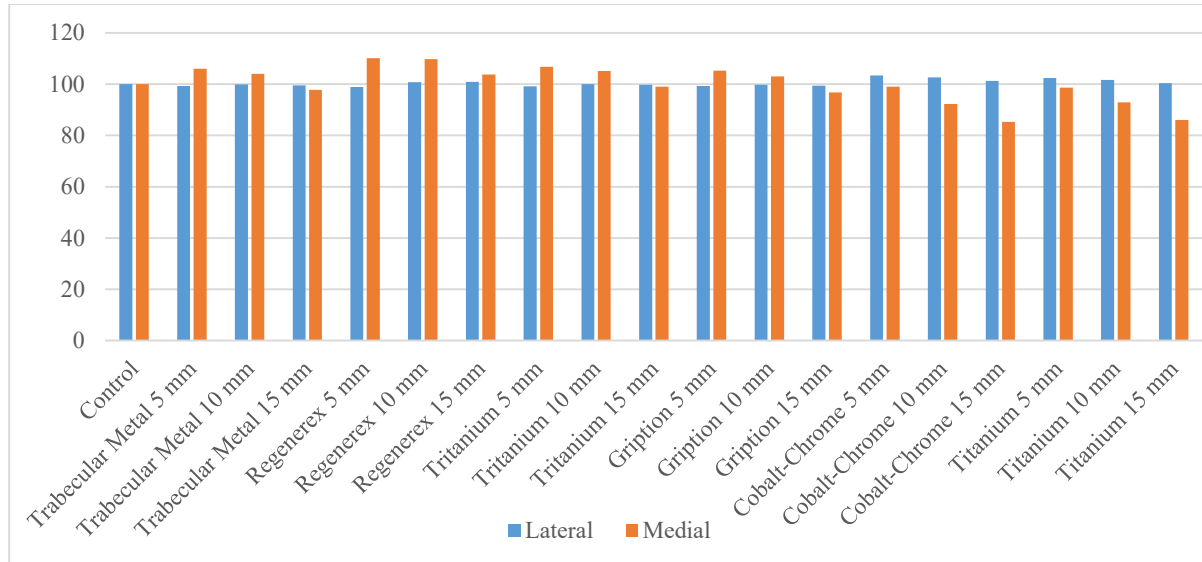


**Figure 88** - Flexion 45°: Average Shear bone stress analysing the local region of interest (depth of 10 mm) and comparing all the trend of all the thicknesses and all the biomaterials to the control model and among them.

Looking at what happens locally, if an augment of porous metal is placed proximally on the medial side of the tibia, there is no variation in terms of shear stress on the lateral side, always compared to that of control model. While the insertion of a porous augment induces an increase of the shear stress which is maximum for a thickness of 5 mm. A rise of 10% is visible for an augment of 5 mm, made of Regenerex which is the porous metal with the lowest stiffness. Furthermore, it is possible to see that if an augment of 15 mm is placed on the medial side of the tibia, the gap between the shear stress distribution of the control model and that of a model with an augment, made of any biomaterial is reduced dramatically.

For the conventional metals, it is possible to notice the same trend but at lower level: no change for the lateral side, while analysing the medial side, the average shear stress is similar to that of the control model if an augment of 5 mm is implanted (both Co-Cr and Ti), but if an augment of 15 mm is considered, the value falls to 85 and 86% for Co-Cr and Ti, respectively.

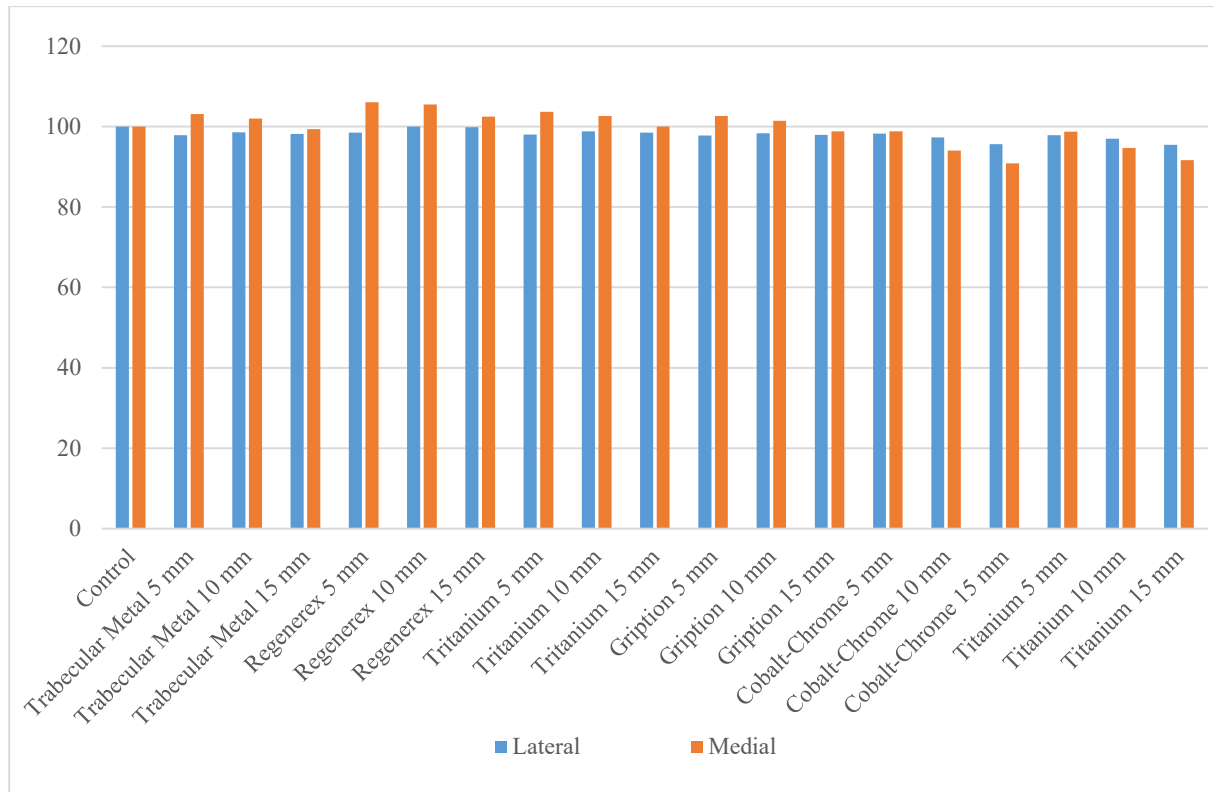


**Figure 89** - Flexion 45°: Average Shear bone stress analysing the global region of interest (depth of 50 mm) and comparing all the trend of all the thicknesses and all the biomaterials to the control model and among them.

Globally, the same pattern is visible but with a lower gap: the medial average shear stress reaches the minimum of 90% at a thickness of 15 mm for conventional metals, while the value of the shear stress is almost that of control if an augment of 15 mm made of Trabecular Metal or Tritanium is implanted.

#### 4.1.6 Shear stress: flexion angle of 90°

For each configuration, a flexion angle of 90° is set and an augment of 5 – 10 – 15 mm is placed on the medial side of the tibia. In the following figures, a graphical overview is reported:

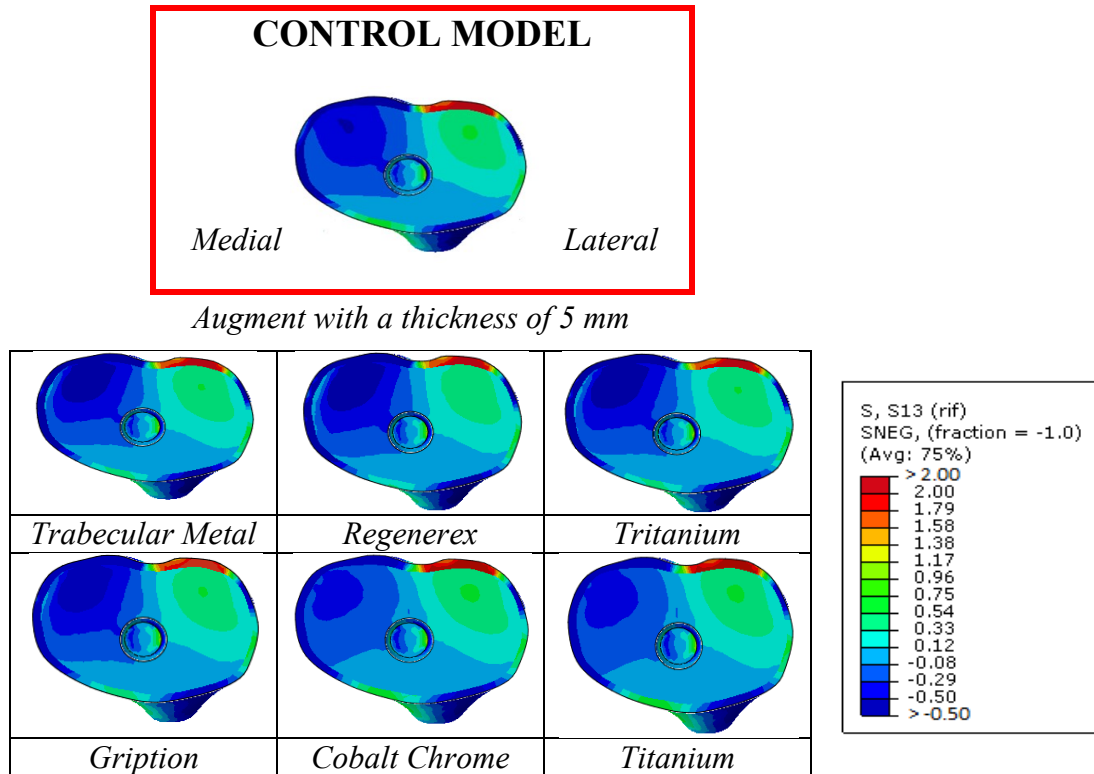


**Figure 90** - Shear stress distribution at tibia-augment interface for a flexion angle of 90° and an augment of 5 mm.

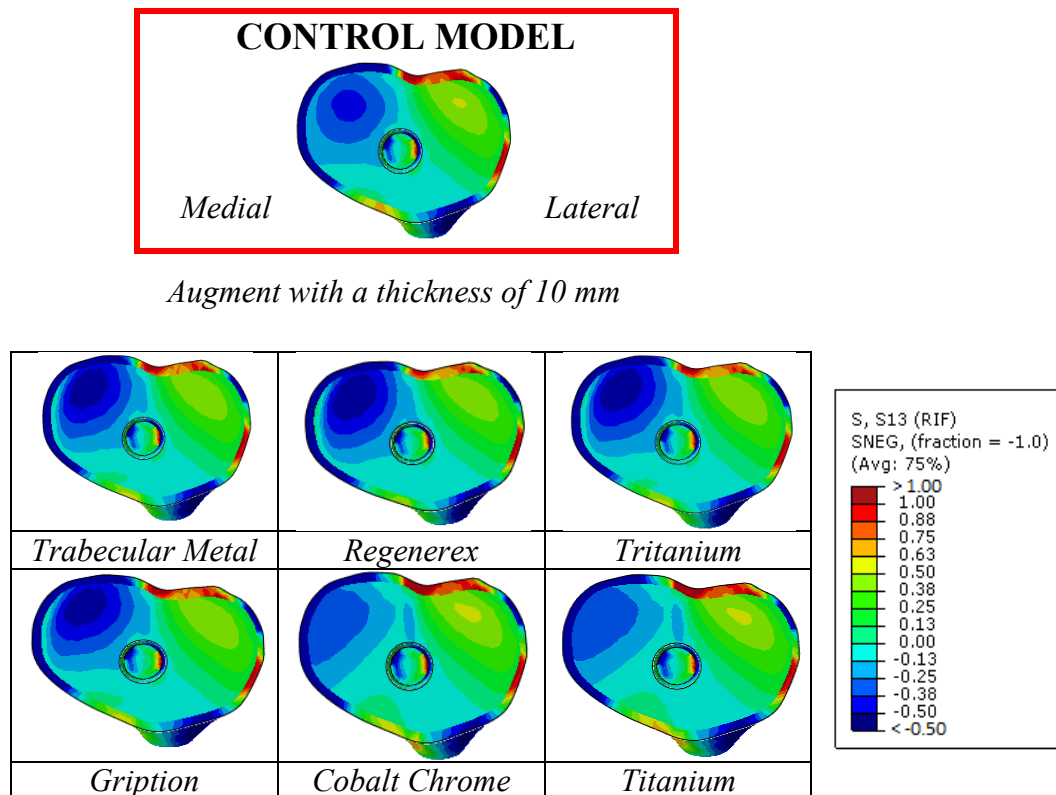


**Figure 91**- Shear stress distribution at tibia-augment interface for a flexion angle of 90° and an augment of 10 mm.

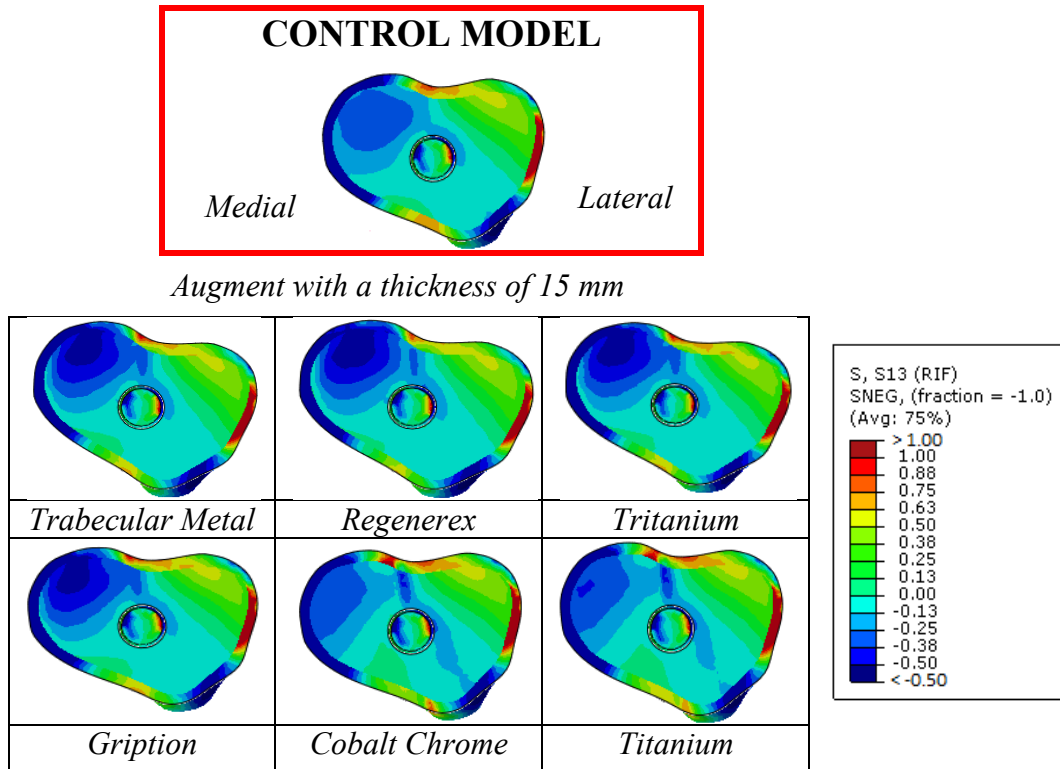


**Figure 92** - Shear stress distribution at tibia-augment interface for a flexion angle of 90° and an augment of 15 mm.

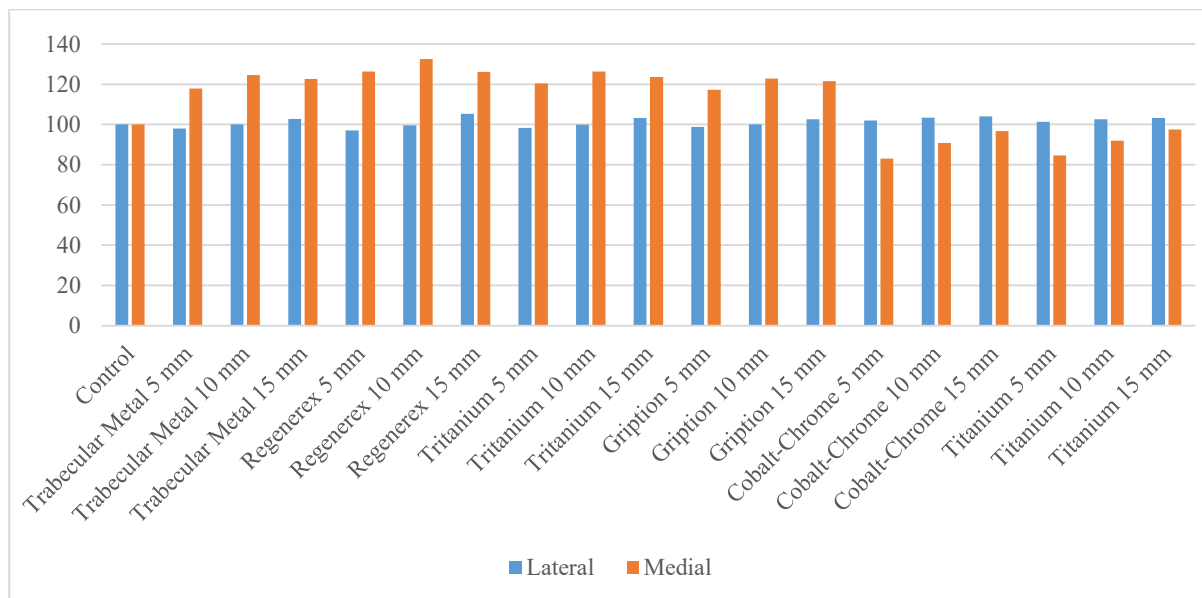


**Figure 93** - Flexion 90°: Average Shear bone stress analysing the local region of interest (depth of 10 mm) and comparing all the trend of all the thicknesses and all the biomaterials to the control model and among them.

Locally, by considering the porous metals, it is possible to notice that the sharpest rise (from 10 – 33%) in terms of the average shear stress is on the medial side, while on the lateral there is no significant variation. Furthermore, the peak in terms of shear stress is visible when an

augment of 10 mm is placed on the medial tibial side: in particular, when it is made of Regenerex, the shear stress reaches a maximum of 133%. Looking at the conventional metals, the most critical condition appears when an augment of 5 mm is implanted: there is a reduction of 17% for Co-Cr and 15% for Ti.

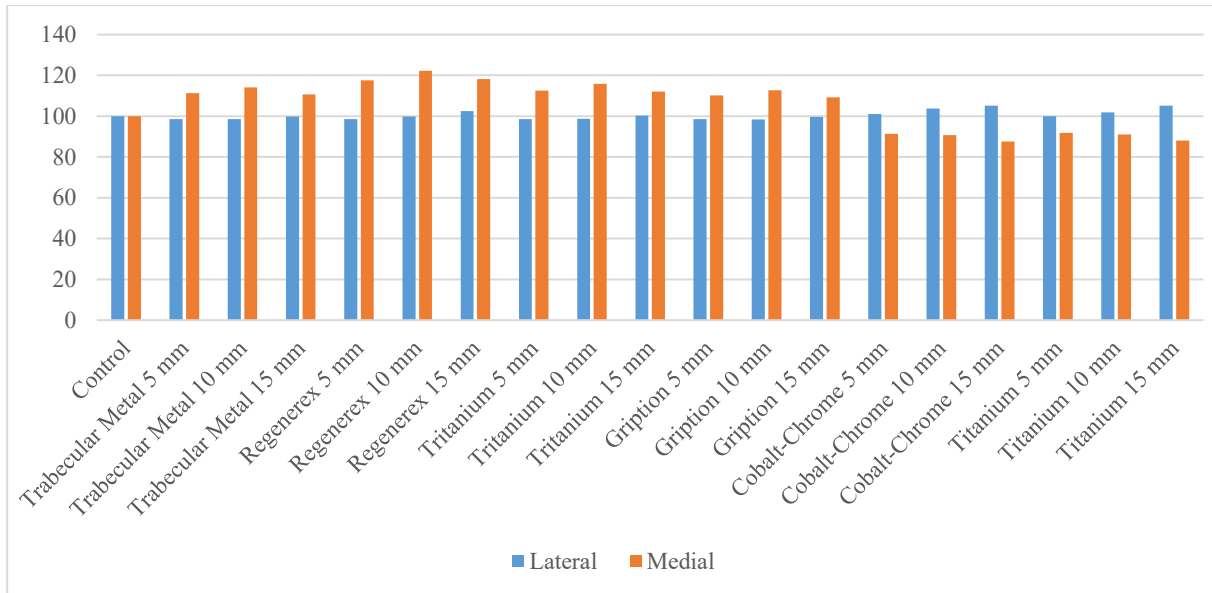


**Figure 94** - Flexion 90°: Average Shear bone stress analysing the global region of interest (depth of 50 mm) and comparing all the trend of all the thicknesses and all the biomaterials to the control model and among them.

Globally, the pattern is the same that it is possible to notice at the local level, but the increase and the decrease of the shear stress is milder for porous and solid metals respectively.

## 4.2 Femoral model

In this section, the same analysis of the tibial model will be carried out for the femoral model. The results obtained from the FEA are shown in terms of the average Von Mises and shear stress at the interface bone-augment, taking into account the three flexion angles ( $0^\circ$  -  $45^\circ$  -  $90^\circ$ ), the two different thicknesses for the distal femoral augment (5-10 mm), the two different thicknesses for the posterior femoral augment (5-10 mm) and the several biomaterials (porous: Trabecular Metal, Regenerex, Tritanium and Gription; solid: Cobalt – Chrome and Titanium). Each analysed configuration will be compared to the others and to the control model.

### 4.2.1 Von Mises stress: flexion angle of $0^\circ$

In this paragraph, the change in bone Von Mises stress caused by the insertion of a distal and then a posterior augment of 5 – 10 mm, placed on the medial condyle of the femur is investigated, comparing all the porous and solid biomaterials. For each configuration, a flexion angle of  $0^\circ$  is set and the “Control Model” is defined as that model where no augment is implanted. With the purpose of comparing the effects of the insertion of an augment, a graphical overview of the Von Mises stress distribution at the bone-augment interface is shown in the following figures.

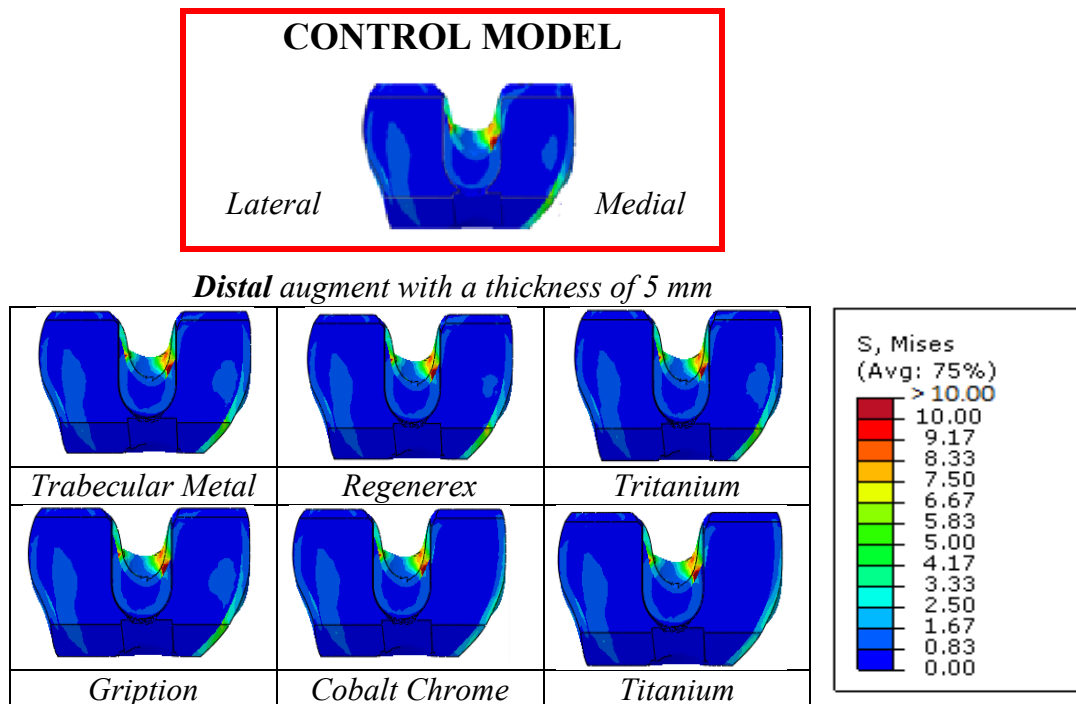
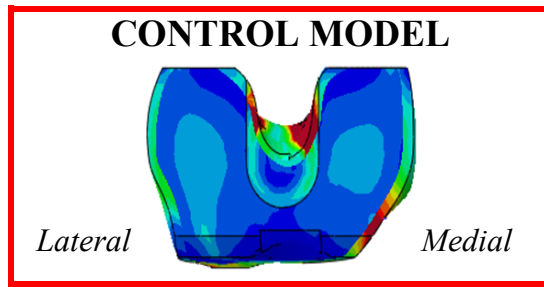


**Figure 95** - Von Mises stress distribution at femur – augment interface for a flexion angle of  $0^\circ$  and a distal augment of 5 mm



*Distal augment with a thickness of 10 mm*

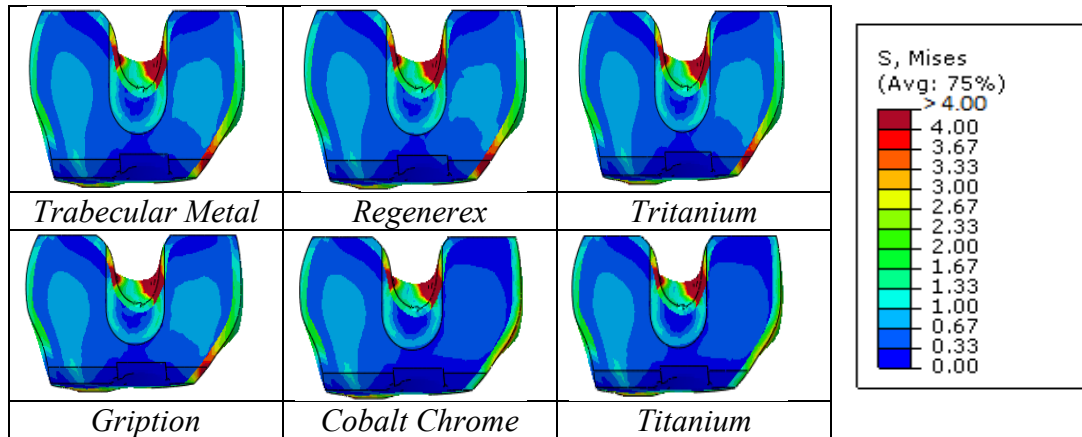
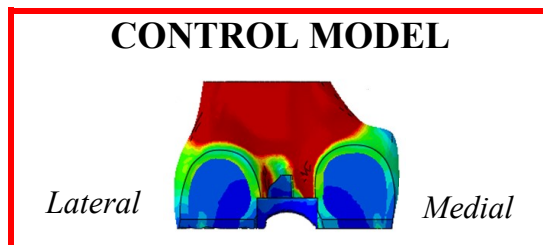


**Figure 96** - Von Mises stress distribution at femur – augment interface for a flexion angle of 0° and a distal augment of 10 mm



*Posterior augment with a thickness of 5 mm*

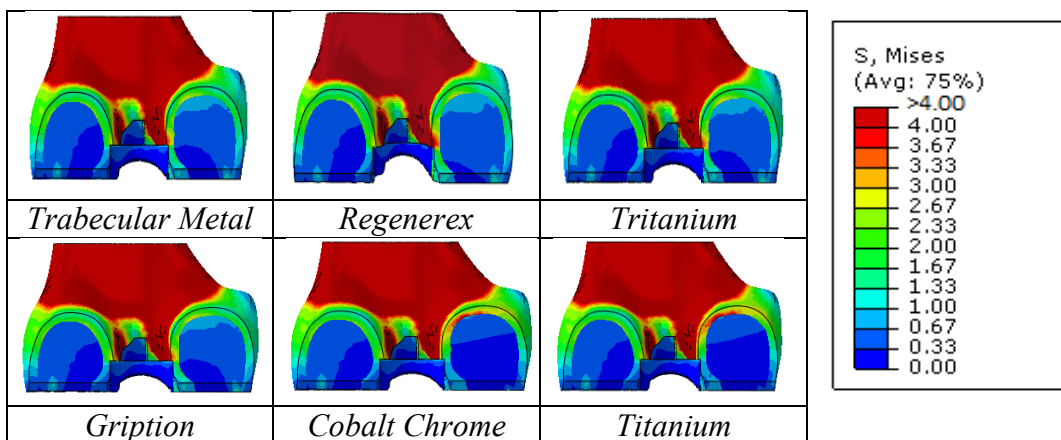


**Figure 97** - Von Mises stress distribution at femur – augment interface for a flexion angle of 0° and a posterior augment of 5 mm

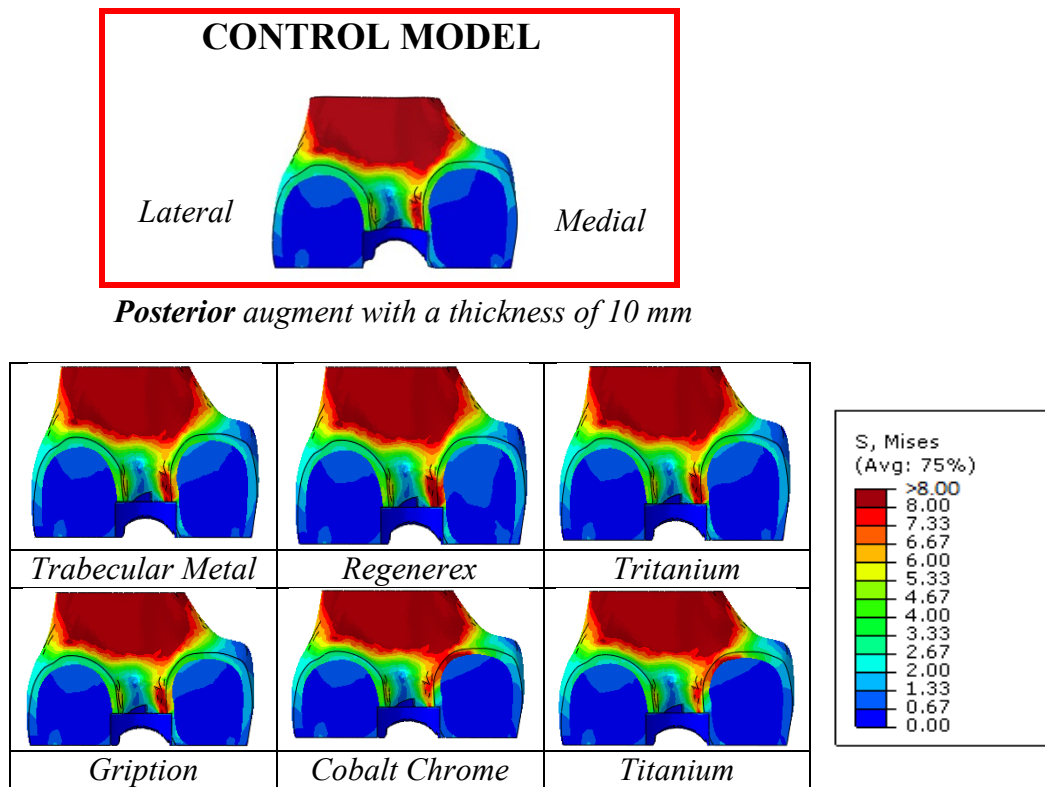


**Figure 98** - Von Mises stress distribution at femur – augment interface for a flexion angle of  $0^\circ$  and a posterior augment of 10 mm

The graphical overviews of the average Von Mises stress at the interface bone – augment, for both these positions (distal and posterior) point out that the stress distribution on the lateral side is very close to that of reference model for each configuration (posterior and distal), for each thickness of the augment (5 or 10 mm) and for each material (both porous and solid). For both positions, the main change in terms of bone stress is visible on the medial side.

The quantitative values are reported as follows, for both cases, considering the local and global effects.

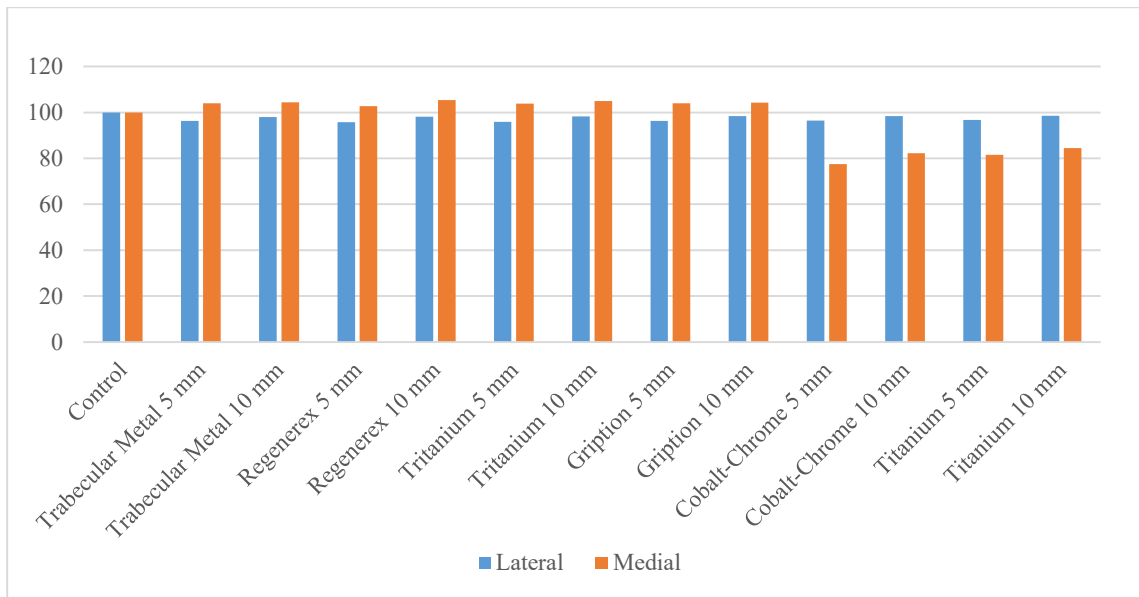


**Figure 99** - Flexion 0°: Average Von Mises bone stress analysing the local region of interest (depth of 10 mm), comparing all the trend of all the thicknesses and all the biomaterials to the control model and among them, and considering an augment placed distally on the medial femoral condyle.

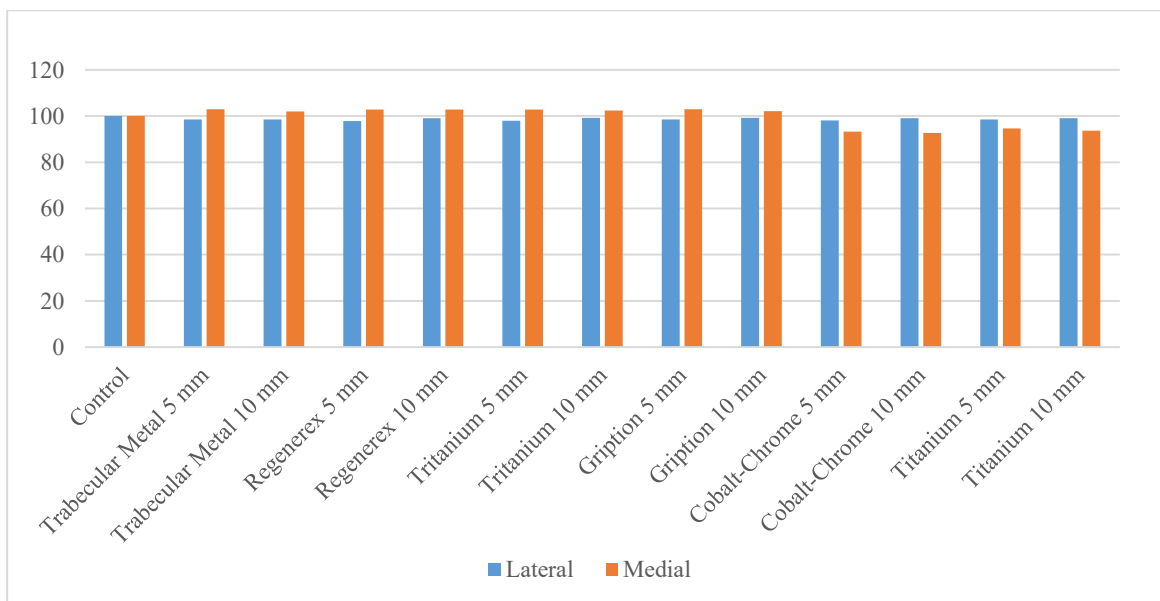


**Figure 100** - Flexion 0°: Average Von Mises bone stress analysing the global region of interest (depth of 50 mm), comparing all the trend of all the thicknesses and all the biomaterials to the control model and among them, and considering an augment placed distally on the medial femoral condyle.

As stated above, these values demonstrate numerically what it is possible to highlight in the graphical overviews. Locally, no significant change occurs on the lateral side, in term of bone stress, for both types of materials (porous and dense): a slight decrease of the 4% for a thickness of 5 mm and a reduction of the 2% for the thickness of 10 mm.

Von Mises stress distribution varies especially on the medial side, where the rate of increase goes from 2% for an augment of 5 mm made of Regenerex to 5.5 % for an augment of 10 mm made of Regenerex. While a very slight increase ( $< 1\%$ ) takes place by passing from a thickness of 5 mm to a 10 mm (for the other porous materials). Analysing the behaviour of the conventional metals, there is a sharp drop of the average Von Mises stress of 22% for Co – Cr augment with a thickness of 5 mm. This fall is reduced to 20% for Co-Cr augment with a thickness of 10 mm. This same trend is visible for Ti but the decrease goes from 18.5% (5 mm) to 16% (10 mm).

Globally, Von Mises stress does not change both on the lateral side and medial side ( $< 1\%$ ) for porous metals, and for all the thicknesses. Looking at the conventional metals, there is no change in terms of bone stress laterally, while a reduction occurs on the medial side ( $< 10\%$ ).

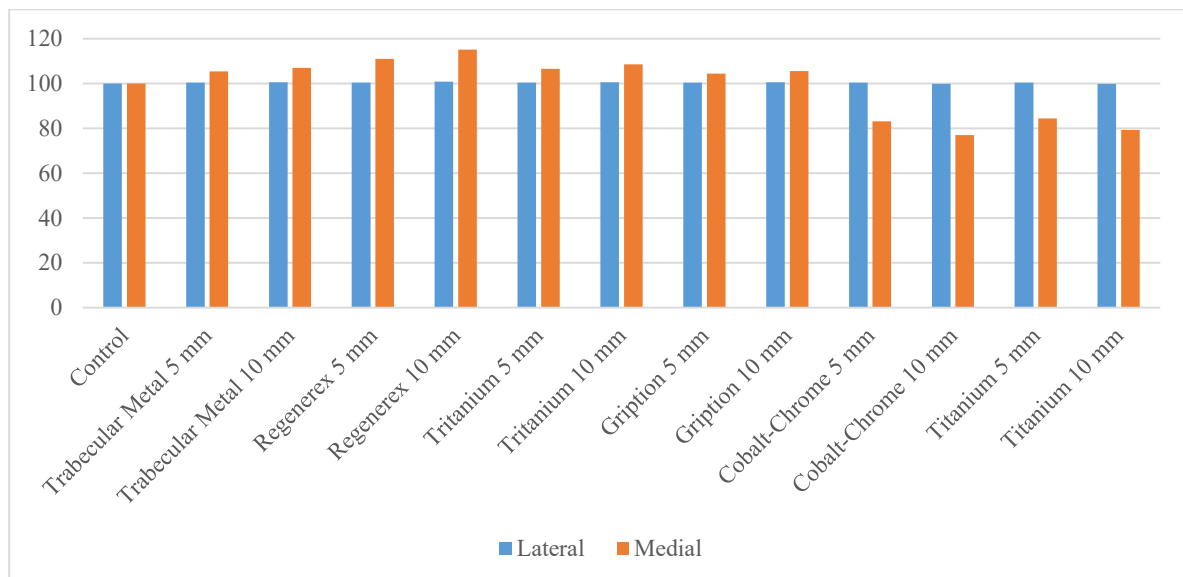


**Figure 101** - Flexion 0°: Average Von Mises bone stress analysing the local region of interest (depth of 10 mm), comparing all the trend of all the thicknesses and all the biomaterials to the control model and among them, and considering a posterior augment placed on the medial femoral condyle.

Locally, analysing what induces the insertion of a posterior augment, it is possible to notice a similar trend to that caused by a distal augment. The lateral side is not subjected to change in terms of bone stress, both for porous and solid metals.

The main change occurs on the medial side:

- For porous metals there is an increase of the bone stress up to 15% for a Regenerex augment with a thickness of 10 mm. Furthermore, passing from 5mm to 10 mm there is a slight increase for stiffer porous metals, while for Regenerex there is an increase of 4%.

- For solid metals there is the opposite trend: a reduction of approximately 15-17% for a thickness of 5 mm and a fall of about 21-23% for a thickness of 10 mm.

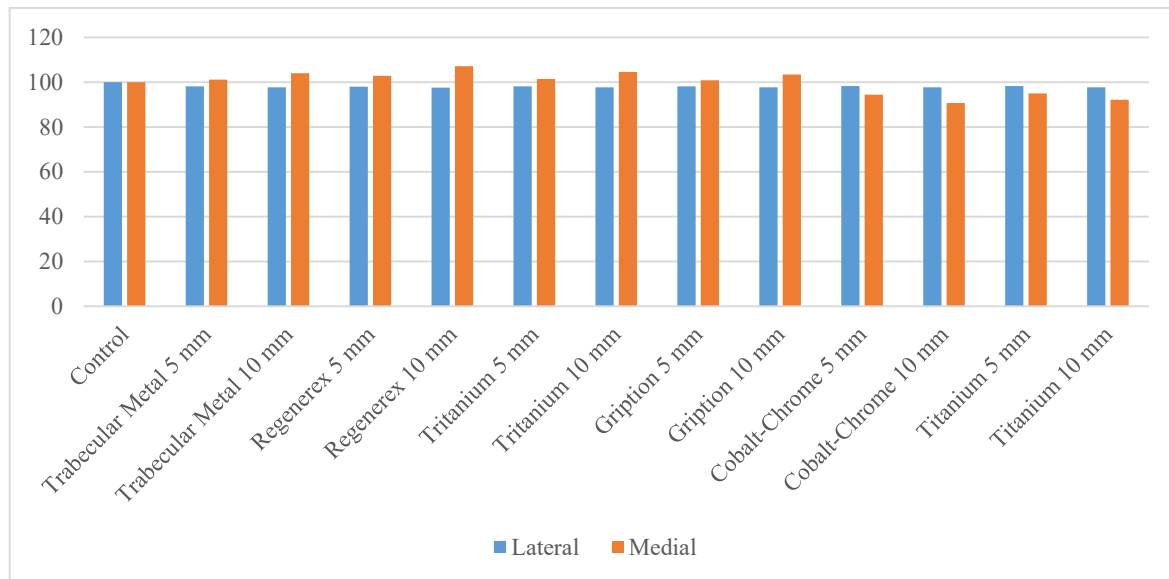


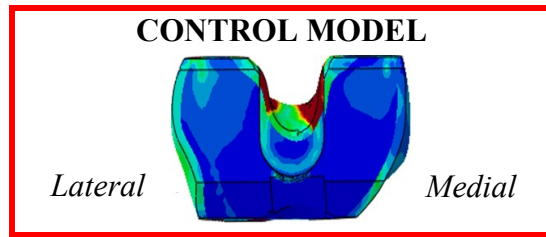
**Figure 102** - Flexion 0°: Average Von Mises bone stress analysing the global region of interest (depth of 50 mm), comparing all the trend of all the thicknesses and all the biomaterials to the control model and among them, and considering a posterior augment placed on the medial femoral condyle.

Globally, the pattern is the same but the gap is reduced for both types of materials. No change occurs on the lateral side, while for the medial side:

- Porous metals present a rise less than 10%.
- Conventional metals show a reduction less than 10%.

#### 4.2.2 Von Mises stress: flexion angle of 45°

In this paragraph, the change in bone Von Mises stress caused by the insertion of a distal and then a posterior augment of 5 – 10 mm, placed on the medial condyle of the femur is investigated, comparing all the porous and solid biomaterials. For each configuration, a flexion angle of 45° is set and the “Control Model” is defined as that model where no augment is implanted. With the purpose of comparing the effects of the insertion of an augment, a graphical overview of the Von Mises stress distribution at the bone-augment interface is shown in the following figures.



*Distal augment with a thickness of 5 mm*

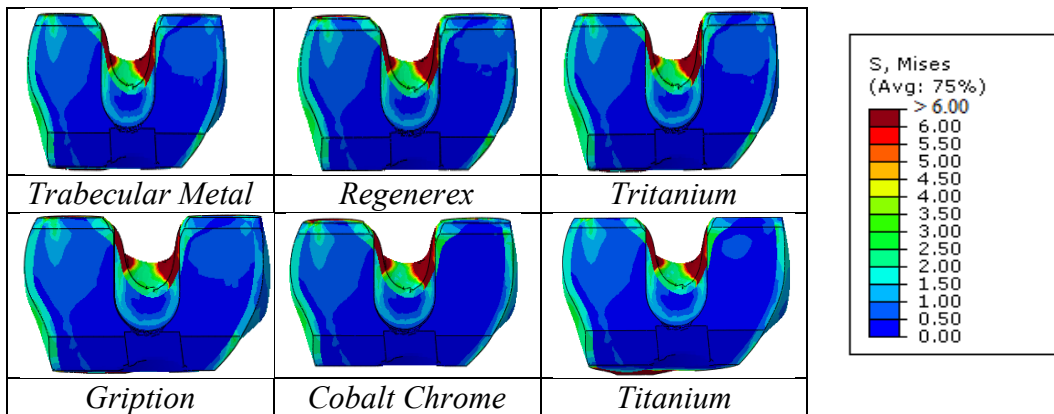
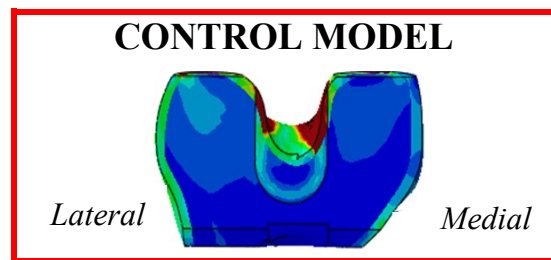


**Figure 103** - Von Mises stress distribution at femur – augment interface for a flexion angle of 45° and a distal augment of 5 mm



*Distal augment with a thickness of 10 mm*

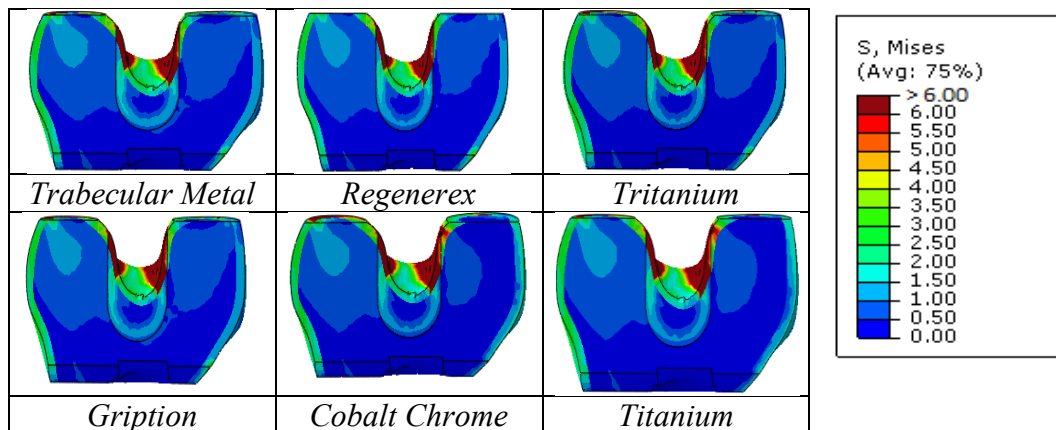
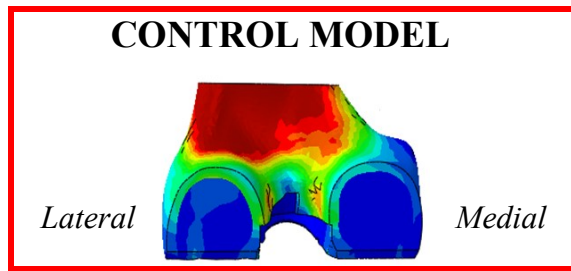


**Figure 104** - Von Mises stress distribution at femur – augment interface for a flexion angle of 45° and a distal augment of 10 mm



*Posterior augment with a thickness of 5 mm*

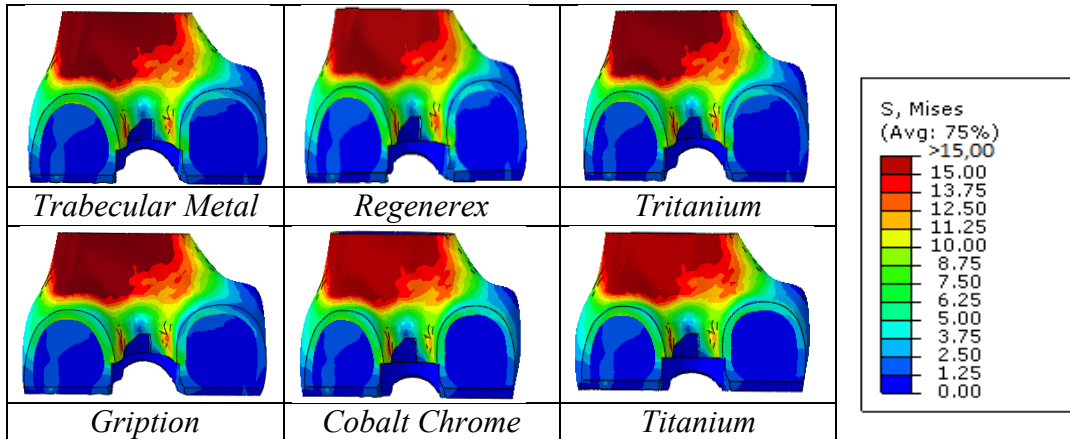
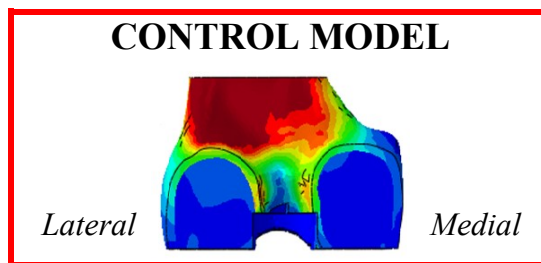


**Figure 105** - Von Mises stress distribution at femur – augment interface for a flexion angle of 45° and a posterior augment of 5 mm



*Posterior augment with a thickness of 10 mm*

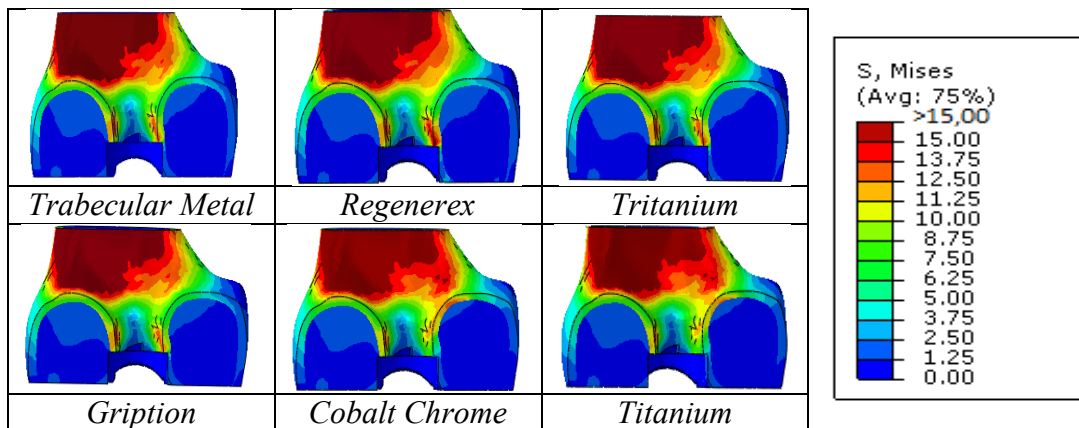


**Figure 106** - Von Mises stress distribution at femur – augment interface for a flexion angle of 45° and a posterior augment of 10 mm

Looking at the graphical overviews, the main change in terms of bone stress occurs on the medial side, while no significant variations are reported on the lateral side, both for porous and solid metals.

The quantitative values are reported as follows, for both cases, considering the local and global effects.

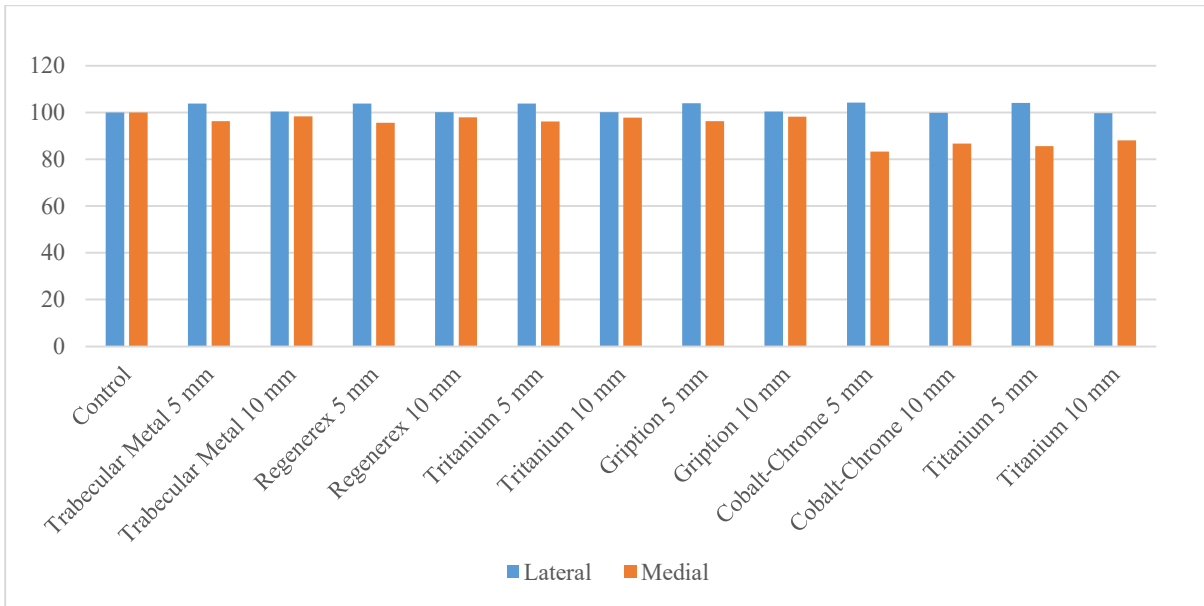


**Figure 107** - Flexion 45°: Average Von Mises bone stress analysing the local region of interest (depth of 10 mm), comparing all the trend of all the thicknesses and all the biomaterials to the control model and among them, and considering a distal augment placed on the medial femoral condyle.

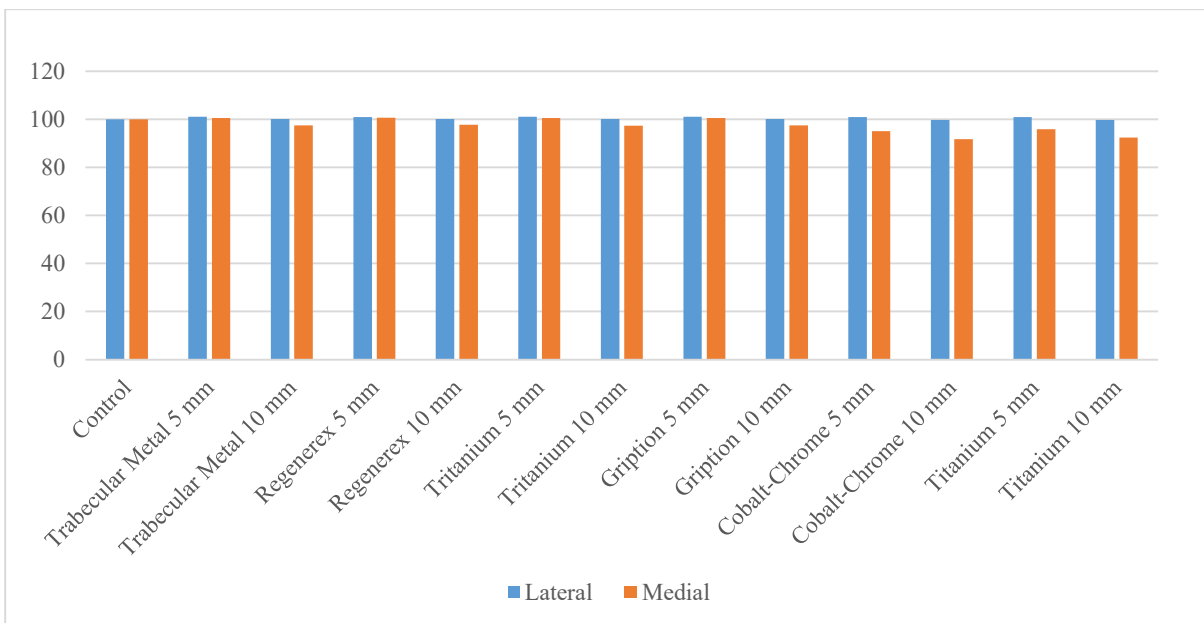


**Figure 108** - Flexion 45°: Average Von Mises bone stress analysing the global region of interest (depth of 50 mm), comparing all the trend of all the thicknesses and all the biomaterials to the control model and among them, and considering a distal augment placed on the medial femoral condyle.

Observing the quantitative values of the average Von Mises stress caused by the insertion of an augment distally on the medial side of the femur:

- Locally, a porous augment of 5 mm leads to an increase and a decrease in terms of bone stress of almost 4% on the lateral and medial side, respectively.
- A conventional augment causes the same trend for the lateral side (increase of 4% for an augment of 5 mm) while it induces a reduction of 15-16.5% and 12.5-13.5 % with a thickness of 5 mm and 10 mm, respectively, on the medial side.

Globally, the change of bone stress is reduced dramatically: in fact, it is possible to notice that all porous metals show a behaviour that is very close to that of control model! Analysing the conventional metals, the reduction of Von Mises stress is less than 10%.

The quantitative analysis carried out to show the effects of a posterior augment demonstrates that an increase of bone stress (up to 22% for Regenerex and a thickness of 10 mm) appears on the medial side when the augment is made of a porous metal. This increase is lower when a thickness of 5 mm is considered. No significant variations are induced on the lateral side both for porous and conventional metals. The opposite pattern is visible with a solid metal: there is a reduction of Von Mises which is maximum when an augment of 10 mm is implanted (up to 23.5%). Globally, the gap is reduced for both types of materials.

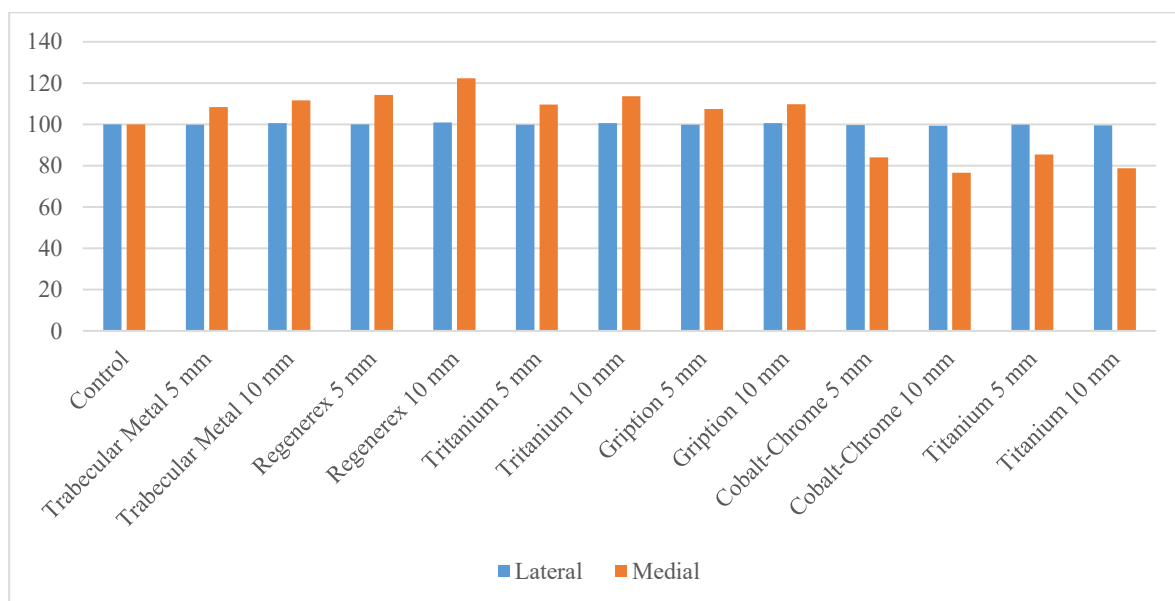


**Figure 109** - Flexion 45°: Average Von Mises bone stress analysing the local region of interest (depth of 10 mm), comparing all the trend of all the thicknesses and all the biomaterials to the control model and among them, and considering a posterior augment placed on the medial femoral condyle.

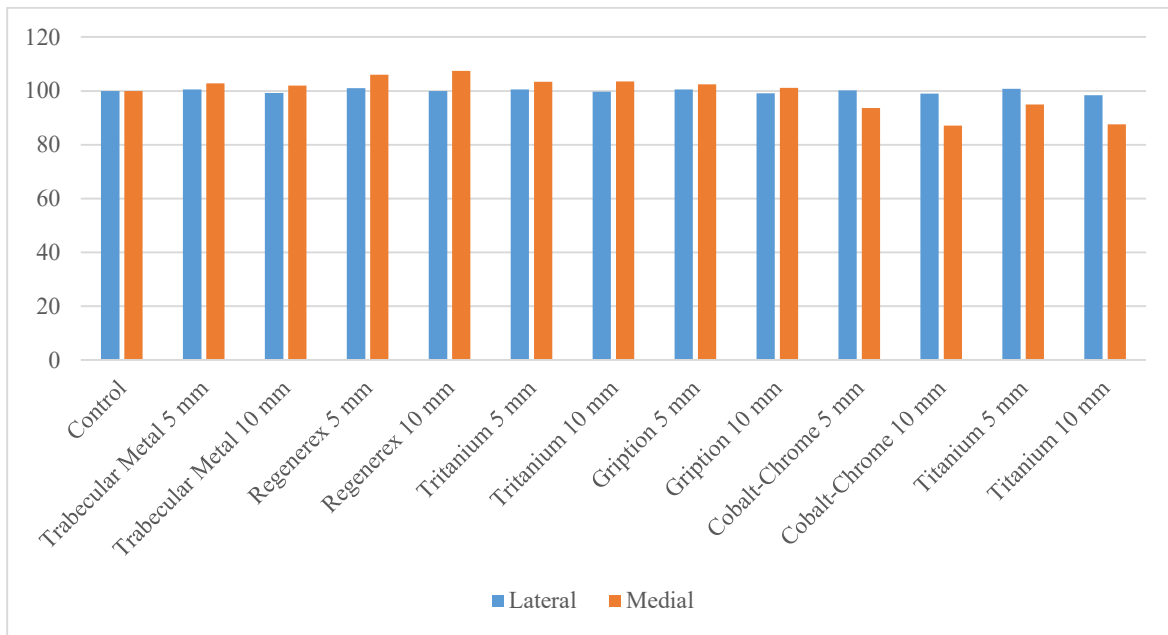


**Figure 110** - Flexion 45°: Average Von Mises bone stress analysing the global region of interest (depth of 50 mm), comparing all the trend of all the thicknesses and all the biomaterials to the control model and among them, and considering a posterior augment placed on the medial femoral condyle.

### 4.2.3 Von Mises stress: flexion angle of 90°

It is evaluated the insertion of a distal and then a posterior augment of 5 – 10 mm, placed on the medial condyle of the femur is investigated, comparing all the porous and solid biomaterials. For each configuration, a flexion angle of 90° is set and the “Control Model” is defined as that model where no augment is implanted. A graphical overview of the Von Mises stress distribution at the bone-augment interface is shown in the following figures.

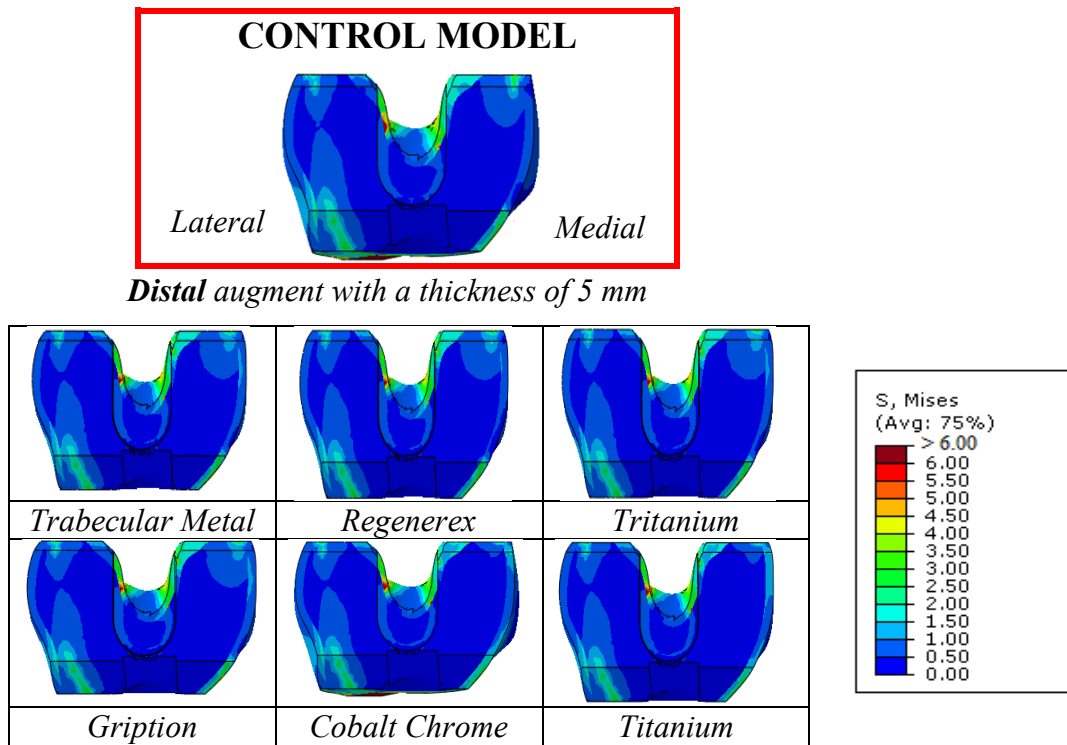


Figure 111 - Von Mises stress distribution at femur – augment interface for a flexion angle of 90° and a distal augment of 5 mm

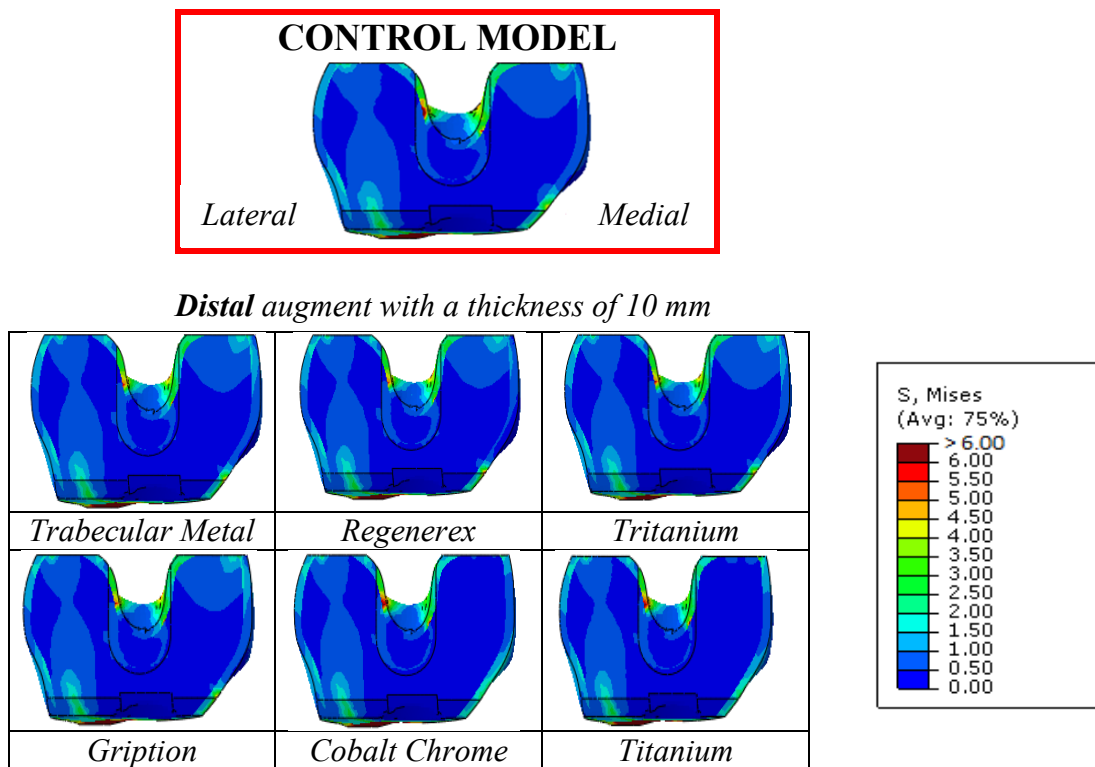
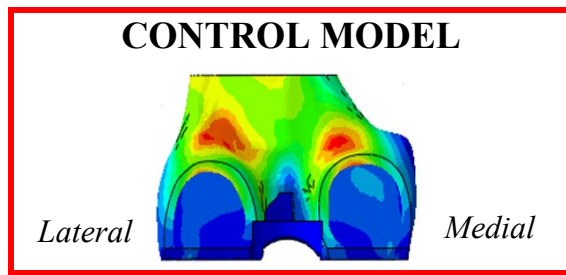
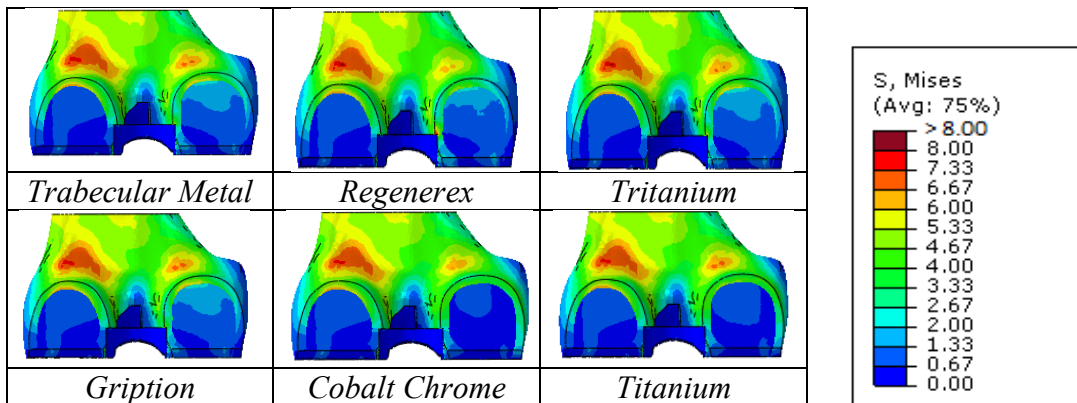


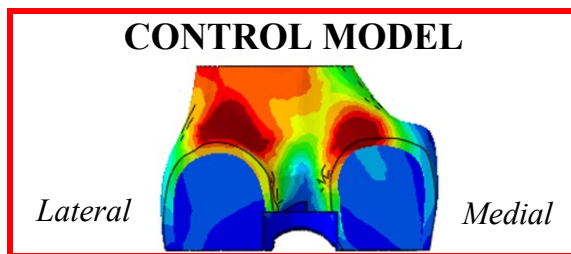
Figure 112 - Von Mises stress distribution at femur – augment interface for a flexion angle of 90° and a distal augment of 10 mm



*Posterior augment with a thickness of 5 mm*



**Figure 113** - Von Mises stress distribution at femur – augment interface for a flexion angle of 90° and a posterior augment of 5 mm



*Posterior augment with a thickness of 10 mm*

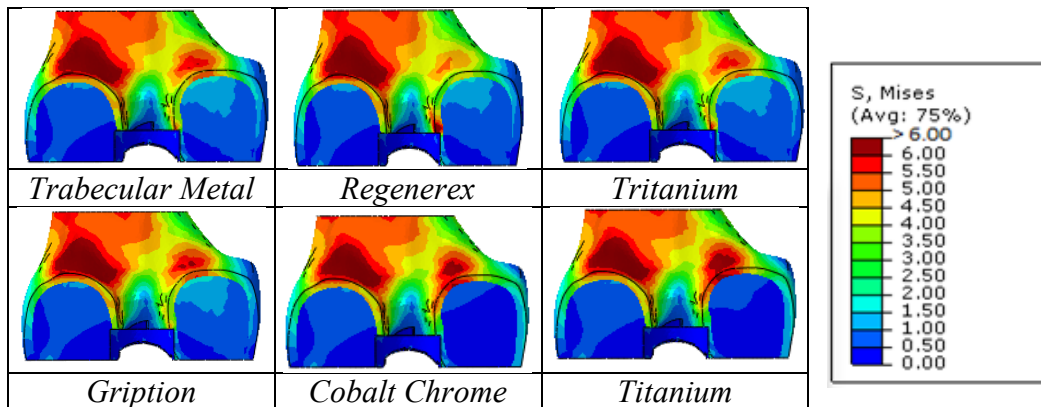


**Figure 114** - Von Mises stress distribution at femur – augment interface for a flexion angle of 90° and a posterior augment of 10 mm

By comparing these configurations, it is possible to notice that for a distal augment, regardless of the thickness, Von Mises stress distribution is close to that of control model not only on the lateral side but also to the medial, considering the porous metals. On the other hand, if the augment is placed on the posterior side of the femur, the main change is visible on the medial side, both for porous and dense metals. A quantitative comparison between the different configurations is reported in the following figures.

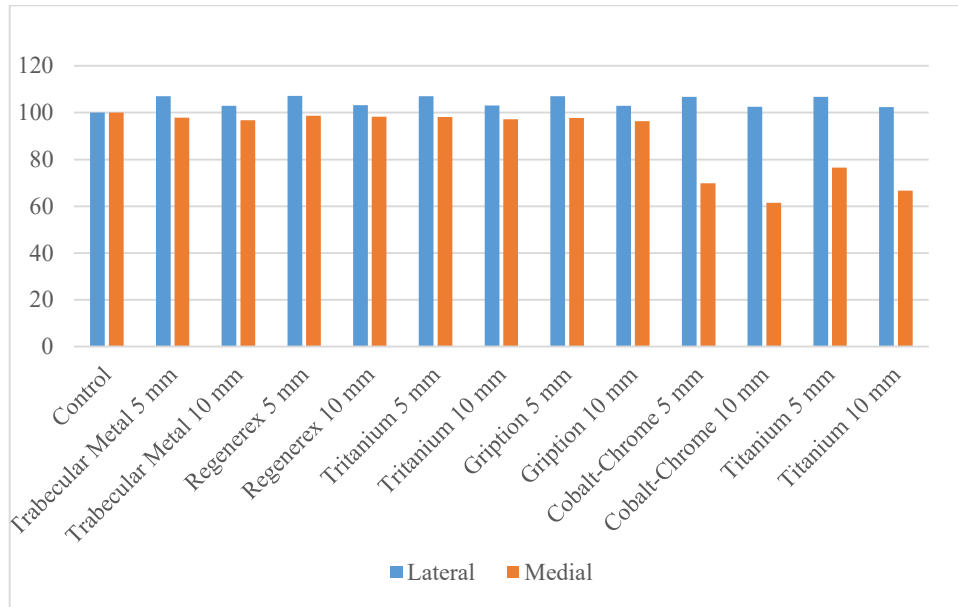


**Figure 115** – Flexion 90°: Average Von Mises bone stress analysing the local region of interest (depth of 10 mm), comparing all the trend of all the thicknesses and all the biomaterials to the control model and among them, and considering a distal augment placed on the medial femoral condyle.

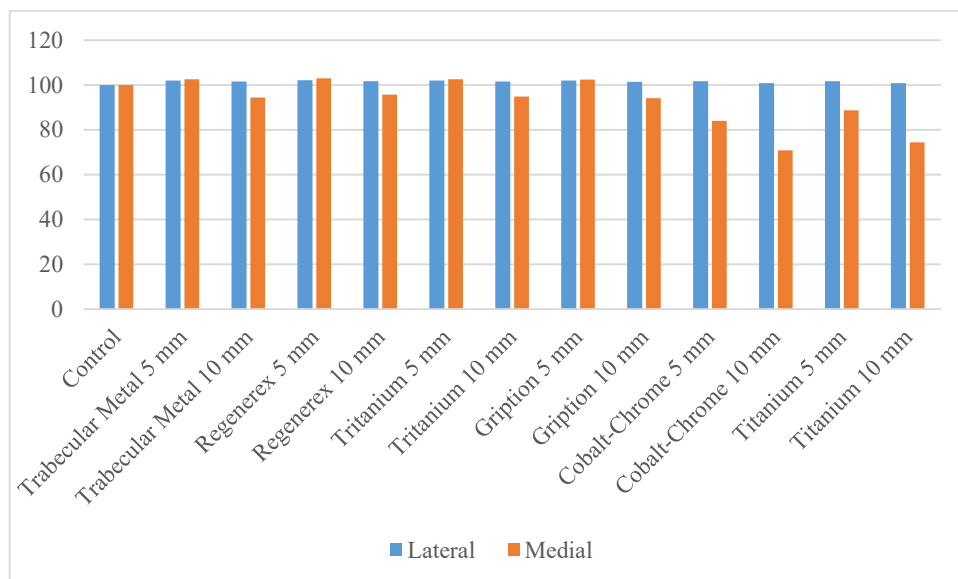


**Figure 116** - Flexion 90°: Average Von Mises bone stress analysing the global region of interest (depth of 50 mm), comparing all the trend of all the thicknesses and all the biomaterials to the control model and among them, and considering a distal augment placed on the medial femoral condyle.

As observed in the graphical overviews, looking what happens in the local region, the insertion of a distal augment made of a porous metal, regardless of the thickness, does not induce a relevant variation in terms of bone stress both on the lateral and medial side (maximum reduction for the medial side is 4% and also the maximum increase for the lateral side is 4%). On the opposite side, Co-Cr and Ti cause a most important reduction of the Von Mises stress on the medial side, which is dependent on the thickness: the reduction is 24-30% for a thickness of 5 mm and 33-39% for a thickness of 10 mm. Globally, the pattern is the same, but the gap has been reduced.

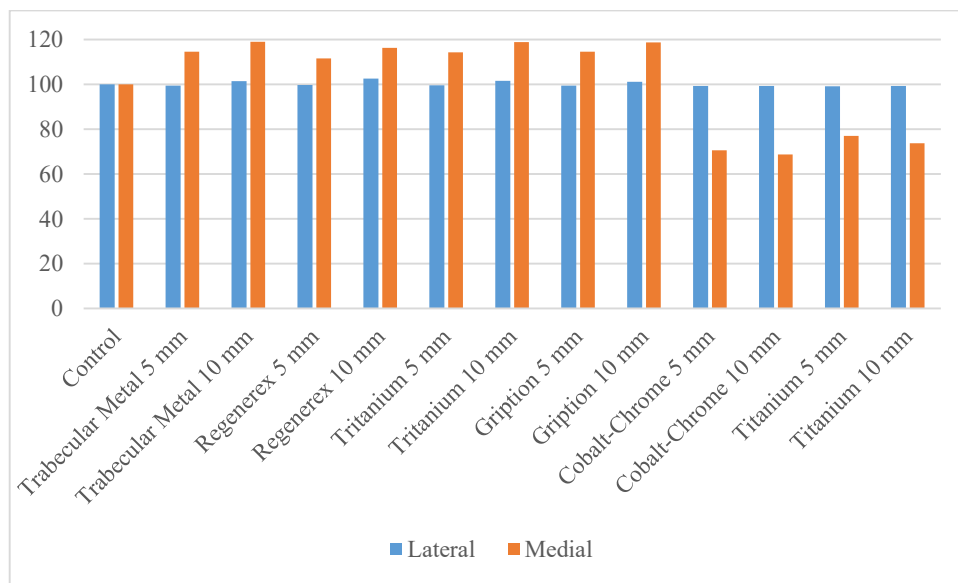


**Figure 117** – Flexion 90°: Average Von Mises bone stress analysing the local region of interest (depth of 10 mm), comparing all the trend of all the thicknesses and all the biomaterials to the control model and among them, and considering a posterior augment placed on the medial femoral condyle.

The trend shown in the previous figure highlights that if a posterior augment is implanted, the lateral side is not subjected to a significant change in terms of bone stress, while an increase of Von Mises stress is reported on the medial side for the porous metals. The higher occurs when a thickness of 10 mm is considered, but the difference in terms of average stress between a thickness of 5 and 10 mm is not relevant. For the conventional metals, the main variation appears on the medial side where it is possible to notice a relevant decrease in terms of bone stress (up to 30%): there is no difference if the thickness of the augment is changed.

Globally, also for these configurations, the trend is the same of the local region, but the gap is reduced.

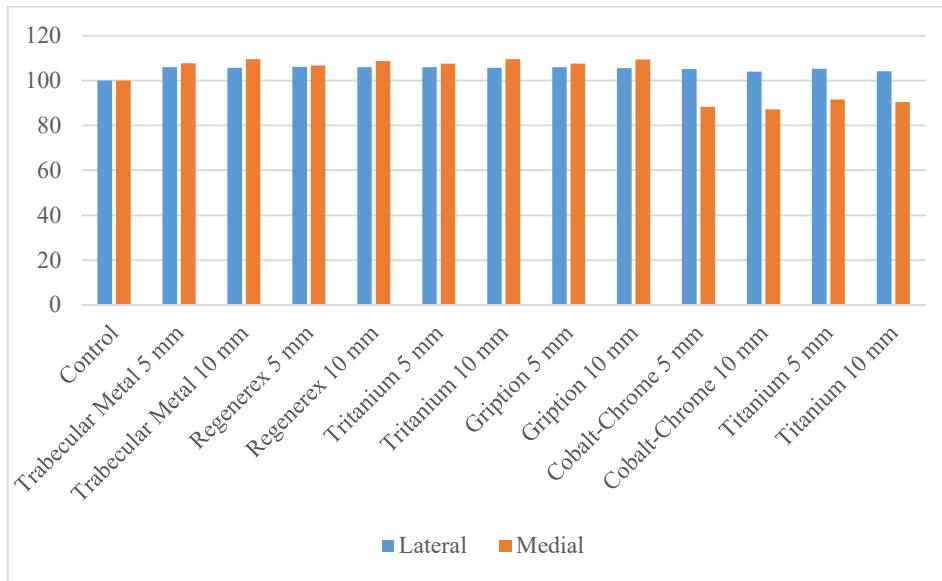
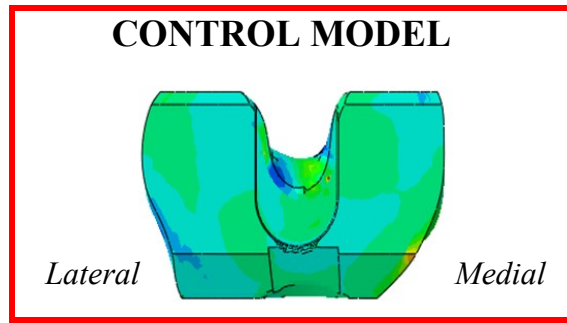


**Figure 118** - Flexion 90°: Average Von Mises bone stress analysing the global region of interest (depth of 50 mm), comparing all the trend of all the thicknesses and all the biomaterials to the control model and among them, and considering a posterior augment placed on the medial femoral condyle.

#### 4.2.4 Shear stress: flexion angle of 0°

In the following paragraphs the distribution of the bone shear stress caused by the insertion of an augment is investigated: the effects of a distal and then a posterior augment of 5 – 10 mm, placed on the medial condyle of the femur is analysed, comparing the behaviour of the porous and solid biomaterials. For each configuration, a flexion angle of 0° is set and the “Control Model” is defined as that model where no augment is implanted. A graphical overview of the shear stress distribution at the bone-augment interface is shown in the following figures.



*Distal augment with a thickness of 5 mm*

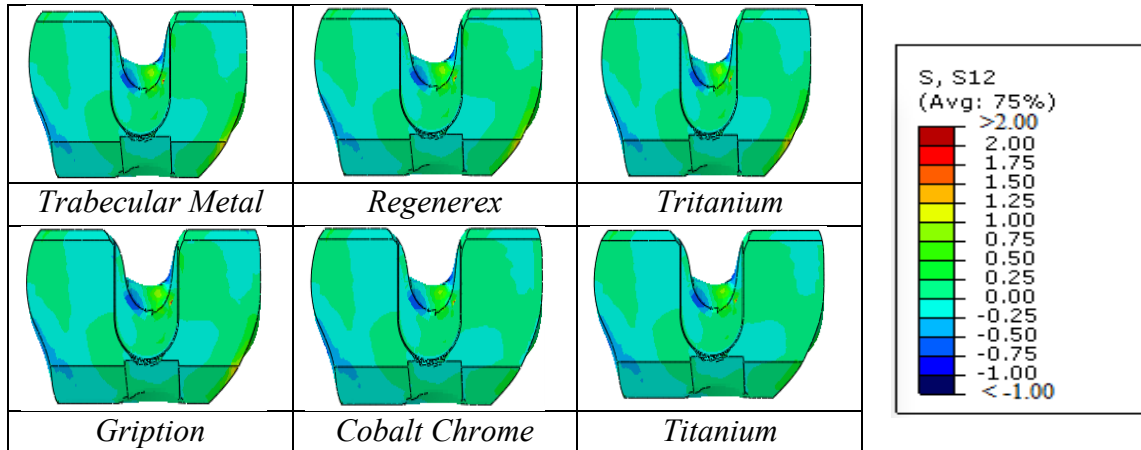
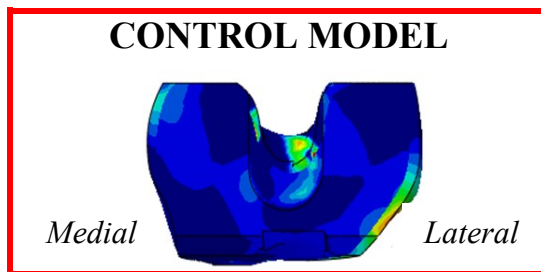


**Figure 119** - Shear stress distribution at femur – augment interface for a flexion angle of 0° and a distal augment of 5 mm



*Distal augment with a thickness of 10 mm*

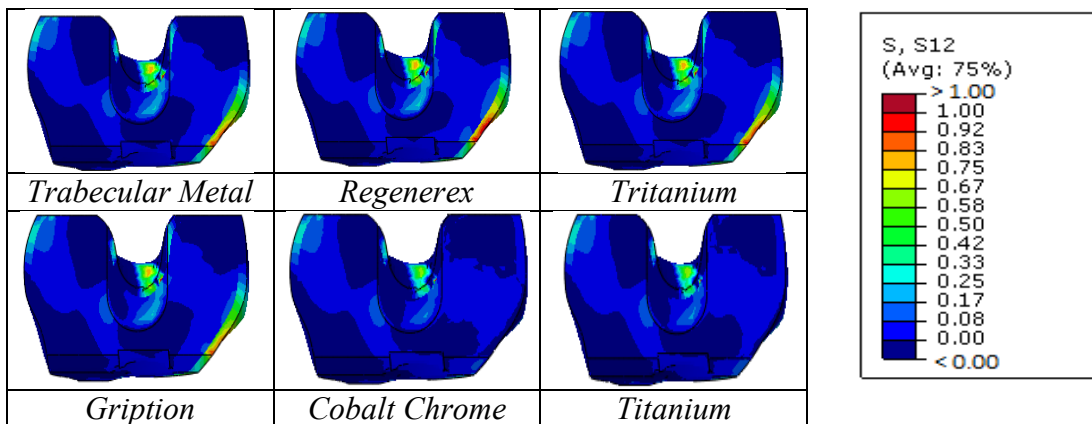
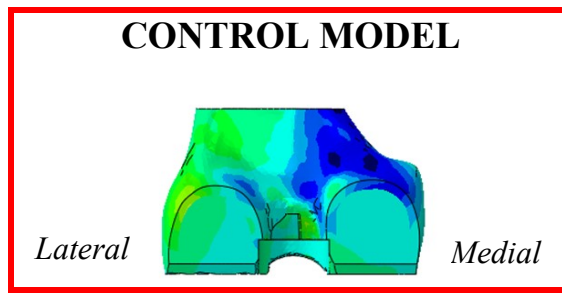


**Figure 120** - Shear stress distribution at femur – augment interface for a flexion angle of 0° and a distal augment of 10 mm



Posterior augment with a thickness of 5 mm

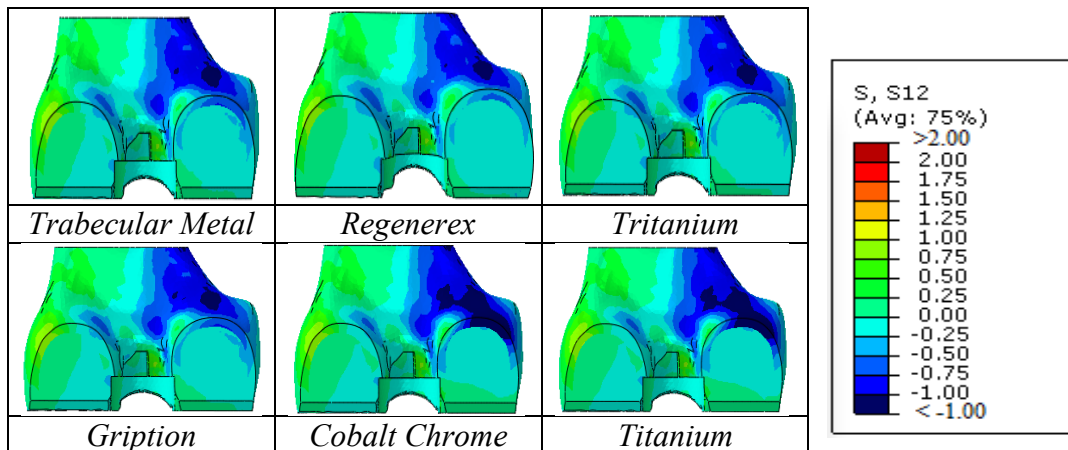
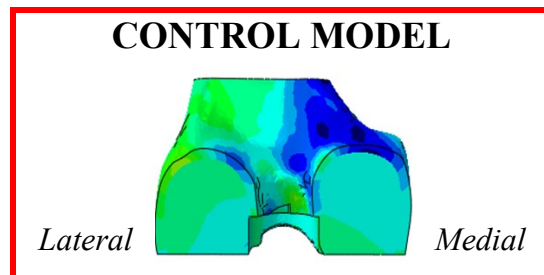


Figure 121 - Shear stress distribution at femur – augment interface for a flexion angle of 0° and a posterior augment of 5 mm



Posterior augment with a thickness of 10 mm

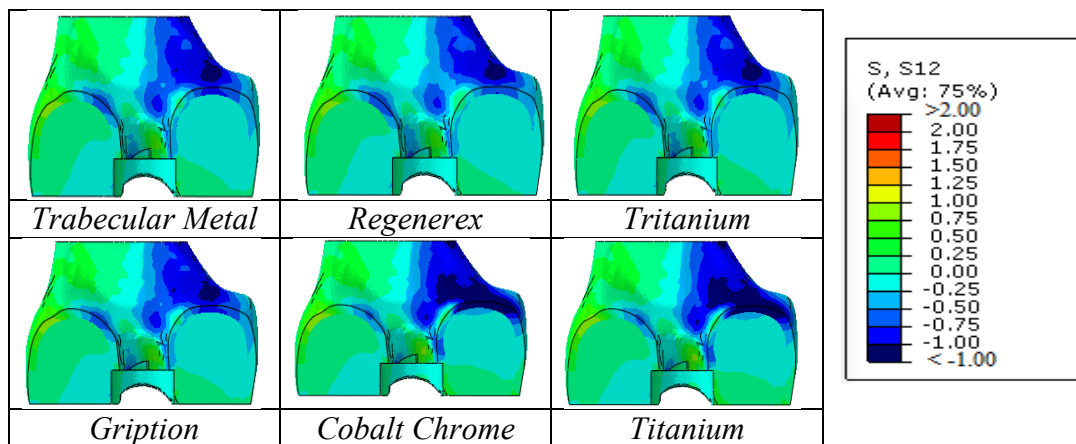
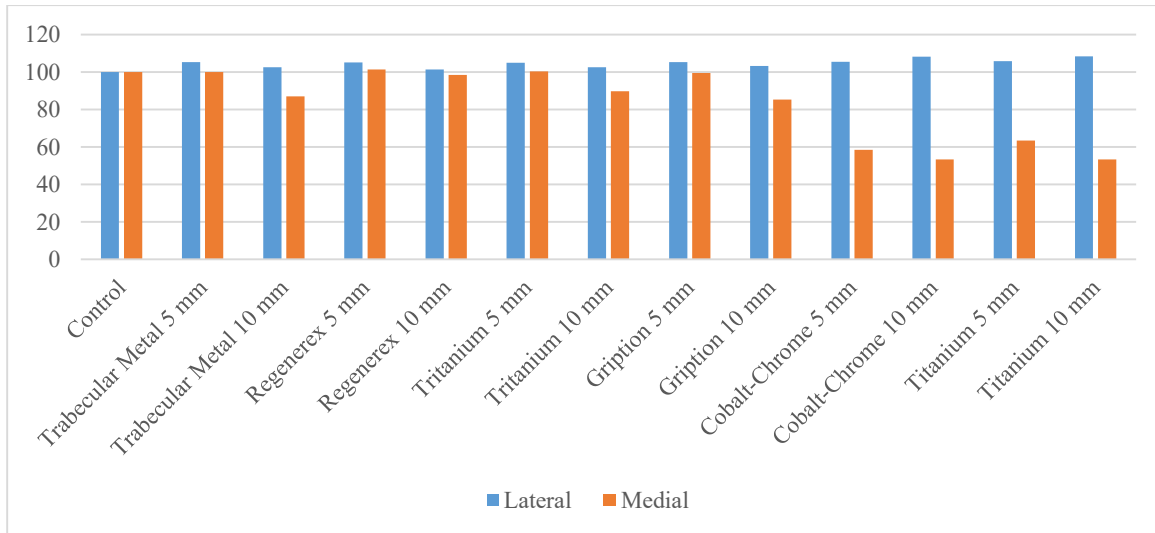


Figure 122 - Shear stress distribution at femur – augment interface for a flexion angle of 0° and a posterior augment of 10 mm

The same considerations expressed for the distribution of Von Mises stress caused by the insertion of an augment are worth also for the shear stress: looking at these graphical representations, it is possible to notice that the lateral side is not subjected to a significant variation, while the main change occurs on the medial side both for porous and solid metals. The results obtained by a quantitative analysis are reported in the following figures.



**Figure 123** - Flexion 0°: Average shear bone stress analysing the local region of interest (depth of 10 mm), comparing all the trend of all the thicknesses and all the biomaterials to the control model and among them, and considering a distal augment placed on the medial femoral condyle.

Analysing the local effects of a distal augment placed on the medial side of the femur, it is possible to notice that the most significant change in terms of shear bone stress is showed on the medial side, both for porous and solid metals. A decrease is reported for both types:

- For porous metals the average shear stress is very close to that of control model if a thickness of 5 mm is considered, while a decrease (up to 15% for Gription) is reported if an augment of 10 mm is implanted. For the lateral side there is a slight increase (up to 5%).
- For the conventional metals, the trend is the same of porous metals but the variations on the medial side are more relevant (up to 47% for a thickness of 10 mm), while an increase less than 10% occurs on the lateral side.

Globally, the pattern is the same, but the offset of the shear stress from the control model for conventional metals is reduced (39%), while the values reported for the porous metals are almost the same of local analysis.

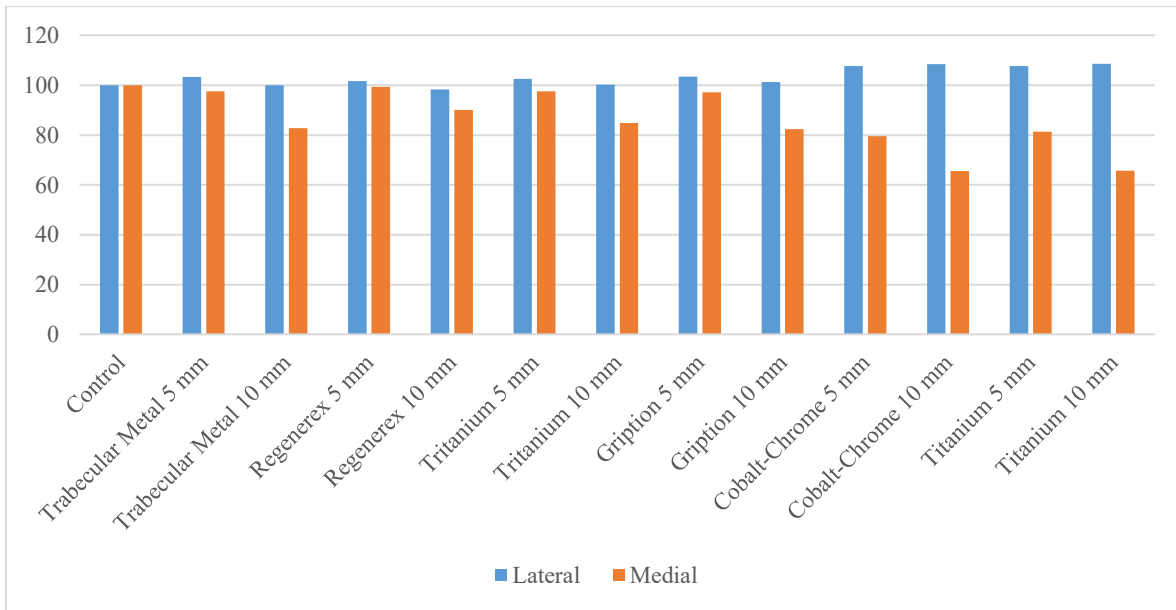


**Figure 124** - Flexion 0°: Average shear bone stress analysing the global region of interest (depth of 50 mm), comparing all the trend of all the thicknesses and all the biomaterials to the control model and among them, and considering a distal augment placed on the medial femoral condyle.

Furthermore, looking at what happens if a posterior augment is placed on the medial side of the femur, it is possible to notice that there is no change in terms of shear stress (<5%) for the lateral side. Analysing the value reported for the medial side, the following bar graph shows that if a porous metal is used, shear stress does not change significantly also on the medial side: the maximum increase is almost of 9% for a thickness of 10 mm.

For the conventional metals, there has been an increase more marked: up to 30% for a Co-Cr augment of 10 mm.

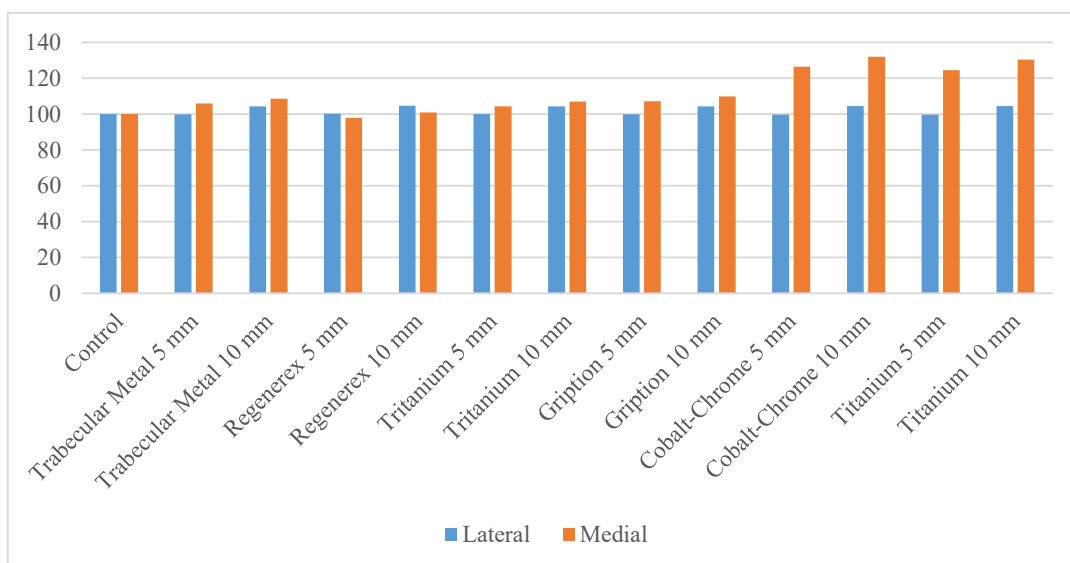


**Figure 125** - Flexion 0°: Average shear bone stress analysing the local region of interest (depth of 10 mm), comparing all the trend of all the thicknesses and all the biomaterials to the control model and among them, and considering a posterior augment placed on the medial femoral condyle

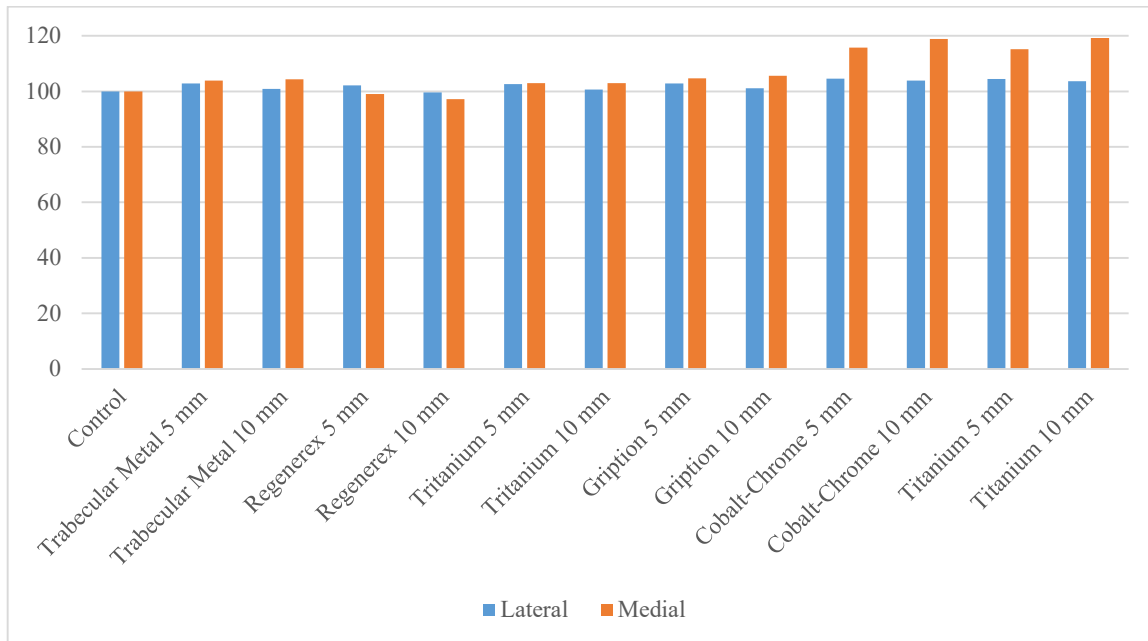


**Figure 126** - Flexion 0°: Average shear bone stress analysing the global region of interest (depth of 50 mm), comparing all the trend of all the thicknesses and all the biomaterials to the control model and among them, and considering a posterior augment placed on the medial femoral condyle.

Globally, data analysis demonstrates that shear stress distribution with a porous augment is very close to that of control model also for the medial side, regardless of the thickness. If a solid augment is implanted the increase is reduced to approximately 20%.

#### 4.2.5 Shear stress: flexion angle of 45°

In this section the distribution of the bone shear stress caused by the insertion of an augment is investigated: the effects of a distal and then a posterior augment of 5 – 10 mm, placed on the medial condyle of the femur is analysed, comparing the behaviour of the porous and solid biomaterials. For each configuration, a flexion angle of 45° is set and a graphical overview of the shear stress distribution at the bone-augment interface is shown in the following figures.

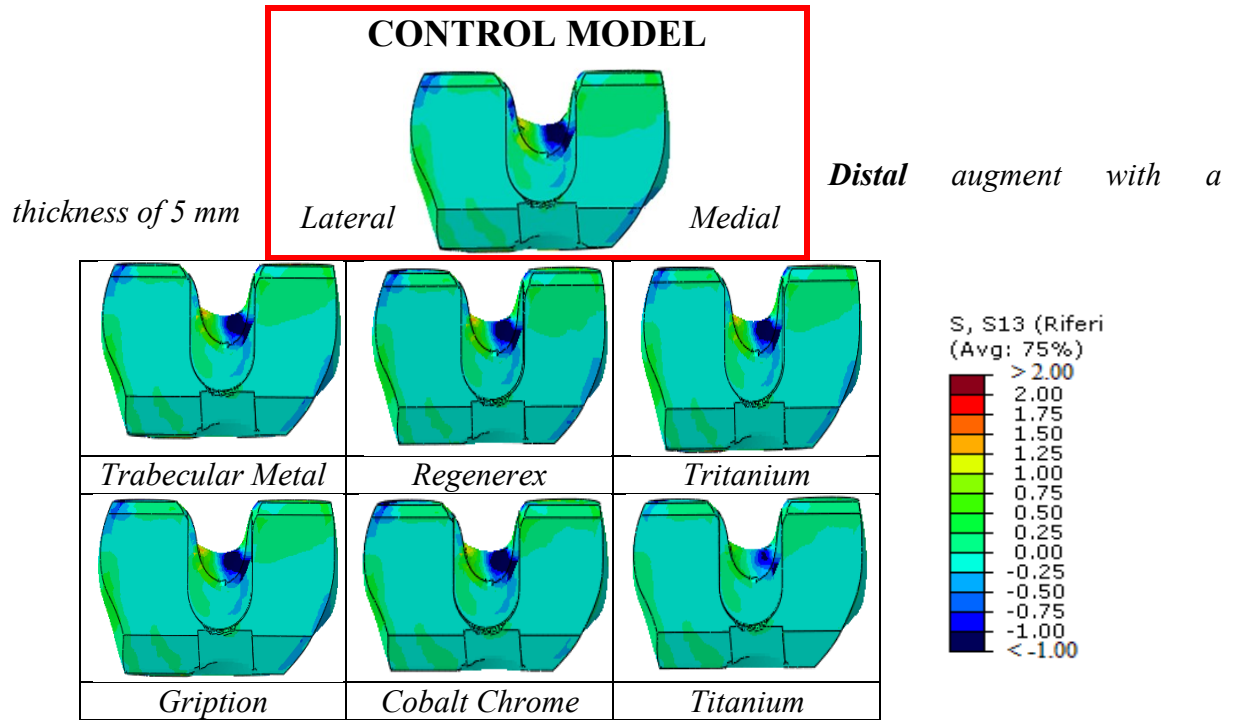


**Figure 127** - Shear stress distribution at femur – augment interface for a flexion angle of 45° and a distal augment of 5 mm

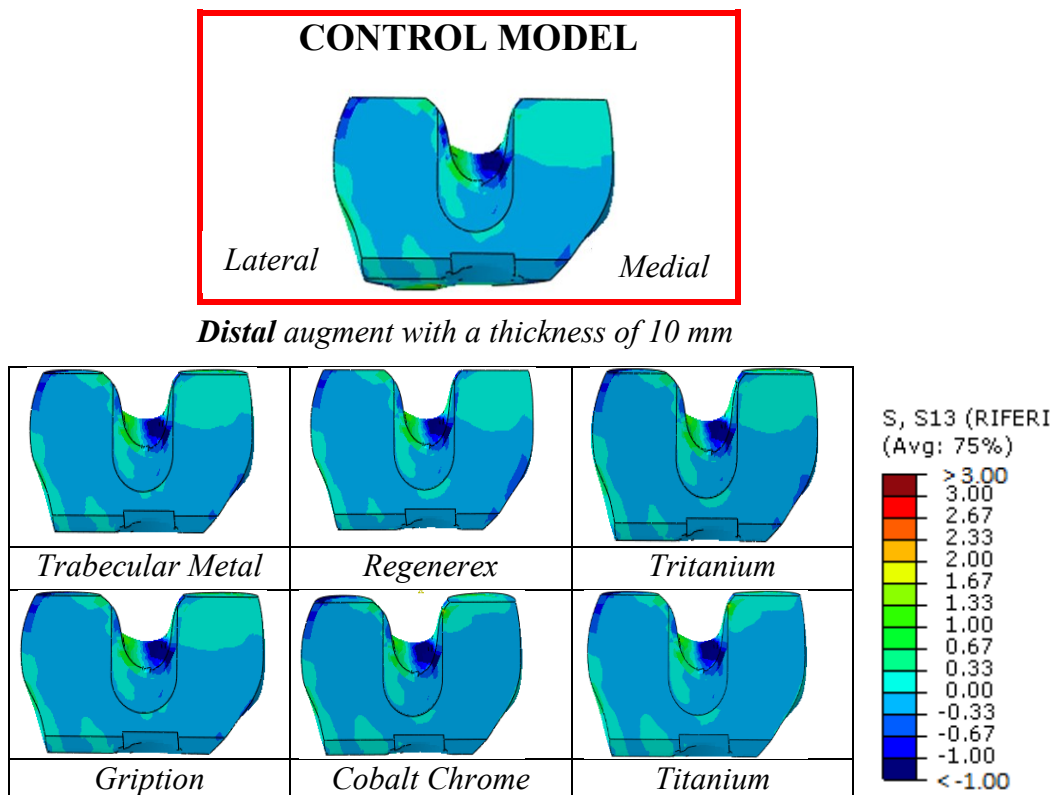


**Figure 128** - Shear stress distribution at femur – augment interface for a flexion angle of 45° and a distal augment of 10 mm.

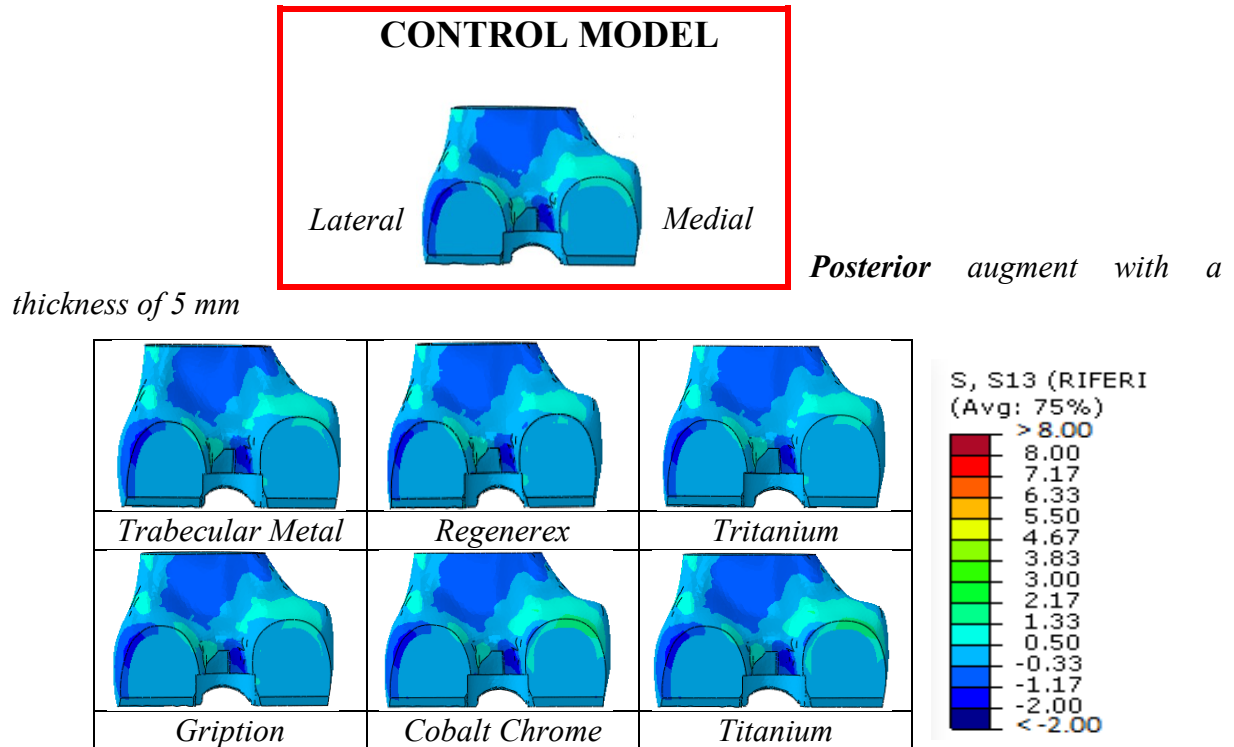


**Figure 129** - Shear stress distribution at femur – augment interface for a flexion angle of 45° and a posterior augment of 5 mm

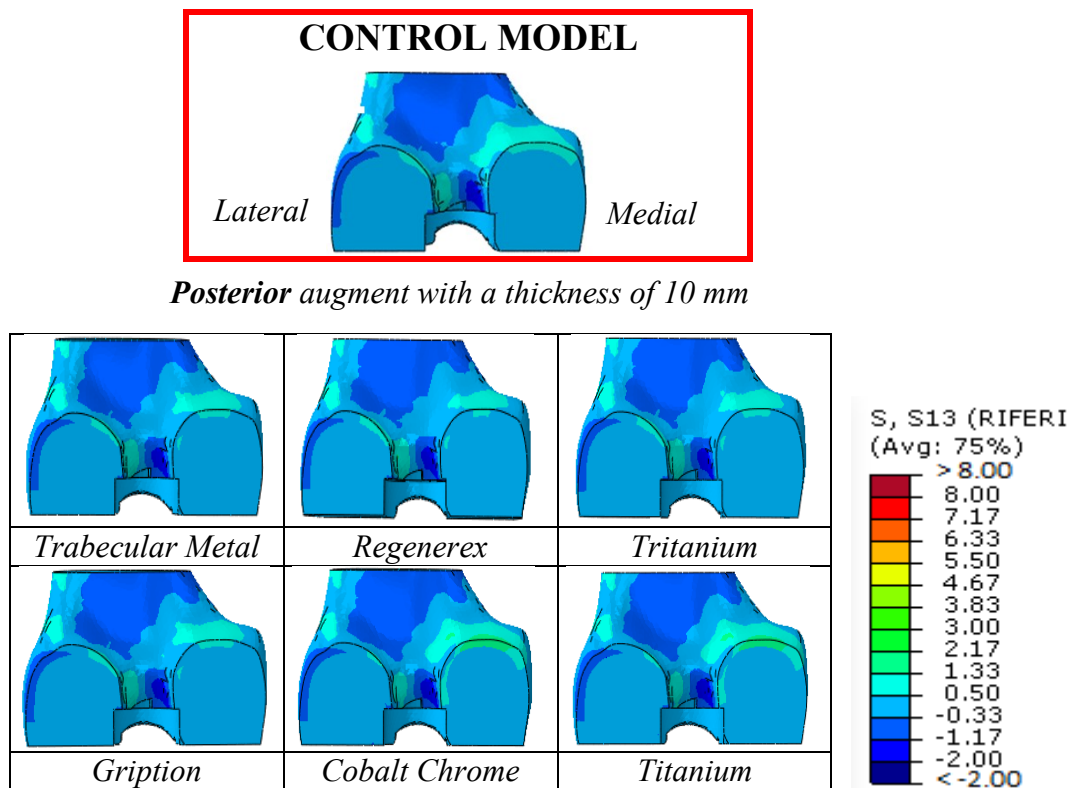


**Figure 130** - Shear stress distribution at femur – augment interface for a flexion angle of 45° and a posterior augment of 10 mm

The quantitative values are displayed in the following figures.

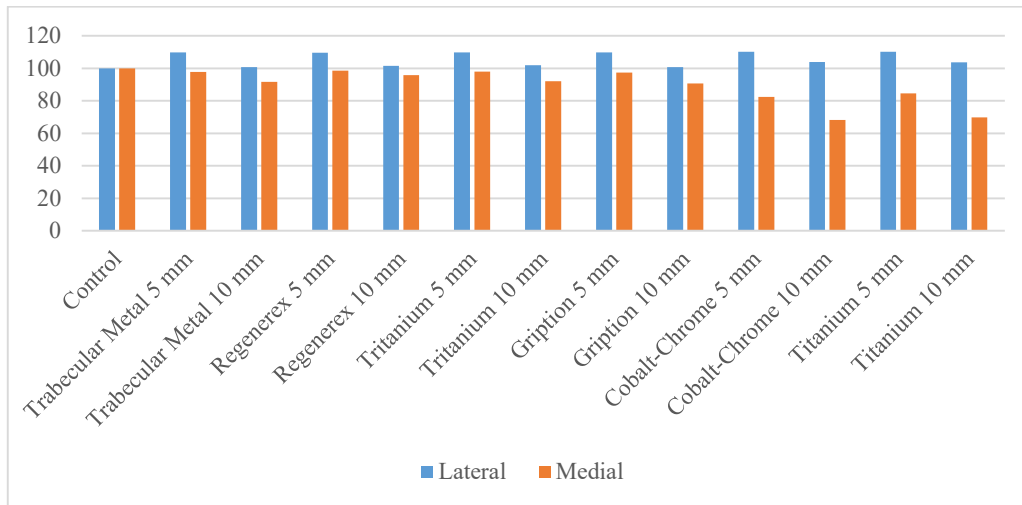


**Figure 131** - Flexion 45°: Average shear bone stress analysing the local region of interest (depth of 10 mm), comparing all the trend of all the thicknesses and all the biomaterials to the control model and among them, and considering a distal augment placed on the medial femoral condyle.

Analysing the quantitative values locally, it is possible to state that an augment of 5 mm, regardless of the material, varies the distribution of the average shear stress on the lateral side, inducing a maximum increase of approximately 10% for both types of materials. On the medial side, bone shear stress is very close to that of the reference model for the porous metals (only a slight reduction: 2-3%), while the convention metals cause a decrease of 16-17%. If an augment of 10 mm is implanted to treat bone loss, porous metals induce a reduction up to 8-9% in terms of shear stress but this variation is most relevant for the dense metals: 30 - 34%. Globally, the trend is the same but as for a flexion angle of 0°, the offset from the control model has been reduced for both categories.

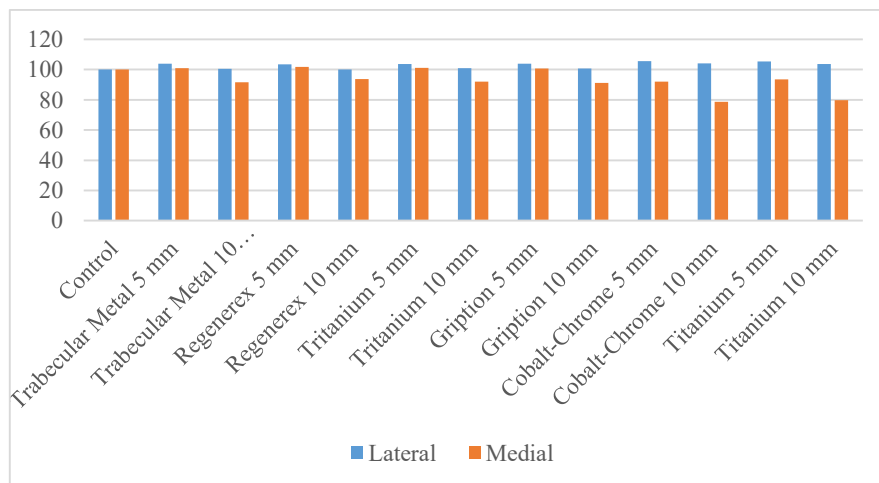


**Figure 132** - Flexion 45°: Average shear bone stress analysing the global region of interest (depth of 50 mm), comparing all the trend of all the thicknesses and all the biomaterials to the control model and among them, and considering a distal augment placed on the medial femoral condyle.

Analysing the results obtained if a posterior augment is placed on the medial side of the femur, it is possible to highlight that locally, there is no significant change in terms of shear stress on the local side for both porous (reduction up to 6%) and solid metals (increase up to 6%). It is possible to notice the main variation occur on the medial side:

- A porous augment causes a reduction up to 17% (Regenerex) if is considered a thickness of 5 mm; while for a thickness of 10 mm is very close to that of control model.
- A solid augment induces an increase up to 27% (Co-Cr) if is implanted an augment of 10 mm; while for a thickness of 5 mm leads to a decrease less than 5%.

Globally, the trend is the same for both types of material: the most critical configuration is that with a posterior augment of 5 mm: it causes an increases of approximately 20% on the medial side and also a reduction on the lateral side that it is most significant for the dense metals, so it is more convenient to use an augment made of porous metals.

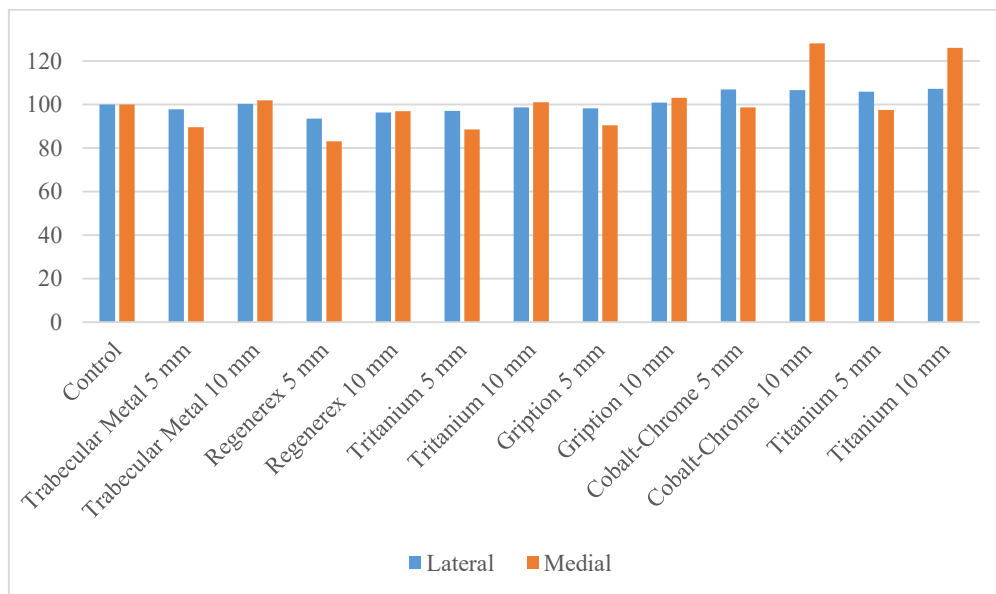


**Figure 133** - Flexion 45°: Average shear bone stress analysing the local region of interest (depth of 10 mm), comparing all the trend of all the thicknesses and all the biomaterials to the control model and among them, and considering a posterior augment placed on the medial femoral condyle.

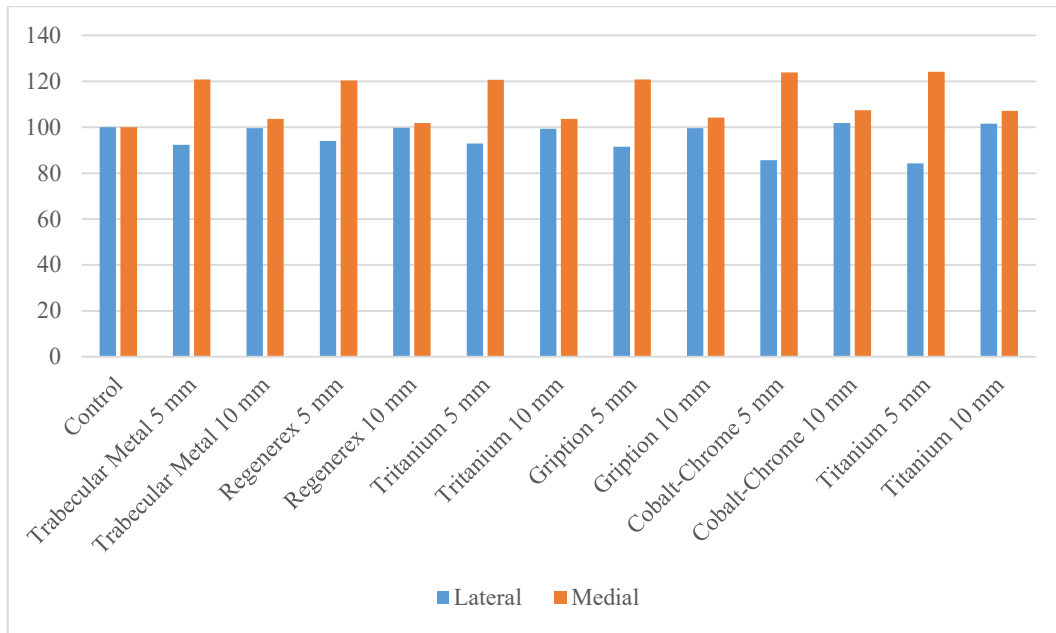


**Figure 134** - Flexion 45°: Average shear bone stress analysing the global region of interest (depth of 50 mm), comparing all the trend of all the thicknesses and all the biomaterials to the control model and among them, and considering a posterior augment placed on the medial femoral condyle.

#### 4.2.6 Shear stress: flexion angle of 90°

In this section, the effects of a distal and then a posterior augment of 5 – 10 mm, placed on the medial condyle of the femur is analysed. For each configuration, a flexion angle of 90° is set and graphical overviews are reported:

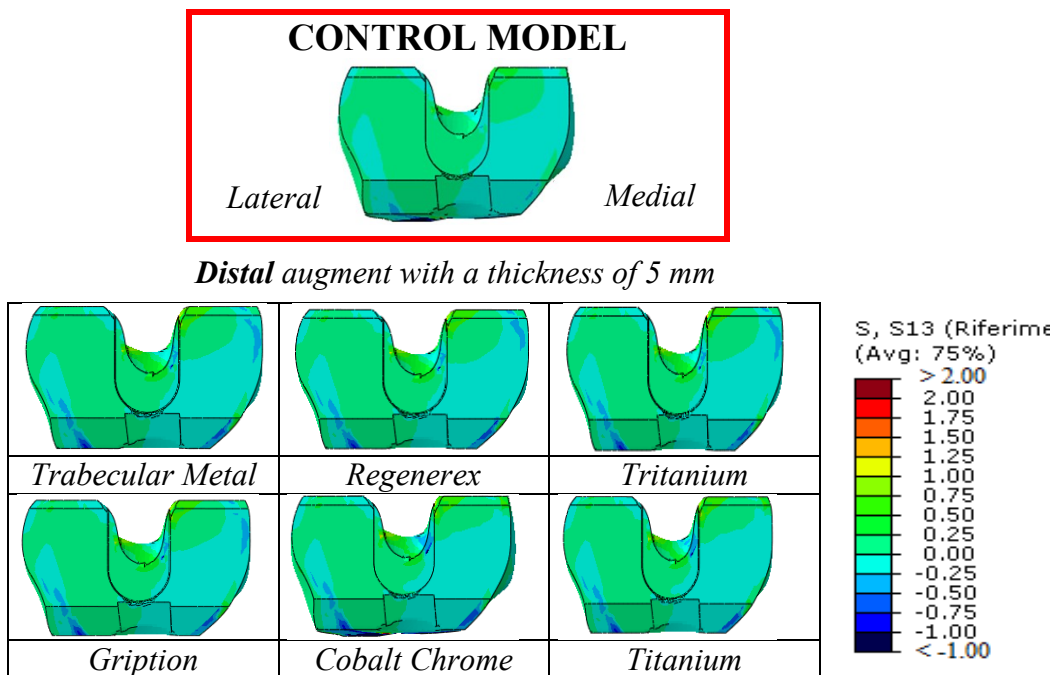


**Figure 135** - Shear stress distribution at femur – augment interface for a flexion angle of 90° and a distal augment of 5 mm

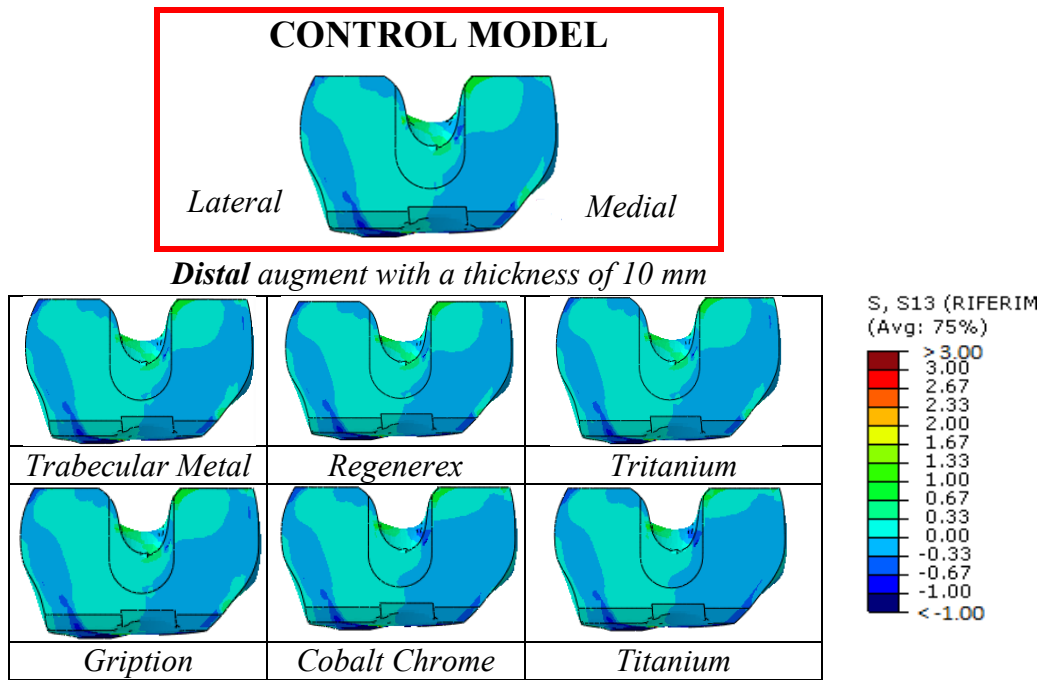


**Figure 136** - Shear stress distribution at femur – augment interface for a flexion angle of 90° and a distal augment of 10 mm

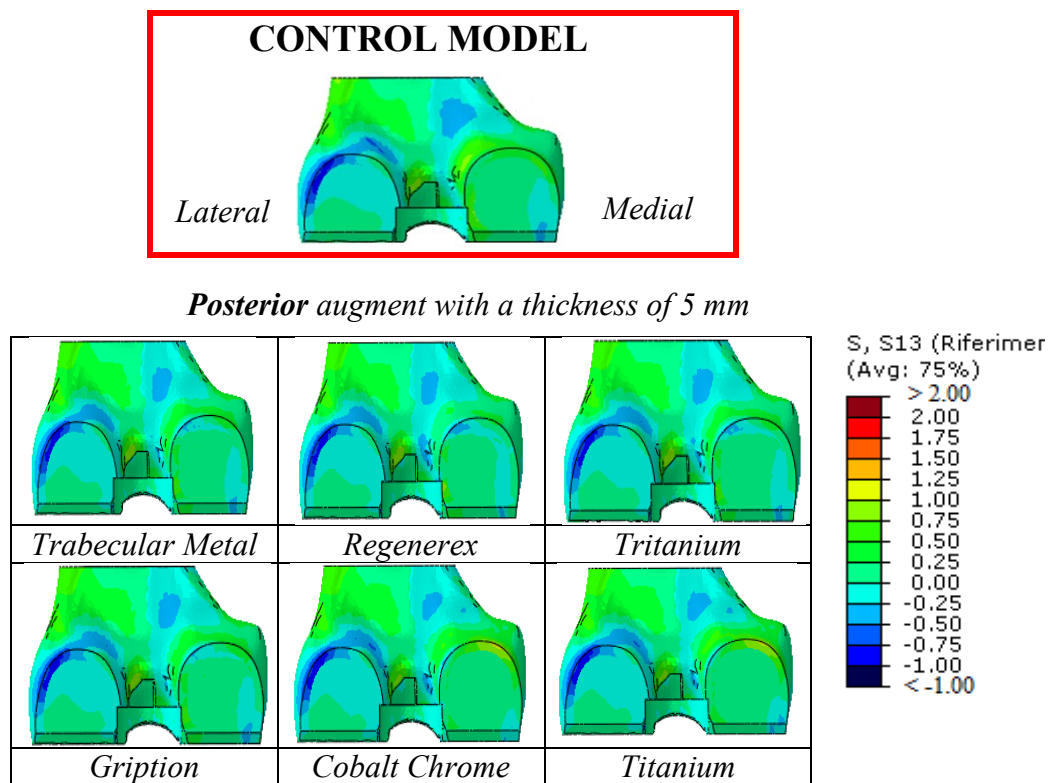


**Figure 137** - Shear stress distribution at femur – augment interface for a flexion angle of 90° and a posterior augment of 5 mm

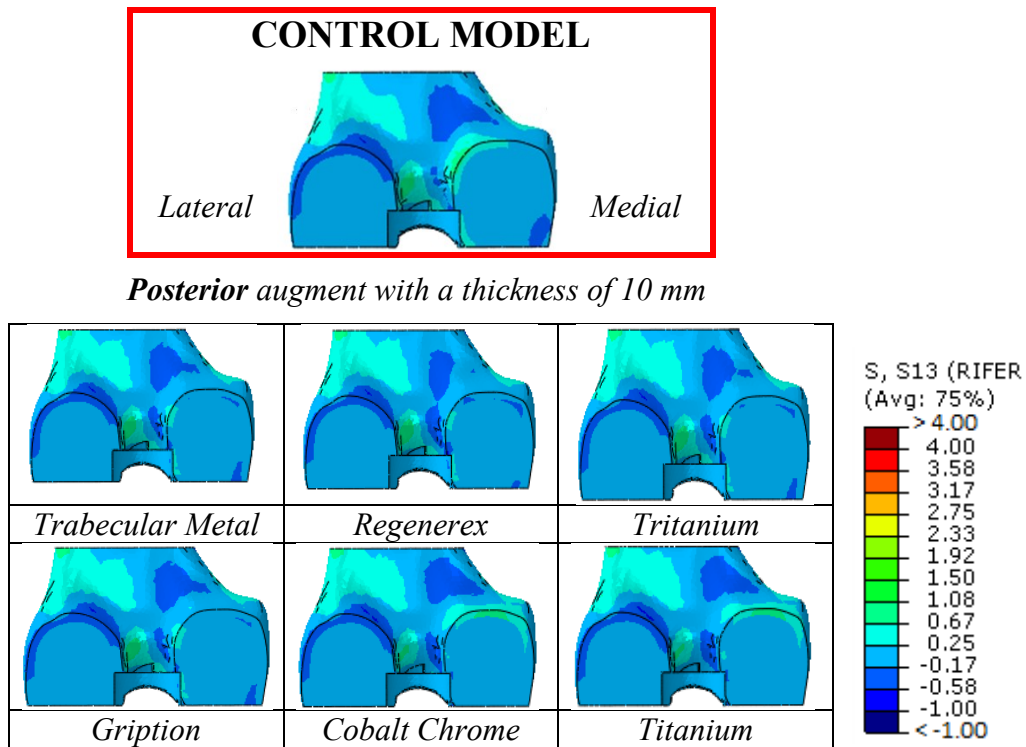


**Figure 138** - Shear stress distribution at femur – augment interface for a flexion angle of 90° and a posterior augment of 10 mm

At first glance, these graphical overviews show that the lateral side is not subjected to a great change in terms of shear stress for all the considered configurations. The relevant variation occurs on the medial side. The results are reported in the following bar graphs.

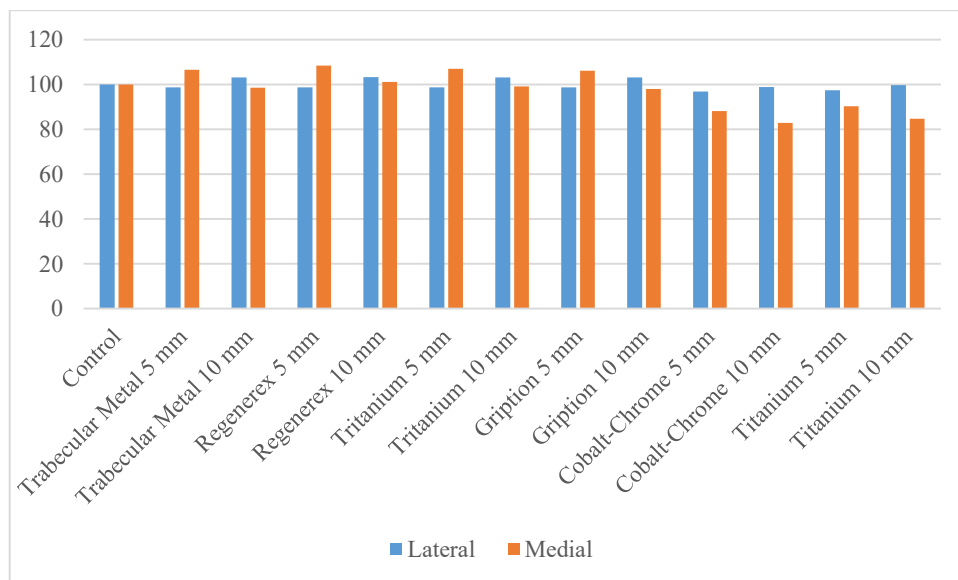


**Figure 139** - Flexion 90°: Average shear bone stress analysing the local region of interest (depth of 10 mm), comparing all the trend of all the thicknesses and all the biomaterials to the control model and among them, and considering a distal augment placed on the medial femoral condyle.

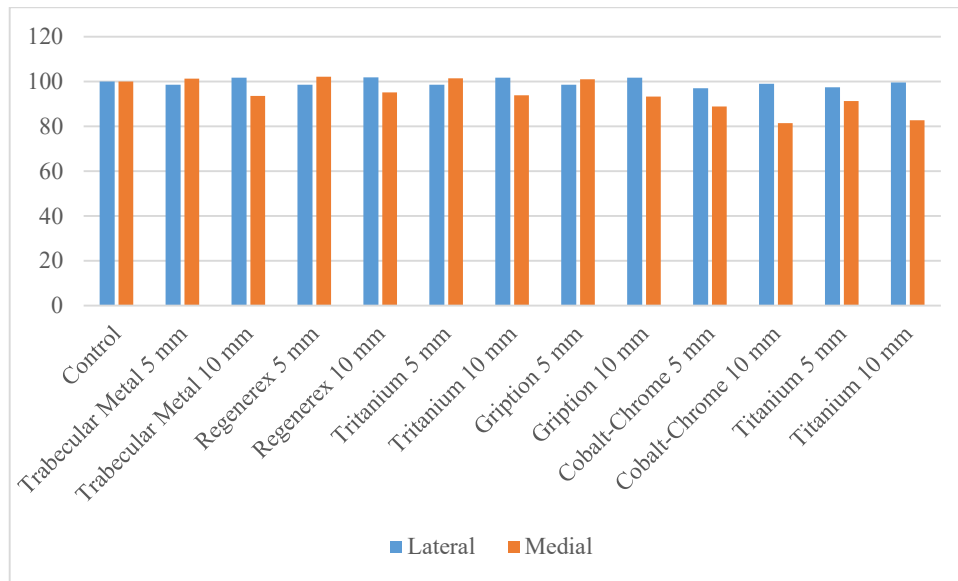


**Figure 140** - Flexion 90°: Average shear bone stress analysing the global region of interest (depth of 50 mm), comparing all the trend of all the thicknesses and all the biomaterials to the control model and among them, and considering a distal augment placed on the medial femoral condyle.

As previously stated, the shear stress distribution on the lateral side is close to that of control model for both porous and solid metals (variations less than 3%), if the region close to the augment is investigated. Porous metal augment of 5 mm causes a maximum rate of increase of 8% in shear stress (Regenerex). If a porous augment with a thickness of 10 mm is implanted, there will be a reduction less than 2%. On the other hand, solid metals induce a decrease of approximately 10% for a thickness of 5 mm and about 20% for a thickness of 10 mm.

Globally, if a porous augment of 5 mm is implanted, shear stress distribution is similar to that of control model for both sides (lateral and medial), while there is a decrease less than 10% if a thickness of 10 mm is considered.

Instead, conventional metal produces more significant change also globally (up to 20% for a thickness of 10 mm).

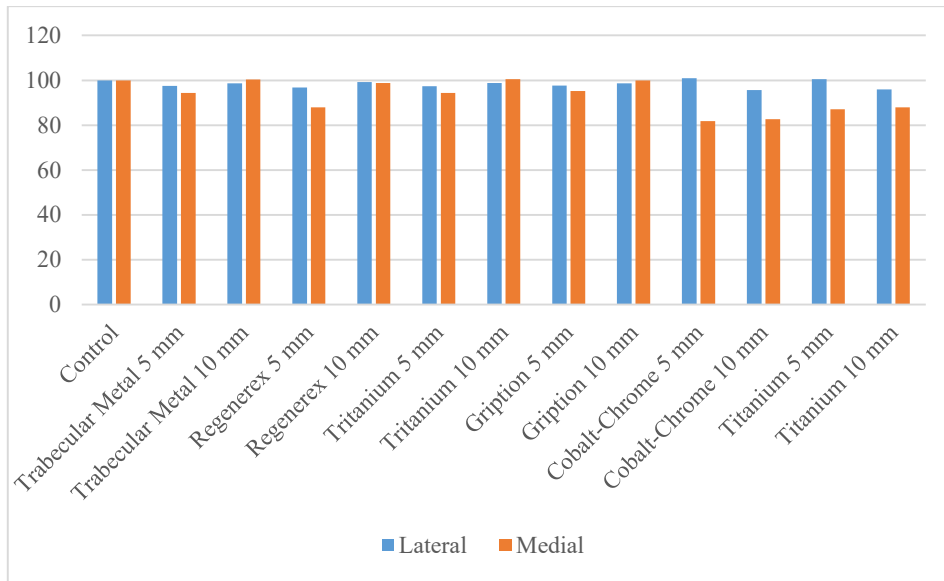


**Figure 141** - Flexion 90°: Average shear bone stress analysing the local region of interest (depth of 10 mm), comparing all the trend of all the thicknesses and all the biomaterials to the control model and among them, and considering a posterior augment placed on the medial femoral condyle.

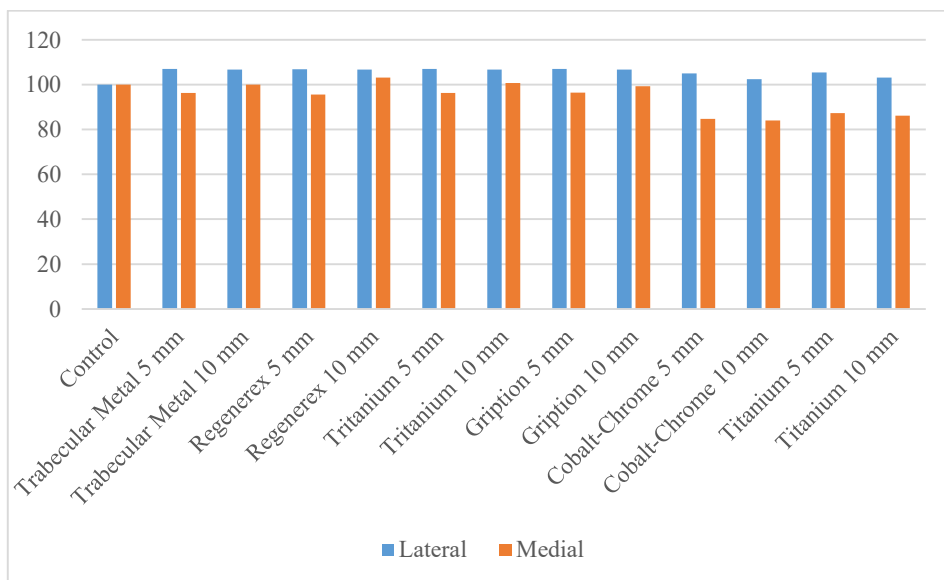


**Figure 142** - Flexion 90°: Average shear bone stress analysing the global region of interest (depth of 50 mm), comparing all the trend of all the thicknesses and all the biomaterials to the control model and among them, and considering a posterior augment placed on the medial femoral condyle.

# Chapter 5

## Discussion

This study is carried out in order to analyse the change in terms of bone stress when an augment is inserted, coupled with the TKA femoral component or the TKA tibial tray, with the purpose of restoring bone stock.

The aim of this work was to evaluate how different thicknesses, different materials and different flexion angles affect bone stress distribution.

It is fundamental to select the most appropriate technique for the treatment of bone deficiencies because this choice influences the success of the revision procedure. Therefore, in order to allow long-term lifespan of the implant, it is crucial to ensure that stress and strain distributions on the host bone are as close as possible to those of the reference model (no augment is inserted) [99].

Furthermore, this study, as also other research, presents some limitations which are related to some assumptions:

- Bone structures are modelled based on only one anatomy, without taking into account possible variations. But, according to literature, this hypothesis has been already used in other biomechanical analysis [100].
- According to previous validated models [59, 64] a linear elastic isotropic material model is assumed for the ligaments: they are modelled as beams where a preload is applied.
- Currently, there are not enough available data about the mechanical behaviour of the bone at the micro and nano structural level [67] due to the complexity of their behaviour: bone structure is heterogeneous, viscoelastic and anisotropic [67, 71] Therefore, according to literature [59, 67, 69], it is assumed that all the materials adopted in this model are considered linear elastic and this hypothesis provides the possibility to compare the behaviour of all the materials adopted qualitatively. Furthermore, it isn't taken into account the porosity of the bone structure because this work isn't interested in the investigation of the implant-bone behaviour at microscopic level [59]. Therefore, taking into consideration these hypotheses, the bony structures behaviour is assumed transversely isotropic for the cortical bone, while linear isotropic for cancellous bone [70].

- According to literature [59, 67, 69], it is assumed that all the materials adopted in this model are considered linear elastic and this hypothesis provides the possibility to compare the behaviour of all the materials adopted qualitatively.
- In this research, medial bone injuries are analysed because several studies [90, 101] have shown that medial defects often occur during revision and primary TKA.

It is possible to conclude that the results obtained through the FEA are in agreement with those reported in literature, in particular for the change in bone stress caused by the insertion of a medial tibial augment. By analysing different techniques for treating the same bone defects, Completo *et al.* [90] found out that the insertion of a filled cemented wedge made of CO-Cr causes no change on the lateral side (5%) and a reduction of bone stress of 23% on the medial side. According to Fehringer *et al.* [102], the most relevant variation occur on the medial side, while no significant change is reported on the lateral side.

This study shows that the insertion of a metal block augment varies the stress distribution mainly on the medial side (where the step wedge is placed), while the lateral side is not subjected to a relevant variation.

By analysing the Von Mises stress variations caused by the insertion of an augment characterized by different parameters (positions, thicknesses, flexion angles and materials), it is possible to notice that leading feature responsible of these changes is the stiffness of the adopted material. On the other hand, position (distal, proximal or posterior), thickness (5, 10 and 15 mm) and flexion angle (0°, 45° and 90°) do not have a sensible influence on the bone stress. The following figures demonstrate this aspect:

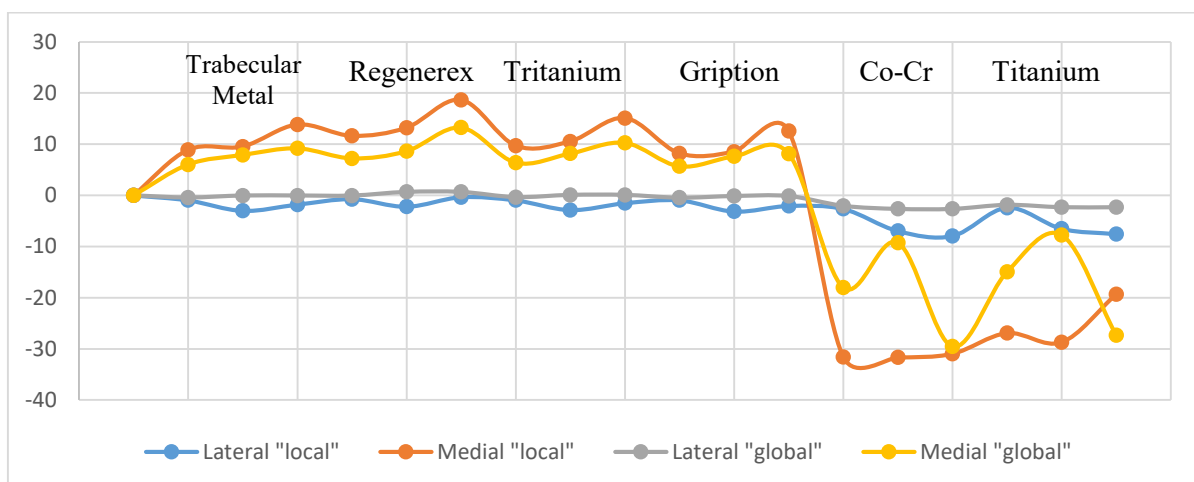


**Figure 143** – Variations of Von Mises stress for a tibial distal augment: flexion angle 0°.

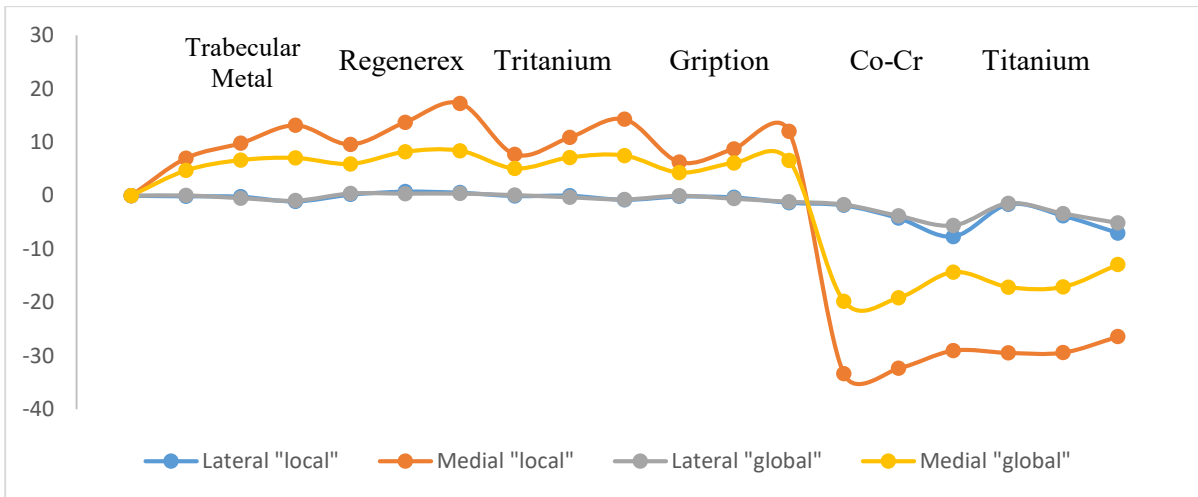


Figure 144 - Variations of Von Mises stress for a tibial distal augment: flexion angle 45°.

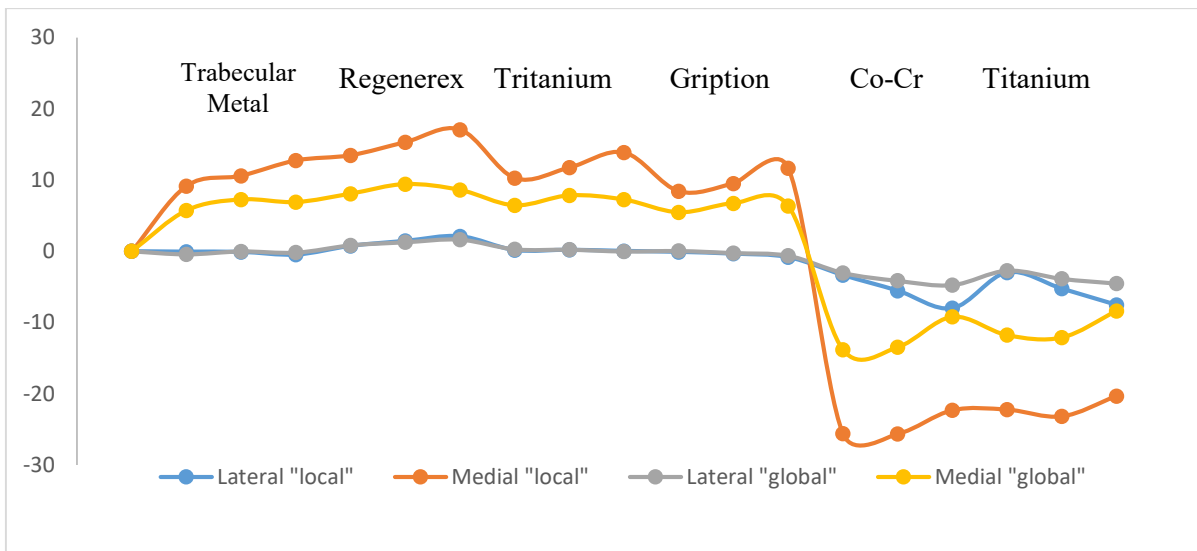


Figure 145 - Variations of Von Mises stress for a tibial distal augment: flexion angle 90°.

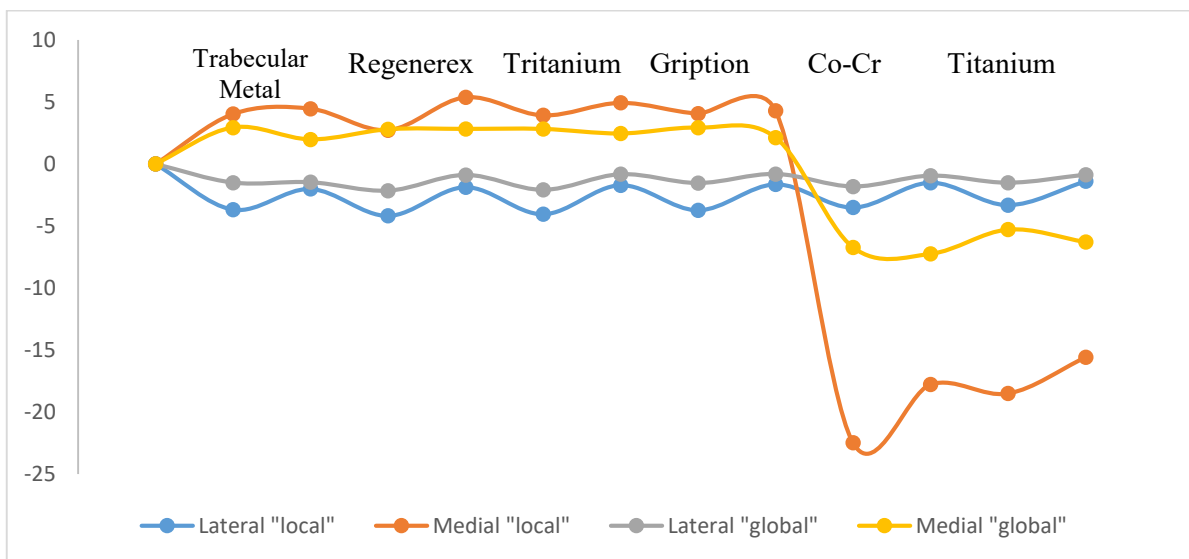


Figure 146 - Variations of Von Mises stress for a femoral distal augment: flexion angle 0°.

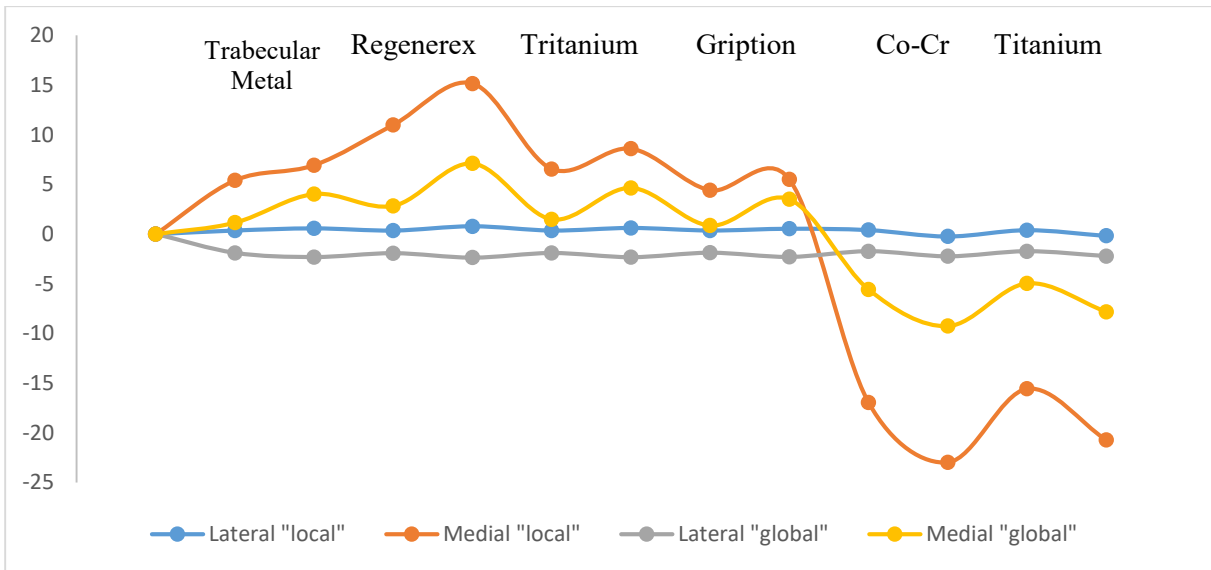


Figure 147 - Variations of Von Mises stress for a femoral posterior augment: flexion angle 0°.

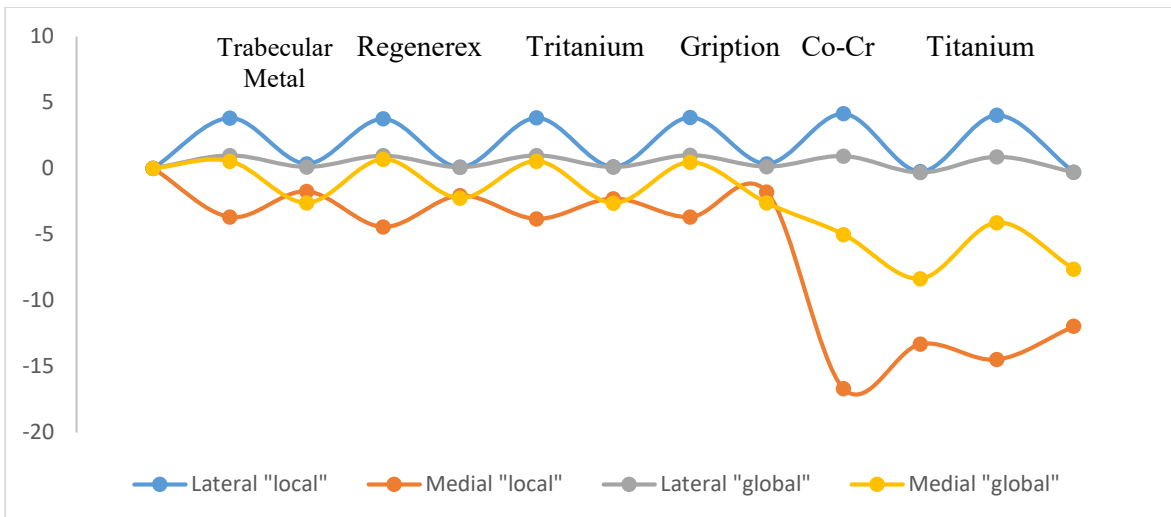


Figure 148 - Variations of Von Mises stress for a femoral distal augment: flexion angle 45°.

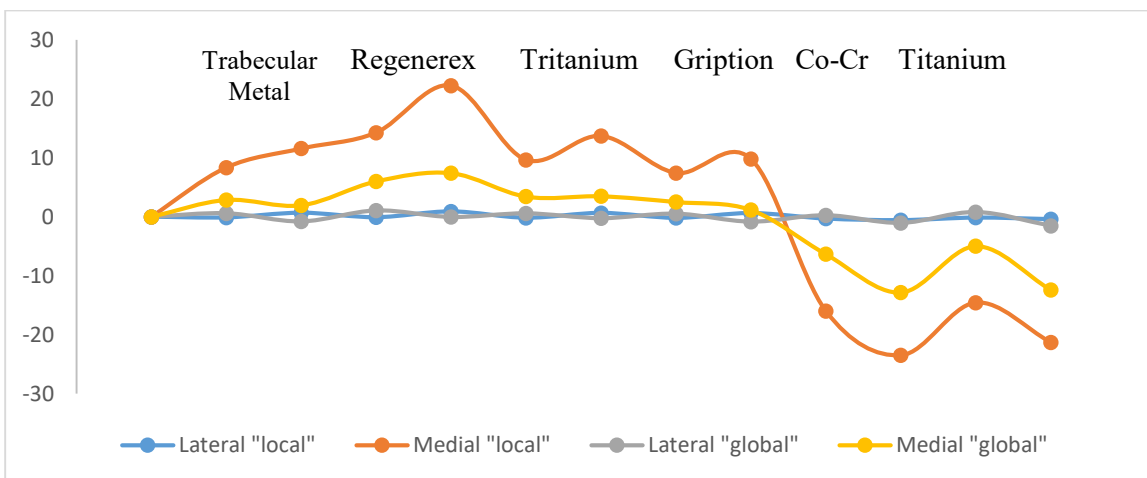
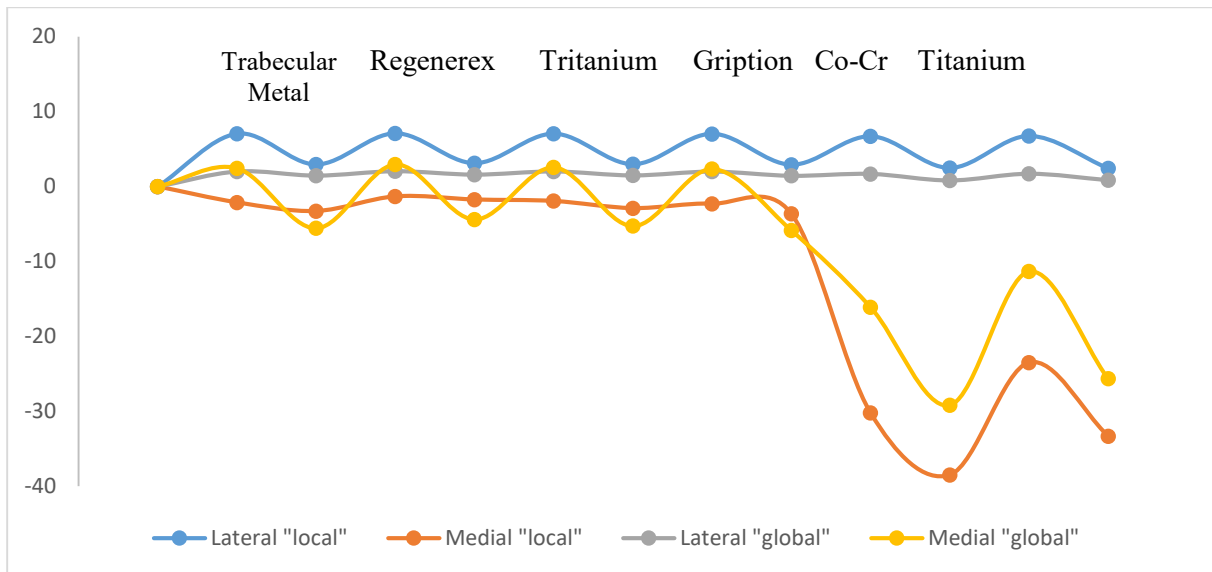
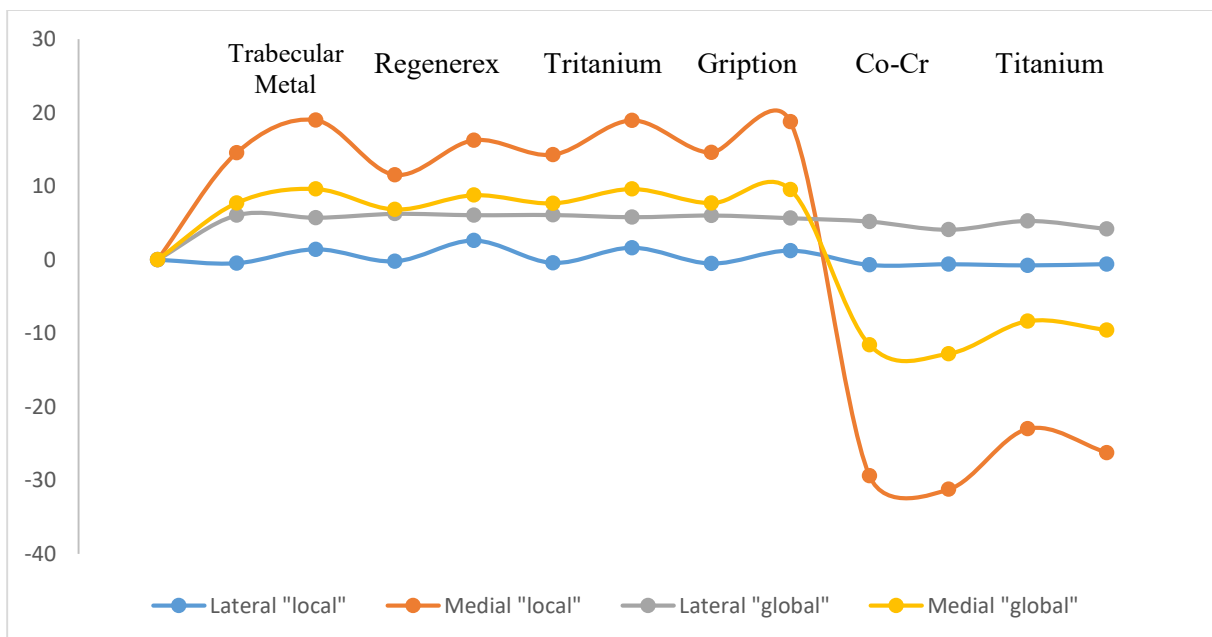


Figure 149 - Variations of Von Mises stress for a femoral posterior augment: flexion angle 45°.



**Figure 150** - Variations of Von Mises stress for a femoral distal augment: flexion angle 90°.



**Figure 151** - Variations of Von Mises stress for a posterior augment: flexion angle 90°.

By observing these results, it is possible to conclude that it is advisable to use a material which has an elastic modulus as close as possible to that of cancellous bone. Therefore, porous metals represent a good alternative to the conventional metals because solid materials cause very marked variations on Von Mises stress distribution in the surrounding host bone. So, the use of porous materials could lead to a reduction of the loosening rate.

Furthermore, the following figures report the variation in terms of shear stress: in this case, it is possible to demonstrate that porous metals allow also a better bone shear stress distribution, if compared to that of conventional metals. The only critical configuration is when a tibial augment made of Regenerex with a thickness of 15 mm is implanted: if a flexion angle of 90° is considered, the change in terms of shear stress is around 32%, while if a conventional metal is adopted for treat this tibial defect, there will be a variation which is less than 20%.

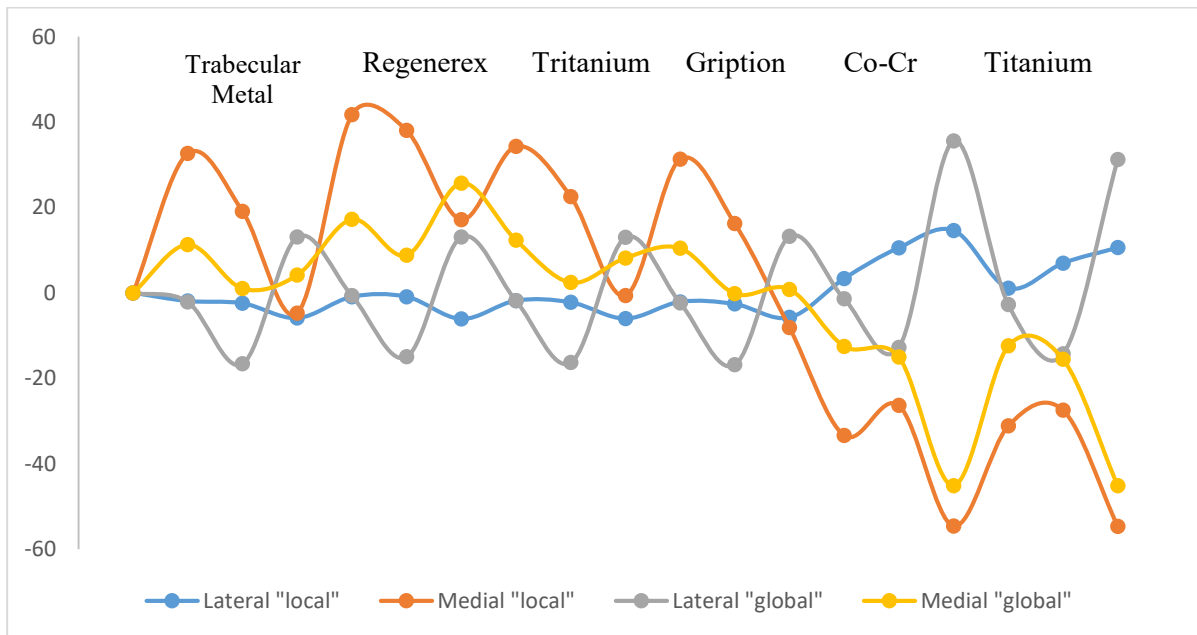


Figure 152 - Variations of shear stress for a tibial distal augment: flexion angle 0°.

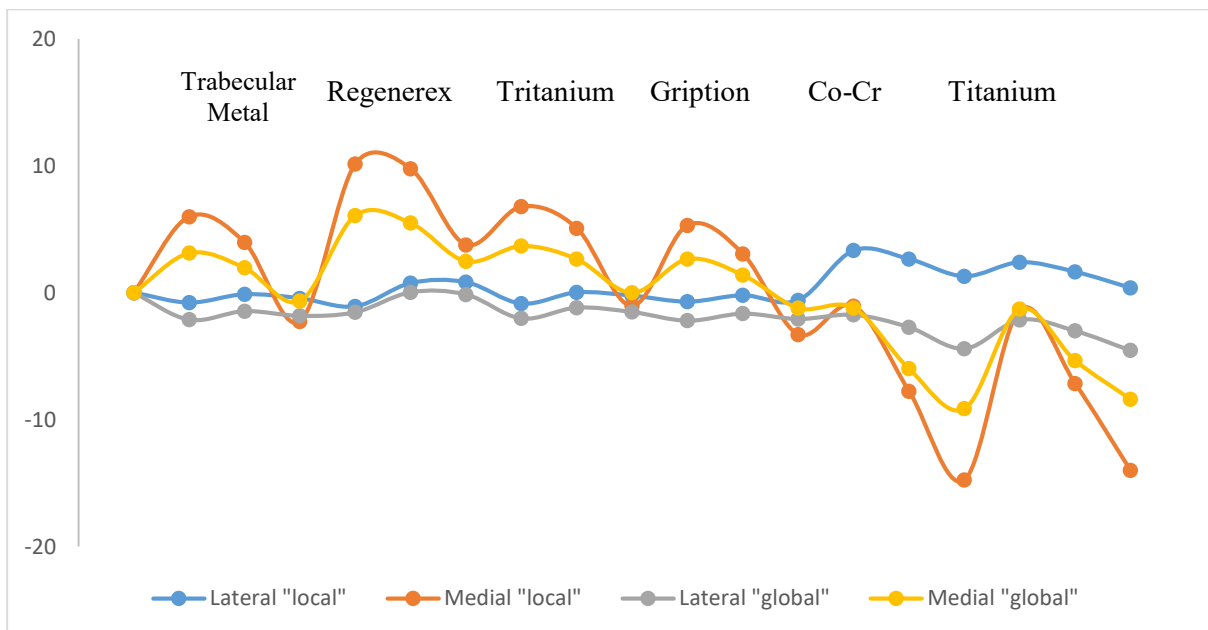
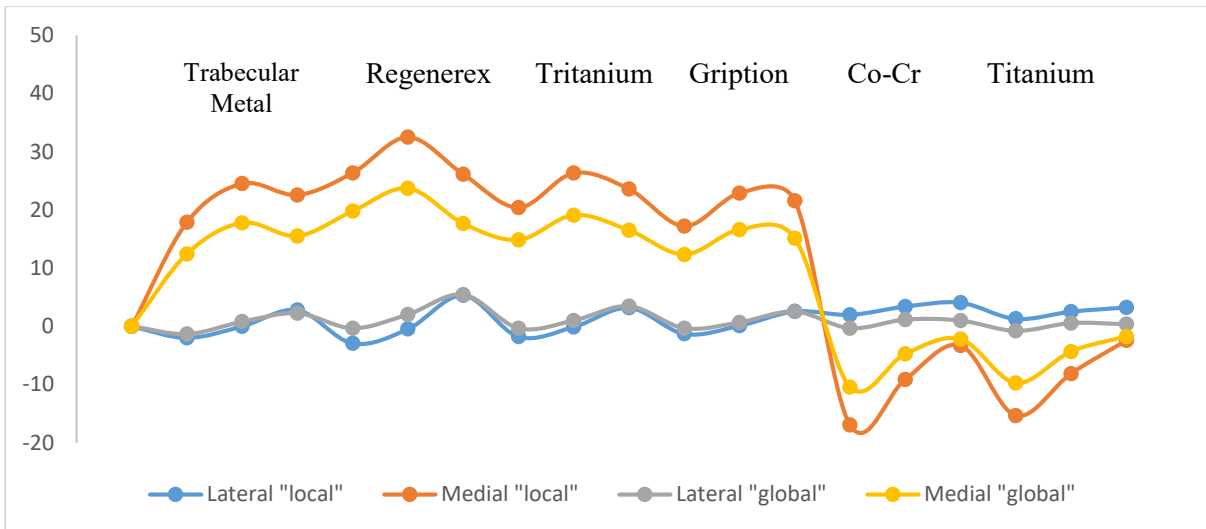
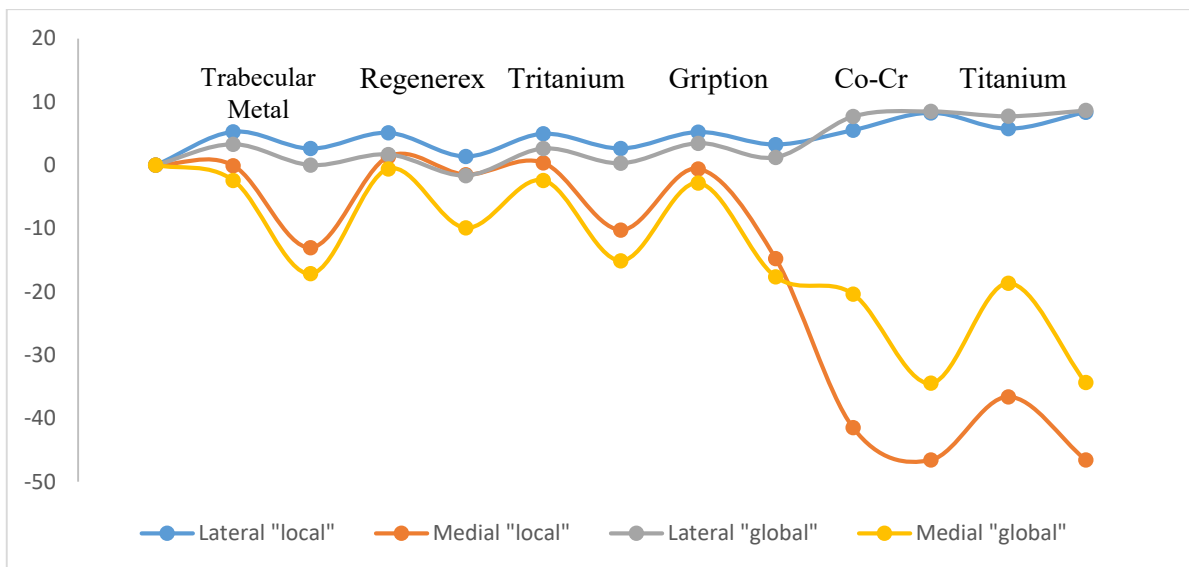


Figure 153 - Variations of shear stress for a tibial distal augment: flexion angle 45°.



**Figure 154** - Variations of shear stress for a tibial distal augment: flexion angle 90°.



**Figure 155** - Variations of shear stress for a femoral distal augment: flexion angle 0°.

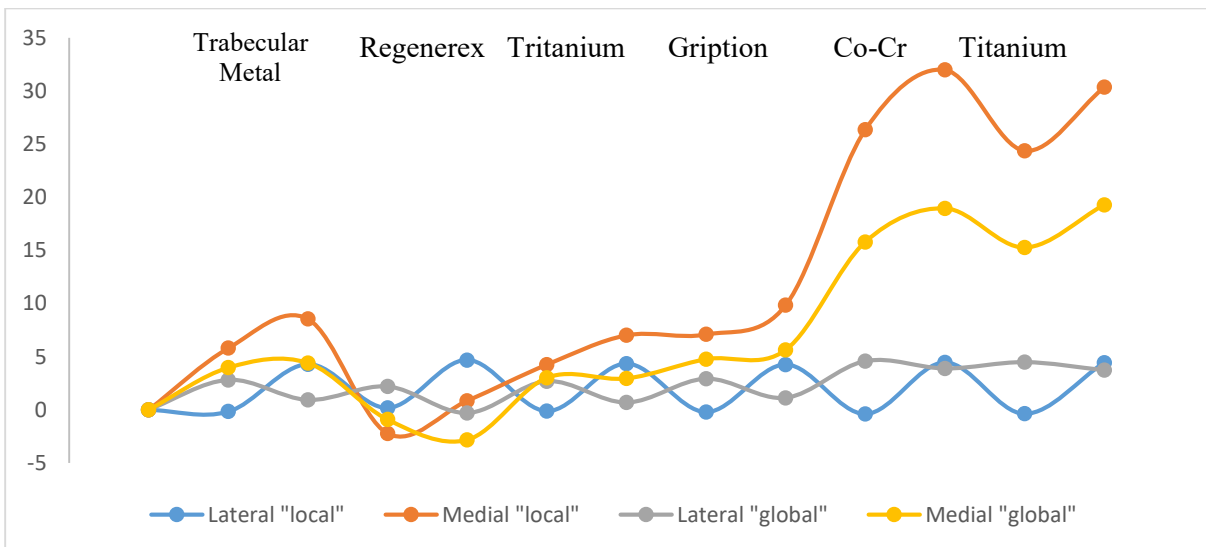


**Figure 156** - Variations of shear stress for a femoral posterior augment: flexion angle 0°.

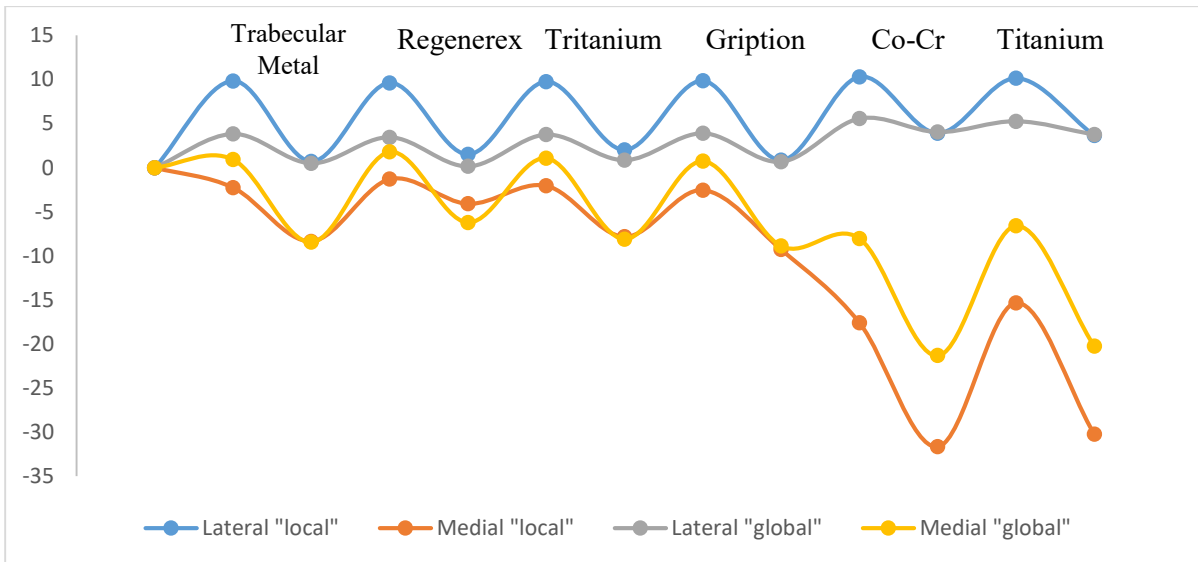


**Figure 157** - Variations of shear stress for a femoral distal augment: flexion angle 45°.

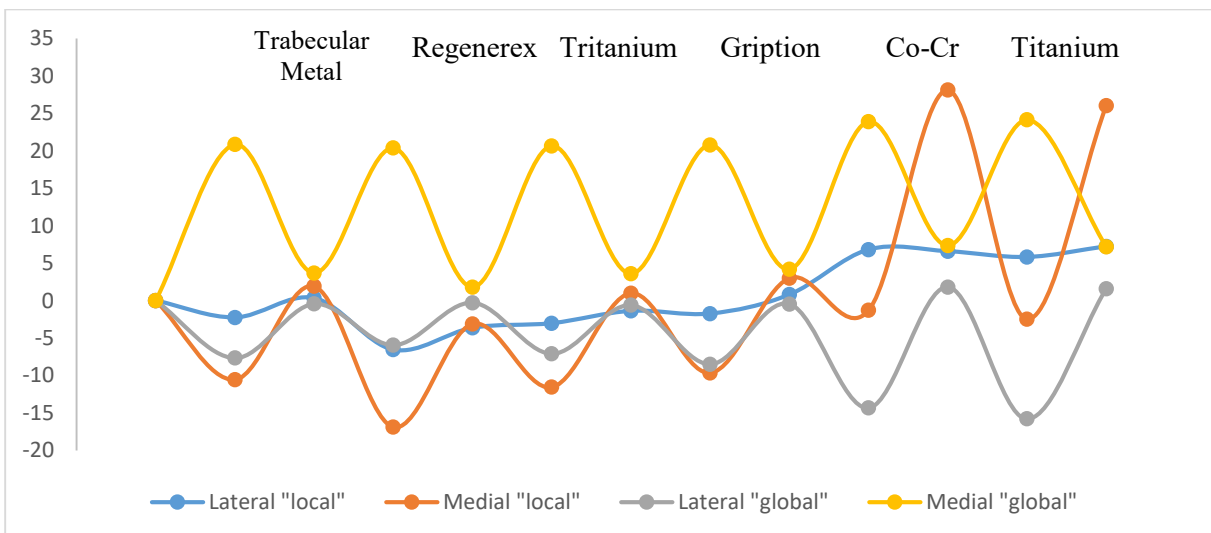


**Figure 158** - Variations of shear stress for a femoral posterior augment: flexion angle 45°.

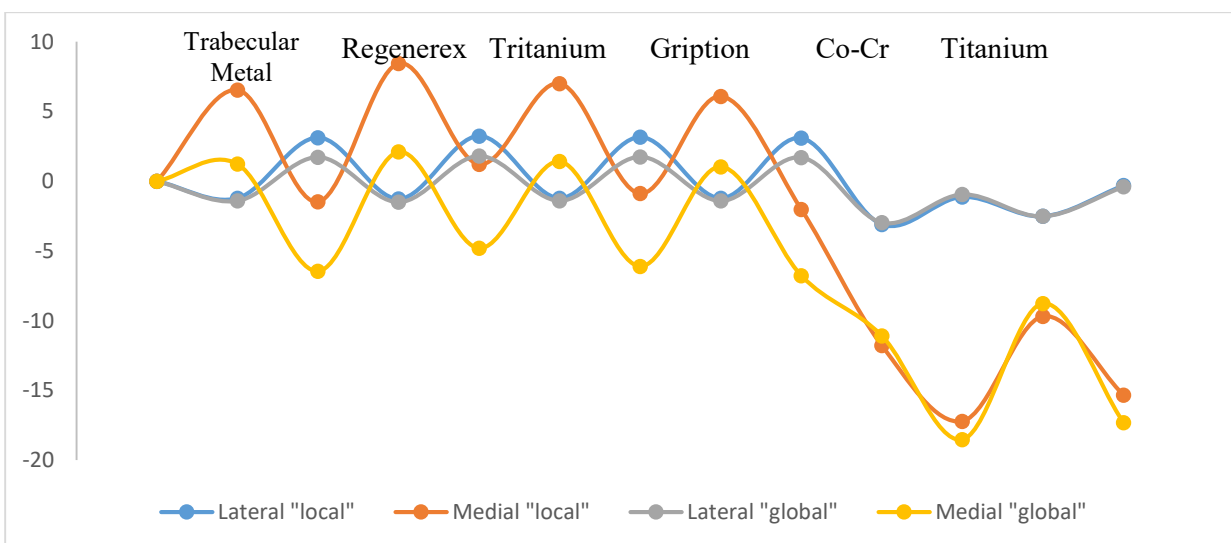


**Figure 159** - Variations of shear stress for a femoral distal augment: flexion angle 90°.

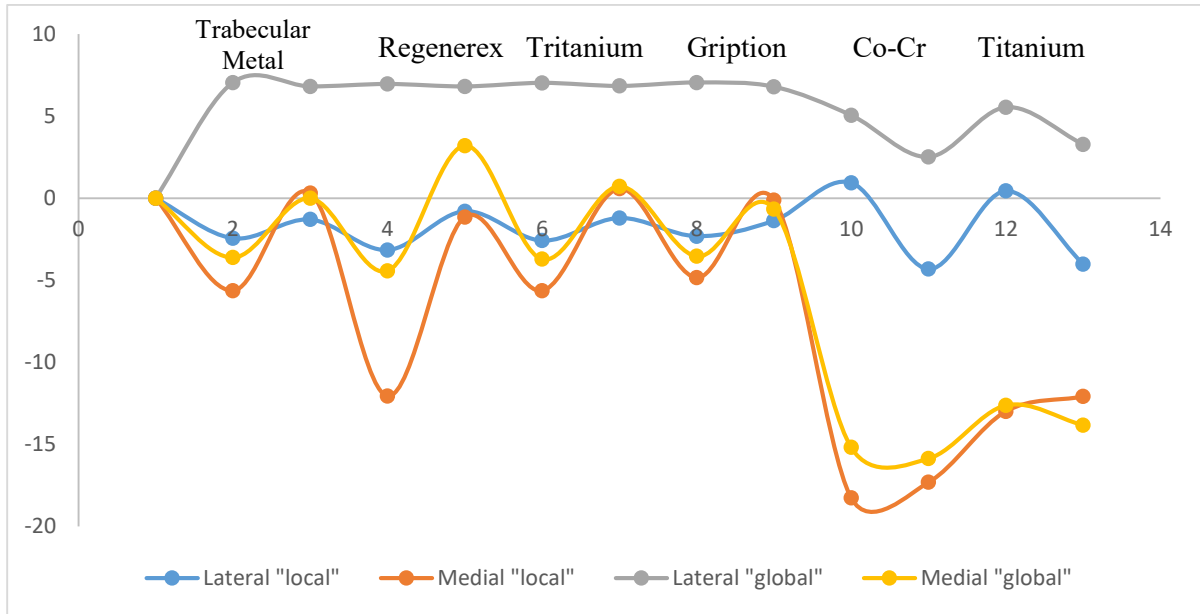


**Figure 160** - Variations of shear stress for a femoral posterior augment: flexion angle 90°.



# Bibliography

- [1] *Knee anatomy*. Available: [https://www.physio-pedia.com/Knee#cite\\_note-p1-1](https://www.physio-pedia.com/Knee#cite_note-p1-1)
- [2] Dr. Chung A. *Knee Anatomy, Function and Common Problems*. Available: <https://www.healthpages.org/anatomy-function/knee-joint-structure-function-problems/>
- [3] Leslie Samuel. *Functional anatomy of the knee: movement and stability*. Available: <http://www.interactive-biology.com/3992/functional-anatomy-of-the-knee-movement-and-stability/>
- [4] U.S. National Library of Medicine. *Knee arthroscopy - series—Normal anatomy*. Available: [https://medlineplus.gov/ency/presentations/100117\\_1.htm](https://medlineplus.gov/ency/presentations/100117_1.htm)
- [5] U.S. National Library of Medicine. *Synovial fluid*. Available: <https://medlineplus.gov/ency/imagepages/19698.htm>
- [6] *Applied anatomy of the knee*. Available: [http://www.orthopaedicmedicineonline.com/downloads/pdf/B9780702031458000879\\_web.pdf](http://www.orthopaedicmedicineonline.com/downloads/pdf/B9780702031458000879_web.pdf)
- [7] M. Saavedra, J. Navarro-Zarza, P. Villasenor-Ovies, J. Canoso, A. Vargas, K. Chiapas-Gasca, C. Hernández-Díaz, A. Kalish. *Clinical Anatomy of the Knee*. *Reumatol Clin*. 2012;8(S2):39–45
- [8] L. Inverarity. *Ligaments of the knee joint*. Available: <https://www.verywellhealth.com/ligaments-of-the-knee-joint-2696388>
- [9] Prof. P.P. Mariani. *Anatomia del ginocchio*. Available: <https://www.pierpaolomariani.it/anatomia-del-ginocchio>
- [10] B. K. Madetti, S. R. Chalamalasetti, S. K. Bolla Pragada. *Biomechanics of knee joint — A review article*. *Front. Mech. Eng.* 2015, 10(2): 176–186
- [11] Prashant Komdeur, Fabian E. Pollo, Phd, and Robert W. Jackson, Md. *Dynamic knee motion in anterior cruciate impairment: a report and case study*. *BUMC Proceedings* 2002;15:257–259.
- [12] E. S. Grood, W. J. Suntay. *A Joint Coordinate System for the Clinical Description of Three-Dimensional Motions: Application to the Knee*. Giannestras Biomechanics Laboratory, Department of Orthopaedic Surgery, University of Cincinnati Medical Center, Cincinnati, Ohio 45267.
- [13] K. J. Hamelynck, J.L. Briard, M. J. Pappas. *Biomechanics of Total Knee Arthroplasty (TKA)*. K. J. Hamelynck et al. (eds.), *LCS® Mobile Bearing Knee Arthroplasty* © Springer-Verlag Berlin Heidelberg 2002
- [14] H. Tateishi. *Indications for Total Knee Arthroplasty and Choice of Prosthesis*. *JMAJ* 44(4): 153–158, 2001
- [15] Prof. A. Moroni. *Artroplastica di ginocchio*. Available: <http://www.profantoniomoroni.com/artroplastica-di-ginocchio/>
- [16] OrthoInfo. *Revision Total Knee Replacement*. Available: <https://orthoinfo.aaos.org/en/treatment/revision-total-knee-replacement/>

- [17] F.S.L. Bobbert, K. Lietaert, A.A. Eftekhari, B. Pouran<sup>1</sup>, S.M. Ahmad, H. Weinans, A.A. Zadpoor. *Additively manufactured metallic porous biomaterials based on minimal surfaces: a unique combination of topological, mechanical, and mass transport properties*. Acta Biomaterialia. Volume 53, 15 April 2017, Pages 572 – 584.
- [18] Rachel M. Frank, David Fabi and Brett R. Levine. *Modern Porous Coatings in Orthopaedic Applications*. S. Nazarpour (ed.), Thin Films and Coatings in Biology, Biological and Medical Physics, Biomedical Engineering.
- [19] J. Muth, M. Poggie, G. Kulesha, R. M. Meneghini. *Novel Highly Porous Metal Technology in Artificial Hip and Knee Replacement: Processing Methodologies and Clinical Applications*. JOM, Vol. 65, No. 2, 2013
- [20] Mediaswanti K, Wen C, Ivanova EP, Berndt CC, Malherbe F, et al. (2013). *A Review on Bioactive Porous Metallic Biomaterials*. J Biomim Biomater Tissue Eng 18: 104
- [21] C.E. Wen, Y. Yamada, P.D. Hodgson. *Fabrication of novel TiZr alloy foams for biomedical applications*. Materials Science and Engineering C 26 (2006) 1439–1444.
- [22] C. E. Wen, Y. Yamada, K. Shimojima, Y. Chino, T. Asahina, M. Mabuchi. *Processing and mechanical properties of autogenous titanium implant materials*. Journal of materials science: materials in Medicine 13 (2002) 397-401.
- [23] *Resistenza dei biomateriali*.  
Available: [http://dma.ing.uniroma1.it/users/scicostr\\_c1/CapVIIIBioStruttureArtificiali.pdf](http://dma.ing.uniroma1.it/users/scicostr_c1/CapVIIIBioStruttureArtificiali.pdf)
- [24] M.I.Z. Ridzwan, Solehuddin Shuib, A.Y. Hassan, A.A. Shokri and M.N. Mohamad Ibrahim, 2007. *Problem of Stress Shielding and Improvement to the Hip Implant Designs: A Review*. Journal of Medical Sciences, 7: 460-467.
- [25] UW Radiology. *The Painful Joint Prosthesis*. Department of Radiology. University of Washington.  
Available: <https://rad.washington.edu/about-us/academic-sections/musculoskeletalradiology/teaching-materials/online-musculoskeletal-radiology-book/the-painful-joint-prosthesis/>
- [26] J. S. Nyman. *Long stemmed total knee arthroplasty with interlocking screws: a computational bone adaptation study*. Journal of Orthopaedic Research 22 (2004) 51-57.
- [27] T. Robalo. *Analysis of bone remodeling in the tibia after total knee prosthesis*. Available: <https://pdfs.semanticscholar.org/2e24/ca16989924cd63471ab871fc957c22524282.pdf>
- [28] J. S. Nyman. *Long stemmed total knee arthroplasty with interlocking screws: a computational bone adaptation study*. Journal of Orthopaedic Research 22 (2004) 51-57.
- [29] S. J. Simske, R. A. Ayers, T. A. Bateman. *Porous material for bone engineering*. Materials Science Forum Vol. 250 (1997) pp 151-182.
- [30] S. Bose, S. Tarafder, A. Bandyopadhyay. *Hydroxyapatite coatings for metallic implants*. Saenz et al. (1999).
- [31] M. Mourm D. Das, T. Winkler, E. Hoenig, G. Mielke, M. Morlock, A. F. Schilling. *Advances in Porous Biomaterials for Dental and Orthopaedic Applications*. Materials 2010, 3, 2947-2974
- [32] F. Matassi, A. Botti, L. Sirleo, C. Carulli, M. Innocenti. *Porous metal for orthopaedics implants*. Clinical Cases in Mineral and Bone Metabolism 2013.

- [33] Karel Lietaert, Ruben Wauthle and Jan Schrooten. *Porous Metals in Orthopedics*. Springer International Publishing AG 2018
- [34] Elia Marin & L. Fedrizzi & L. Zagra. *Porous metallic structures for orthopaedic applications: a short review of materials and technologies*. Eur Orthop Traumatol (2010) 1:103–109
- [35] Jeetram Prajapati. *Metal foam by space holder technique*. ISBN: 978-93-86171-35-1.
- [36] Ahmed Niameh Mehdy Alhusseny, Adel Nasser and Nabeel M J Al-zurfi. *High-Porosity Metal Foams: Potentials, Applications, and Formulations*.
- [37] E. A. Lewallen, S. M. Riester, C. A. Bonin, H. M. Kremers, A. Dudakovic, S. Kakar, R. C. Cohen, J. J. Westendorf, D. G. Lewallen. *Biological Strategies for Improved Osseointegration and Osteoinduction of Porous Metal Orthopedic Implants*. TISSUE ENGINEERING: Part B Volume 21, Number 2, 2015
- [38] O. K. Kamynina, I. Gotman, E. Gutmanas, A. E. Sytschev, S. G. Vadchenko and E. N. Balikhina. *Combustion Synthesis of Porous Ti–Co Alloys for Orthopedic Applications*. ISSN 1061-3862, International Journal of Self-Propagating High-Temperature Synthesis, 2009, Vol. 18, No. 2, pp. 102–108. © Allerton Press, Inc., 2009.
- [39] A. S. H. Makhlof. *Current and advanced coating technologies for industrial applications*. Woodhead Publishing Limited, 2011
- [40] Tarun Garg, Onkar Singh, Saahil Arora & R.S.R. Murthy. *Scaffold: A Novel Carrier for Cell and Drug Delivery*. *Critical Reviews™ in Therapeutic Drug Carrier Systems*, 29(1), 1–63 (2012)
- [41] Naznin Sultana and MinWang. *PHBV/PLLA-based composite scaffolds fabricated using an emulsion freezing/freeze-drying technique for bone tissue engineering: Surface modification and in vitro biological evaluation*. Published 18 January 2012
- [42] Yazhou Wang, Bochu Wang, Guixue Wang, Tieying Yin, Qingsong Yu. *A novel method for preparing electrospun fibers with nano-/micro-scale porous structures*. Published online: 18 April 2009
- [43] Sean V Murphy & Anthony Atala. *3D bioprinting of tissues and organs*. Nature Biotechnology VOLUME 32 NUMBER, 8 AUGUST 2014
- [44] K. Prasad, O. Bazaka, M. Chua, M. Rochford, L. Fedrick. *Metallic Biomaterials: Current Challenges and Opportunities*. Materials 2017, 10, 884
- [45] Ibrahim Ozbolat and Yin Yu. *Bioprinting towards Organ Fabrication: Challenges and Future Trends*. TBME-01840-2012
- [46] C. Gao, S. Peng, P. Feng, C. Shuai. *Bone biomaterials and interactions with stem cells*. Citation: Bone Research (2017) 5, 17059
- [47] B. Levine. *A New Era in Porous Metals: Applications in Orthopaedics*. ADVANCED ENGINEERING MATERIALS 2008, 10, No. 9
- [48] A. A. Pasa, M. L. Munford. *Electrodeposition*. Encyclopedia of Chemical Processing.
- [49] N. Koju, P. Sikder, Y. Ren, H. Zhou, S.B. Bhaduri. *Biomimetic coating technology for orthopedic implants*. Current Opinion in Chemical Engineering 2017, 15:49–55
- [50] H. Cao, X. Liu. *Activating titanium oxide coatings for orthopaedic implants*. Volume 233, 25 October 2013, Pages 57–64

- [51] V. K. Balla, S. Bodhak, S. Bose and A. Bandyopadhyay. *Porous Tantalum Structures for Bone Implants: Fabrication, Mechanical and In vitro Biological Properties*. Acta Biomater. 2010 August ; 6(8): 3349–3359
- [52] B. Levine, S. Sporer, C. J Della Valle, J. J. Jacobs, W. Paprosky. *Porous Tantalum in Reconstructive Surgery of the Knee*. *J Knee Surg*. 2007;20:185-194.
- [53] Zimmer Biomet. *Trabecular Metal*. Available: <http://www.zimmer.co.uk/medical-professionals/our-science/common/trabecular-metal-technology.html>
- [54] S.A. Hacking, J.D. Bobyn, K.-K. Toh, M. Tanzer, J.J. Krygier. *Fibrous tissue ingrowth and attachment to porous tantalum*. © 2000 John Wiley & Sons, Inc.
- [55] Stryker. *Engineered for bone*. Available: [http://www.stryker.com/builttofuse/media/assets/3434TriC\\_TechSummaryTRICC-BR-4\\_15542HINC.PDF](http://www.stryker.com/builttofuse/media/assets/3434TriC_TechSummaryTRICC-BR-4_15542HINC.PDF)
- [56] Depuy. *GRIPTION® Porous Coating*. Available: <https://emea.depuyorthopedics.com/hcp/hip/products/qs/gription-porous-coating>
- [57] T. P. Andriacchi, T. S. Stanwyck, J. Galante. *Knee biomechanics and Total Knee Replacement*. The Journal of Arthroplasty Vol. 1 No.3 September 1968.
- [58] J. F. Keating, A. H. R. W. Simpson, C. M. Robinson. *The management of fractures with bone loss*. ©2005 British Editorial Society of Bone and Joint Surger.
- [59] B. Innocenti, S. Pianigiani. Biomechanical Analysis of Augments in Revision Total Knee Arthroplasty. Proceedings VII Meeting Italian Chapter of the European Society of Biomechanics (ESB-ITA 2017) 28-29 September 2017, Rome – Italy.
- [60] S. W. Wiesel. *Operative Techniques in Orthopaedic Surgery*. 13 luglio 2010
- [61] J. K. Lee, C. H. Choi. *Management of tibial bone defects with metal augmentation in primary total knee replacement*. The British Editorial Society of Bone & Joint Surgery, 22 Buckingham Street, London.
- [62] S. Tsukada, M. Wakui, M. Matsueda. *Metal block augmentation for bone defects of the medial tibia during primary total knee arthroplasty*. *J Orthop Surg Res*. 2013 Oct 20;8:36.
- [63] B. Innocenti, S. Pianigiani. *The use of finite element modelling to improve biomechanical research on knee prosthesis*. Nova Science Publisher, Inc. Jan 1 2015.
- [64] B. Innocenti, ÖF. Bilgen, L. Labey, GH. van Lenthe, JV. Sloten, F. Catani. *Load sharing and ligament strains in balanced, overstuffed and understuffed UKA. A validated finite element analysis*. *J Arthroplasty*. 2014 Jul;29(7):1491-8.
- [65] D. Kluess, J. Wieding, R. Souffrant, W. Mittelmeier and R. Bader. *Finite Element Analysis in Orthopaedic Biomechanics*. © 2010 The Author(s).
- [66] K. Halonen. *Validation and application of computational knee joint models*. Publications of the University of Eastern Finland Dissertations in Forestry and Natural Sciences No 187.
- [67] J.Y. Rho, L. Kuhn-Spearing, P. Zioupos. *Mechanical properties and the hierarchical structure of bone*. Available online 19 November 1998.
- [68] A.C. Godest, M. Beaugonin, E. Haug, M. Taylor, P.J. Gregson. *Simulation of a knee joint replacement during a gait cycle using explicit finite element analysis*. Available online 2 January 2002.
- [69] S. Kopparti P, G. Lewis. *Influence of three variables on the stresses in a three-dimensional model of a proximal tibia-total knee implant construct*. *Biomed Mater Eng*. 2007;17(1):19-28.

- [70] O. Kayabasi, B. Ekici. *The effects of static, dynamic and fatigue behavior on three-dimensional shape optimization of hip prosthesis by finite element method*. © 2006 Published by Elsevier Ltd.
- [71] E.E. Gdoutos, D.D. Raftopoulos, J.D. Baril. *A critical review of the biomechanical stress analysis of the human femur*. Available online 5 May 2003.
- [72] . GEMINI® SL® Total Knee Replacement cementable / cementless with TiCaP®
- [73] . GEMINI® SL® Total Knee Replacement The complete system for greater versatility in total knee arthroplasty.
- [74] J. Brihault, A. Navacchia, S. Pianigiani, L. Labey, R. De Corte, V. Pascale, B. Innocenti. *All-polyethylene tibial components generate higher stress and micromotions than metal-backed tibial components in total knee arthroplasty*. *Knee Surg Sports Traumatol Arthrosc*. 2016 Aug;24(8):2550-9.
- [75] B. Innocenti, J. Bellemans, F. Catani. *Deviations From Optimal Alignment in TKA: Is There a Biomechanical Difference Between Femoral or Tibial Component Alignment?* *J Arthroplasty*. 2016 Jan;31(1):295-301.
- [76] M. Soenen, M. Baracchi, R. De Corte, L. Labey, B. Innocenti. *Stemmed TKA in a Femur With a Total Hip Arthroplasty Is There a Safe Distance Between the Stem Tips?* *J Arthroplasty*. 2013 Sep;28(8):1437-45.
- [77] M. Vaninbrouckx, L. Labey, B. Innocenti, J. Bellemans. *Cementing the femoral component in total knee arthroplasty: Which technique is the best?* *Knee*. 2009 Aug;16(4):265-8
- [78] J. Vanlommel, J.P. Luyckx, L. Labey, B. Innocenti, R. De Corte, J. Bellemans. *Cementing the Tibial Component in Total Knee Arthroplasty Which Technique is the Best?* *J Arthroplasty*. 2011 Apr;26(3):492-6
- [79] D. Waanders, D. Janssen, K.A. Mann, N. Verdonchot. *The mechanical effects of different levels of cement penetration at the cement–bone interface*. *J Biomech*. 2010 Apr 19;43(6):1167-75.
- [80] LINK. GEMINI SL Total Knee replacement. Available: <https://www.linkorthopaedics.com/en/for-the-physician/products/knie/primary/gemini-sl-total-knee-replacement/>
- [81] F. Galbusera, M. Freutel, L. Dürselen, M.D' Aiuto, D. Croce, V. Sansone, B. Innocenti. *Material models and properties in the finite element analysis of knee ligaments: a literature review*. Published online 17 November 2014.
- [82] J. P. Whittaker, R. Dharmarajan, A. D. Toms. *The management of bone loss in revision total knee replacement*. Published Online 1 Aug 2008
- [83] Advanced BIOFOAM. Available: <http://www.osimplantes.com.br/produtos/files/microport/joelho/Advance%20Base%20Biofoam%201.pdf>
- [84] W. R. Taylor, M. O. Heller, G. Bergmann, G. N. Duda. *Tibio-femoral loading during human gait and stair climbing*. First published: 01 January 2006
- [85] K. Sasaki and R. R. Neptune. *Contributions of leg muscles to the axial knee joint contact force during normal walking*.
- [86] T. Ingrassia, L. Nalbone, V. Nigrelli, D. Tumino, V. Ricotta. *Finite element analysis of two total knee joint prostheses*. First Online: 14 June 2012
- [87] E.A. Elia, P.A. Lotke. *Results of revision total knee arthroplasty associated with significant bone loss*. *Clin Orthop* 1991;271:114-21.
- [88] P.A. Lotke, R.Y. Wong, M.L. Ecker. *The use of methylmethacrylate in primary total knee replacements with large tibial defects*. *Clin Orthop* 1991;270:288-94.
- [89] D.E. Hockman, D. Ammeen, G.A. Engh. *Augments and allografts in revision total knee arthroplasty: usage and outcome using one modular revision prosthesis*. *J Arthroplasty* 2005;20:35-41.

- [90] JA. Rand. *Bone deficiency in total knee arthroplasty: use of metal wedge augmentation*. Clin Orthop 1991;271:63-71.
- [91] MG. Brand, RJ. Daley, FC. Ewald, RD. Scott. *Tibial tray augmentation with modular metal wedges for tibial bone stock deficiency*. Clin Orthop 1989;248:71-9.
- [92] J. P. Whittaker, R. Dharmarajan, A. D. Toms, *The management of bone loss in revision total knee replacement*. Published Online:1 Aug 2008
- [93] JM. Cuckler. *Bone loss in total knee arthroplasty: graft augment and options*. J Arthroplasty 2004;19(Suppl 1):56-8.
- [94] AE. Pour, J. Parvizi, N. Slenker, JJ. Purtill, PF. Sharkey. *Rotating hinged total knee replacement: use with caution*. J Bone Joint Surg [Am] 2007;89-A:1735-41.
- [95] BD. Springer, FH. Sim, AD. Hanssen, DG. Lewallen. *The modular segmental kinematic rotating hinge for nonneoplastic limb salvage*. Clin Orthop 2004;421:181-7.
- [96] RJ. Harrison Jr, MM. Thacker, JD. Pitcher, HT. Temple, SP. Scully. *Distal femur replacement is useful in complex total knee arthroplasty revisions*. Clin Orthop 2006;446:113-20.
- [97] JD.Bobyn, GJ.Stackpool , SA, Hacking, M, Tanzer, J.Krygier. Characteristics of bone ingrowth and interface mechanics of a new porous tantalum biomaterials. J Bone Joint Surg [Br] 1999;81-B:907-14.
- [98] RM .Meneghini, DG. Lewallen , AD ,Hanssen. *Use of porous tantalum metaphyseal cones for severe tibial bone loss during revision total knee replacement*. J Bone Joint Surg [Am] 2008;90-A:78-84.
- [99] A. Completo, R. Duarte, F. Fonseca, J. A. Simões, A. Ramos, C. Relvas (2013). Biomechanical evaluation of different reconstructive techniques of proximal tibia in revision total knee arthroplasty: An in-vitro and finite element analysis. Clinical Biomechanics, 28(3), 291–298.
- [100] B. Innocenti, E. Truyens, L. Labey, P. Wong, J. Victor and J. Bellemans. Can medio-lateral baseplate position and load sharing induce asymptomatic local bone resorption of the proximal tibia? A finite element study. Journal of Orthopaedic Surgery and Research 2009.
- [101] S. Tsukada1, M. Wakui and M. Matsueda. Metal block augmentation for bone defects of the medial tibia during primary total knee arthroplasty Tsukada et al. Journal of Orthopaedic Surgery and Research 2013, 8:36
- [102] Fehring TK, Peindl RD, Humble RS. Modular tibial augmentations in total knee arthroplasty. Clin Orthop. 1996; 327:207.

# Acknowledgements

Giunta alla fine di questo percorso fondamentale per la mia vita, ritengo sia doveroso ringraziare tutti coloro che mi sono stati sempre vicini, sostenendomi, incoraggiandomi quando sembrava che avessi perso la fiducia in me stessa.

Ringrazio la mia relatrice, la Prof.ssa Cristina Bignardi per avermi dato, grazie alla realizzazione di questo lavoro, la possibilità di poter ampliare le mie conoscenze in un campo non propriamente meccanico, per la totale disponibilità e comprensione.

Ringrazio il Prof. Bernardo Innocenti per avermi seguita nel mio percorso di tesi all'estero permettendomi di maturare conoscenze più approfondite nell'ambito della biomeccanica.

Ringrazio la mia famiglia la quale mi ha consentito di realizzare i miei sogni, sostenendomi, supportandomi ed essendomi vicina sempre, anche nei momenti di debolezza e difficoltà, nonostante la distanza. Un ringraziamento particolare va alla mia mamma che durante questo percorso universitario, ma in generale nella vita, mi è sempre vicina, ha sempre creduto in me e ha cercato sempre di incoraggiarmi nonostante i miei alti e bassi.

Ringrazio Torino per avermi dato l'opportunità di conoscere una persona, che poi è diventata un fulcro fondamentale nella mia vita: Emma, la mia coinquilina. La nostra è nata come una semplice conoscenza dovuta alla convivenza, ma poi per me è diventata più di una sorella. Lei è stata quella persona che ha sopportato tutte le mie ansie quotidiane, le mie paure, che mi ha consolata, ma che mi ha anche spronata a non arrendermi, che mi ha insegnato a lottare per quello che si vuole. Quello che ammiro di lei è la sua grinta, la sua energia: è il mio punto di riferimento.

Desidero inoltre ringraziare i miei amici, quelli veri, che ci sono sempre nonostante tutto e nonostante la lontananza, che ti offrono sempre una spalla su cui piangere, ma che ti fanno anche ridere e che ti tirano su il morale, quando ogni cosa sembra andar storto.

